U.S. Department
of Transportation
**Federal Railroad
Administration**

Analytic Studies of the Relationship Between Track Geometry Variations and Derailment Potential at Low Speeds

Office of Research and
Development
Washington DC 20590

Fred B. Blader

The Analytic Sciences Corporation
One Jacob Way
Reading MA 01867

FRA/ORD-83/16
DOT-TSC-FRA-83-3

September 1983
Final Report

Technical Report Documentation Page

1. Report No.	2. Government Accession No.	3. Recipient's Catalog No.
FRA/ORD-83/16		PB84 129329

4. Title and Subtitle
ANALYTIC STUDIES OF THE RELATIONSHIP BETWEEN TRACK GEOMETRY VARIATIONS AND DERAILMENT POTENTIAL AT LOW SPEEDS

5. Report Date: September 1983
6. Performing Organization Code: TSC-DTS-76

7. Author(s)
Fred B. Blader

8. Performing Organization Report No.: DOT-TSC-FRA-83-3

9. Performing Organization Name and Address
The Analytic Sciences Corporation*
One Jacob Way
Reading MA 01867

10. Work Unit No. (TRAIS): RR319/R3305
11. Contract or Grant No.: DTRJ-57-80-C-00062

12. Sponsoring Agency Name and Address
U.S. Department of Transportation
Federal Railroad Administration
Office of Research and Development
Washington DC 20590

13. Type of Report and Period Covered: Final Report Oct 1981-Mar 1983
14. Sponsoring Agency Code: RRD-12

15. Supplementary Notes
*Under contract to: U.S. Department of Transportation
Research and Special Programs Administration
Transportation Systems Center
Cambridge MA 02142

16. Abstract

This report describes analytical studies carried out to define the relationship between track parameters and safety from derailment. Problematic track scenarios are identified reflecting known accident data. Vehicle response is investigated in the 10-25 mph speed range, using an analytic model of a freight vehicle to identify critical values of body roll, and incipient wheel drop and rail climb, on track with weak lateral restraint. The track model includes gauge variation as well as alignment and cross-level in curves and the vehicle represents a 100-ton hopper car. Model results compare well with experimental results.

Safe values for gauge and crosslevel are identified for curved track containing lateral cusps at outer rail joints with and without cross-level cusps at staggered joints. Safe values of alignment are identified for sinusoidal alignment variation with constant gauge on tangent track and in curves up to 10 degrees. Recommendations are made on improvements to the computational efficiency and accuracy of the simulation and on further efforts required to identify completely safe values for track over the range of speeds, vehicle types and track conditions encountered in service.

17. Key Words
Computer Simulation, Mathematical Dynamic Curving, Hunting, Wheel Rail Forces, Profiles, Derailment, Track Geometry, Track Safety Standards

18. Distribution Statement
DOCUMENT IS AVAILABLE TO THE PUBLIC THROUGH THE NATIONAL TECHNICAL INFORMATION SERVICE, SPRINGFIELD, VIRGINIA 22161

19. Security Classif. (of this report)	20. Security Classif. (of this page)	21. No. of Pages	22. Price
UNCLASSIFIED	UNCLASSIFIED	154	

Form DOT F 1700.7 (8-72) Reproduction of completed page authorized

PREFACE

As part of the Track Safety Research Program of the Office of Research and Development of the Federal Railroad Administration (FRA), the Transportation Systems Center (TSC) has been conducting and directing both analytical and experimental studies. These studies aim to define the relationships between track design and maintenance parameters and the safety and performance resulting from the dynamic interaction of the track and train. They are intended to provide the basis for improved track design and maintenance specification that can be directly related to the safe and efficient performance of the rail transportation system. Efforts conducted under this program have included:

- Statistical Correlation of Railcar Accident Data and Freight Car Characteristics Conducted at TSC (Ref. 1)
- Development of a data base of engineering parameters characterizing the physical parameters and configurations of railway rolling stock by Pullman-Standard Corporation (Ref. 2).
- Development of analytic characterizations of track geometry variations found in existing track by ENSCO Corporation (Ref. 3)
- Analytic studies of the relation between track geometry variations and derailment potential conducted by The Analytic Sciences Corporation (TASC)
- Field tests and demonstrations conducted in cooperation with the Railroad Industry and the American Railway Engineering Association (AREA).

This report describes the work conducted by TASC on the analytic studies over the years 1977 through 1982 and represents the contributions on the engineering model and analysis of Dr. Fred Blader, John A. Elkins, Dr. Narayan A. Acharya, Paul W. Berry, Dr. Harish C. Dhingra, Dr. Joseph W. Griffin, Dr. Robert L. Jeffcoat, and Dr. James H. Taylor, and on the computer work of Kathy Baribeau, Dr. David S. Biekasa, Bill Kuklinski, and Peter Zammuto.

The work described in the report is primarily intended to support the study of track safety performance standards and has been used by those in government (FRA, TSC), the American Railway Engineering Association (AREA) and the railroad industry, particularly the Association of American Railroads (AAR), responsible for addressing these standards and safety during rail transportation.

The model improvements and results will also be of interest to the rail vehicle manufacturing industry to aid in assessing the response of particular vehicles to track geometry.

The author wishes to thank Dr. Herbert Weinstock, the TSC Technical Monitor, for his tireless work in guiding and criticizing the work and for providing the framework within which the new approximations were introduced to the computer program, SIMCAR, used in the study.

METRIC CONVERSION FACTORS

Approximate Conversions to Metric Measures

Symbol	When You Know	Multiply by	To Find	Symbol
	LENGTH			
	AREA			
	MASS (weight)			
	VOLUME			
	TEMPERATURE (exact)			
°F	Fahrenheit temperature	5/9 (after subtracting 32)	Celsius temperature	°C

*1 in = 2.54 (exactly). For other exact conversions and more detailed tables, see NBS Misc. Publ. 286, Units of Weights and Measures, Price $2.25, SD Catalog No. C13.10:286.

Approximate Conversions from Metric Measures

Symbol	When You Know	Multiply by	To Find	Symbol
	LENGTH			
mm	millimeters	0.04	inches	in
cm	centimeters	0.4	inches	in
m	meters	3.3	feet	ft
m	meters	1.1	yards	yd
km	kilometers	0.6	miles	mi
	AREA			
cm^2	square centimeters	0.16	square inches	in^2
m^2	square meters	1.2	square yards	yd^2
km^2	square kilometers	0.4	square miles	mi^2
ha	hectares ($10,000\ m^2$)	2.5	acres	
	MASS (weight)			
g	grams	0.035	ounces	oz
kg	kilograms	2.2	pounds	lb
t	tonnes (1000 kg)	1.1	short tons	
	VOLUME			
ml	milliliters	0.03	fluid ounces	fl oz
l	liters	2.1	pints	pt
l	liters	1.06	quarts	qt
l	liters	0.26	gallons	gal
m^3	cubic meters	35	cubic feet	ft^3
m^3	cubic meters	1.3	cubic yards	yd^3
	TEMPERATURE (exact)			
°C	Celsius temperature	9/5 (then add 32)	Fahrenheit temperature	°F

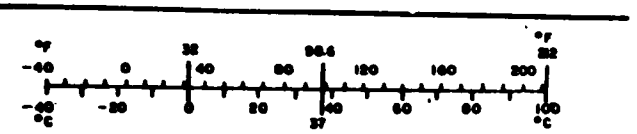

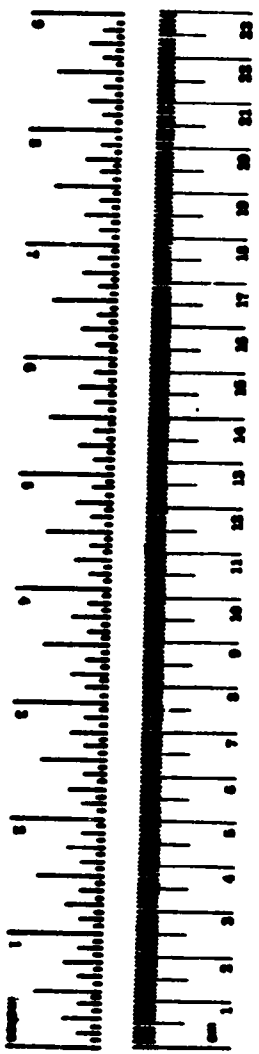

TABLE OF CONTENTS

TABLE OF CONTENTS (Continued)

LIST OF FIGURES

LIST OF FIGURES (Continued)

LIST OF FIGURES (Continued)

LIST OF FIGURES (Continued)

LIST OF FIGURES (Contined)

LIST OF TABLES

SUMMARY

The Track Safety Research Program aims to define the relationship between track parameters and safety under track train interaction. Investigation of track geometry data indicated that the deviations are generally large amplitude, infrequent occurrences, primarily controlled by staggered jointed rail effects. Dominant scenarios chosen from a study of the derailment statistics between January 1976 and September 1978 are found to be,

- Rock and roll and tangent track 10-25 mph
- Alignment-gauge and cross level variation in curves 10-25 mph.

The former scenario has been studied and reported by the Transportation Systems Center (TSC) using an MIT model. The latter is the primary subject of this study. An advance in freight car modeling is described to include gauge variation not available in existing models and to improve the computational efficiency at low speeds. The peak wheel rail forces on the truck leading axles, predicted by the computer program developed, are shown to be in reasonable agreement with data obtained in perturbed track tests and tests on Union Pacific and Chessie System track.

Parametric studies are reported relating gauge, alignment, cross level and curvature variations to rail car safety and wheel rail forces to assist in defining limits for safe operation between 10 and 25 mph. The results suggest:

a) For new wheel and rail profiles which generally provide the worst curving performance, the computer simulation SIMCAR provides valid performance predictions.

b) For speeds less than 25 mph the response to outer rail cusped track, showing both gauge and alignment variation in curves, is not sensitive to speed. The forces generated tend to spread the rail.

c) Under minimal lateral track restraint conditions, incipient wheel drop is predicted as the most likely derailment mode on curved track with outer rail cusps.

d) On 10° curves, with outer rail cusps and cusped cross-level variation, the combined response presents a more severe derailment likelihood than is presented by the separate studies of response to gauge and cross-level variation.

e) Sinusoidal track alignment variations, with constant gauge at speeds below 25 mph, are predicted to produce severe gauge spreading forces, especially for wavelengths of 50 ft and below. The wavelength producing the largest forces varies with curvature.

f) A set of geometric track values for gauge, alignment and cross-level in curves have been identified, within which no derailment is predicted for the loaded 100 ton hopper car simulated.

1. INTRODUCTION

1.1 BACKGROUND

During the past decade, there have been extensive efforts by both Government and industry to establish a better understanding of the dynamic interactions in the track/train system as a function of train operating practices, terrain and track geometry. Significant work has been accomplished under the International Government Industry Track/Train Dynamics Program administered by the Association of American Railroads (AAR), (Ref. 4), towards defining options for controlling dynamic aspects of train operation to limit excessive train action resulting in potentially unsafe conditions. Several mathematical models were developed under this program.

A sample of concurrent efforts to predict the dynamic behavior of trains and cars is listed under Ref. 5. These advances in predicting railcar response to track geometry variations have made it possible to reevaluate and redefine current track geometry and maintenance specifications in terms of their relationship to the safety-related dynamic response of rail cars and trains. In 1970, when the current FRA Track Safety Standards were initially formulated, track design and maintenance practice was based on limited empirical data, tradition, and intuitive judgments, that could not be subjected to precise engineering analysis. The specification represented a consensus of the best judgment of qualified engineers based upon current and varying individual railroad practices.

1.2 OBJECTIVE

The purpose of the studies reported here is to apply the improved state-of-the-art in dynamic modeling to establish direct relationships between variations in track geometry and dynamic performance of rail cars. These relationships are then applicable to the development of specifications which establish the maximum tolerable track geometry variations that can be permitted, assuring safety from derailment.

1.3 APPROACH

Initial results obtained (Ref. 3) indicated that for a wide range of track geometry measurements, track geometry variations could be represented mathematically as a stationary random process described completely by a limited number of parameters. These parameters also appeared to correlate well with the assigned track classes. Accordingly, the initial studies conducted under this contract were directed towards development of a probabilistic approach to be applied to existing rail vehicle dynamics models giving derailment statistics as a function of the statistical track geometry parameters. Further investigation of the track geometry data, however, indicated that the track geometry deviations governing the track classes, to which a segment of track was assigned, were generally large amplitude, infrequent occurrences. These were on one hand obscured by the statistical processing of the data and on the other hand too large and too frequent to be considered part of the identified stationary random process. In addition, in the lower classes of track, where most accidents were found to occur, (Ref. 1), the track geometry gauge deviations were found to be controlled primarily by half staggered jointed rail effects.

Analysis of accident data and experience of the AREA Ad Hoc Committee on Track Safety Performance Standards also indicated that railroad accidents were not purely random occurrences that were extensions of normal operation conditions but could be associated with particular track and operation conditions. Accordingly, the government/industry efforts were redirected towards a "scenario approach." Representative problematic track geometry situations were defined and associated representative vehicles having a high incidence of derailment were analyzed to establish limits on track geometry variations to prevent derailment. A more complete description of the "scenario approach" and an identification of the highest priority scenarios for controlling numbers of accidents is given in Chapter 2 of this report.

The highest priority scenario was studied in an analysis by TSC (Ref. 6) making use of a simplification of the "Freight Car Model" of the Government/Industry Track Train Dynamics Program developed by Mechanical Engineering Department of the Massachusetts Institute of Technology (Ref. 7) which has been demonstrated to be in good agreement with experimental data. This study resulted in the definition of a cross-level index for controlling harmonic roll derailments induced by cross-level variation. It was further evaluated in a pilot application of the Chessie System and in tests on the Boston and Maine in August 1982.

The second highest priority as discussed in Chapter 2 was the combined effect of alignment, gauge, curvature and cross-level on high center of gravity cars in operation at speeds between 10 and 25 mph. Attempts to apply the Library of Rail Vehicle Dynamics Programs acquired under this effort (Appendix A) resulted in the discovery of two significant difficulties. First, the programs that predicted rail forces were designed for higher operation speeds and were not computationally efficient at lower operating speeds. More importantly, the existing programs failed to treat gauge variations that normally occur with alignment variations on lower track classes. This resulted in the prediction of wheel rail forces for wavelengths of the order of 39 feet, much higher than those normally observed in field measurements. Accordingly, as discussed in Chapter 3, the existing rail vehicle models were modified to improve the wheel rail forces representation. New algorithms were identified and used to improve the computational efficiency of the program, SIMCAR.

The peak wheel/rail forces on the truck leading axles, predicted by the program, were found to be in general agreement with data obtained in track tests, as discussed in Chapter 4.

Parametric studies relating gauge, alignment, and curvature variations to rail car safety and wheel rail forces were conducted to define limits of track geometry variations which would be tolerable for operations between 10 and 25 mph. The results of these studies are presented in Chapter 5. As discussed these results are believed to be conservative due to the simulation of new wheel/rail geometry and a friction coefficient that would be typical of clean dry rail.

2. STUDY METHODOLOGY

2.1 INTRODUCTION

The primary emphasis of the work conducted in this effort is the analysis of the safety-related dynamic response of freight cars, subjected to track geometry variations representing operating conditions and track geometry deviation conditions that are typical of train derailment situations. The highest priority was identified at the Transportation Systems Center from the number of derailments attributed to track geometry contained in the records of the FRA Railroad Accident/Incident Reporting System (RAIS) over the period January 1976 to September 1978 inclusive.

Quantitative measures of dynamic response were identified that could be directly related to the proximity to derailment or track structural failure. In the studies described here, the effects of track geometry variations were assessed using car body displacements (roll-angle) or wheel displacements (wheel lift and drop), that implied a derailment condition. Critical force and force ratios necessary for evaluation of track structural adequacy were also identified as required outputs of the computations.

Finally, analysis tools were examined for studying the scenario, their capability for predicting the performance measures, the types of geometry deviations possible, vehicle characteristics depicted, and computational efficiency. The models were improved and the resulting computer simulation applied to the study described in Chapter 5.

The following sections provide a more detailed discussion of the scenarios, processes and measurements, and analysis tools investigated for the study of derailment due to track geometric deviations.

2.2 DERAILMENT SCENARIOS

Table 2.2-1 provides a tabulation of the number of derailments on mainline track attributed to track geometry causes between 1976 and 1979 for the speed ranges associated with current FRA track safety standards. Based upon the results of the vehicle accident correlation studies described in Ref. 1, the Track Geometry Characterization Studies, Ref. 3, and discussions with Railroad Industry representatives, the derailment scenarios listed in Table 2.2-2 were identified. They include cars, track geometry, and operational conditions representative of a major portion of accidents in the categories of Table 2.2-1. Two scenarios appear to dominate the accident statistics. Both are associated with high-cg loaded hopper cars.

Inadequacies encountered in existing models, the necessity for model modification, and delays in the availability of model comparative results from track tests and track data, restricted the results reported here to Scenario 2. The freight car model was developed sufficiently to complete running in the 10-25 mph and to provide a satisfactory basis for investigation of higher speed freight car scenarios.

2.2.1 Scenario 1 - Cross-Level on High Center of Gravity (CG) Cars, 10-25 mph

The rock-and-roll scenario (cross-level response) involves operation of high-cg cars at above 10 but less than 25 mph. At these speeds, alternating low joints in staggered rails provided track cross-level input frequency coincident with the car's poorly-damped natural roll mode. This speed range is consistent with the existing FRA track classification No. 2. Although not apparent from Tables 2.2-1 and 2.2-2, variation in alignment, gauge, and curvature also affects the tendency to derail in this mode. This is seen more clearly in Table 2.2-3 for all vehicles. It has been possible, to investigate certain aspects of this response using models without wheelrail creep forces or any track degrees of freedom. Car yaw motion has also been neglected in these studies. Such a model (Ref. 7) was used by the Transportation Systems Center (Ref. 6) to determine the cross level amplitude boundaries between safe and dangerous operation. The results have been used to support investigation into track geometry requirements to reduce number of accidents resulting from this scenario.

In this study, safety-related dynamic performance was defined by maximum wheel lift and peak carbody roll angle. An example of the latter is given in Fig. 2.2-1, which also shows the comparative result from the SIMCAR program using the revised model, described in Chapter 3, designed for the combined study of varying alignment, gauge, and curvature. For comparison, the track was straight and gauge set tight in SIMCAR, the conditions prevailing in the MIT model study. Comparisons are given for cross-level variations of 1 in. and 5/8 in. One outcome of the TSC study was a proposed track figure-of-merit relating the cross level deviation permissible to a moving cross-level average.

TABLE 2.2-1

DERAILMENTS DUE TO TRACK GEOMETRY (Ref. 1)

GOVERNING SCENARIOS FOR TRACK STANDARDS PRELIMINARY LIST

SPEED	ALIGNMENT	GAUGE	SURFACE	CROSSLEVEL
10-25	Alignment induced roll High CG Loaded Hopper Curve BJR 3 + 59*	83	Pitch or Bounce Loaded Autorack Tangent BJR 8 8	Harmonic Roll High CG Loaded Hopper Tangent BJR 1 312
25-40	Alignment Induced Roll High CG Unloaded Hopper Curve BJR 4 37	9	Pitch or Bounce Loaded TOFC Tangent BJR 9 0	Harmonic Roll High CG Unloaded Hopper Tangent BJR 2 37
40-60	Discontinuity Resp. Light Car Discontinuity (Frog) 7 14	3	Pitch or Bounce TOFC Tangent BJR 10 0	Harmonic Roll High CG Loaded Box Tangent BJR 5 4
60-80	Discontinuity Resp. Locomotive Discontinuity (Frog) 13 0	Hunting Empty Flat Tangent CAR, Gauge Change 11 0	Pitch or Bounce Locomotive Tangent BJR 12 0	Lateral/Vertical Resp Locomotive Spiral Entry/Exit 6 6
80-110	Discontinuity Resp. Locomotive Discontinuity (Comp) 14 0	Hunting Passenger Gauge Change 16 0	0	Lateral/Vertical Resp Passenger Spiral Entry/Exit 15 0

+ Priority
* Total no. of accidents

TABLE 2.2-2

DERAILMENT SCENARIO PRIORITY BASED ON ACCIDENT STATISTICS

PRIORITY AND NO.	SCENARIO DESCRIPTION	NUMBER OF ACCIDENTS
1	Cross-level-induced response of high-cg loaded hopper on tangent bolted-joint rail: 10-25 mph	312
2	Alignment-gauge response of high-cg loaded hopper on curved bolted-joint rail: 10-25 mph	142
3	Alignment-gauge response of unloaded hopper car on curved track: 25-40 mph	46
4	Cross-level induced response of unloaded hopper car on tangent bolted-joint rail: 25-40 mph	37
5	Alignment-gauge response of light box car on tangent track: 40-60 mph	17
6	Lateral-yaw response of locomotive during spiral entry-exit 40-60 mph	6

2.2.2 Scenario 2 - Alignment-Gauge Response of High CG Cars, 10-25 mph

The number of accidents resulting from the second scenario in Table 2.2-2 is also large. The speed range of this scenario, derailments due to alignment and gauge, is again below 25 mph. Although derailments below 10 mph are apparent from Table 2.2-3, they are unlikely to be associated with mainline running, are relatively inexpensive, and there remains some doubt as to the interpretation of their cause. They are excluded from this scenario as they were from that of harmonic roll. The car is similar to that of Scenario 1, having a high center of gravity. The loaded 100 ton hopper, with truck centers close to rail length and old suspension elements, is known to be a bad actor when operating over staggered bolted rail joints. Alignment and gauge response are generally associated with lateral rail misalignment. In curves, this implies wide gauge and alignment variation due to rail spreading forces at joints particularly on the outer rail. Tangent track has been included in this scenario for completeness.

TABLE 2.2-3
DERAILMENTS VS SPEED AND TRACK GEOMETRY DEFECTS

(CAUSE CODES) MAINLINE TRACK, UM/RAIS '77 DATA

SPEED (MPH)	TOTAL DERAILMENTS	DERAILMENTS DUE TO EXCESSIVE TRACK GEOMETRY DEVIATION				
		CROSSLEVEL	WIDE GAUGE	ALIGNMENT	SUPERELEVATION	PROFILE
0 - 9.9	415	88	121	22	6	4
10 - 15	619	198	53	28	18	5
15.1 - 20	255	60	10	13	9	2
20.1 - 25	230	54	10	18	8	0
25.1 - 30	181	29	3	16	4	0
30.1 - 35	79	1	3	10	1	0
35.1 - 40	130	7	3	11	0	0
40.1 - 45	71	0	1	8	0	0
45.1 - 50	85	4	2	5	1	0
50.1 - 55	27	0	0	1	0	0
55.1 - 60	22	0	0	0	0	0
60.1 - 65	7	0	0	0	0	0
65.1 - 70	9	0	0	0	0	0
70.1 - 75	1	0	0	0	0	0
75.1 - 80	0	0	0	0	0	0
	2,131	441	206	132	47	11

At 10 mph and above, total derailments - 1,716.

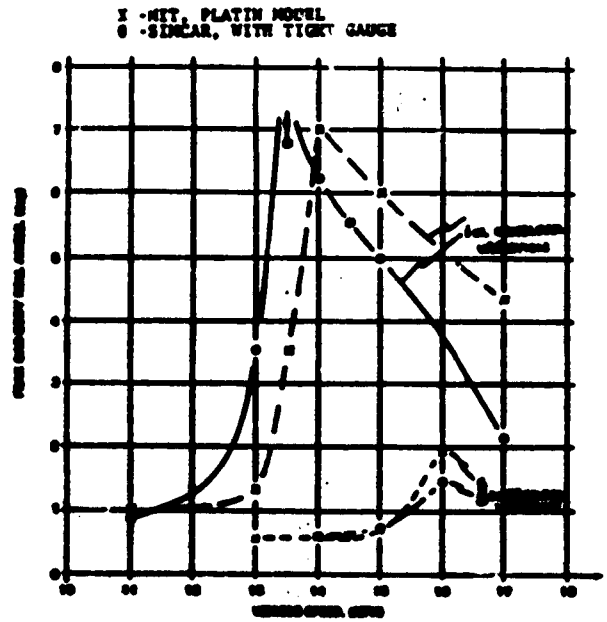

Figure 2.2-1 Comparison of Peak Car Body Roll Angle from MIT and SIMCAR Computer Programs

A particular feature of this scenario is that the lateral misalignment of each rail, particularly where the rails are staggered and jointed, renders their gauge an important variable. Although universally specified in track standards, none of the models collected and listed in Appendix A allowed for the study of gauge as an input variable, an essential feature for this study.

Roll angle is less likely to reach dangerous levels at low speed than in Scenario 1. However, wheel lift in the form of rail climbing is possible under extreme curving with large lateral forces, especially where the vertical force is reduced. Under extreme wide gauge, whether static or due to dynamic gauge spreading, the wheelset may "drop in" between the rails. Simulation requires a model capable of producing criteria to suit these forms of derailment. In the study described in Chapter 5, the modified model of Chapter 3 was used.

2.2.3 Scenario (Combined 1 and 2) - Cross-Level and Alignment, Gauge Response, 10-25 mph

As described under Scenario 1, the effect of combined alignment, gauge and cross level variation in curves (Scenarios 1 and 2) is believed by some railway personnel to be responsible for derailments of high cg cars which might not have occurred under either scenario separately. In particular, unloading of the flanging wheel while being driven laterally by the force on the heavily loaded non-flanging wheel is a potentially hazardous situation. If this occurs, relating track standards solely to results of separate studies under Scenarios 1 and 2 may lead to conditions in which the track crosslevel, alignment and gauge combine to give unforeseen derailment potential. TSC has already recognized this possibility and has carried out tests under combined conditions on the Chessie System. This issue is also addressed in the model improvements outlined in Chapter 3, and incorporated into the SUNCAR program. The modified model has both the roll characteristics necessary for Scenario 1, and truck and wheel/rail characteristics for dynamic curving including varying gauge. No other model was found suitable for this study as modeled.

The measures chosen for identifying safety related dynamic performance are compatible with the separate scenarios. Wheel lift may occur due to vertical motion of the wheel in Scenario 1 or, less likely, due to large lateral to vertical force ratio resulting in wheel climb, as in the second scenario. Body roll is affected in the combined scenario by coupling of the crosslevel and lateral excitation of the wheelsets and also to a lesser extent by track compliance. Wheel drop may occur where the instantaneous dynamic gauge exceeds the critical distance between wheel flange and opposite wheel outer tread and must be avoided.

2.2.4 Scenarios 3 and 4 - Cross-Level and Alignment, Gauge Response, 25-40 mph

These scenarios, listed in Table 2.2-2, are a continuation of Scenarios 1 and 2 at speeds of 25 to 40 mph, consistent with existing FRA track Class 3. A speed of 40 mph is just above the lowest speed at which hunting takes place, for light cars with badly worn wheels. At these low critical speeds, the kinematic wavelength is close to the length of a single jointed rail and may prove to be a problem. The reduction in effective lateral damping may give rise to large lateral oscillations when forced by track alignment. This oscillation is described more specifically under Scenario 5. The investigation of sinusoidally varying alignment, close to the kinematic wavelength, is reported in Chapter 5. In Scenarios 3 and 4, the light car natural frequencies are higher than those for a laden car by a factor approaching 2. Thus, roll excitation of the laden car at 18 mph, produces a similar resonance near 36 mph in the unladen car. Reduced vertical forces at higher speeds contribute to larger instantaneous lateral to vertical force ratios on the wheel.

The model requirements for simulating these conditions are similar to those for Scenarios 1 and 2 with some changes in emphasis where particular suspension frequencies influence the response. Gauge variations remain important. Measurement of wheel drop and lateral excursion beyond flange contact (rail climb) are again appropriate as measurements of derailment. Forces are used to compare the model and test results.

2.2.5 Scenario 5 - Alignment, Gauge Response and Hunting, 40-60 mph

Light cars with worn wheels on dry track will hunt. The speeds indicated in this scenario are consistent with existing FRA Class 4 Track. The condition variables for hunting to occur include rail and wheel profiles, variations in track alignment, gauge and curvature, track surface conditions, lightness of the car and truck geometry and stiffness as maintained. Tramming (dynamically induced out-of-squareness of the truck plan) is an important feature of hunting and leads to the wheel attacking the rail in a potential climbing situation. Heavy cars are less susceptible

to this problem. The hunting oscillation is frequently associated with car body yaw. As mentioned in previous scenarios, the damping may be low enough at sub-critical speeds to cause large amplitude responses to sinusoidal track inputs. Lateral rail alignment variations can excite the oscillation into becoming self-sustaining. This is typical of suspensions with nonlinear characteristics such as those found in freight cars. Body yaw response is large when the car truck center distance is nearly equal to 1 1/2 rail lengths on staggered jointed track. Although there is a potential for climbing derailment, hunting is also of a concern as a cuase of subsequent track, vehicle and lading failure. Simulation models of hunting require an accurate representation of wheel rail conditions. For this reason and because of the potential for component failure and wear, forces are important. Many models exist for the study of hunting in freight cars (Ref. 8). They include random excitation of the vehicle with nonlinear characteristics using describing functions to "linearize" the model. Present model results show some divergence from known behavior when friction coefficients change. The derailment record supports a requirement of hunting study to improve the understanding of the effect of rail dynamic inputs during hunting.

2.2.6 Scenario 6 - Lateral, Yaw Response in Spirals, 40-60 mph

Derailments descriptive of this scenario have occurred on particular 3-axled locomotives. Extensive tests have been carried out on these and other vehicles in attempts to identify the cause of these derailments. The computer program CURVELOCO (No. 038 Appendix A) was a particular attempt to simulate this scenario. The lateral-yaw frequency is excited by track geometry within this speed range, permissible under FRA classification No. 4, particularly in curve entry and exit spirals. Dynamic unloading of the wheels has also been observed. Importance is therefore attached to the transient forced response of the vehicle and the effective damping in each mode. Although the geometric relationship of wheel to rail adequately defines the derailment condition in simulations, tests to derailment are not generally carried out. Total lateral force was monitored in tests at TTC to indicate the proximity to track panel shift and lateral and vertical forces and their ratio were used to indicate derailment potential. Forces are therefore a necessary part of model comparison with test results.

2.3 ANALYSIS TOOLS

The rail vehicle dynamics library (RVDL), described in Appendix A, was collected to select programs for use in the parametric studies of rail vehicle response to track input, identified in the scenario of the preceding sections. Figure 2.3-1 relates known vehicle modes and natural frequencies to known vibration source wavelengths over the speed range for each scenario. The scenarios discussed are related to wavelengths due to rail discontinuities and rail alignment errors and include response due to truck kinematic activity during hunting.

Caution is necessary in interpretation of Figure 2.3-1 into modeling requirements. The nonlinear characteristics of rail vehicles, particularly freight vehicles, give rise to transient response and harmonic phenomena having higher frequency components than those indicated. In addition, the truck modes described assume a primary suspension not used in the freight vehicle but universal in the design of locomotives. Table 2.3-1 summarizes the extended frequency range of interest in each scenario together with the modes of oscillation needed in the model for accurate assessment of frequency response. Due to the complex nature of the wheel/rail interaction forces and uncertainties in wheel and rail profiles and friction behavior, many of the models collected in Appendix A have included highly simplified representations of the lateral wheel/rail force characteristics. In models for predicting hunting behavior, the wheel/rail force characterization has been limited to use of linear creep characteristics with a quasi-linearization of the "gravitational stiffnesses" and "effective conicities" resulting from wheel/rail geometry contact forces and moments. These models have generally neglected friction saturation effects and the large spin creep lateral forces in flange contact and have assumed constant track gauge.

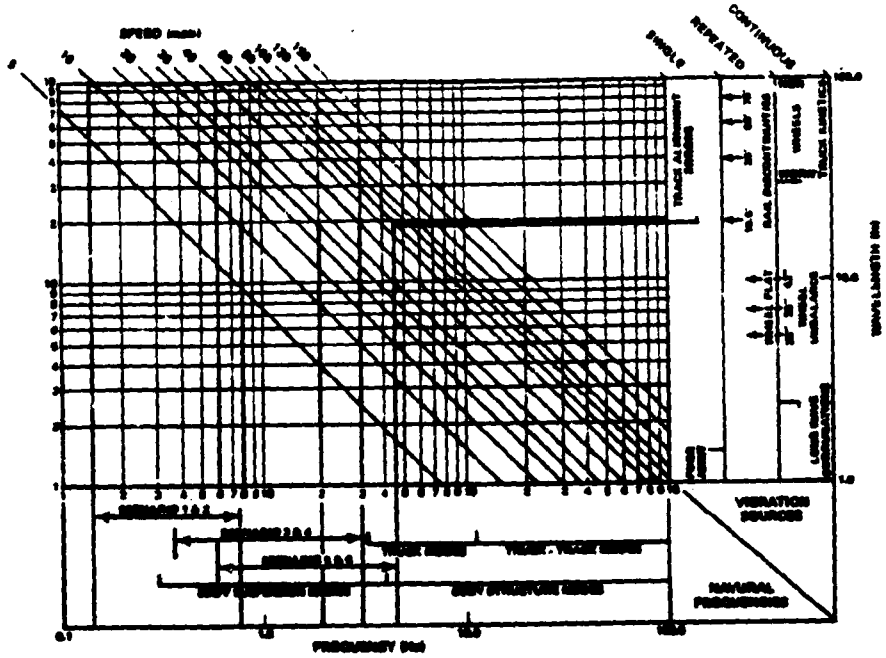

Figure 2.3-1 Coupled Rail Vehicle Dynamics

TABLE 2.3-1

MODAL REQUIREMENTS FOR VEHICLE MODELS

SCENARIO	FREQUENCY RANGE	MODE
1,2	0.1-4.0 Hz	Rigid Body Suspension
3,4	0.3-12.0 Hz	Rigid Body Suspension, Body Structural
5,6	0.6-22 Hz	Rigid Body Suspension, Body Structural, Truck Suspension

The models for lateral response to track irregularities have in some cases assumed that the alignment variations are much larger than the flange clearance and that the wheels follow the lateral track geometry perfectly. This is satisfactory for computing the net forces on the car and truck, but can be expected to provide errors in the individual wheel forces, and is unsuitable for studies of proximity to derailment. In other cases, the models assume the linear creep relationships and effectively assume an infinite flange clearance.

Other models divided the wheel/rail forces into a tread region governed by linear creep forces and a vertical flange where forces are governed by an effective rail stiffness. None of these models provide the potential for wheel climb to occur. For alignment variations typical of lower classes of track, as discussed earlier in this chapter, the gauge variations are significant compared to the alignment variations and have a significant effect on the rail car response and wheel/rail forces. Chapter 3 compares the wheelset displacements and wheel/rail forces of the model developed under this effort with other published material.

It was found necessary to develop an improved representation of the wheel/rail force relationships which included gauge variation and wheel climb capabilities. In order to permit generation of results in a short time frame, a modification of the wheel/rail force models using linear creep forces in the tread range and a nonlinear force representation on the flange was made to permit wheel climb to be studied. As shown in Chapter 3, this representation is a good approximation for new standard AAR profiles on new rail.

Numerical integration programs which model the wheel/rail creep forces were

found to be computationally inefficient at low speeds because of large eigenvalues, which do not influence the solution. The program SIMCAR used in the study here employs state reduction to remove the effect of these from the dynamic calculation.

Freight vehicle response programs developed previously treated large amplitude roll using models with zero flange clearance, while the models that treated lateral response did not account for large amplitude roll. Since the combined effect may be important, the model described in Chapter 3 contains both.

2.4 DERAILMENT PROCESSES AND MEASURES

Section 2.2 set out the nature of the derailment process for the particular scenarios identified from the derailment statistics. In this section the derailment processes, which are not the result of track failure, are identified in more detail and related to the measures used in the revised model and simulation study reported in Chapters 3 and 5. Derailment, as discussed here, represents the cessation of guidance provided by the rails to the wheelsets and is characterized by movement perpendicular to the direction of travel. In particular, the wheel may lift from the rail surface, and/or may move laterally as when the flange climbs over the rail, or when the outside of the non-flanging wheel moves inside the gauge face of the rail. These three derailment conditions are referred to as wheel lift, wheel climb and wheel drop.

Wheel lift is principally associated with the static and dynamic effects of variation in crosslevel. Statically, a torsionally stiff freight car can exhibit wheel unloading and wheel lift if the rate of crosslevel variation along its length exceeds the capability of the suspension and body to twist. This condition is more prevalent with lightly loaded cars having constant contact sidebearers. In this static situation, derailment generally follows unloading of the flanging wheel in curves where a lateral force is sustained. Dynamic wheel lift occurs when the vehicle suspension rolls about a low center excited by crosslevel variation at low joints on staggered jointed track or at high overbalance speed in curves. Wheel lift is therefore descriptive of an impending carbody rollover or of a potential unrestrained lateral movement. Wheel climb is frequently associated with partial wheel unloading. With the wheelset attacking the rail, and the flanging wheel lightly loaded vertically, the non-flanging wheel carries an increase over static load and the lateral force developed by the non-flanging wheel may drive the flanging wheel on to and over the rail. The wheel lateral to vertical force ratio, L/V, has been used (Ref. 16) to indicate proximity to derailment conditions in this mode and is especially important for monitoring test measurements. Derailment indices pertinent to the study reported in Chapter 5 are discussed in the following sections.

2.4.1 Body Roll Angle

A threshold was chosen from the experience gained from other studies of the rock and roll phenomenon (Ref. 7). A value of ±5.0 degrees is considered excessive. For the loaded hopper car investigated, this angle occurs well after rotation over the sidebearer and centerplate separation commences as discussed in Appendix B. A sample plot of roll angle against time, from the SIMCAR model described in Appendix B, is given in Fig. 2.4-1, for severe roll in a 10 degree curve with gauge and alignment variation. Although roll derailment is predicted, i.e., the angle exceeds ±5.0 degrees, it is accompanied by wheel climb as seen in Fig. 2.4-1.

2.4.2 Wheel Lift and Rail Climb

In earlier studies, a value of 0.5 inch was used to signify an excessive height of the wheel tread above the rail in cross level response. The model of Platin (Ref. 7) has been used by TSC in this regime with wheel lift as a primary index of derailment. For the Association of American Railroads (AAR) 1/20 profile, 0.5 inch approximates the height beyond which the flange angle decreases. The value of wheel lift at the tape-line during rail climb may be calculated from the lateral wheel rail movement and knowledge of the profiles as given in Fig. 2.4-2. It suggests derailment if the wheel moves more than 0.1 inch beyond initial flange contact. Distance beyond flange contact is a monitored output from SIMCAR. Figure 2.4-3 illustrates the results for the case previously illustrated in roll. The graph indicates the time history of the position of the flange beyond initial contact with the rail. Rail climb derailment is shown to occur simultaneously with the exceedance of 5° roll angle shown in Fig. 2.4-1 for the same case.

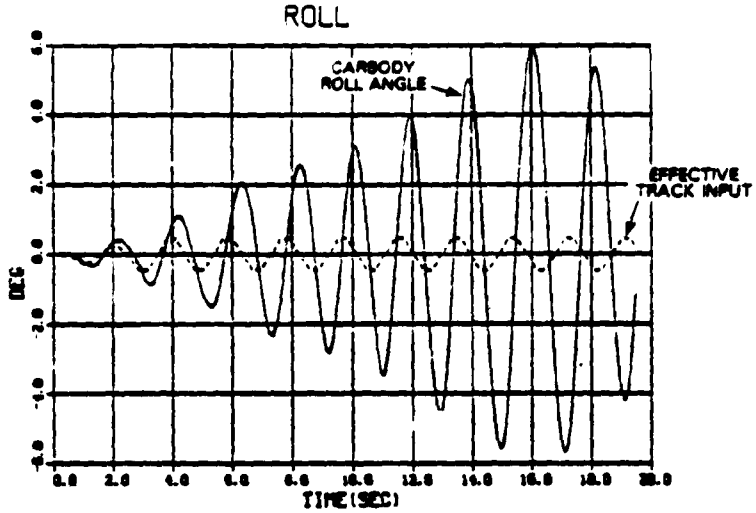

Figure 2.4-1 Severe Roll in a 10 Degree Curve 14 mph

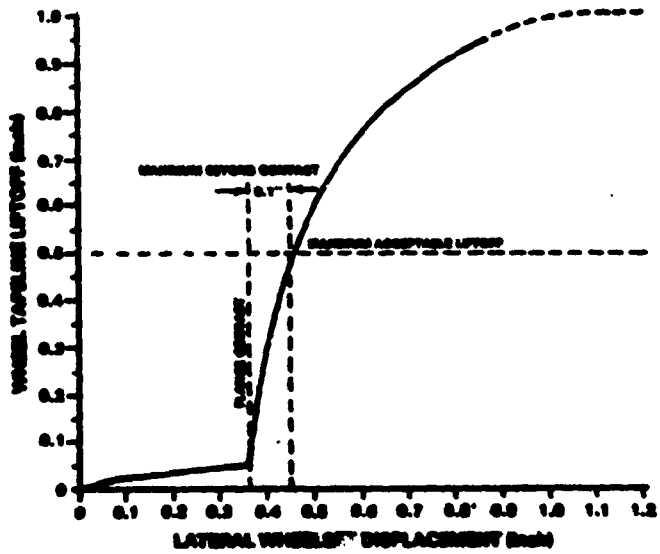

Figure 2.4-2 Wheel Lift vs Lateral Displacement New AAR Wide Flange Wheel Profile

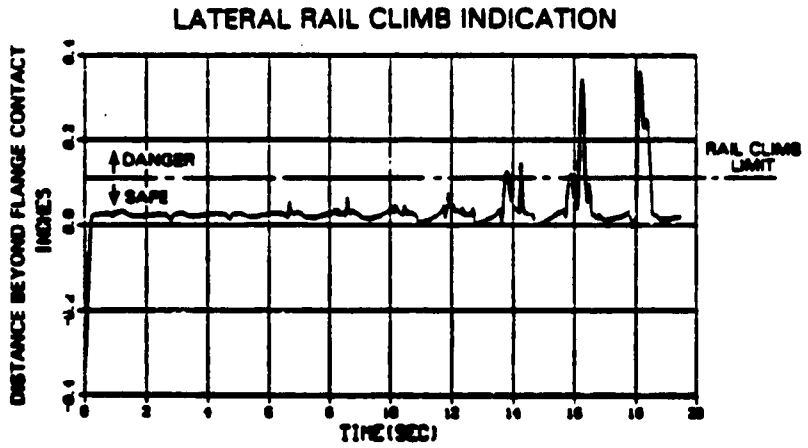

Figure 2.4-3 Severe Rail Climb Under Severe X-Level and Alignment Perturbations in a 10 Degree Curve -

2.4.3 Wheel Drop

The "distance to wheel drop" for new wide flange wheels is defined by the equation,

$$\text{distance} = 0.5\,(64.5 \pm 0.3 - \text{instantaneous track gauge}) - y_{wheel}\ ,\ \text{inches}$$

where, y_{wheel} is the wheelset lateral position relative to the track center line. The wheelset must also avoid approaching wheel drop by a significant safety margin. A value of zero represents a derailment and is a primary index. A safety margin of 1.25 in. shown in Fig. 2.4-4, representing a maximum gauge of 59 in., has been used for the cases studied in this report. This gives the distance to the wheel drop limit as,

$$\text{distance} = 3.07'' - \text{instantaneous flangeway clearance}$$

The instantaneous flangeway clearance for rigid track is available as an output from the computer program SIMCAR, and is illustrated in Fig. 2.4-5. The true clearance will have additional gauge increases due to rail deflection. A representation of this effect, used in Chapter 5, is illustrated in Fig. 2.4-6, which plots lateral force against distance to wheel drop directly. The limiting lateral rail deflection for the softest rail flexibility thought acceptable for track restraint specification is plotted and the value of the deflection for the low rail established. The rail deflection curve for the high rail, plotted from the low rail deflection point, gives a limit above which the computed points would indicate a derailment. This does not happen in the illustration used. This form of derailment will be seen to be important in the results given in Chapter 5.

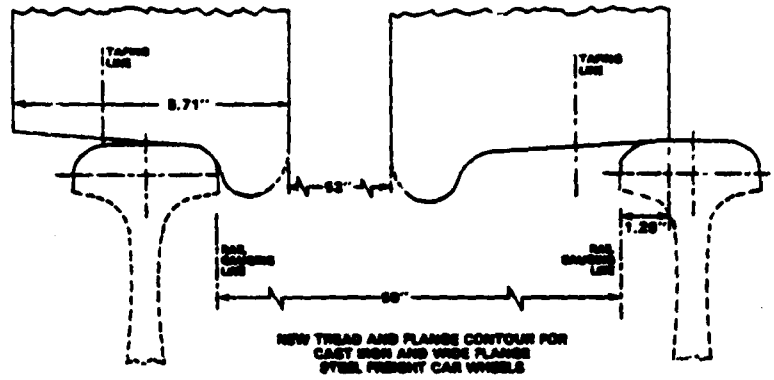

Figure 2.4-4 Wheel/Rail Contact Geometry for AAR Standard Freight Car Wheel on AREA Standard Rail at 59 in. Rail Gauge with Wheelset Displaced at Laterally 1.5 in.

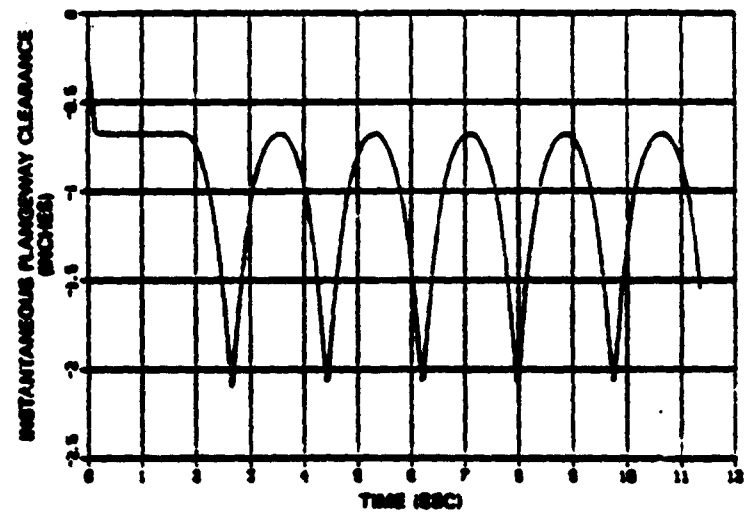

Figure 2.4-5 Instantaneous Clearance with Severe Lateral Rail Cusps on a 15 Degree Curve

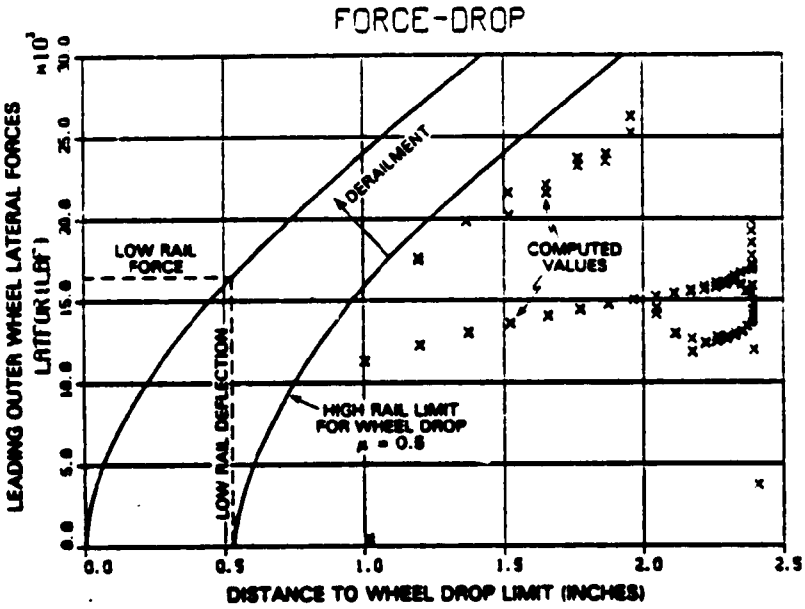

Figure 2.4-6 Leading Outer Wheel Lateral Force Against Distance to Wheel Drop - 15 Degree Curve with Outer Rail Cusps (See Also Fig. 2.3-4)

3. FREIGHT VEHICLE MODEL

3.1 INTRODUCTION

The model used to study the effect of track irregularities on freight vehicles represents a typical freight vehicle having two 3-piece trucks. The general arrangement is shown in Fig. 3.1-1. Values of the parameters for a loaded 100 ton Hopper Car are given in Appendix C.

The body of the vehicle rests on the centerplate of the bolster which in turn rests on the spring groups at the center of each sideframe. Each spring group contains two spring loaded friction snubbers giving damping in the vertical and lateral directions. Each sideframe rests on two bearings, one on each axle, through bearing adaptors which slot into the sideframe above the bearings. The body contains body bolsters over each truck. Sidebearers are located between the body and truck bolsters. A general view of a freight vehicle is given in Fig. 3.1-2. The truck bolster moves laterally with the body, yaws with the wheelsets, and rolls relative to both.

3.2 MODEL SUMMARY

3.2.1 Degrees of Freedom

The freight car model is described in terms of the following sixteen degrees of freedom:

- Rigid Body
  1. Lateral displacement (y_c)
  2. Vertical displacement (z_c)
  3. Roll angle (ϕ_c)
  4. Pitch angle (θ_c)
  5. Yaw angle (ψ_c)
- Flexible Body
  6. Twist (ξ_x)
  7. Vertical bending (ξ_y)
  8. Lateral bending (ξ_z)
- Truck A
  9. Lateral displacement (y_A)
  10. Wheelset (bolster) yaw angle (ψ_A)
  11. Sideframe yaw angle (δ_A)

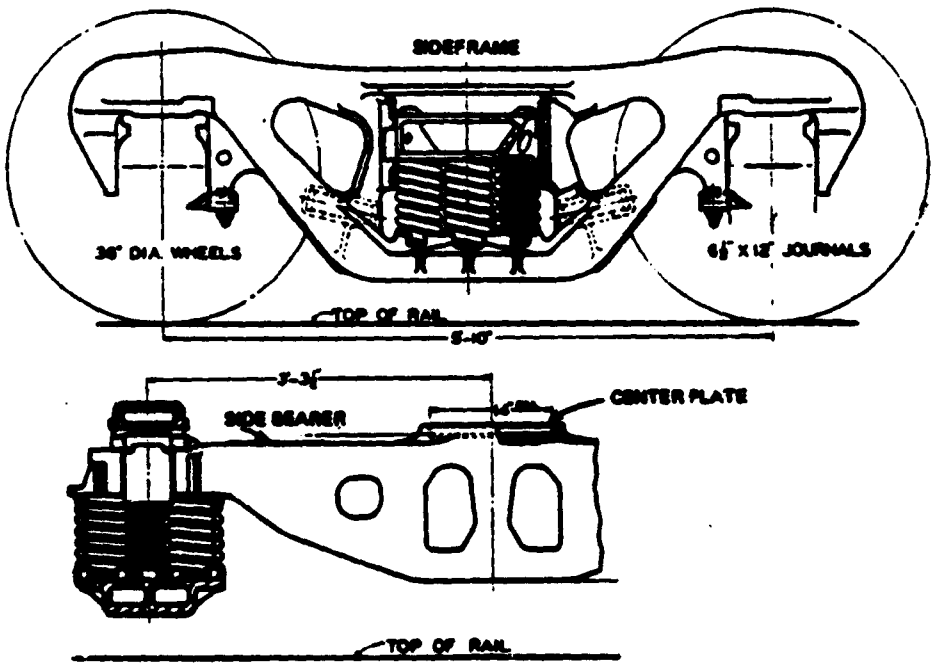

Figure 3.1-1 3-Piece Truck

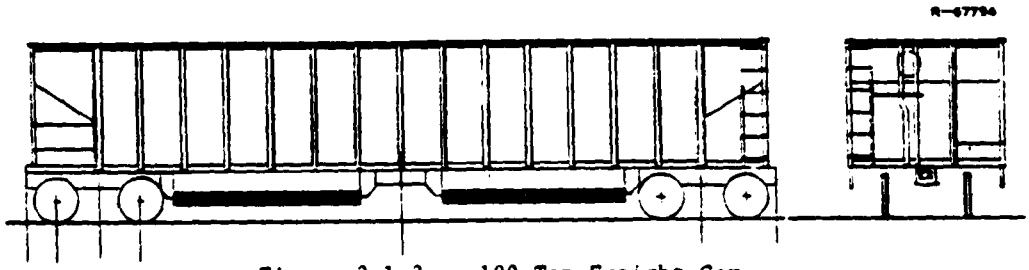

Figure 3.1-2 100-Ton Freight Car

- Truck B

  12. Lateral displacement (y_B)
  13. Wheelset (bolster) yaw angle (ψ_B)
  14. Sideframe yaw angle (δ_B)

- Bolsters A and B

  15. Roll angle on A (ϕ_{BA})
  16. Roll angle on B (ϕ_{BB})

A full description of the equations governing the model behavior i given in Appendix B.

3.2.2 Nonlinearities

The most complex system characteristics are associated with the wheel/rail interaction which are discussed fully in Section 3.3. The remaining suspension nonlinearities are constructed in piecewise linear form, and are discussed in Appendix B. They comprise,

- Roll moment - to allow for sidebearing clearance and rotation about the edge of the centerplate
- Snubbing forces - friction in the suspension between bolster and sideframe in vertical movement
- Centerplate friction - yaw friction between the centerplate and body
- Tram (truck out of square) stiffness - sudden increase in stiffness with increasing angle between the wheelsets and sideframes as the clearances are taken up
- Lateral suspension stiffness - sudden increase in lateral stiffness as the clearance between the sideframe and bolster is taken up
- Vertical suspension stiffness - to permit bottoming of the springs and movement about free length of the springs.

3.2.3 Track Inputs

Provision is made in the models for sinusoidal and jointed rail shapes, the latter being constructed from an exponential form. The rail joints may be staggered or symmetric. Provision is also made for varying the perturbation amplitudes in segments of track length, so that test tracks of known shape may be represented in constant curvature with alignment, gauge, and cross-level variations. The 19 inputs calculated in the model from the chosen rail shapes, described more completely in Appendix B, are

- Lateral unbalance in curve
- Apparent along track difference in wheel velocity over rails due to different rail lengths in the curve
- Track yaw angle in curve at each truck relative to body
- Track lateral alignment at each axle
- Mean track vertical position at each truck
- Mean track vertical rate of position change at each truck
- Mean cross-level angle at each truck
- Mean rate of cross-level angle change at each truck
- Rail/wheel flange semi-clearance at each axle.

3.3 RAIL/WHEEL MODEL

The rail/wheel model used in the work reported is an approximate one based initially on the work of Sweet, L.M., Sivak, J.A., and Putman, W.F. carried out for TSC at Princeton University (Ref. 18). In this investigation, theoretical and experimental results were obtained for a wheelset, constrained laterally and in yaw for particular rail and wheel profiles and coefficients of friction between 0.45 and 0.52. The experimental work used a one-fifth scale model and LEXAN was used for wheels and rails to provide a proper scale for the rail/wheel forces.

The results suggested that it might be possible to use a linear model on the tread with terms added to the wheelset yaw moment and lateral force upon flange contact. These additional values were initially presumed to be a function solely of lateral position beyond flange contact. However subsequent modification has made the approximations more complex and more accurate relative to other models and published data.

In the following description of the approximate model developed for the computer program SIMCAR, each wheel/rail force or moment is given in terms of the local wheelset coordinates, y or ψ, and their derivatives. These are linearly related to the motion variables chosen for equations of motion in Appendix B.

3.3.1 Lateral Wheel Force

Forces on the tread due to spin-creep and the lateral component of the normal at contact are assumed to be small and are neglected. Choosing y to represent local wheelset lateral movement and ψ the local yaw angle relative to the track, the wheel tread creepages are

$$\text{longitudinal, } v_x = \pm\left(\frac{\alpha}{r_o} y + \frac{\beta}{V}\dot{\psi}\right)$$

right wheel + ve

$$\text{lateral, } v_y = \left(\frac{\dot{y}}{V} - \psi\right), \text{ both wheels}$$

where

- $(\dot{})$ - derivative with respect to time
- α - tread cone semiangle, assumed constant and small
- r_o - mean rolling radius
- β - lateral half distance between rail/wheel contact points
- v - velocity along track.

The linear lateral force characteristic for each wheel, for small creepages and contact angles, is,

$$F_y = F_{22}\left(\frac{\dot{y}}{V} - \psi\right)$$

where

- F_{22} - linearized lateral creep coefficient.

It is known from Carter's work that these creep coefficients are a function of vertical load. Thus,

$$F_{22} = F_{22static}\, R^{2/3}$$

where

- R - ratio of actual to nominal static vertical load for the wheel under consideration ($= \frac{V}{V_{static}}$)

The linearized relationship for lateral force by any wheel becomes,

$$F_y = F_{22static}\, R^{2/3}\left(\frac{\dot{y}}{V} - \psi\right)$$

Under large creepages, the tangential force in the contact area will saturate, becoming equal to the limiting friction force in the direction of slipping for the conditions chosen. The direction of slipping is given by the creepages. Hence, the lateral direction cosine, is given by,

$$C_y = \frac{\left(\frac{\dot{y}}{V} - \psi\right)}{\sqrt{\left(\frac{\alpha}{r_o} y + \frac{\beta}{V}\dot{\psi}\right)^2 + \left(\frac{\dot{y}}{V} - \psi\right)^2}}$$

Thus, the limiting lateral force on any wheel is $(C_y \mu V)$ where,

- μ = coefficient of friction on the tread

The lateral force on any wheel increases rapidly when the flange is contacted, due to the rapid increase in contact angle. In full slip, with no longitudinal component, the value of lateral to vertical force ratio on a flanging wheel, at large angle-of-attack to the rails, may reach that suggested by Nadal (Ref. 9),

$$\frac{L}{V} = \frac{\tan\delta - \mu}{1 + \mu \tan\delta}$$

where

δ = flange angle.

Under conditions of full lateral slippage, a non-flanging wheel has a value of $\frac{L}{V} \approx \mu$. Upon flanging, the approximation used here assumes an additional lateral force which is solely the function of distance beyond flange contact shown in Fig. 3.3-1. The increase in value is introduced progressively for analytic purposes by the leading slope K_{LEAD}. The maximum value is chosen to provide, for large slippage in the lateral direction, a value for the sum of tread and flange forces on the flanging wheel equal to that due to Nadal. The resulting maximum value due to the additional flange contact force is,

$$\frac{L}{V} = \mu + \frac{\tan\delta - \mu}{1 + \mu \tan\delta} = \frac{(1+\mu^2)\tan\delta}{1 + \mu \tan\delta}$$

The lateral force, L, is assumed proportional to the instantaneous vertical force, V.

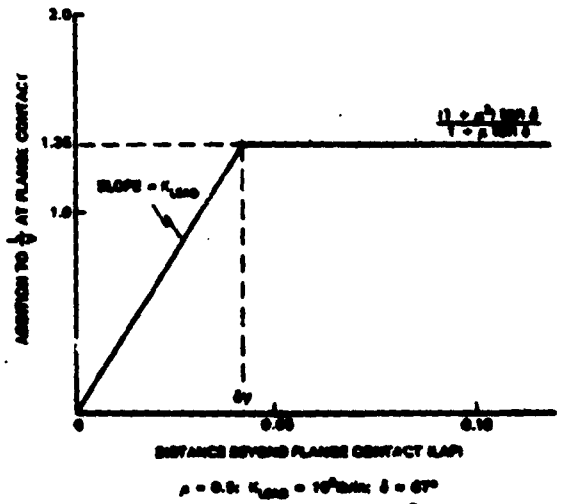

Figure 3.3-1 Increase in $\frac{L}{V}$ at Flange Contact

3.3.2 Wheelset Moments

The yaw moment on a non-flanging wheelset for small creepages and angles is approximately,

$$T_z = 2B\, F_{11} \left(\frac{a}{r_o} y + \frac{B}{V} \dot{\psi}\right)$$

where

F_{11} = longitudinal linear creep coefficient.

In the approximate model, no adjustment is made to the longitudinal creep coefficient in tread contact to account for variations in the vertical wheel loads below saturation. However, the moment is saturated in a manner similar to that for the lateral force. The longitudinal direction cosine for tread contact is,

$$C_x = \frac{\left(\frac{a}{r_o} y + \frac{B}{V} \dot{\psi}\right)}{\sqrt{\left(\frac{a}{r_o} y + \frac{B}{V} \dot{\psi}\right)^2 + \left(\frac{\dot{y}}{V} - \psi\right)^2}}$$

Hence, the limiting longitudinal force on any wheel is $C_x \mu V$. The maximum possible moment on the wheelset if no flanging occurs is,

$$T_{max} = 2BC_x \mu V_{static}.$$

V_{static} occurs under equal wheel loads, R=1. An adjustment is made for other values. If R=0 then no moment is possible since no longitudinal force can exist on one or other of the wheels. A factor F_M between 0 and 1, linear in R, is used to account for this. The total saturated moment becomes,

$$T_z = F_M \cdot 2B\, C_x\, \mu\, V_{static}$$

Flange contact with one rail has the effect of a sudden increase in rolling radius and a resulting yaw moment which steers the wheelset around towards the track centerline. In addition, there is generally a change in the rotational velocity of the wheelset necessitated by torque equilibrium requirements about its axis. Flange contact generally produces saturation at the non-flanging wheel contact with the rail and provides a limiting friction

condition. The longitudinal component of this friction force has therefore been used to approximate the total yaw moment.

In order to establish the longitudinal component of the friction force, a value of longitudinal creep on the non-flanging wheel was initially derived assuming single point contact on the flanging wheel for the new AAR 1/20 wheel on new 132 lb/yd AREA rail. However it was found necessary to modify this expression to reflect the two point contact for these profiles when flanging and to allow for change in the wheelset rotational speed. Thus,

longitudinal creep, v_x

$$= \left(\frac{LAP}{\delta_y}\right)^{0.3} \left(0.0042 + 1.636 \frac{LAP}{R_o}\right)$$

where

LAP - distance beyond initial flange contact

δ_y - see Fig. 3.3-5 - lead distance

R_o - mean rolling radius.

The expression was obtained as a heuristic fit to published data. The expression for the longitudinal direction cosine on the non-flanging wheel is,

$$C_{flx} = v_x \Big/ \sqrt{\left[v_x^2 + v_y^2\right]}$$

where

v_x = longitudinal creep, given above

v_y = linear lateral creep $(\psi - \frac{\dot{y}}{V})$

This resulting maximum yaw moment on an equally loaded wheelset (R=1) is,

$$T_{flx} = C_{flx} \cdot 2B \cdot \mu V_{static}$$

or in dimensionless terms,

$$\frac{T_{flx}}{2BV_{static}} = \mu C_{flx}$$

As with the non-flanging wheelset the yaw moment can only exist in the presence of non-zero wheel loads and is assumed to be a maximum when the wheels are equally laden at the static value. Thus, for any vertical force ratio on the flanging wheel,

$$R = \frac{V}{V_{static}},$$

$$\frac{T_{flx}}{2BV_{static}} = \mu F_M C_{flx}$$

where F_M has the value given in Fig. 3.3-2.

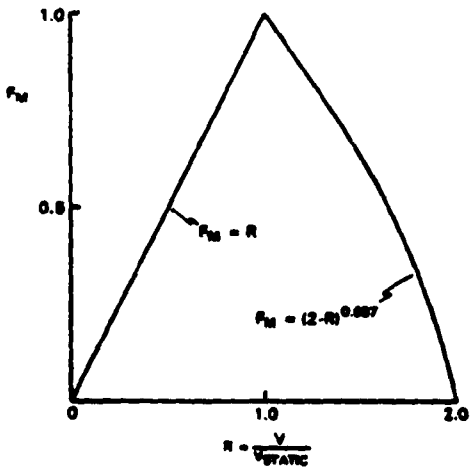

Figure 3.3-2 Yaw Moment Factor for Flanging Wheel R

3.3.3 Total Wheelset Characteristics for SUCAR

The dynamic response of the vehicle as modeled to rail/wheel forces and moments is a consequence of the total effect on both wheels. These are presented here in terms of the net lateral force, P, and the yaw moment, M. They are made non-dimensional by division by the axle load, W, and the maximum friction moment, μBW, respectively. The values chosen for illustration, and later for comparison to the Kalker look-up model are for the new AAR 1/20 wheel on new AREA 132 lb/yd rail with $\mu = 0.375$. The maximum flange angle is $\delta = 67°$ and the tread cone angle, $\alpha = 0.05$ radians.

The total axle lateral to vertical force ratio, P/W, is shown in Fig. 3.3-3 against ψ, the yaw angle of attach. This may be interpreted as the negative lateral creepage, $(\psi - \dot{y}/V)$, in a dynamic circumstance. Thus, the curve for $|y| < 0.325$ in., is the

approximation for the lateral tread creepage characteristic, including saturation but shown in a negative sense. As previously discussed in Section 3.3.1, the value of lateral force on the flanging wheel decreases with yaw angle to the Nadal limit. In practice negative angles of attack during flanging are limited to the trailing axle under dynamic conditions and to hunting. Consequently, the characteristic in this regime does not impact the study reported here. However, it is apparent from Fig. 3.3-3 that the present characteristic is inaccurat in this region. A more correct model such as that discussed in Refs. 16, 17, 18 does not have symmetry suggested by the simplified form used here. This is due to the change in the direction of the flange force. In the limit this gives an expression for the Nadal value on the flanging wheel,

$$\frac{L}{V} = \frac{\tan \delta + \mu}{1 - \mu \tan \delta}$$

and for the total force on the axle,

$$\frac{P}{V} = \frac{2\mu + (1-\mu^2) \tan \delta}{1 - \mu \tan \delta}$$

using values $\mu = 0.375$ and $\delta = 67°$,

$$\frac{P}{V} = 23.8 \text{ (Nadal, } \psi << 0)$$

Although very much larger than the apparent asymptote in Fig. 3.3-3, this Nadal value will only be approached well outside the range of angles shown and no negative value of angle of attack has been observed in the results produced for a flanging wheel.

Variation of the lateral force, P/W beyond flange contact is apparent from Fig. 3.3-3 and more easily seen in the cross plot of P/W against y shown in Fig. 3.3-4. These values occur during saturation on the non-flanging wheel and are affected by the increase in longitudinal creepage and the resulting rotation of the slip vector towards the direction of travel. The result is a further increase in P/W for positive angle ψ and a decrease for negative ψ. The values for negative ψ in Fig. 3.3-4 further illustrate the inaccuracy discussed for this regime. The total lateral force characteristic remains unaffected by curvature of the track.

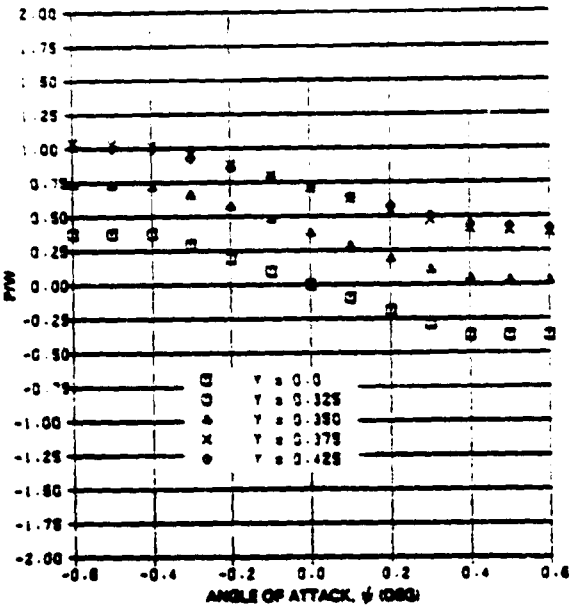

Figure 3.3-3 Approximate Wheel/ Rail Interaction: P/W vs ψ

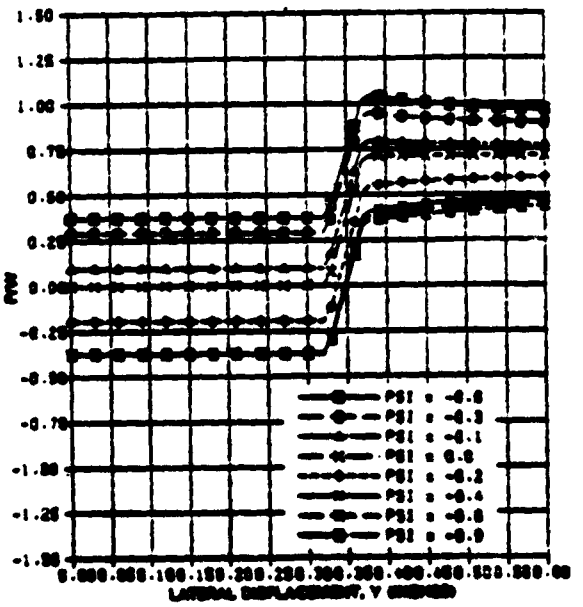

Figure 3.3-4 Approximate Wheel/ Rail Interaction: P/W vs y

The non-dimensional moment M/μBW is shown in Figs. 3.3-5, 3.3-6, 3.3-7, 3.3-8, for curves of 0, 5, 10, 15 degrees, respectively. The principal difference between these curves is in the region of tread contact where the lateral offset of the wheelset for equilibrium in the curve is apparent.

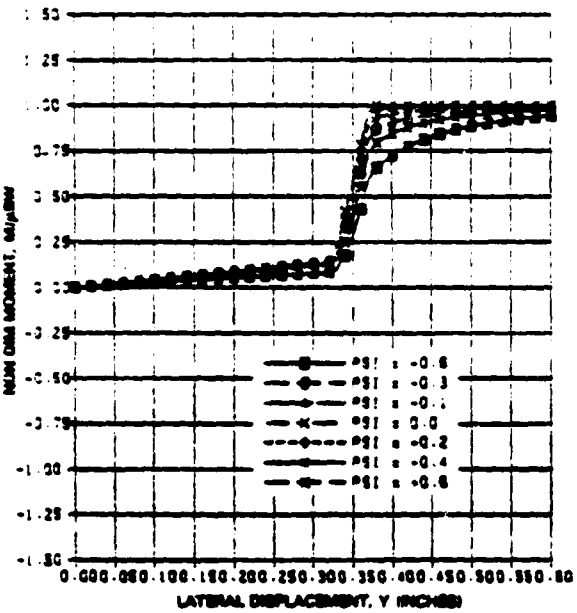

Figure 3.3-5 Approximate Wheel/ Rail Interaction: M/μBW vs y Tangent Track

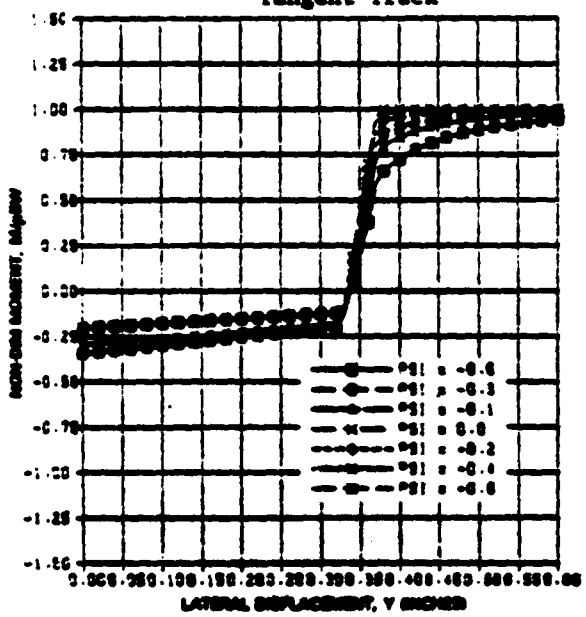

Figure 3.3-6 Approximate Wheel/ Rail Interaction: M/μBW vs y 5° Curve

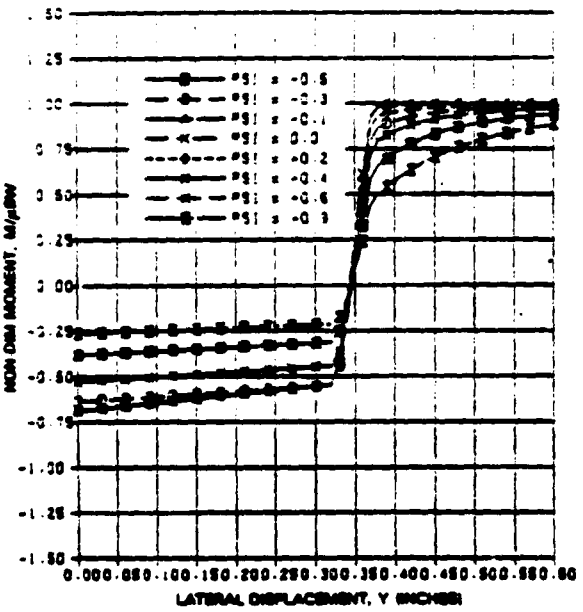

Figure 3.3-7 Approximate Wheel/ Rail Interaction: M/μBW vs y 10° Curve

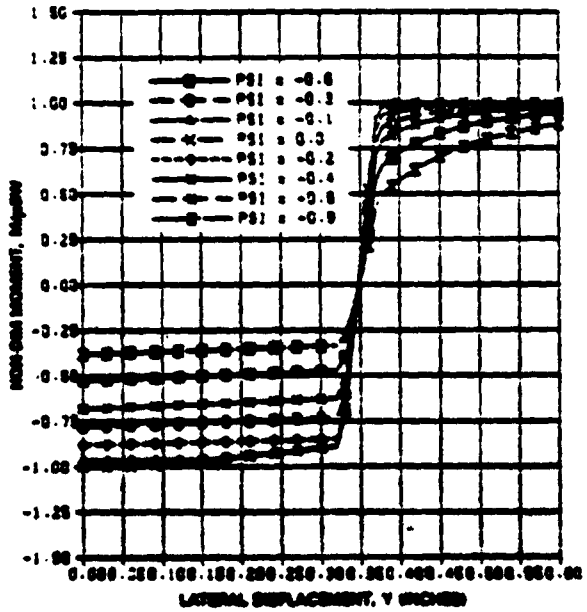

Figure 3.3-8 Approximate Wheel/ Rail Interaction: M/μBW vs y 15° Curve

Beyond flange contact the moment which comes from the saturated longitudinal component of the tangential friction force, depends solely on the direction of slippage. In the approximation used here this is independent of curvature and approaches full longitudinal slippage with increasing y.

3.4 COMPARISON OF APPROXIMATE RAIL/WHEEL CHARACTERISTICS WITH THE ELKINS MODEL

3.4.1 Historical Background

Prior to the 1960's steady-state curving predictions were performed using a method, (Refs. 10 and 11), in which the treads of each wheel were considered to be cylindrical and forces were developed by sliding friction. The direction of the force was aligned with the direction of the slippage vector. Additional lateral forces were developed by the flange when it came into contact with the gauge face of the rail.

The linear relationships between creep force and creepage first formulated by Carter (Ref. 12), were applied to the problem of predicting the curving behavior of railroad vehicles by Boocock (Ref. 13) and Newland (Ref. 14).

The curving models were then refined to include the effects of gravitational stiffness and spin creep, which were significant with worn or profiled wheels, particularly when contact occurred near the flange root. The analyses conducted using the linear creep theory, considered flange contact as a condition to be avoided and, therefore, at the limit of the analysis. However, the limitation occurred for almost all vehicles on curves having a radius of greater than 2,000 ft (3°), and for most vehicles on much larger radius curves, whereas the major problems of rail wear and track damage were occurring on smaller radius curves.

At this point, two different approaches were pursued. The desire to have wheel profiles which would remain approximately the same shape throughout their life, led to the development of profiled wheels. These profiles were found to give only a single point of contact with the rail for most of the rail profiles, new or worn, found in practice. In order to evaluate the performance of these profiled wheels, detailed analytical models of the wheel/rail interaction were developed. These models made use of Kalker's nonlinear creep theory (Ref. 15), which had become available at about this time. As a result, models were created including the nonlinearities arising from both the single point contact wheel/rail geometry and the creep force creepage relationships, inherent in Kalker's nonlinear theory. This approach is described in the work at British Rail of Gilchrist and Brickle (Ref. 16), Elkins and Gostling (Ref. 17), and in the United States by Sweet and Sivak (Ref. 18). Experimental results for lateral force and yaw moment were obtained from both full scale experiments and model tests, which gave good agreement with the predicted wheel/rail forces.

Models at AAR (Ref. 19) and Battelle (Ref. 20) in the United States, used a completely different approach. The concepts of Porter and Boocock-Newland were combined, to produce a model which calculated tread forces from the linear creep force relationships for a straight tapered wheel, and introduced a lateral force on an implicitly vertical flange.

A recent advance by Elkins at TASC, using the theory of Elkins and Gostling (Ref. 16), but allowing two points of contact on the flanging wheel, has given extremely accurate force and moment predictions on the flanging wheel when compared to test results carried out for the Urban Mass Transportation Administration on the Washington Metropolitan Transit Authority by TSC. The Elkins model is widely accepted as being the most accurate currently available and has now been validated for a number of profiles giving both single and two-point contact. It is therefore described in more detail and used below as a standard against which the simpler model described in this report is compared.

3.4.2 The Effect of Rail/Wheel Profiles on Forces and Moments

In 1977, resulting from studies carried out at British Rail, Elkins and Gostling published "A General Quasi-Static Curving Theory for Railway Vehicles," (Ref. 17). The paper described a model, validated by experiment for single point contact, which used measured cross-sectional geometry of wheels and rails to insert the rail/wheel forces and moments into the equilibrium equations. The forces in the plane of contact and moments about its perpendicular were obtained from the Kalker table book (Ref. 15), extended to include values of contact patch ellipticity up to 10, permitting accurate assessment up to derailment.

Further improvements were made to the model in Ref. 22 and the addition of two points of rail/wheel contact, at TASC in Ref. 23. The model and resulting computer simulation are used for evaluating the accuracy of the simplified model of wheel/rail forces and moments described above.

In the model by Elkins, the position and angles of the points of contact and a knowledge of the angular velocity of the axle about its bearing axis ϕ, are used to calculate longitudinal, lateral creepages and spin at all points of contact. The angular velocity of the wheelset $\dot{\phi}$ is calculated from considerations of torque balance as discussed in Ref. 17. The creepage equations for each point of contact are identical to those described in Refs. 17 and 22 and are not repeated here.

The net force and moment on the axle are made up of components of the normal and tangential forces on each of the points of contact, with the tangential forces being dependent upon the normal forces and the previously discussed creepages. The tangential or creep forces are highly nonlinear functions of the creepages and the contact patch geometry and are calculated from Kalkers nonlinear table of force/creepage relationships in the manner described in Ref. 17.

For a single point of contact on each wheel, the vertical load and the wheelset kinematics uniquely define the normal and, therefore, the tangential forces at the contact point. However, when two points of contact exist, there is a range of values of normal and tangential force, which may occur at the two points of contact, for a given vertical wheel load and wheelset kinematics.

Although, the lateral force and yaw moment cannot be separately defined for this lateral displacement, there is a unique relationship between them. Plots of axle yaw moment against lateral force provide a convenient means of comparing the steering characteristics of the wheel/rail geometries discussed in this report and later comparing the SIMCAR and Elkins characteristics.

A direct comparison is given for the case of equal wheel loads and three different profile assumptions in Figs. 3.4-1, 3.4-2, and 3.4-3. The cases chosen represent the lead axle angle-of-attack in steady-state in curves of 0, 5, and 10 degrees. The profile assumptions are single and two-point contact with new AAR 1/20 wheel profiles on 132 lb/yard AREA rail section, and a worn wheel profile used by Canadian National researchers (Ref. 25) (called CNA) on a worn rail profile shown in Fig. 3.4-4 and discussed more fully in Section 3.4.3.

The figures show that the correct assumption of two point with the new AAR 1/20 wheel gives a lower steering moment for any chosen lateral force. This increases the lateral force in equilibrium conditions during curving. The CNA profile, which represents an average worn condition, generally results in a higher steering moment. The exception occurs at the flange root where two point contact occurs. This is noticeable in Fig. 3.4-1. It should be noted that all characteristics given in this chapter terminate arbitrarily beyond maximum flange angle.

It is possible to conclude from these results that the new AAR 1/20 wheel on new 132 lb/yard, rail which has contact separately with flange and tread, contributes a lower steering effect to the axle and provides the highest potential for derailment. The simplified characteristic has therefore been designed to simulate this condition with greatest accuracy.

3.4.3 Comparison of SIMCAR with Elkins' Results - New Profiles

In order to compare the values of wheelset moment and lateral force on the flanging wheel, descriptive of the steering characteristics represented by the model, a matrix of values was chosen. For the leading wheelset, the angle-of-attack used was calculated to represent steady-state curving. The chosen values were,

Curvature	ϕ (Angle-of-Attack)
0°	0.0°
5°	0.3°
10°	0.6°
15°	0.9°

Each result was computed for load ratio $R = \frac{V}{V_{static}} = 0.5; 1.0; 1.5$. The static wheel load is 32,868 lb.

In addition, results representing the trailing axle were chosen with zero angle-of-attack over the same range of curvatures for R = 1.0. The comparison was carried out for a value of $\mu = 0.375$, and $\delta = 67°$, also used in the simulation of the results given in Chapter 5. Figures 3.4-5, 3.4-6 and 3.4-7 show a complete set of SIMCAR characteristics of $M/\mu BW$ (axle moment) against P/W (axle lateral force) for the chosen values above. Representative values of the characteristic are repeated in later figures in comparison with the characteristic by Elkins, using the Kalker tables, for new AAR 1/20 wheel profiles on new AREA 132 lb rail at a standard

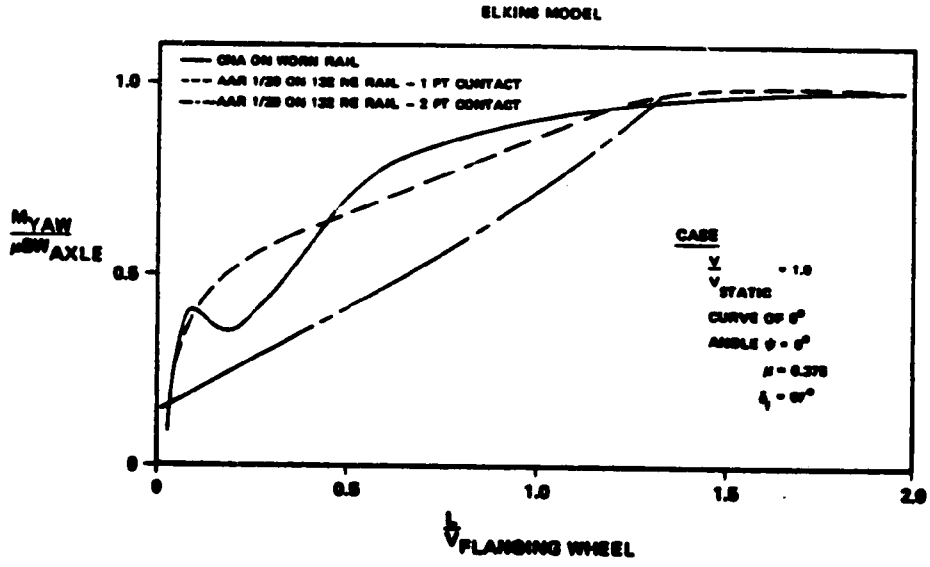

Figure 3.4-1 Axle Yaw Moment M/μBW vs Flanging Wheel L/V

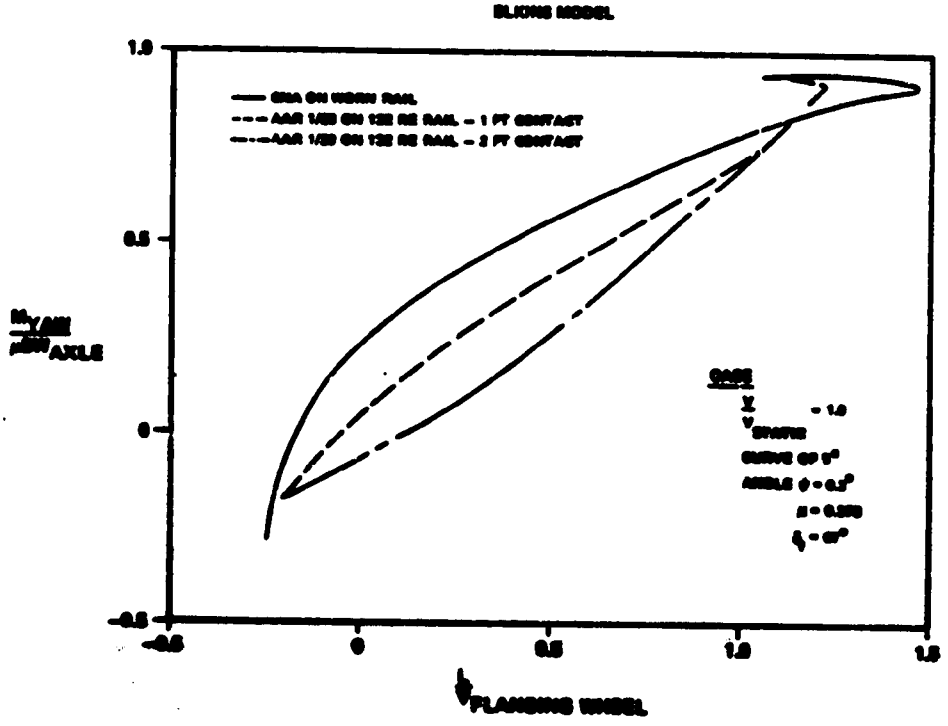

Figure 3.4-2 Axle Yaw Moment M/ BW vs Flanging Wheel L/V

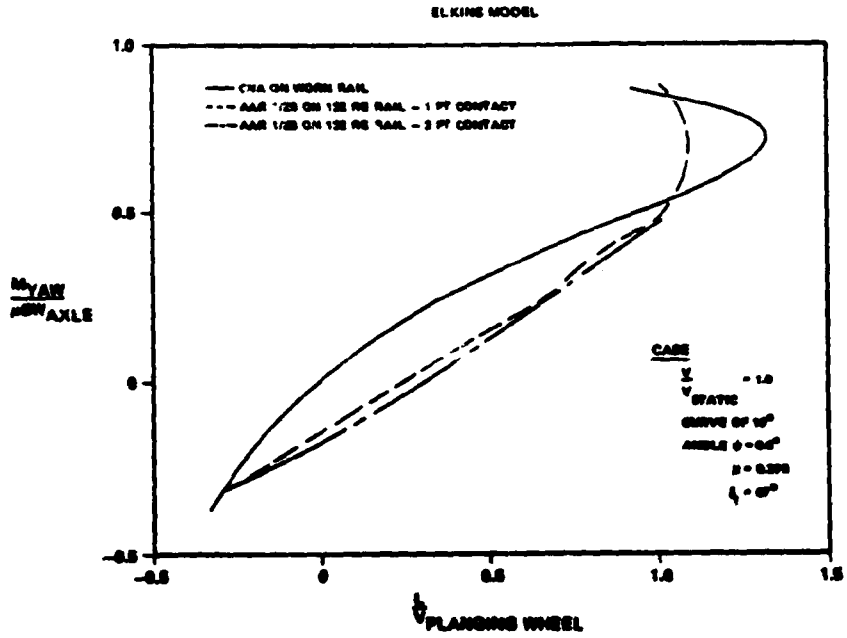

Figure 3.4-3 Axle Yaw Moment M/μEW vs Flanging Wheel L/V

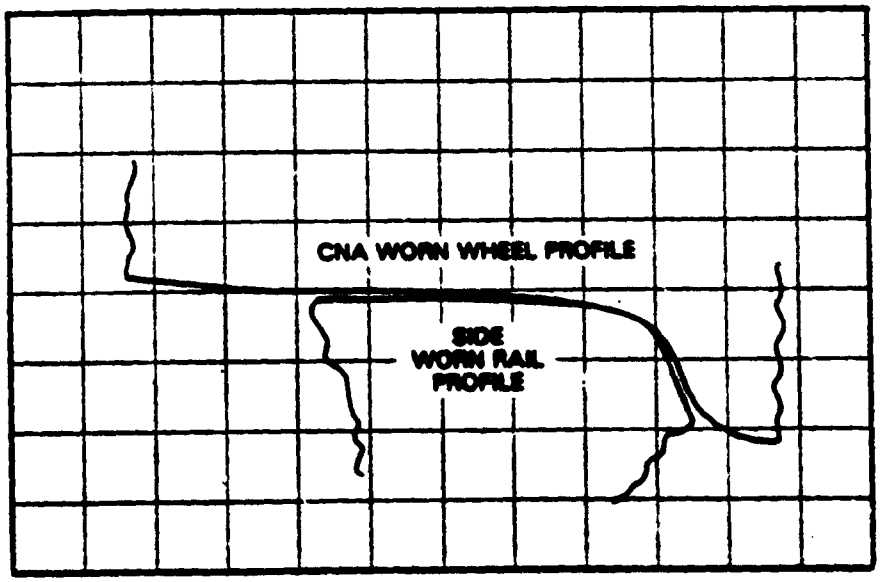

Figure 3.4-4 CNA on Worn Rail Profiles

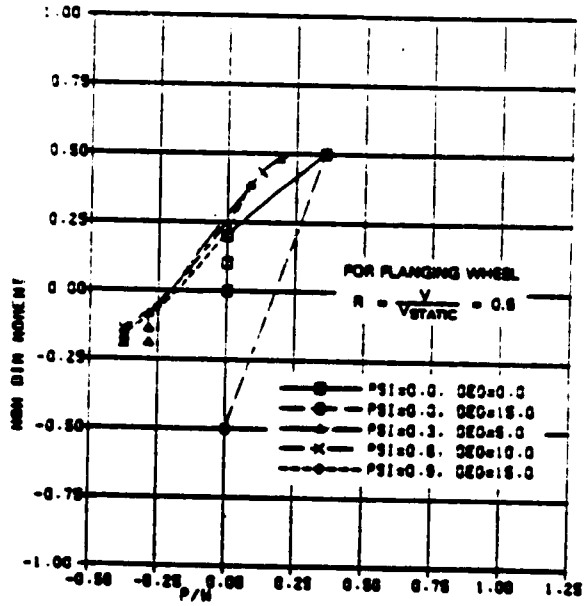

Figure 3.4-5 SIMCAR Characteristics:
R = 0.5
New AAR 1/20 Wheel on AREA
132 lb/yd Rail

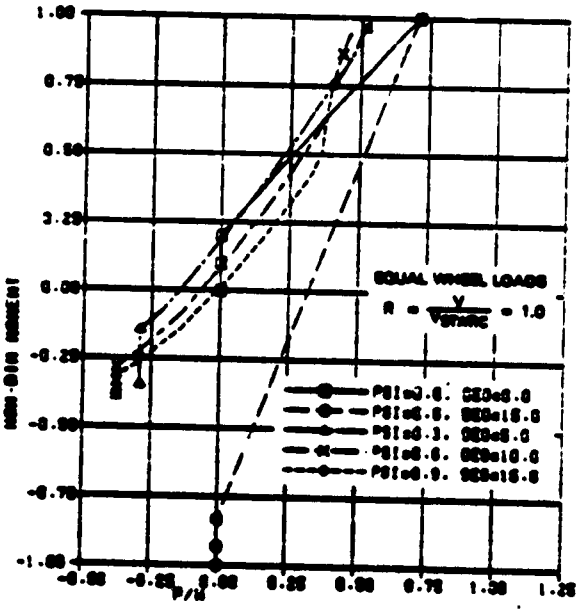

Figure 3.4-6 SIMCAR Characteristics:
R = 1.0
New AAR 1/20 Wheel on AREA
132 lb/yd Rail

gauge of 56½ in. A value of coefficient of friction $\mu = 0.375$ is used throughout.

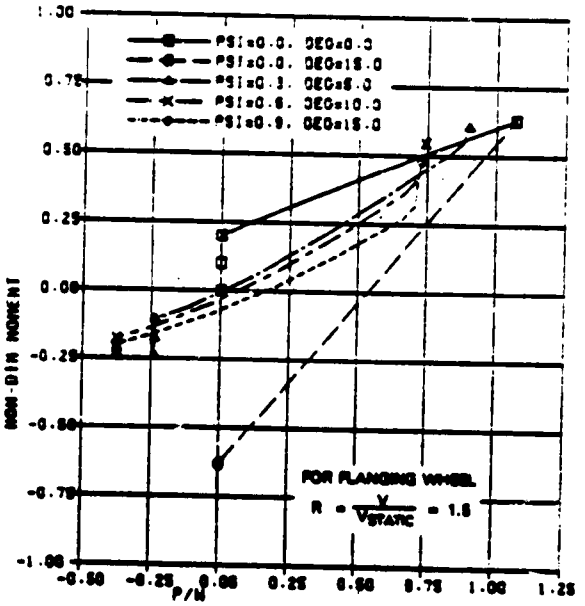

Figure 3.4-7 SIMCAR Characteristics:
R = 1.5
New AAR 1/20 Wheel on AREA
132 lb/yd Rail

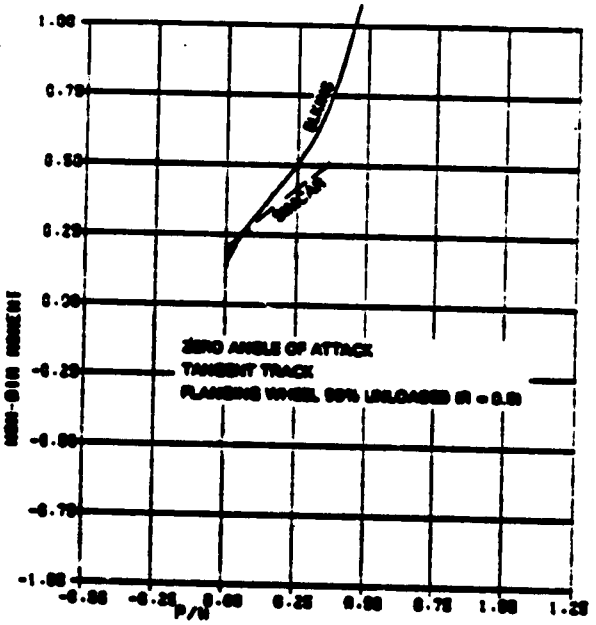

Figure 3.4-8 Comparison of SIMCAR with Elkins: New Profiles $\phi = 0°$; Deg = 0°, R = 0.5

Figures 3.4-8, 3.4-9 and 3.4-10 give the comparison for the range of wheel loading equivalent to zero angle of attack on tangent track. Figure 3.4-9

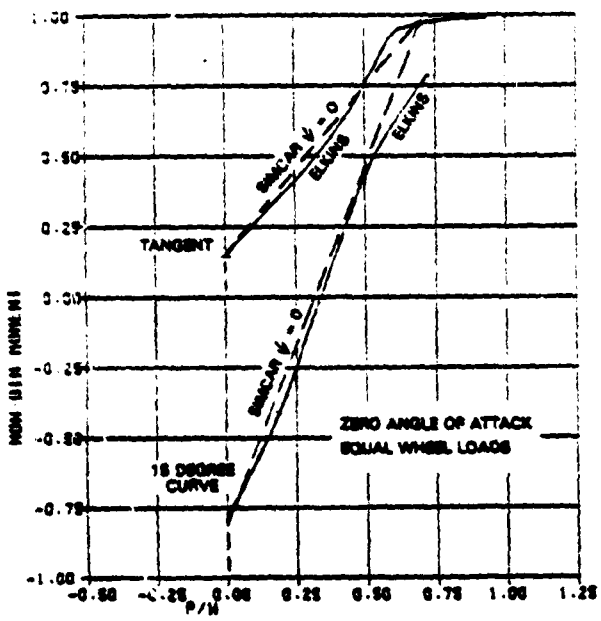

Figure 3.4-9 Comparison of SIMCAR with Elkins: New Profiles ϕ = 0°; Deg = 0° and 15°; R = 1.0

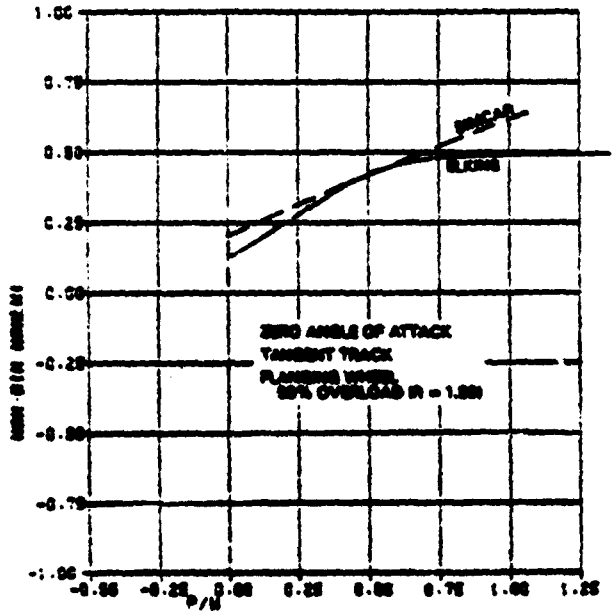

Figure 3.4-10 Comparison of SIMCAR with Elkins: New Profiles ϕ = 0°; Deg = 0°; R = 1.5

also includes zero angle for a 15 degree curve with equal wheel loads, representative of a trailing axle.

Elkins predicts much larger moments for the lightly loaded wheel under large lateral forces. In this regime SIMCAR underestimates the effect of the normal force on the flanging wheel at flange contact. For equal wheel loads this difference is substantially reduced. As shown in Fig. 3.4-10 for an overloaded flanging wheel, SIMCAR overestimates the moment and underestimates the lateral force under similar conditions closest to flange climbing. However, the force and moments indicative of flange climbing by a trailing wheelset are unlikely and these differences do not impact the results in the derailment studies presented here.

The results representative of a leading wheelset in a curve are given in Fig. 3.4-11, 3.4-12, and 3.4-13 for R = 0.5, 1.0, and 1.5 respectively. The SIMCAR characteristics differ little from those due to Elkins. The largest difference occurs on the lightly loaded wheel in which SIMCAR again underestimates the moment during severe climbing lateral forces. The results are therefore conservative under these conditions.

Evidence of the relationship between yaw moment, $M/\mu W$, and lateral force on the flanging wheel alone, L/V, provides similar results to those discussed for total wheelset lateral force, P/W. Figure 3.4-14 provides an example for a 15 degree curve. The overall comparison

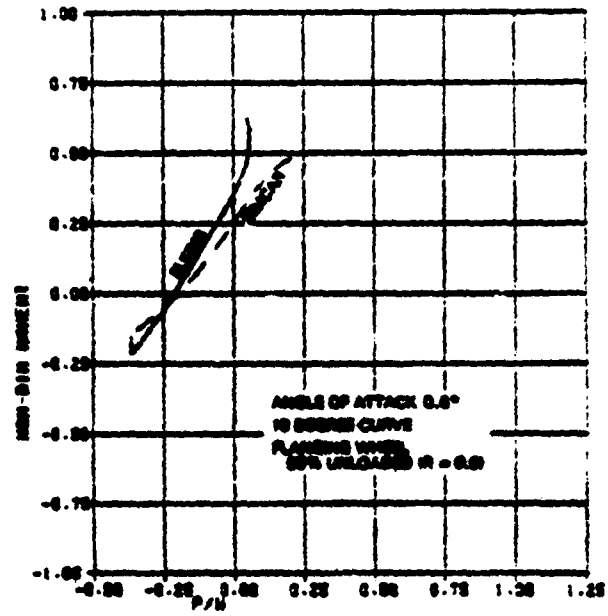

Figure 3.4-11 Comparison of SIMCAR with Elkins: New Profiles ϕ = 0.6°; Deg = 10°; R = 0.5

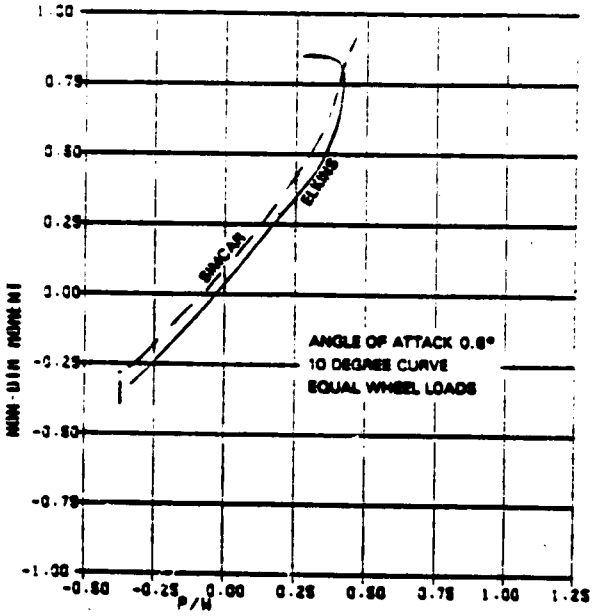

Figure 3.4-12 Comparison of SIMCAR with Elkins: New Profiles ψ = 0.6°; Deg = 10°; R = 1.0

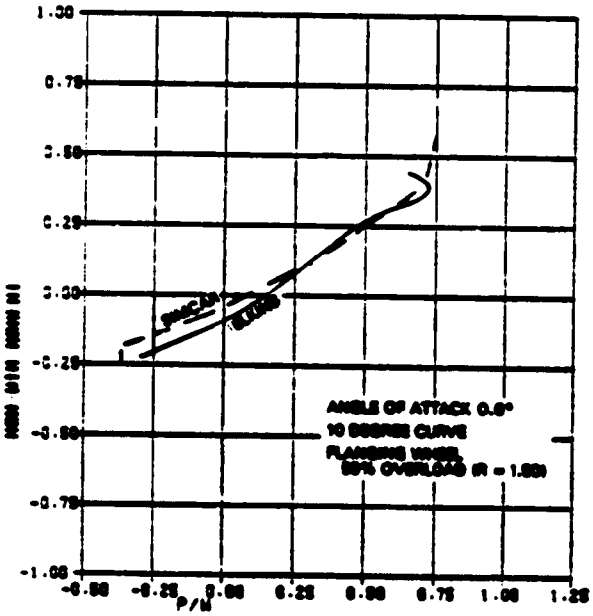

Figure 3.4-13 Comparison of SIMCAR with Elkins: New Profiles ψ = 0.6°; Deg = 10°; R = 1.5

is similar to that for the 10 degree curve for total lateral force given in Fig. 3.4-12. In both cases the Elkins result produces a reduced lateral force

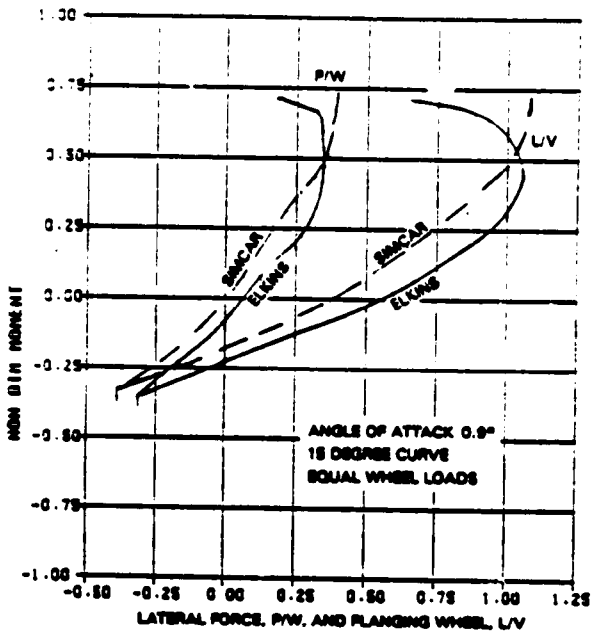

Figure 3.4-14 Comparison of SIMCAR with Elkins: New Profiles ψ = 0.9°; Deg = 15°; R = 1.0

as the wheel climbs the flange in single point contact. The SIMCAR characteristic does not attempt to simulate the regime following flange climb.

The comparisons for R = 1.0 show the closeness designed into the SIMCAR characteristic, by adjusting the expression for longitudinal creepage for equal wheel loads and the particular combination of wheel and rail profiles illustrated.

An alternative representation reflects both yaw moment and lateral force as functions of the displacement beyond flange contact. The model has a leading slope to the lateral force characteristic, K_{LEAD}, up to its maximum value. The model due to Elkins is designed for steady-state analyses and presumes rigid track. In order to provide an equivalent circumstance for both characteristics, the Elkins lateral force has been used to define a lateral displacement following the initial flange contact, similar to that in the SIMCAR characteristic. The moment is then related to the same lateral displacement.

The comparison between the SIMCAR and Elkins' characteristics is given for R = 1 and μ = 0.375 in Fig. 3.4-15 and 3.4-16. The inaccuracy previously

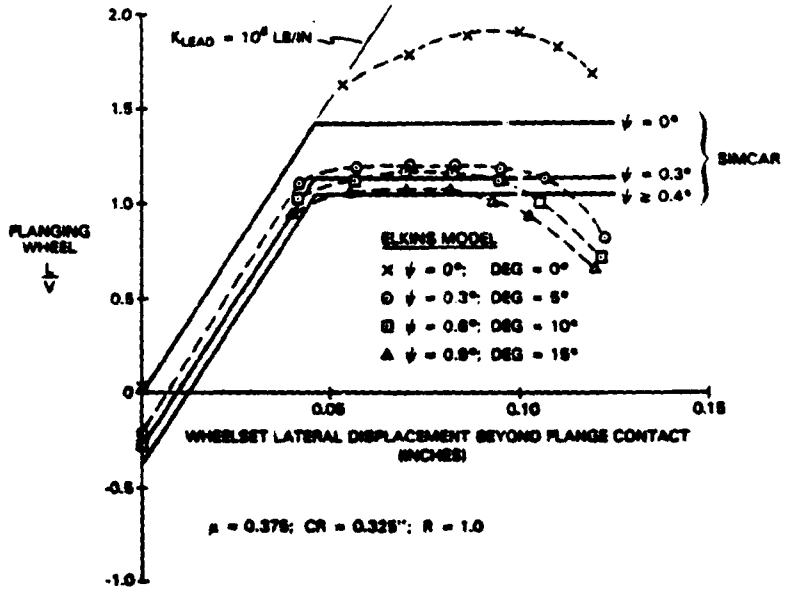

Figure 3.4-15 Flanging Wheel L/V Relationship with y
New AAR 1/20 Wheels on 132 RE Rail

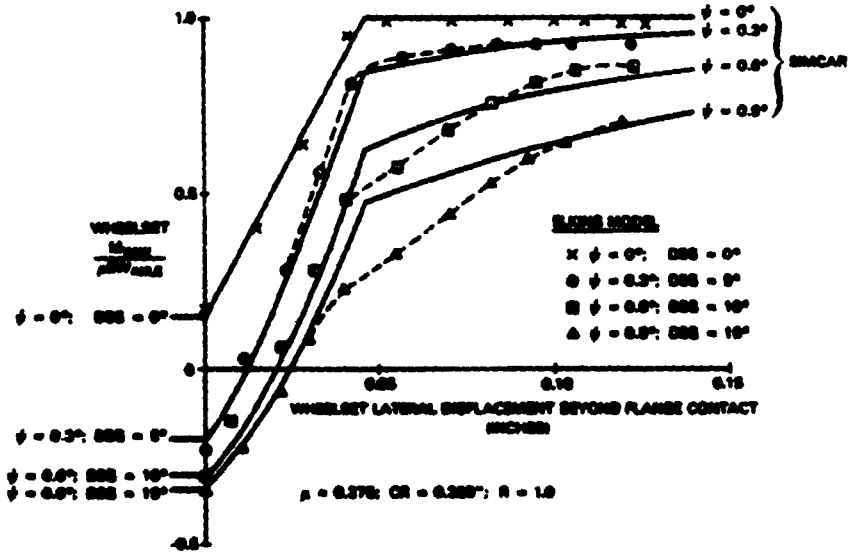

Figure 3.4-16 Yaw Moment Relationship with y
New AAR 1/20 Wheels on 132 RE Rail

noted for values of lateral force at zero angle-of attack, ψ, and following wheel tread separation is apparent in Fig. 3.4-15. The lateral position at derailment is generally indicated by the reduction in the Elkins prediction of $\frac{L}{V}$ in Fig. 3.4-15 and occurs close to 0.10 inch. At this value the steering moment in the SIMCAR approximation in Fig. 3.4-16 is close to that suggested by the Elkins model for both wheelsets

leading to the conclusion that the SIMCAR approximation is accurate in estimating lateral equilibrium forces and moments for the case studied of new wheels and rails.

3.4.4 Comparison of SIMCAR with Elkins' Results - Worn Profiles

In order to investigate the generality of the approximate model used, comparison is made with Elkins' results for two situations representative of worn circumstances of the rail. For this purpose, a measured side worn rail profile was chosen, using a cross-section taken from Ref. 24, p. 54, Fig. 27A. The profile is claimed by the author of the reference to be typical of heavy operation. However, hand measured digitization from the figure for the results presented here may have contributed to some inaccuracy.

Two wheel profiles were investigated. The first was a standard new AAR 1/20 profile which was found to give 2-point contact initially, but a lower flange angle at which tread lift-off commenced. The second was the CMA profile (Ref. 25), now widely used as a "standard" worn wheel, which gave single point contact, except for initial contact with zero angle of attack. In both cases a wide gauge of 57½ inches was chosen, equivalent to a clearance (CR) of 0.825 in.

For standard AAR 1/20 wheel, the results are given in Fig. 3.4-17 to 3.4-19. Figure 3.4-17 shows the steering relationship of dimensionless moment to total lateral force, on the leading flanging wheel, for equal wheel loads, (R=1), and 0, and 15 degree curves. Figure 3.4-18 presents the comparison for lateral force, L/V, against lateral wheelset displacement beyond flange contact, with the Elkins model provided with leading edge slope as discussed in Section 3.4.2. The gauge clearance for the Elkins results is arbitrarily fixed to provide a similar initial contact to that used in the SIMCAR model results plotted. Figure 3.4-19 provides the comparison between the SIMCAR and Elkins results for the yaw moment, M/μBW, against lateral wheelset displacement beyond flange contact.

In general, the approximate characteristic for the chosen worn rail is identical to that for new rail since the model only contains a rudimentary knowledge of the profiles; the tread and flange angles chosen to represent them are similar. However the widened gauge used in the worn rail studies modifies the force and moment values at the start of flange contact due to the increase in

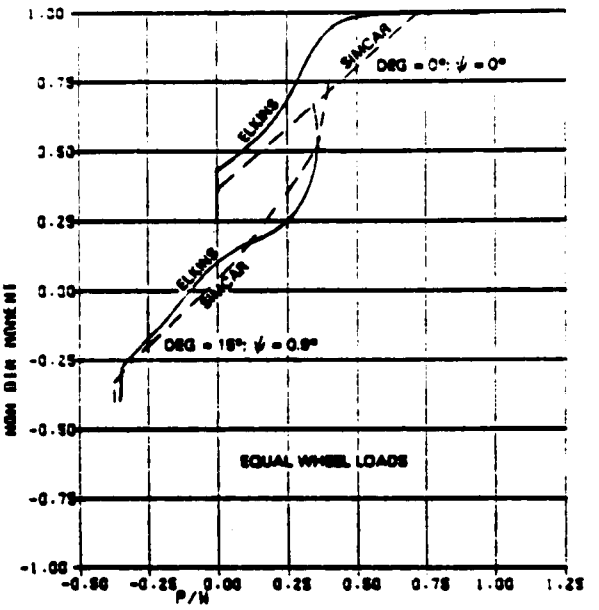

Figure 3.4-17 Comparison of SIMCAR with Elkins: New Wheel/Worn Rail R = 1.0; ψ = 0°, Deg = 0°; ψ = 0.9°, Deg = 15°

the difference in rolling radius between wheels.

The Elkins model reflects both the change in rolling radius and the contact angle for the particular profiles and in this case, for the worn rail, produces a reduced angle at which 2-point contact ceases. This is 42 degrees for the side worn rail as compared to 62 degrees with new rail. The result is a greater difference between the SIMCAR and Elkins model results, especially at zero (or negative) angle of attack on tangent track, where the Elkins model shows an increase in moment at the intermediate value of lateral force on tread and flange.

The results for the CMA profile, here used to represent a worn wheel, and the side worn rail profile, are shown in Figs. 3.4-20, 3.4-21 and 3.4-22. This profile combination provides single point contact throughout the lateral wheelset excursion and hence the initial flange contact is not precisely defined. An attempt is made here to match the curves against lateral position. However, with flangeway clearance resulting from standard gauge, an effective conicity of 0.1⅛ has been assumed as representative of the variation of tread rolling radius difference between

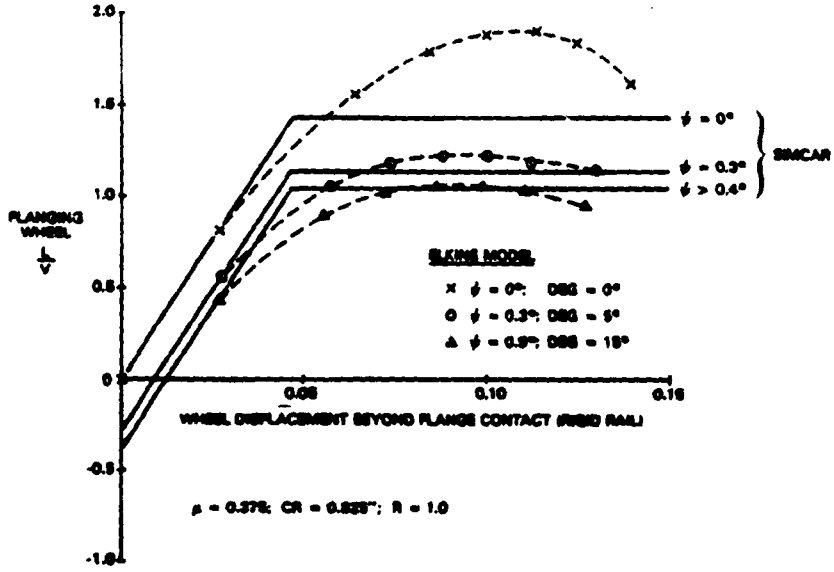

Figure 3.4-18 Flanging Wheel L/V Relationship with y
New AAR 1/20 Wheel on Side Worn Rail

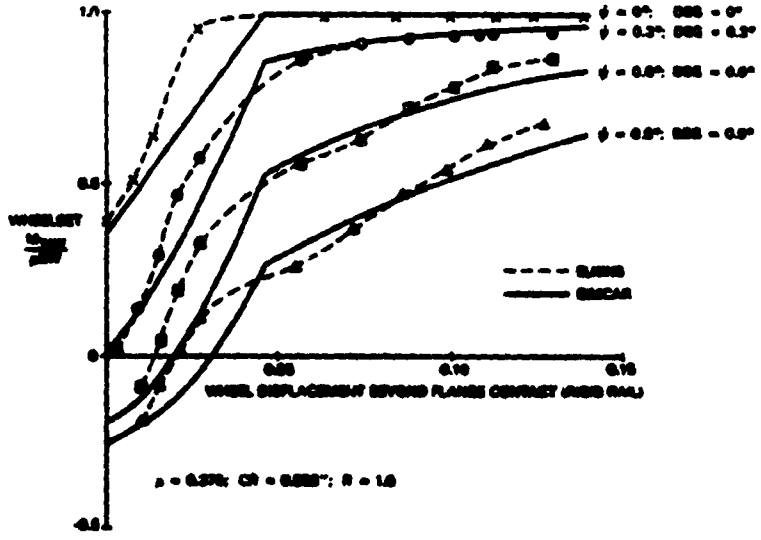

Figure 3.4-19 Yaw Moment Relationship with y
New AAR 1/20 Wheel on Side Worn Rail

wheels with lateral wheelset displacement. With the wide gauge chosen here to represent worn track, giving a flangeway clearance of 0.825 in., the same rolling radius difference at flange contact suggests a proportionally lower effective conicity of 0.071, which has been used here for the tread cone angle in the SIMCAR model. While this leads to a closer flange contact characteristic, it may be deficient for studies

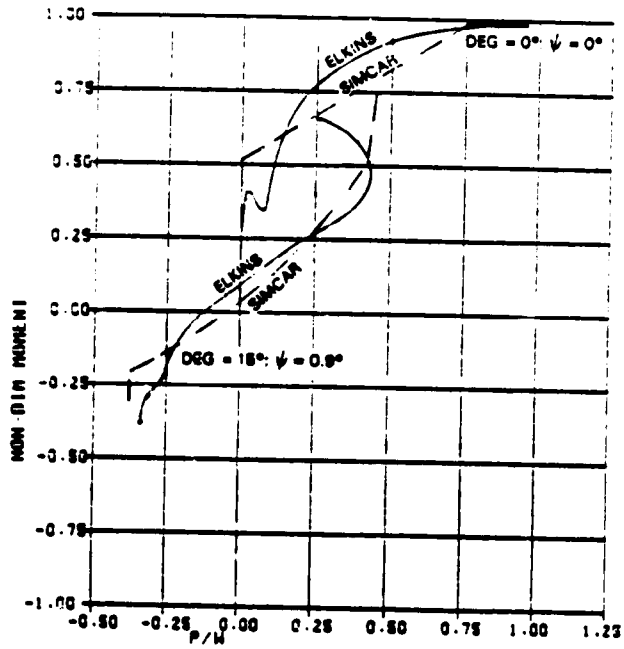

Figure 3.4-20 Comparison of SIMCAR with Elkins: Worn Wheel and Rail R = 1.0; ψ = 0°, Deg = 0°; ψ = 0.9°, Deg = 15°

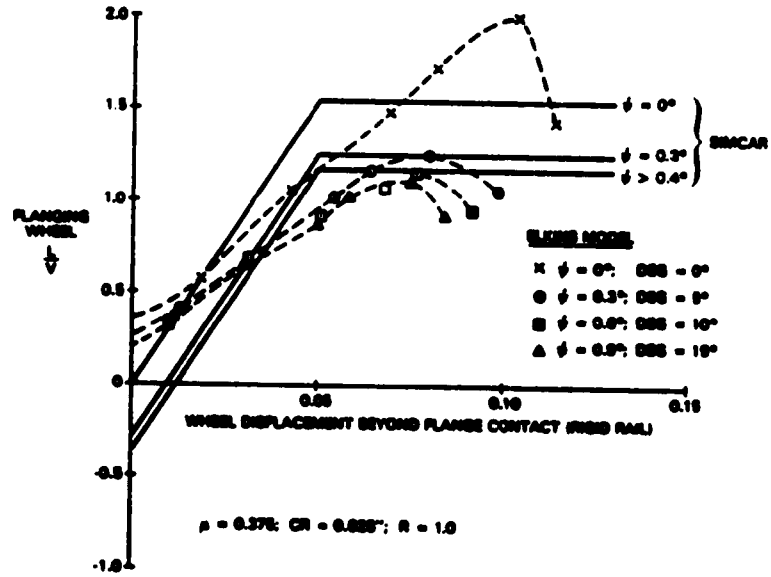

Figure 3.4-21 Flanging Wheel L/V Relationship with y CRA Wheel on Side Worn Rail

dominated by tread contact and may provide inaccuracy in the yaw moment on the trailing axle while not in flange contact.

These graphs, showing the worn wheel/rail profile characteristics, show the limitation of the approximate model of separate tread and flange contact regimes with piecewise linear representations for each. The rudimentary knowledge of the profiles in this model does not permit an accurate nonlinear characteristic in worn tread contact.

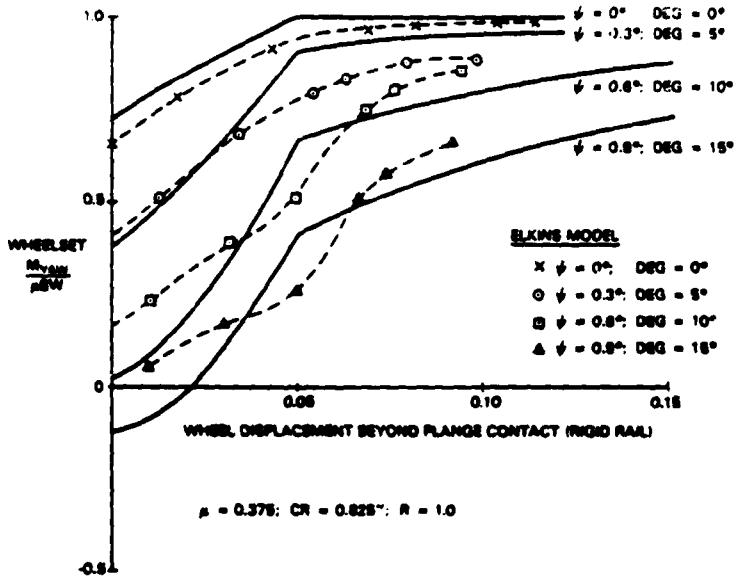

Figure 3.4-22 Yaw Moment Relationship with y CMA Wheel on Side Worn Rail

However, the problem of a representative characteristic with varying gauge and conicity is a general one which would require recalculation of the contact geometry at each step for an accurate model. The model appears to satisfy the requirement well for new straight tapered wheel profiles. Care has been found necessary in its use with wheel profiles which produce single point contact, and an effective conicity which varies with gauge during tread contact, where adjustment of the approximate characteristic has been required.

4. COMPARISON OF 16-DEGREE-OF-FREEDOM FREIGHT CAR MODEL WITH TEST RESULTS

4.1 INTRODUCTION

The modified 16-degree of freedom (DOF) freight car computer model, described in Chapter 3 and Appendices B and C, was designed to be used in studies of freight vehicles near derailment. Simulation allows results to be obtained at a significant reduction in cost relative to full scale testing, but requires that the model be verified as representing the behavior that would be observed in the field. This enables valid results to be obtained with limited amounts of full scale testing. The procedure is outlined in Fig. 4.1-1. The results, used here to seek agreement of dominant vehicle outputs (such as wheel-rail force), are regarded as indication of the basic accuracy of the modeling effort. Data for comparison were available from three sources.

The first data set was generated when a train, composed primarily of loaded 100-ton cars, was run over instrumented track perturbations at the Transportation Test Center in February 1979. The track perturbations had been constructed for locomotive testing under the Perturbed Track Test (PTT) program (Ref. 26). Track instrumentation consisted of a series of rail-mounted strain gauges to measure lateral and vertical wheel-rail forces.

A second set of data for comparison was obtained during loaded 100-ton freight car testing on the Union Pacific railroad during March 1980 (Ref. 27). Instrumented wheelsets were used to measure forces.

A third set of data was produced from tests carried out on the Chessie System Track at Starr, Ohio in spring 1981 (Ref. 28). Instrumented wheelsets were also used in this test.

Finally the program was used to generate results for steady state curving which were compared to published results of a number of test programs for the leading outer wheel force.

4.2 SIMULATION-FIELD TEST COMPARISONS WITH PERTURBED TRACK TEST DATA

The Perturbed Track Tests (PTT) at Pueblo were conducted to compare the response of two six-axle locomotives to

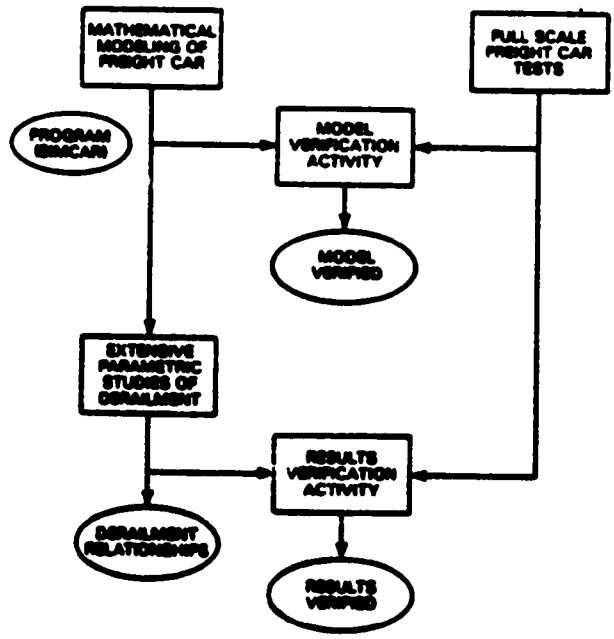

Figure 4.1-1 Model Verification Activity as Related to Overall Project Plan

specific, well-controlled track inputs. To accomplish this objective, two large segments of track were modified to include various large track perturbations. One of these two modified segments was on a 1.5 deg curve (1 inch superelevation) portion of the Train Dynamics Track. During the PTT runs, on-board sensors provided most of the data which was taken. In addition, certain track sections were provided with strain gauges as a check on the on-board data and to measure wheel-rail force on non-instrumented axles. One of the instrumented sections consisted of a "1-inch high rail misalignment". This is a curved track section in which the joints of the high rail are displaced outwards one inch relative to undisturbed track. This causes the wheels to move outwards and causes high wheel-rail forces as the wheel flanges ride up the rail just past the perturbed joint.

Since the area of curving dynamics, including variation in track alignment, cross-level, and gauge, is a unique aspect of the SIMCAR freight car model, advantage was taken of the PTT full-scale test to provide data for verification of this model. Although the PTT runs proper involved locomotive responses, some freight car data were taken as the FAST (Facility for Accelerated Service Testing) train was hauled over the PTT track. Specifically, data was taken on a loaded 100 ton covered hopper car (Ref. 26), and compared to a simulation of the same vehicle using the SIMCAR model.

The result of this comparison is presented in Fig. 4.2-1. Both the lead and trailing axles of the lead truck are shown, and the wheel-rail forces are measured on the outside wheel. The magnitude and signature of the simulation result and the field measurement are close, the differences being within the range of the uncertainties in the field measurements and the vehicle and track parameters.

4.3 SIMULATION-FIELD TEST COMPARISONS FOR UNION PACIFIC TESTS

During March of 1980, a series of instrumented freight car tests were made on the Union Pacific Railroad to support track geometry specification development activity using the test equipment of the FRA Truck Design Optimization Program. As part of these tests, over 300 feet of track was modified to exhibit a series of alignment and gauge deviations. Automatic Location Detector (ALD) targets were placed along the modified section to assist in data reduction. Figure 4.3-1 illustrates the planned test track alignment.

As part of the simulation output, Fig. 4.3-2 illustrates the flange clearance between the static wheel position and the left and right rails obtained from the SIMCAR program. The space between the two wheel flanges has been "removed" from this figure so that wheelset position is displayed as a point on the solid line. Hence, flanging occurs whenever the wheel set position moves outside the flange clearance lines. Periods of flanging can be discerned in this figure. The test was conducted at a speed of 27 mph.

The comparison of actual field measurements (Ref. 27) and simulation results is presented in Fig. 4.3-3. The simulation results were generated using the track perturbations illustrated in Fig. 4.3-1. The comparison of the magnitude of the response between test and simulation results is fair.

Some differences between simulation and test responses are apparent, especially in the first peak, between ALD 2 and 3. Although the simulation predicts only a small force peak due to the short flanging occurrence, the actual track test produced a very large response. As this is the response to the first perturbation, an initial condition disparity could account for this difference. Other differences may again be the consequence of variation between the assumed condition of the wheels and rails which were the same as for the PTT test. It is also probable that details of the track geometry deviated from the ideal layout of Fig. 4.3-1 used in the SIMCAR results.

4.4 SIMULATION - FIELD TEST COMPARISONS WITH STARR TEST DATA

In June 1981, a series of tests were carried out on the Chessie System at Starr, Ohio. These tests were conducted to examine the forces developed on weak track, their effect on gauge and potential for wheel drop, the coupling between cross-level and gauge variation and its effect on cross level index for track safety standards. In particular, for the model used in this report, the test was designed to provide baseline force and response data, under the severe track geometry conditions, for comparison with the results from the computer simulation.

The test consist is shown diagrammatically in Fig. 4.4-1. Three loaded 100 ton hopper cars were used. Instrumented wheelsets on two cars had nominally new,

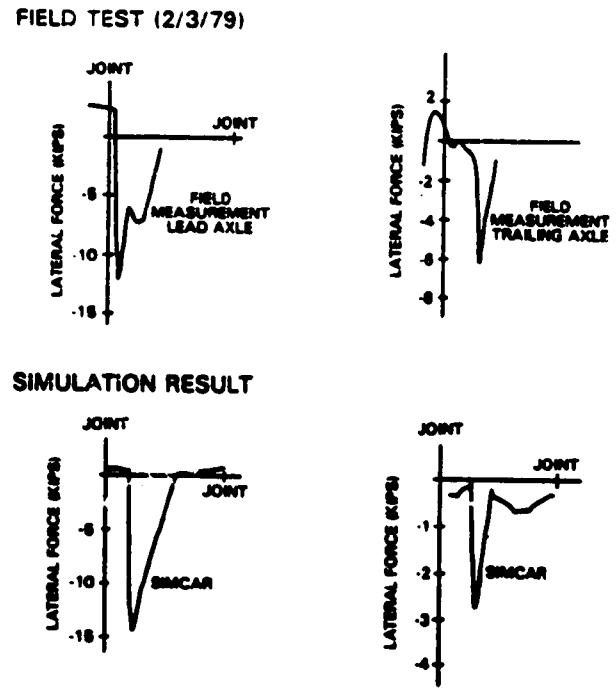

Figure 4.2-1 Wheel-Rail Forces - Measured and Simulated

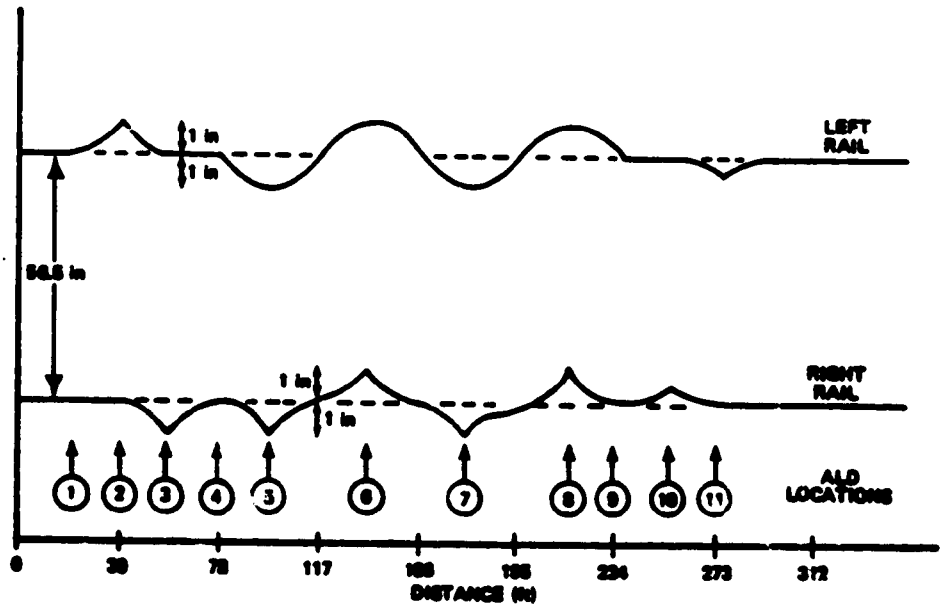

Figure 4.3-1 Test Track Alignment Plan

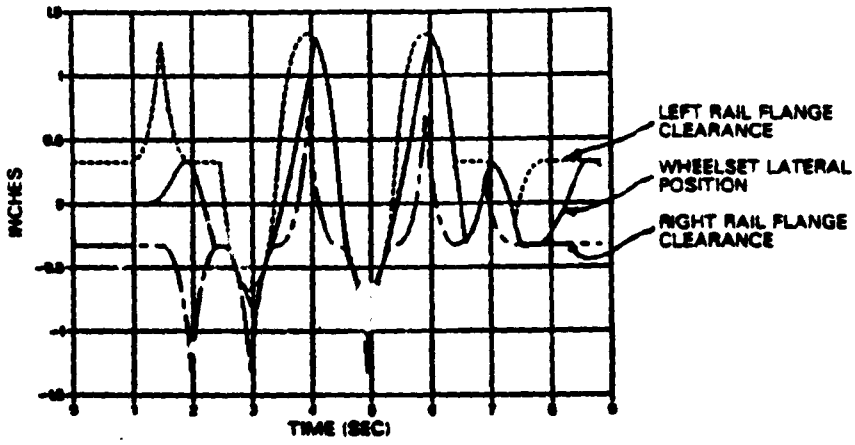

Figure 4.3-2 First Wheelset Lateral Response

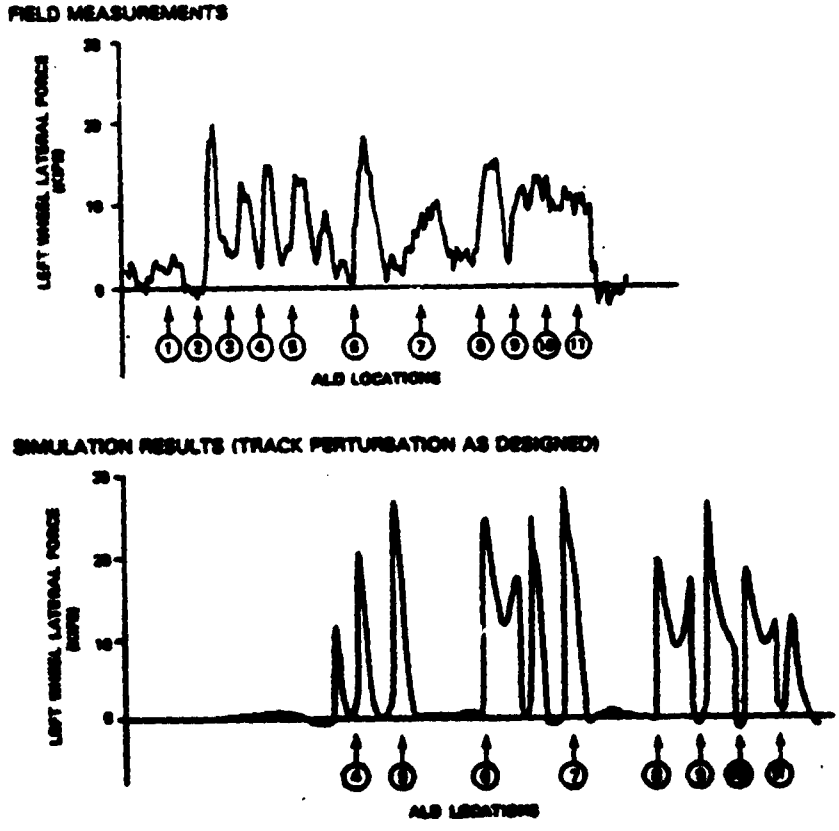

Figure 4.3-3 First Left Wheel Lateral Force - Simulation and Field Test

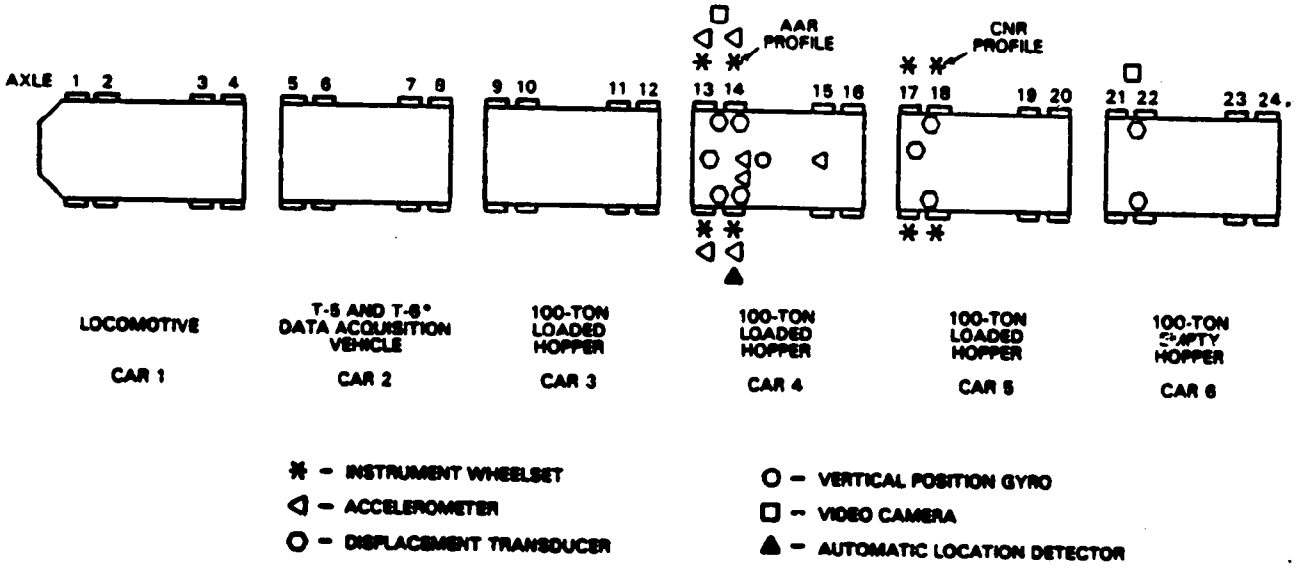

*FOR RUNS ON 6/4 AND 6/5

Figure 4.4-1 Consist Instrumentation

AAR 1/20, and worn, CMA, profiles. Difficulties with the AAR profiled wheelsets resulted in comparison of SIMCAR output being made with the output of the CMA profiled wheelsets on Car 5. For this purpose, an effective conicity of $a = 0.18$ and $\mu = 0.375$ were used.

The loaded hopper car was assumed to have standard 100 ton trucks with characteristics similar to those given in Appendix C. The measured value of truck spacing in the test car of 40.5 feet was used in the simulation. The test vehicle roll characteristic was assumed to be similar to that discussed in Appendices B and C. However, the CG height for the body was estimated as 5 feet above the center plate. This value was estimated by TSC, and reported in Ref. 29, using the simplified M.I.T. rock and roll model (Ref. 7) and data from the test on tangent track with cross level variation.

The track alignment and gauge variation on a six degree curve in test Section 1 is shown in Fig. 4.4-2. The results from this section were used for the comparison with SIMCAR predictions. The measured and simulated results are given in Fig. 4.4-3 at 15 mph. Very little roll was apparent or predicted. The force levels generally correspond well, with some difference during the transition between tight and wide gauge.

In addition to the alignment and gauge variation, a further series of tests were carried out with 3/4 in. cross level variation added during the last rail lengths. Car roll was excited almost to wheel lift as shown in Fig. 4.4-4. The simulated vertical wheel force compares well with that measured, although some variation is apparent at the start due to the existence of joints and dips in the test track exciting an initial value of roll, not simulated. The lateral forces are shown in Fig. 4.4-5. Here the simulation shows good agreement with the measured forces. Since the predictions for track standards, given in Chapter 5, are centered on dynamic curving effects this agreement was considered to be a valuable verification of the model behavior.

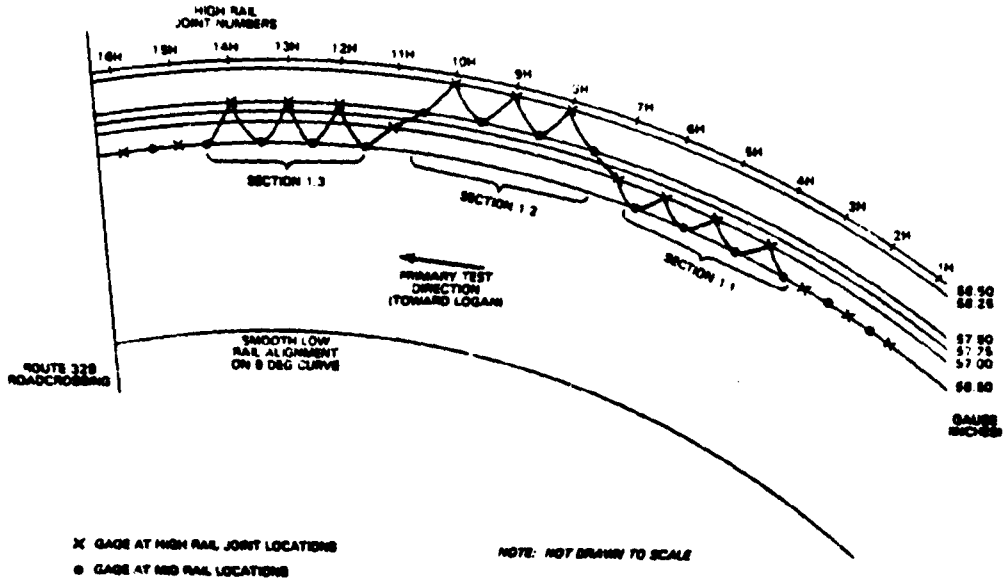

Figure 4.4-2 Perturbation Layout at Starr, Ohio Showing Gauge Specifications on Soft Curve

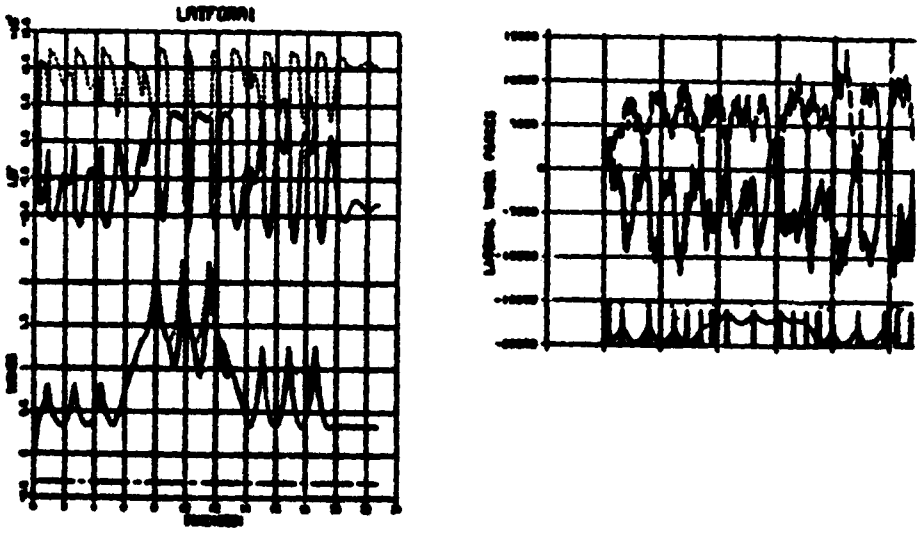

Figure 4.4-3 Test Simulation and Result from Starr, Ohio With Track Layout Shown Above

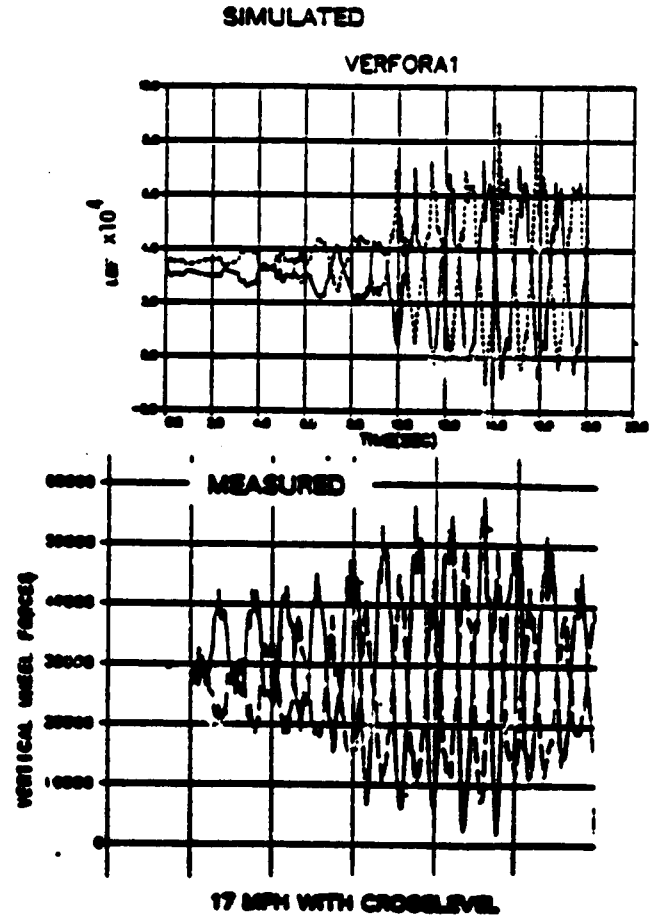

Figure 4.4-4 Simulation and Test Result From Starr, Ohio With Perturbation of Fig. 4.4-2 and 3/4 in. Cross-Level at Last 9 Joints

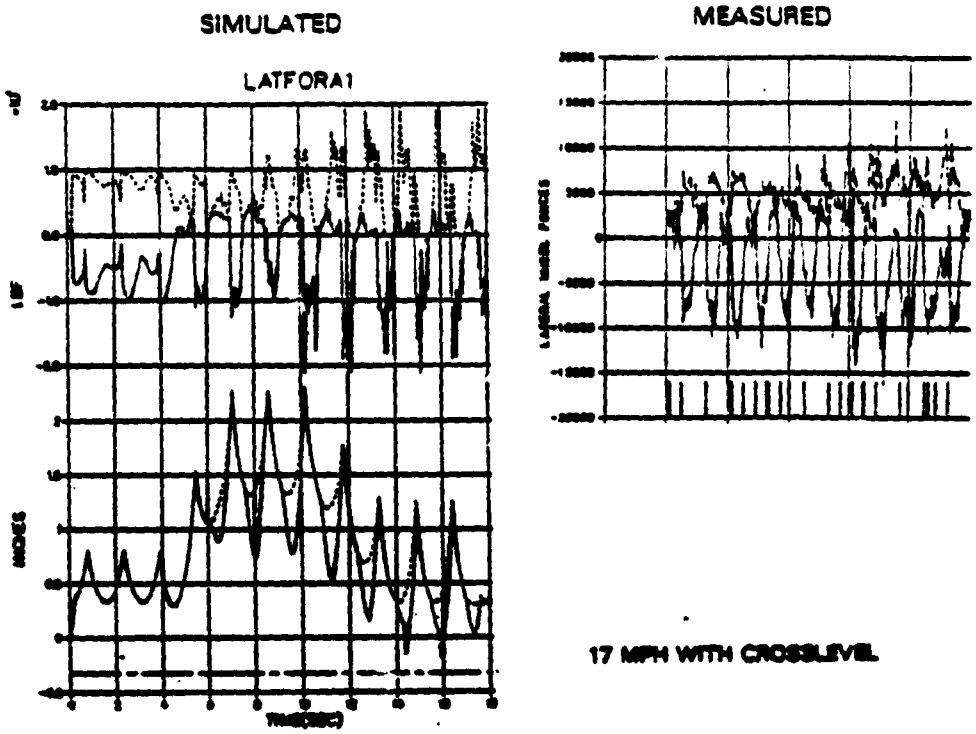

Figure 4.4-5 Simulation and Test Result From Starr, Ohio With Perturbation of Fig. 4.4-2 and 3/4 in. Cross-Level at Last 8 Joints

4.5 COMPARISON OF SIMULATION RESULTS WITH PUBLISHED DATA FROM TESTS IN STEADY CURVES

In order to compare the predictions with as broad a set of recorded test circumstances as possible, a survey was carried out. Published tests were identified for the leading outer wheel force on loaded 100 ton hopper cars with standard 3-piece trucks at near balance speed in curves. The following tests were found suitable.

- Truck Design Optimization Project (TDOP) (Ref. 30)
- Wheel Load Tests at the Facility for Accelerated Service Testing (FAST) (Ref. 31)
- Wear Tests of FAST (Ref. 32)
- Tests on new trucks at Canadian Pacific (CP Rail) (Ref. 33)
- Tests on Union Pacific Track (UP) (Ref. 34).

Since each test condition may and probably will be different, the results given in Fig. 4.5-1 show variation. However, the results show the same trend as the model predictions and have a mean value close to that predicted by the model, adding to the confidence in simulation of the 100 ton hopper car, in curves under service conditions.

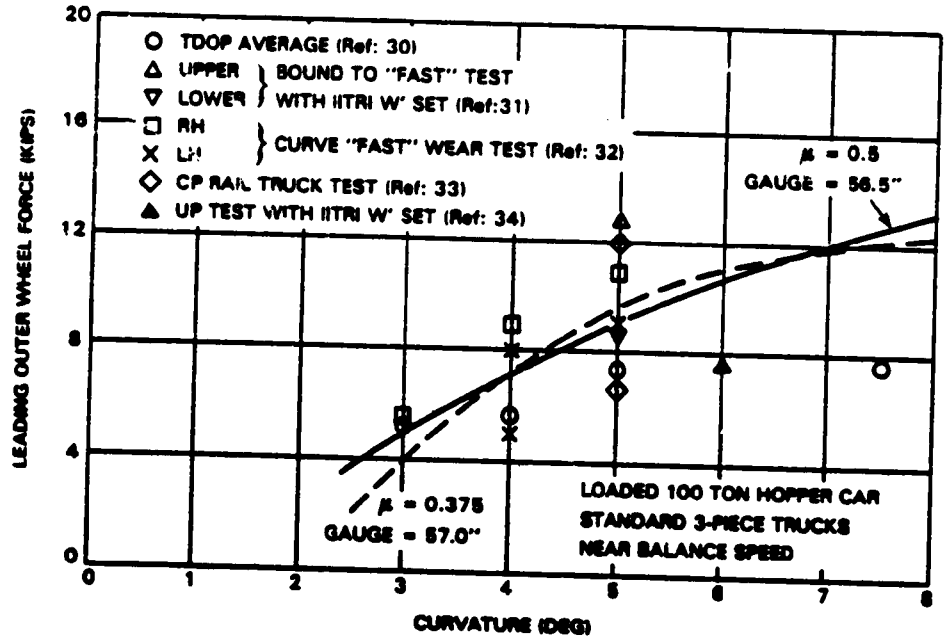

Figure 4.5-1 SIMCAR Steady State Predictions vs Measured Leading Outer Wheel Forces

5. STUDY OF LOW SPEED RESPONSE TO ALIGNMENT, GAUGE AND CROSS-LEVEL VARIATION IN CURVES -100 TON HOPPER CAR

5.1 INTRODUCTION

In the preceding chapters, the objective of the study reported here was described as that required to establish a relationship between track geometry and the safety resulting from vehicle/track dynamic interaction. The study reported in this chapter concerns the response of alignment and gauge variations in curves with and without cross-level variations in the 10-25 mph speed range. The 100 ton hopper car, loaded to a high center of gravity, provides the poorest performance scenario representative of the "real world" situation. The car is chosen to have significant sidebearing clearance (¼ inch) and a truck center spacing close to the rail length.

5.2 LOW SPEED STUDY PLAN AND OUTPUTS

The computer program used in the study of the response of a loaded 100 ton hopper, between 10 and 25 mph, has a list of 87 possible output states, all of which are printed at each chosen step in time. The list was reduced to the following time histories for plotting. Each was produced for the runs listed and discussed.

- Lateral Wheelset Position - axle 1 to observe tracking relative to track geometric input
- Roll Angle - to establish vehicle integrity and confirm lateral weight transfer
- Lateral Forces - axles 1 and 2, to assess the potential for derailment
- Lateral Force - axle 3, to confirm similarity between trucks
- Vertical Force - left wheels, truck A, to observe under and overloading and wheel lift
- L/V - leading left wheel, to observe the classical rail climb value (this is the outer wheel in curving runs)
- L/V - leading right wheel
- Flange to rail overlap - left wheels of leading truck, to observe potential rail climb and wheel drop
- Flange to rail overlap - right wheels of leading truck
- Linear lateral siffness required to prevent wheel drop.

In addition to the above plots, a cross plot was produced by the computer program leading left (outer) wheel force against leading wheelset distance to rail drop, as defined in Section 2.4.3. The left wheel is made the outer wheel in the computed curving runs by choosing a right hand curve. A sample of the plotted output without roll angle, is given in Figs. 5.2-1 through 5.2-11 for a 5 degree curve with 1½ inch outward cusps of the joints on the high rail. The wheel/rail characteristic for this run represents new wheels and the speed is 15 mph. The track is superelevated to give balance at this speed and the gauge is set at 56.5 inch. A friction coefficient of 0.5 is assumed. The result is discussed more fully in Section 5.4.

The planned study separated the work into four basic track scenarios shown in Fig. 5.2-12.

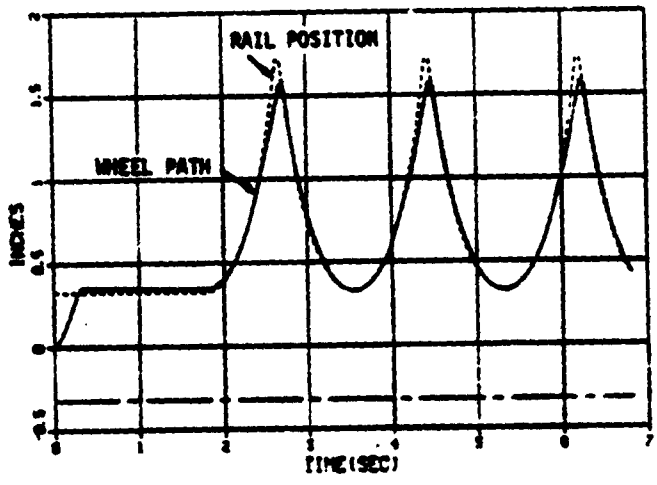

Figure 5.2-1 Lateral Position - Wheelset 1 - Truck A

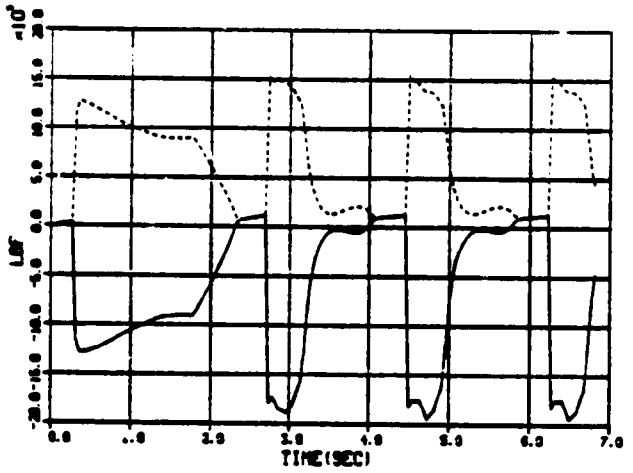

Figure 5.2-2 Lateral Forces - Wheelset 1 - Truck A

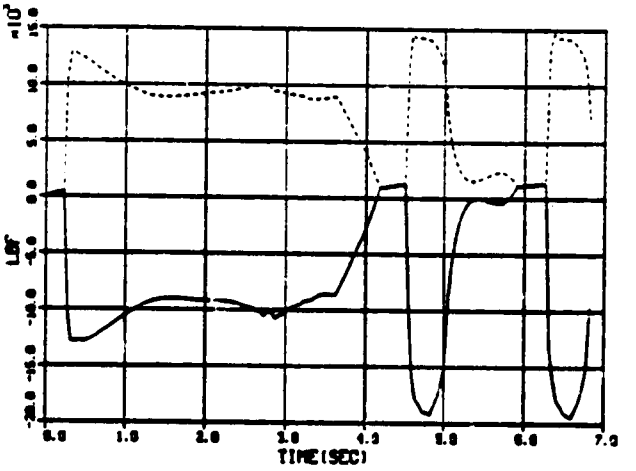

Figure 5.2-4 Lateral Force - Wheelset 2 - Truck B

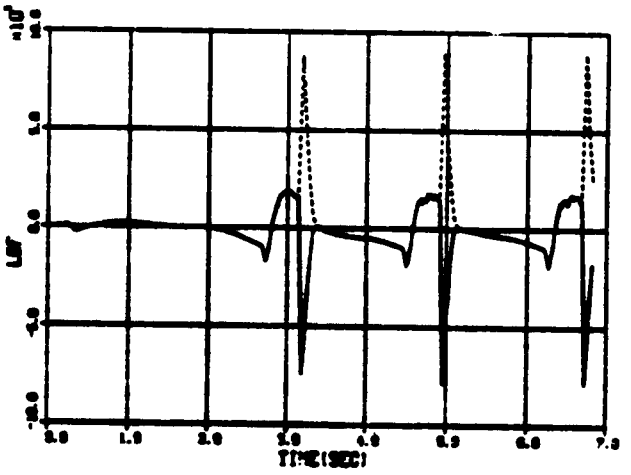

Figure 5.2-3 Lateral Forces - Wheelset 2 - Truck A

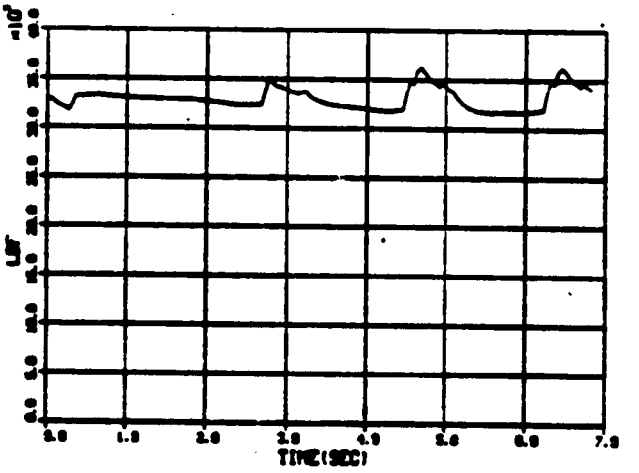

Figure 5.2-5 Vertical Force - Left Wheels - Truck A

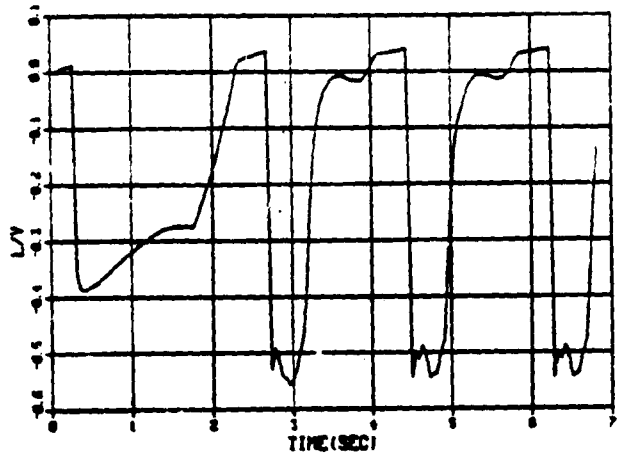

Figure 5.2-6 L/V - Leading Left Wheel - Truck A

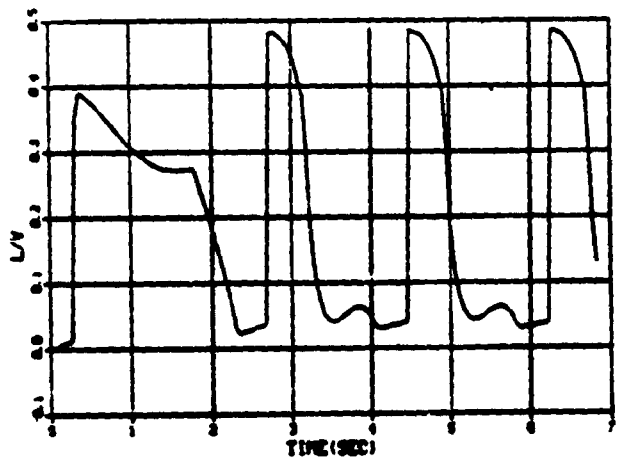

Figure 5.2-7 L/V - Leading Right Wheel - Truck A

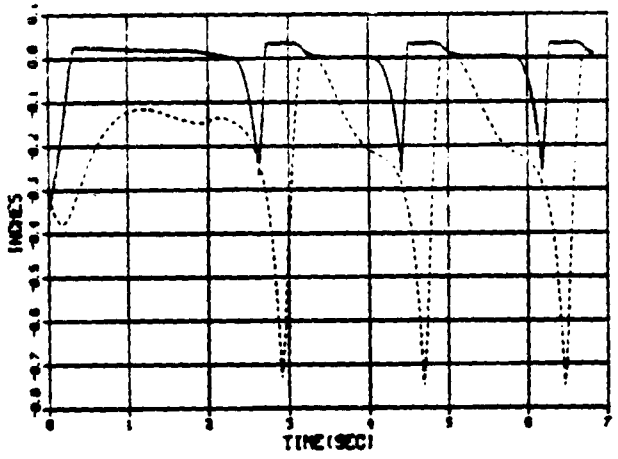

Figure 5.2-8 Flange to Rail Overlap - Left Wheels - Truck A

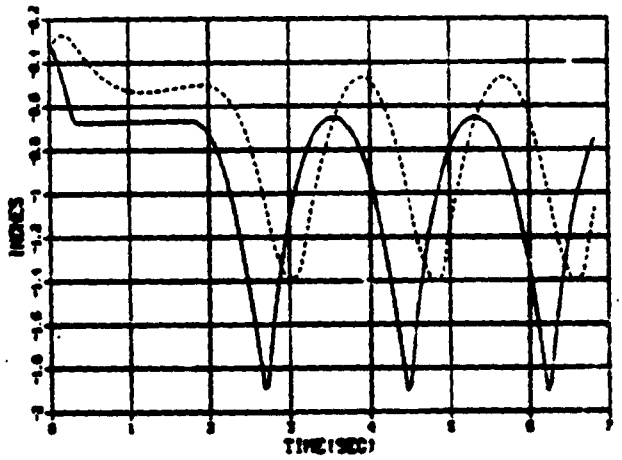

Figure 5.2-9 Flange to Rail Overlap - Right Wheels - Truck A

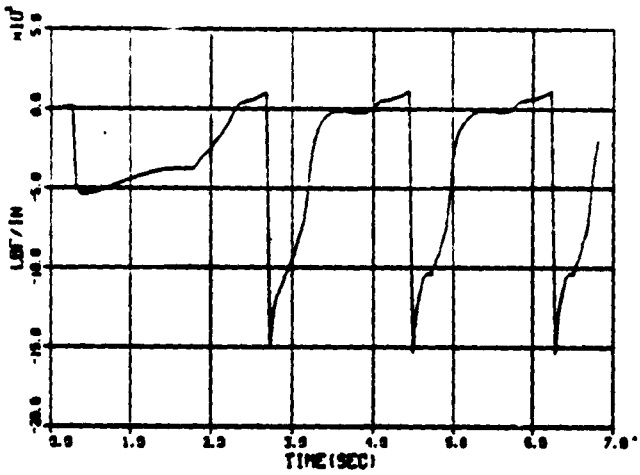

Figure 5.2-10 Linear Lateral Stiffness Required to Prevent Wheel Drop

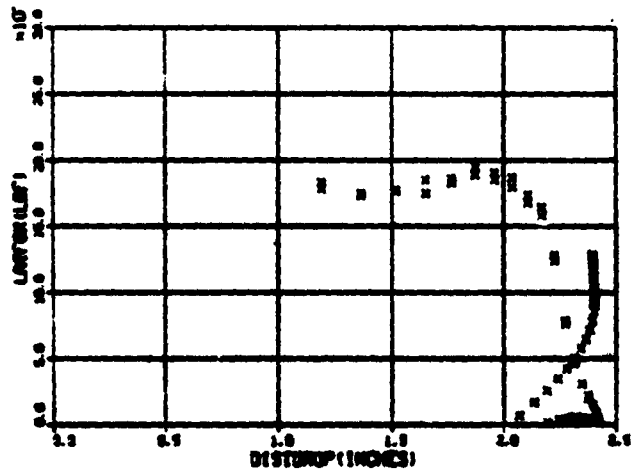

Figure 5.2-11 Leading Outer Wheel Force vs Distance to Leading Wheelset Drop

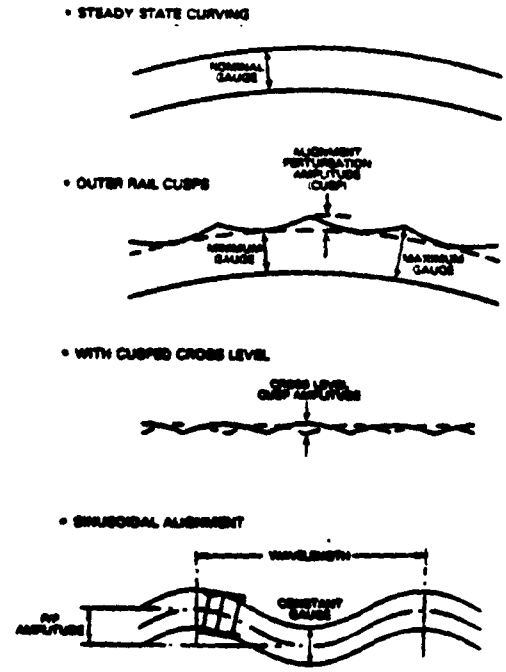

Figure 5.2-12 Track Scenarios

5.2.1 Steady State Curving

In order to provide a check with published behavior, described previously in Section 4.5, and to provide baseline data and information on the mechanics of curving, computer runs were undertaken simulating steady curving on ideal track with constant gauge. The basic run list is given in Table 5.2-1 showing the track superelevations for balanced curving.

In addition to runs carried out solely in steady curves, all other dynamic curving studies were preceded by 2 rail lengths of steady curving to provide appropriate initial conditions. These results were therefore available for further analyses of steady conditions and as a check on computational accuracy and especially to investigate the effect of friction and gauge changes on the response.

TABLE 5.2-1

TRACK SUPERELEVATION FOR BALANCED STEADY STATE CURVING (IN.)

CURVE DEGREES \ VEL MPH	15	20	25
5	0.761	1.353	2.114
10	1.522	2.706	4.059
15	2.283	4.059	6.342

5.2.2 Outer Rail Alignment Cusps

The list of runs planned and carried out under this track scenario is given in Table 5.2-2. These runs were planned to fulfill the following objectives.

- To find the values of minimum and maximum gauge which suggested incipient wheel drop or rail climb for curvatures of 3, 5, 8, 10, 15 degrees, for an appropriately poor scenario of the vehicle/track system.
- To establish the effect of friction using μ = 0.375; 0.5 and curvatures of 5; 10; 15 degrees.
- To establish the effect of speed and unbalance on the results over a speed range of 10 to 25 mph.

5.2.3 Outer Rail Alignment and Cross-level Cusps

The preliminary runs carried out in this study were intended to determine the sensitivity of additional response phenomena due to the combination of alignment, gauge and cross-level variation in curves. Running was limited to the definition of limiting values of outer rail alignment variation, which had not previously resulted in the prediction of incipient wheel drop or rail climb, as defined in Chapter 2.

A run list is given in Table 5.2-3. Minimum gauge was fixed at 56.5 in. for all runs. Maximum gauge was varied between 57.75 in and 56.5 in. Cross-level cusps were limited to 0.5, 0.625, and 0.75 in. A value for the coefficient of friction of 0.5 was used throughout. The study was carried out on a 10 degree curve superelevated to give balance at 15 mph. Speeds were varied between 14 and 16 mph to excite roll responses.

5.2.4 Sinusoidal Alignment Variation

This study was to determine response from track alignment variation alone. The study is divided into runs on tangent track and in 5 degree and 10 degree curves. The run list is given in Table 5.2-4.

Runs on tangent track were included, in order to obtain,

- Survey of the effect of amplitude at wavelength λ of 90 ft and 25 mph to provide baseline values.
- Runs at 5 in. and 3 in. peak/peak amplitudes for a range of λ of 39, 50, 75, 90 ft.
- Investigation of speed effect.
- Identification of critical values just preventing incipient wheel drop prediction.

In curving simulation with sinusoidal alignment variation the runs were arranged to satisfy the following requirements,

- Establish critical values just preventing incipient wheel drop prediction.
- Investigate gauge variation.
- Investigate speed variation.

The results of each of the investigations are discussed in the following sections.

TABLE 5.2-2

RUN LIST FOR OUTER RAIL CUSPS

RUN	BASIC CURVE		GAUGE PERTURBATION		WHEEL/ RAIL		SPEED
NO.	DEG	BALANCE SPEED MPH	MIN. GAUGE in.	MAX. GAUGE in.	PROFILES	μ	MPH
3/1	3	15	56.5	58.0	NEW	0.375	15
3/2			57.0	58.5			
3/3			56.5			0.5	
5/1	5	15	56.5	58.5	NEW	0.375	15
5/2			58.0				
5/3			58.5			0.5	
5/4		25	58.0			0.375	25
5/5			58.5				
5/6		35					35
5/7		45					45
5/8		25					15
5/9							32
5/10							40
5/11							45
5/12		15	57.0	58.0		0.5	15
5/13			56.5	57.75			
5/14			56.0				
5/15				58.0			
5/16			56.5				
8/1	8	15	56.5	58.5	NEW	0.375	15
8/2				58.0			
8/3			57.0	158.5			
10/1	10	15	56/5	58.5	NEW	0.375	15
10/2			57.0				
10/3			56.5	58.0			
10/4				58.5		0.5	
10/5						0.375	
10/6			57.0	57.75		0.5	
10/7			56.0				
10/8			56.5				

TABLE 5.2-2
RUN LIST FOR OUTER RAIL CUSPS (Continued)

RUN	BASIC CURVE		GAUGE PERTURBATION		WHEEL/ RAIL		SPEED
NO.	DEG	BALANCE SPEED MPH	MIN. GAUGE in.	MAX. GAUGE in.	PROFILES	μ	MPH
15/1	15	15	56.5	58.5	NEW	0.375	15
15/2	↓	↓	↓	58.0	↓	↓	↓
15/3	↓	↓	57.0	58.5	↓	↓	↓
15/4	↓	↓	56.5	↓	↓	0.5	↓
15/5	↓	↓	↓	58.0	↓	↓	↓
15/6	↓	↓	57.0	↓	↓	↓	↓
15/7	↓	↓	↓	57.57	↓	0.375	↓
15/8	↓	↓	56.5	↓	↓	0.5	↓
15/9	↓	↓	56.0	↓	↓	↓	↓
15/10	↓	↓	↓	57.5	↓	↓	↓
15/11	↓	↓	57.0	↓	↓	↓	↓

TABLE 5.2-3
RUN LIST OUTER RAIL CUSPS AND X-LEVEL CUSPS

RUN	BASIC CURVE		GAUGE PERTURBATION		X-LEVEL PERTN	WHEEL/ RAIL		SPEED
NO.	DEG	BALANCE SPEED MPH	MIN. GAUGE in.	MAX. GAUGE in.	CUSP AMPLITUDE in.	PROFILES	μ	MPH
x/1	10	15	56.5	57.75	0.0	NEW	0.5	13
x/2	↓	↓	↓	↓	0.5	↓	↓	14
x/3	↓	↓	↓	↓	↓	↓	↓	15
x/4	↓	↓	↓	↓	↓	↓	↓	16
x/5	↓	↓	↓	↓	↓	↓	↓	15
x/6	↓	↓	↓	↓	0.625	↓	↓	↓
x/7	↓	↓	↓	56.5	0.5	↓	↓	↓
x/8	↓	↓	↓	↓	0.625	↓	↓	↓
x/9	↓	↓	↓	↓	0.75	↓	↓	↓

TABLE 5.2-4

RUN LIST FOR SINUSOIDAL ALIGNMENT VARIATION

RUN	BASIC CURVE		ALIGNMENT PERTURBATION		GAUGE	WHEEL/ RAIL		SPEED
NO.	DEG	BALANCE SPEED MPH	WAVE LENGTH in.	DOUBLE AMPLITUDE in.	CONSTANT in.	PROFILES	μ	MPH
T/1	0	-	1080	3.85	56.5	NEW	0.5	25
T/2				3.0				
T/3				5.0	58.0			
T/4			900					
T/5			600					
T/6			468					
T/7			1080	3.0				
T/8			900					
T/9			600					
T/10			468					
T/11			1080					15
T/12			900					
T/13			600					
T/14			468					
T/15			1080	3.5	57.75			
T/16			600	1.0	58.0			
T/17				2.0	57.75			
T/18					58.0			
T/19			1080	4.5	57.75			
T/20					57.5			
T/21			900	3.25	57.75			
T/22			600	1.75				
T/23			468	1.33				
T/24			600	1.5				
T/25				1.125				
T/26								
T/27								35
T/28								45
T/29			600					25
T/30				1.125				5
T/31								60
T/32								80
T/33								100
C/1	5	25	1080	4.5	57.75	NEW	0.5	25
C/2			900	3.25				
C/3			600	1.25				
C/4			468	1.333				

TABLE 5.2-4

RUN LIST FOR SINUSOIDAL ALIGNMENT VARIATION (Continued)

RUN	BASIC CURVE		ALIGNMENT PERTURBATION		GAUGE	WHEEL/RAIL		SPEED
NO.	DEG	BALANCE SPEED MPH	WAVE LENGTH in.	DOUBLE AMPLITUDE in.	CONSTANT in.	PROFILES	μ	MPH
C/5	10	25	1080	4.5	57.75	NEW	0.5	25
C/6			900	3.25				
C/7			600	1.25				
C/8			468	1.333				
C/9	15		1080	4.5				
C/10			900	3.25				
C/11			600	1.25				
C/12			468	1.333				
C/13	10		1080	4.5	57.5			
C/14			900	3.25				
C/15			600	1.25				
C/16			468	1.333				
C/17	15		1080	4.5				
C/18			900	3.25				
C/19			600	1.25				
C/20			468	1.33				
C/21	5				57.75			15

5.3 STEADY-STATE CURVING

As a preliminary to defining the study plan for gauge, alignment and cross-level variation in curves, the program was used to study vehicle performance in steady-state curving. Each dynamic curving run was also preceded by a short section in steady curving as a baseline for the dynamic results, to provide an appropriate initial condition, and to provide additional understanding of curving mechanics. The predicted forces and moments for steady-state curving in 5, 10, and 15 degree curves, at balance speed, are shown in Fig. 5.3-1, for the parameters given. The leading outer wheel sustains the largest force in full flange contact and with its opposite on the inside rail comprises a pair of gauge spreading forces which may become large. In tight curves, there is little moment on the lead axle. The second axle, however, sustains a large moment, but only small lateral forces, due to its nearly radial position.

Thus, the wheel/rail forces are predominantly across-track (lateral) for the leading and along-track (longitudinal) for the trailing axle. An often used estimate provided by test results is the measure of the L/V of the leading inner wheel to estimate μ, the friction coefficient. In the case of the 10 degree curve illustrated in Fig. 5.3-1, this result suggests a μ of 0.34 compared to that of 0.375 used in the computation and representing the fully saturated value. It may be concluded that a small but significant component of the low rail force is along the track. The value of lateral forces for μ = 0.5 is given for the 15 degree curve in Fig. 5.3-2 showing that a potential exists for gauge spreading and rail rollover for track having low rail strength/stiffness or a requirement for a minimum track strength/stiffness.

Figure 5.3-3 shows a graph of wheel/rail forces against curvature for the values of μ = 0.375 given previously, and also for μ = 0.5, over the range of curvatures of 3° to 15°. A gauge of 56.5 in. was used throughout. As expected from the preceding discussion of tight curves with saturated creep forces, the larger coefficient of friction μ, produces larger forces in steady-state curving. There appears to be little difference due to these friction levels between lead outer rail forces below

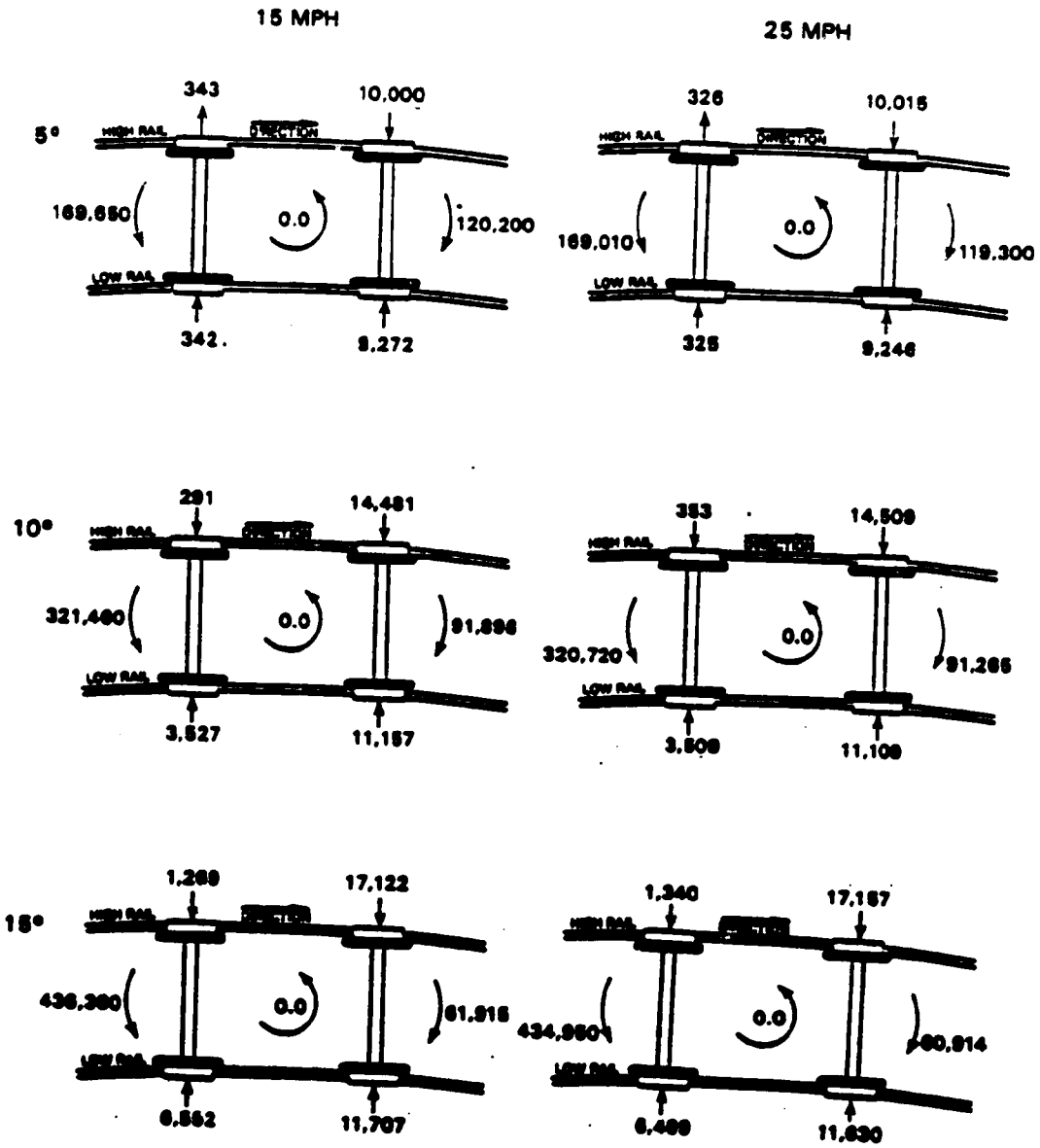

μ = 0.375; GAUGE = 56.5 in.; BALANCED SUPERELEVATION
V = 32,668 lb; μW = 733,367 lb in.; μV = 12,326 lb

Figure 5.3-1 The Effect of Speed and Curvature on SYNCAR Steady State Curving Forces and Moments

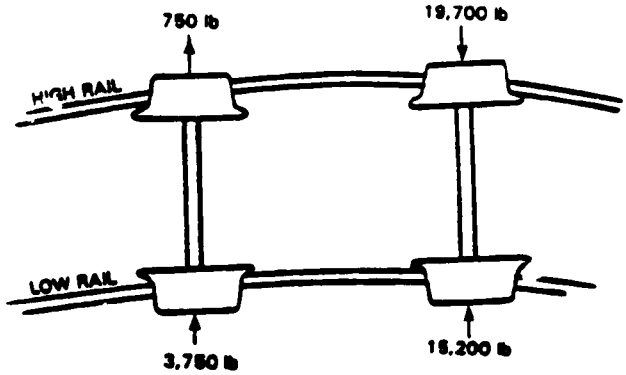

LATERAL FORCES ON TRUCK AXLES NEGOTIATING 15° CURVE WITH NO IRREGULARITY
GAUGE = 56.5 in. $\mu = 0.5$

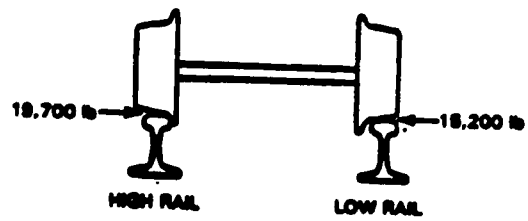

LATERAL GAUGE SPREADING FORCES ON LEAD AXLE OF TRUCK NEGOTIATING 15° CURVE

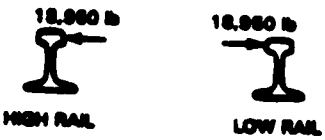

LATERAL FORCES ON RAILS PRODUCED BY TRUCK NEGOTIATING 15° CURVE

Figure 5.3-2 Lateral Steady State Forces for High Friction and Tight Curving

curvatures of 5 degrees, probably due to the combined rotation of the force vector in the contact patch and reduction below full slippage.

Lateral forces were also produced for $\mu = 0.375$, over the same range of curvatures, to assess the effect of gauge changes on steady curving indicated by the SINCAR model. The results are given in Fig. 5.3-4. In tight curves, which tend to produce gross slippage, the lateral forces are not very sensitive to change in gauge. However, in the smaller curvatures, increased gauge, and resulting larger rolling radius difference between wheels produce a larger steering moment on the leading axle. The result is a reduced total (net) lateral force on this axle which is predicted to change sign for the lower curvatures. (The inner wheel lateral force becomes larger than the outer). The individual lateral forces are also less for the wider gauge.

5.4 CURVING WITH HIGH RAIL OUTWARD CUSPS

The objective of the use of high rail cusps in curves in this study was to establish the effect of gauge change within the jointed rail length, under a track geometry perceived to give poor

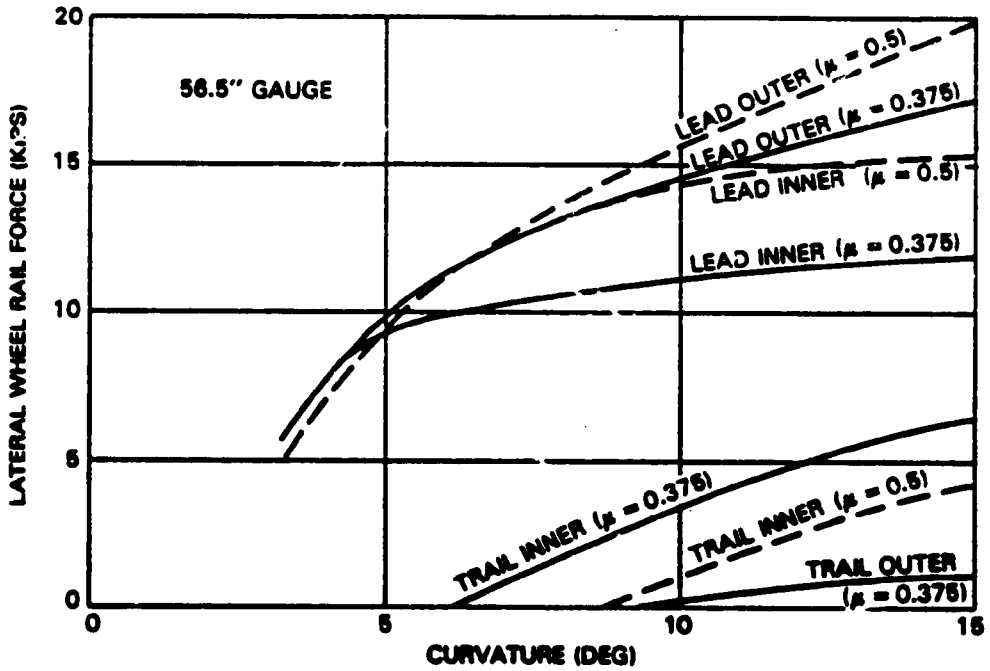

Figure 5.3-3 Effect of Friction Coefficient-Steady State Curving Forces-Loaded 100 Ton Car Balanced Speed - Standard 3-Piece Truck

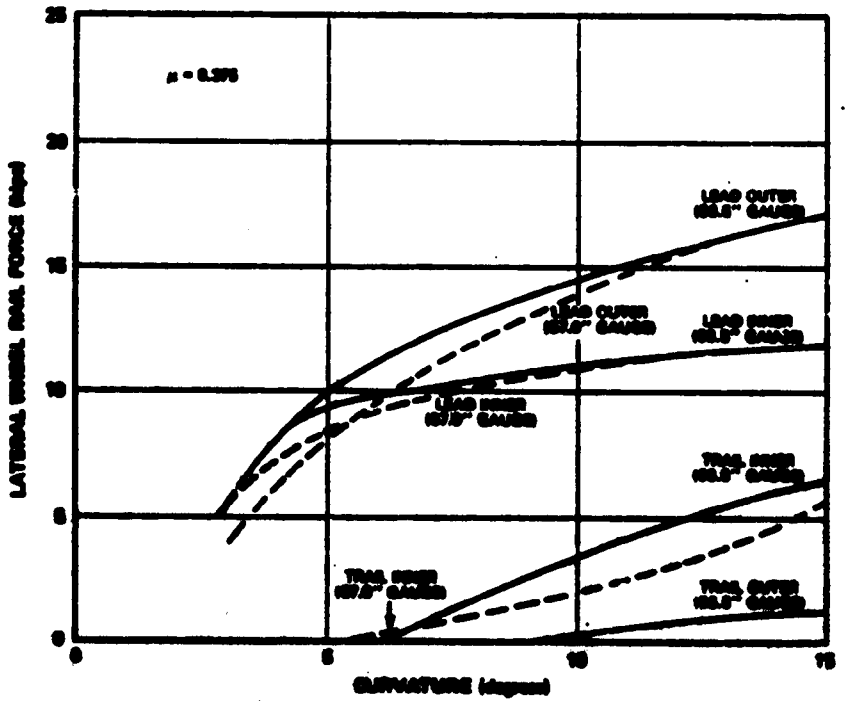

Figure 5.3-4 Effect of Gauge Variation-Steady State Curving Forces-Loaded 100 Ton Car Balanced Speed - Standard 3-Piece Truck

response to the 100 ton hopper car. The curving process under these track perturbation has been illustrated in the sample plotted outputs given in Section 5.2. In particular the graph of wheelset position relative to the track, Fig. 5.2-1, showed that, for this curve, the outer wheel flange of the leading axle remains in contact with the outer rail for most of its length, leaving for a small distance in this case, just prior to the joint, and hitting the rail again just beyond the joint. At the higher track curvatures outer wheel flange separation does not generally take place.

The maximum lateral force occurs on both wheels of the leading axle immediately following the joint at flange contact, where the angle of attack of the wheel to the rail is greatest. This is also illustrated in Fig. 5.2-2. Thus, the maximum or peak force occurs close to the widest gauge at the joint. The joint location is also a potential weakness in lateral restraint on the track. Vertical force varies little during the run, as seen in Fig. 5.2-5. On the low rail, the right, non-flanging - wheel L/V (Fig. 5.2-3) approaches μ = 0.5 for the case illustrated.

Interest in the results presented here is focussed on the worst response for gauge spreading and potential for wheel drop. In this scenario, rail climb appears to be less likely although results were also produced to indicate its occurrence for much larger cusp amplitudes.

Initial runs were carried out using a coefficient of friction, μ, of 0.375 found characteristic of the Starr results given in Chapter 4. With a minimum gauge of 56.5 in., Fig. 5.4-1 shows the effect of varying maximum gauge (or cusp amplitude) on peak outer wheel lateral forces, over the range of curvatures of 3 to 15 degrees. Since the low rail is not perturbed the maximum gauge is the cusp amplitude added to the minimum gauge. The superelevation was set constant to provide balance at the 15 mph running speed. For comparison the Nadal value for this friction level and a new flange angle of 67° is 34, 568 lb. It is not approached by these results, supporting the contention that rail climb prediction is unlikely. As might be expected, both increased curvatures and larger outer rail cusps provide an increase in outer rail force. This increase is not proportional. The results suggest less increase in force for larger values of curvature and cusp amplitude.

The variation in minimum gauge has a lesser effect, as shown in Fig. 5.4-2; the wider the gauge, the lower the peak lateral force on the outer wheel. This result was also produced at a balanced speed of 15 mph throughout. The inner rail force remains approximately constant over the range of curvatures investigated.

For a coefficient of friction of 0.5 and flange angle of 67°, the Nadal value of lateral force becomes 28,007 lb. It is clearly more likely that rail climb take place in high curvatures, with the higher level of friction more typical of dry running. The effect of this is shown in the results summarized in Fig. 5.4-3 for a minimum gauge of 56.5 in. and a maximum gauge of 58.5 in. The lateral force for the higher friction coefficient approaches that suggested by Nadal as indicative of rail climbing. However, as later results will show, the rail spreading forces are sufficient to cause wheel drop at smaller values of cusp amplitude, or maximum gauge, than those indicating rail climb here.

The preceding results show the expected trends in behavior and support the contention and observations of tests, such as those performed at Starr, Ohio and described in Chapter 4, that rail spreading is the more likely cause of derailment, especially where the lateral track stiffness is low. The remaining discussion in this scenario is devoted to the assessment of largest values of gauge which are predicted not to give incipient wheel drop under dynamic wide gauge on weak track. Curves of 5, 10 and 15 degrees are used in this investigation. The distance to wheel drop is calculated using the method described in Section 2.4.3. Incipient wheel drop is investigated by comparing the computed outer wheel lateral force and distance to wheel drop to those permissable from the high rail stiffness, after subtracting the spreading due to the low rail. The low rail force is assumed to be constant for these runs, at a value close to the limit, appropriate to the chosen coefficient of friction. The results computed are for μ = 0.5.

Figures 5.4-4 and 5.4-5 show the results for the 5 degree curve. For the smaller maximum gauge of Fig. 5.4-4, the results do not approach the limit set by the track stiffness. However, in Fig. 5.4-5, the result for a minimum gauge of 56.5 in. and a maximum of 58.0 in. touches the high rail stiffness characteristic, above which incipient wheel drop is predicted. This was the result used for the sample output given

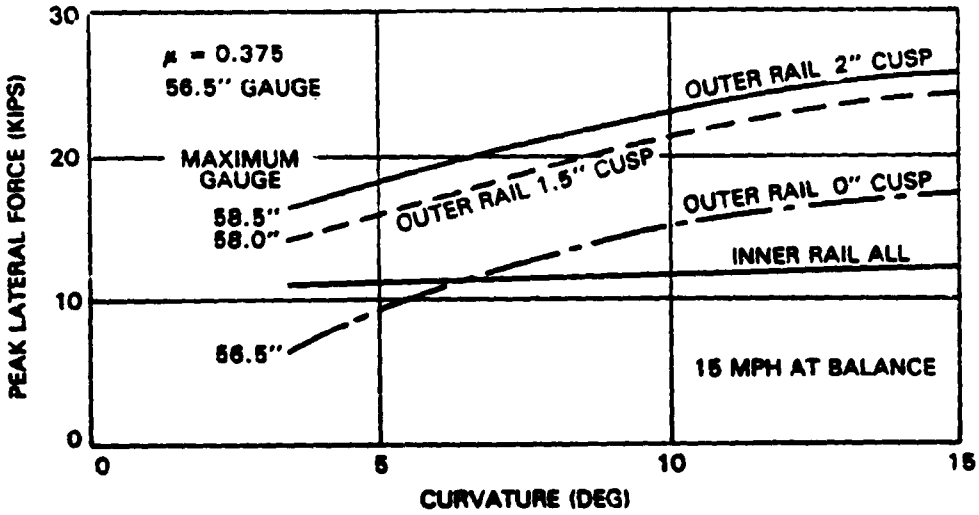

Figure 5.4-1 Effect of Cusp Amplitude, Peak Wheel Rail Forces, for Lead Axle Negotiating Curve with Outward Cusps

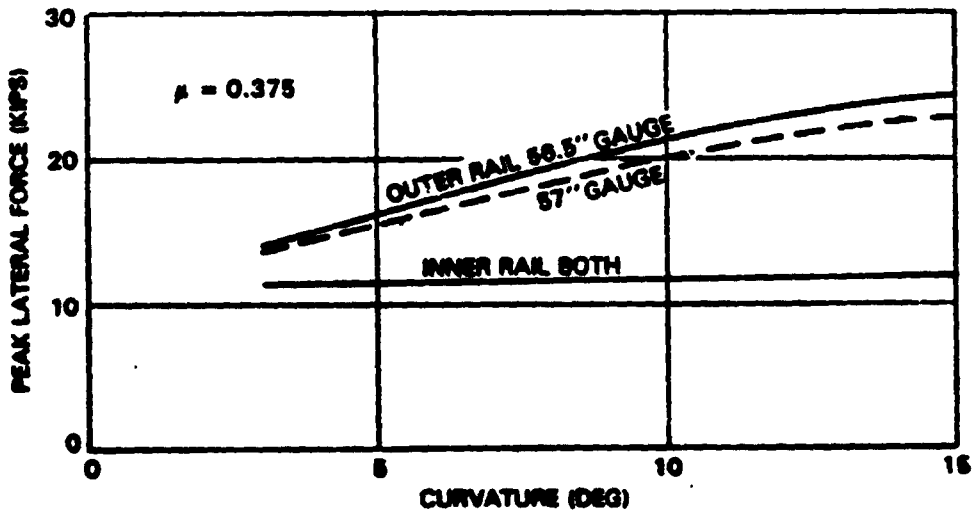

Figure 5.4-2 Effect of Minimum Gauge Variation, Peak Wheel Rail Forces on Lead Axle, Negotiating Curve With 1.5" Outward Cusps

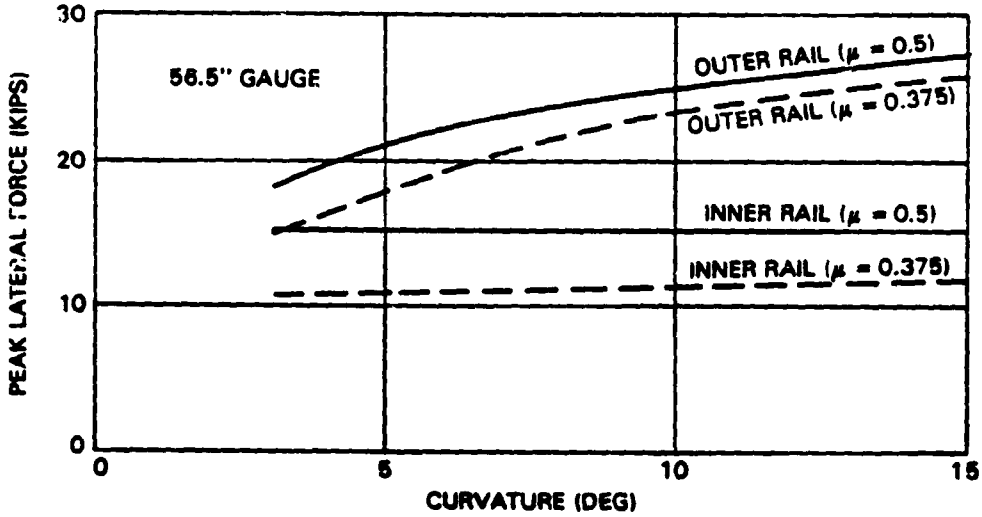

Figure 5.4-3 Effect of Friction Coefficient, Peak Wheel Rail Forces for Lead Axle, While Negotiating Curve with 2" Outward Cusps

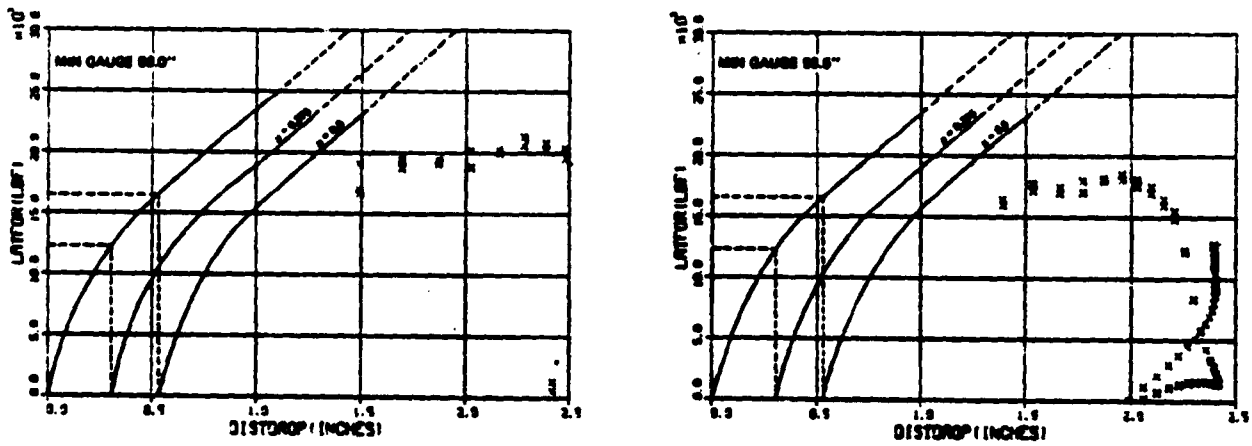

Figure 5.4-4 Wheel Drop Tendency in a 5 Degree Curve Maximum Gauge 57.75 in.

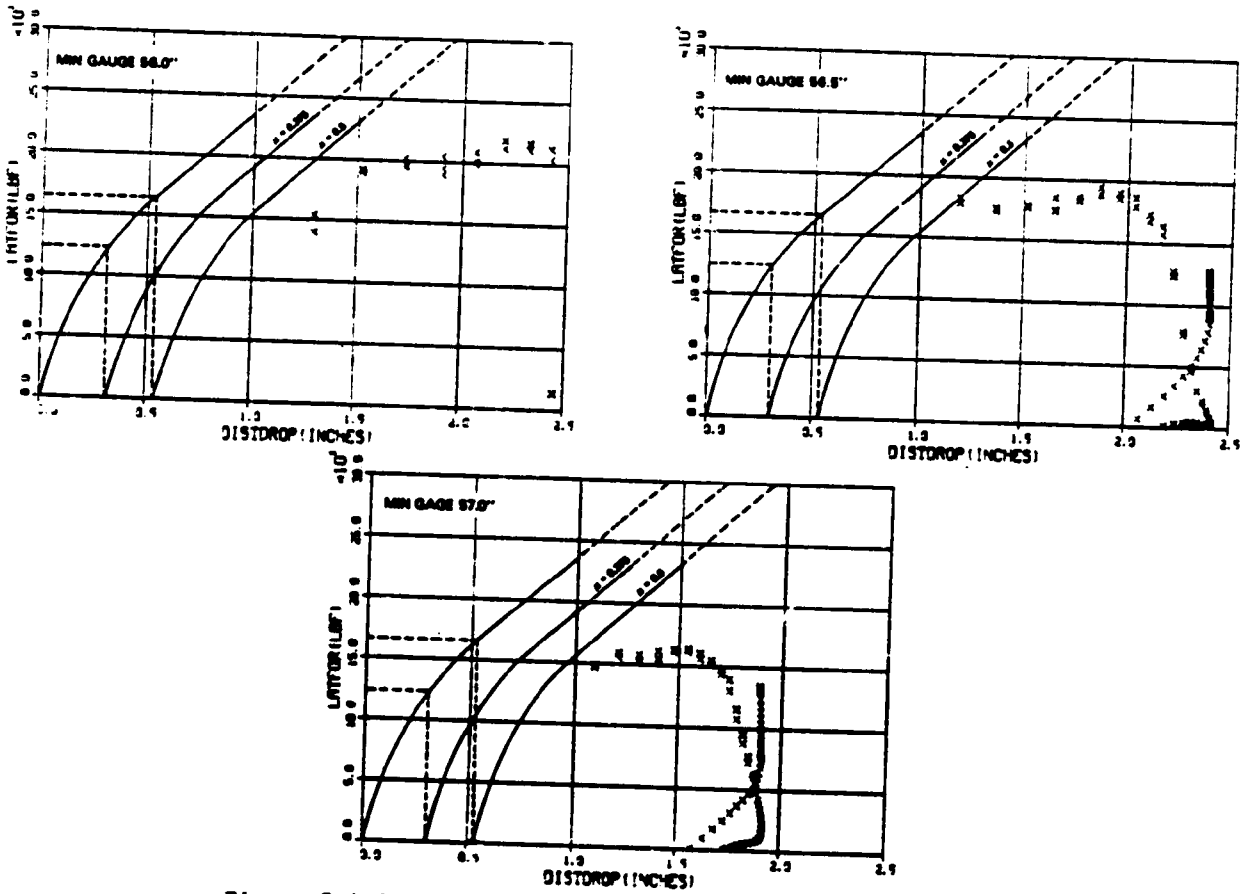

Figure 5.4-5 Wheel Drop Tendency in a 5 Degree Curve Maximum Gauge 58.0 in.

previously in Fig. 5.2-1 through 5.2-11. The small peak in lateral force on the leading edge of the time history in Fig. 5.2-2 contributes to the value indicating incipient wheel drop. Since no such peak is observed in Fig. 5.2-4 for the leading axle of the trailing truck, it may be "analytical", rendering the result slightly conservative.

For the 10 degree curve, the results for a maximum gauge of 57.75 in., are given in Fig. 5.4-6. In this case the result for tight minimum gauge of 56.0 in. show a clear prediction of exceedance of the wheel drop line for $\mu = 0.5$. This result is slightly different from the other 10 degree results in that the outer wheel flange leaves the gauge face of the rail for a short distance and even hits the low rail briefly, as shown by the wheelset path in Fig. 5.4-7. However all the results for a maximum gauge of 57.75 in. in 10 degree curves show a proximity to the incipient wheel drop limit. It is generally recognized that a wide gauge of 59 in. can cause wheel drop. This is consistent with the result given here since the incipient wheel drop limit, chosen in Section 2.4.3, represents a margin of safety of 1.25 in. of tread overlap by the wheel on the low rail.

The results for the computer simulation in the 15 degree curve for the maximum gauge of 57.75 in. are given in Fig. 5.4-8. Both minimum gauges produce an exceedance of the incipient wheel drop limit. A safer condition is identified from Fig. 5.4-9 for a maximum gauge of 57.5 in. Although the lateral forces reach similarly high values, the reduction in clearance of 0.25 in. is adequate to prevent incipient wheel drop.

All the results discussed above have been produced for a hypothetic curve at a 15 mph balance speed. Running at 3 in. overbalance represents a 5% transfer of load to the outer wheel, lowering

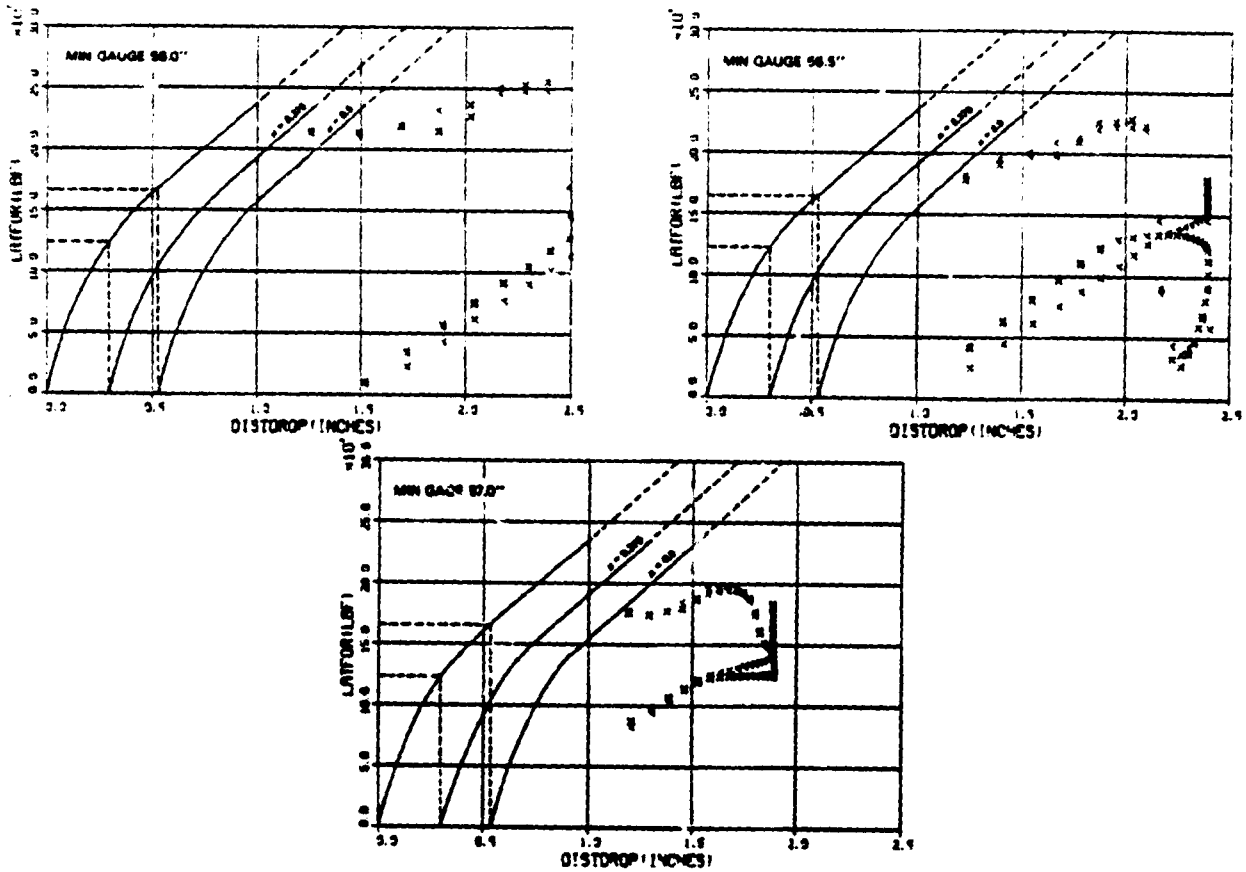

Figure 5.4-6 Wheel Drop Tendency in a 10 Degree Curve
Maximum Gauge 57.75 in.

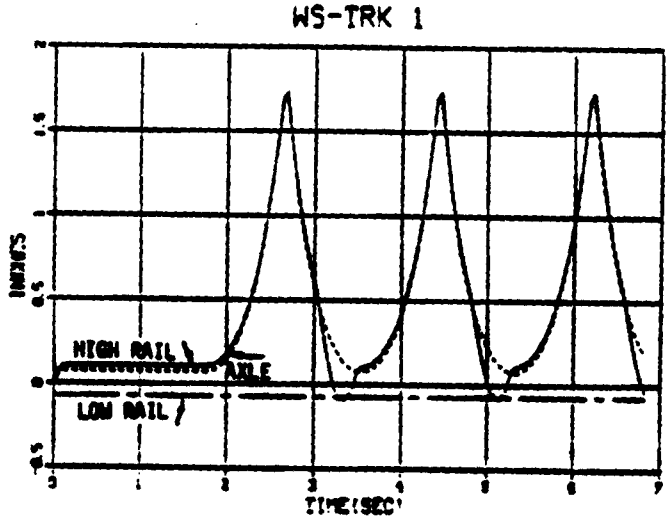

Figure 5.4-7 High and Low Leading Wheel Clearances
10 Degree Curve
15 mph at Balance; $\mu = 0.5$
Minimum Gauge 56.0 in.
Maximum Gauge 57.75 in.

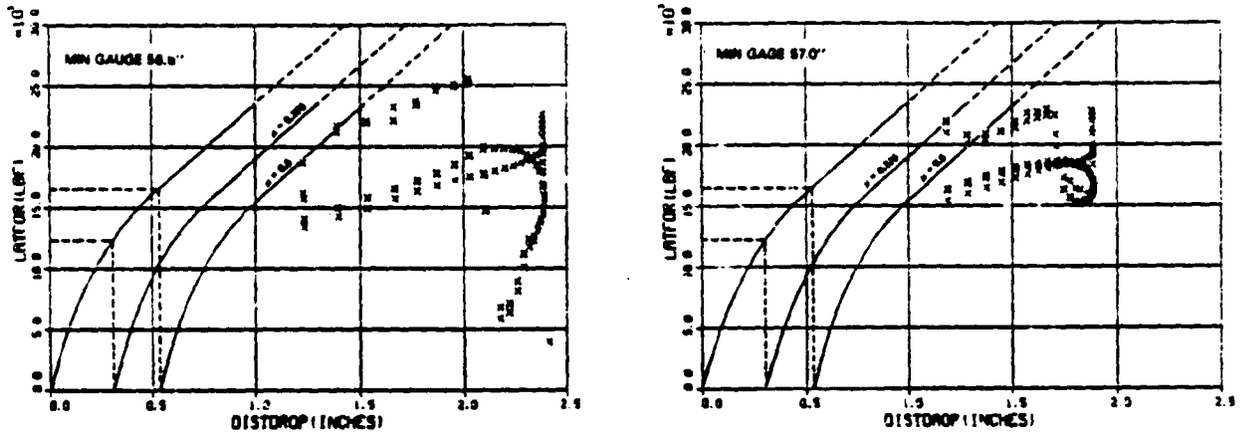

Figure 5.4-8 Wheel Drop Tendency in a 15 Degree Curve Maximum Gauge 57.75 in.

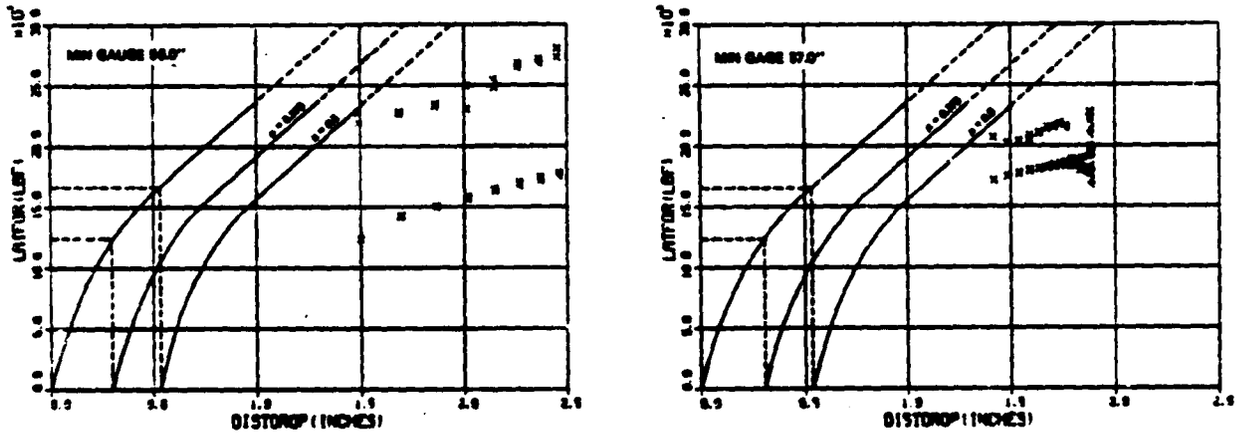

Figure 5.4-9 Wheel Drop Tendency in a 15 Degree Curve Maximum Gauge 57.5 in.

of the inner, and a resulting increase in the outer peak wheel lateral force. Figure 5.4-10 shows that for 3 in. overbalance the reduced inner rail force permits a 10% higher outer rail force for a 12 degree curve in the region of 20,000 lb without wheel drop. This is shown in Fig. 5.4-11 to be just over that predicted in the same curve for the outer rail at the 3 in. overbalanced condition. It may be concluded that the results are not seriously affected by under or overbalanced running in the range considered normal for freight vehicles.

5.5 CURVING WITH COMBINED HIGH RAIL ALIGNMENT AND CROSS LEVEL CUSPS AT JOINTS

In the preceding section the response of the 100 ton hopper was reported for a track scenario with alignment cusps in the high rail alone. There exists the possibility that, if these are combined with a cross level input, coupling

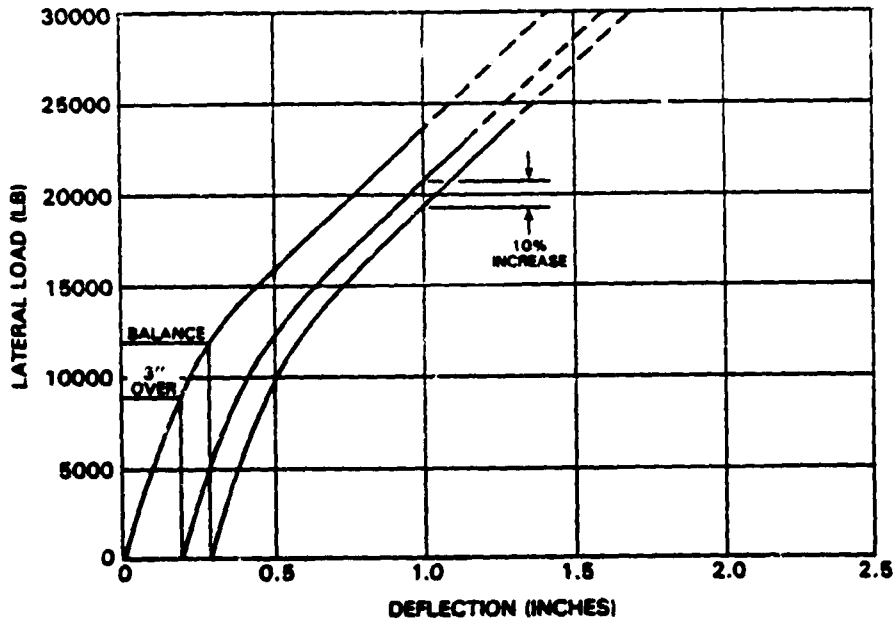

Figure 5.4-10 Modification to Rail Restraint Capacity at 3 in. Overbalance in 12 Degree Curve

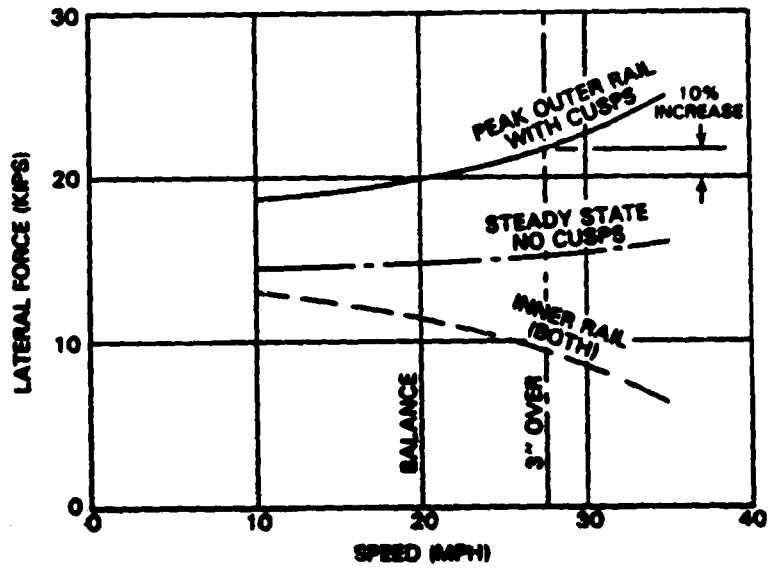

Figure 5.4-11 Effect of Cant Deficiency in 12 Degree Curving $\mu = 0.5$; New Profiles; Minimum Gauge - 56.5 in.; Maximum Gauge - 57.75 in. (in Cusps)

will take place, rendering the response to the combination worse than each individual scenario. This might lead to the requirement for a further limitation of track geometry to prevent a new potential for derailment. The computer predictions in this combined scenario were carried out to examine whether the response produced worse results than those in the previous section for alignment and gauge alone or the periodic cross level cusps studies by

TSC and used to verify the simulation program in Section 2.2 (see also Ref. 6 and 7).

One manner in which the response to the combined inputs might cause rail climb is that of a lateral disturbance during dynamic wheel unloading in roll. The study therefore concentrated on roll angle, lateral and vertical forces and the tendency to climb the rail, as indicated by the excursion of the wheel beyond flange contact. A 10 degree curve with elevation for balance at 15 mph is used throughout.

The response in roll is shown in Fig. 5.5-1 for ½ in. and 5/8 in. cross level cusps at the speed of 14 mph close to the roll resonance. The roll angle amplitude is large and suggests an angle above 5° for the 5/8 in. input. The run for the same speed at the lower crosslevel of ½ in. was significantly lower. These results suggest that body roll in curves is not greatly different from that in tangent track and is not strongly influenced by outer rail alignment variations within the limits studied here. (Note: these graphs have a different scale for roll angle.)

Figure 5.5-2 presents a comparison of lateral forces for the same runs. In general the lateral forces exceed 20,000 lb. However, the critical information on performance lies in the phasing with the dynamic vertical load given in Fig 5.5-3. The roll resonance leads to complete unloading of the wheels for the 5/8 in. cross-level. (A small negative vertical force is indicated due to the fact that the snubbing force as modeled does not cease at wheel lift off.)

The results for the 15 mph run, with 5/8 in. crosslevel cusps, reveals that the left (outer) wheel lifts off just prior to 16.5 sec. into the run. This just preceeds the maximum roll angle in this cycle. At the same instant the outer wheel lateral force is zero and the "non-flanging" wheel force is 10,000 lb. However immediately following this the flanging wheel lateral force approaches 20,000 lb with a vertical force of approximately 10,000 lb. Thus an L/V of 2 is sustained for a significant time. The result is a rail climb derailment indicated more clearly by the value of left wheel flange overlap of the rail (DYLF 12) in Fig. 5.5-4. This overlap on the outer

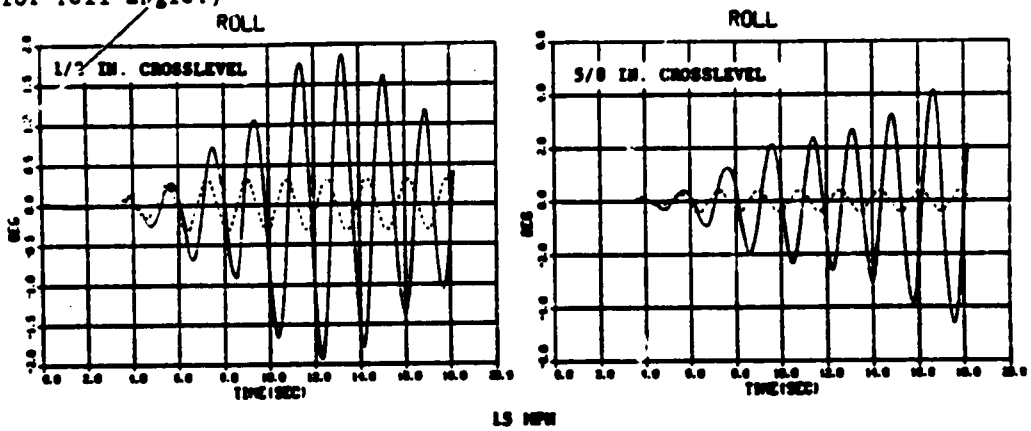

Figure 5.5-1 Roll Response of 100 Ton Car to Crosslevel Variations in 10° Curve with Gauge Varying from 56-1/2 in. - 57-3/4 in. (1-1/4 in. Cusp)

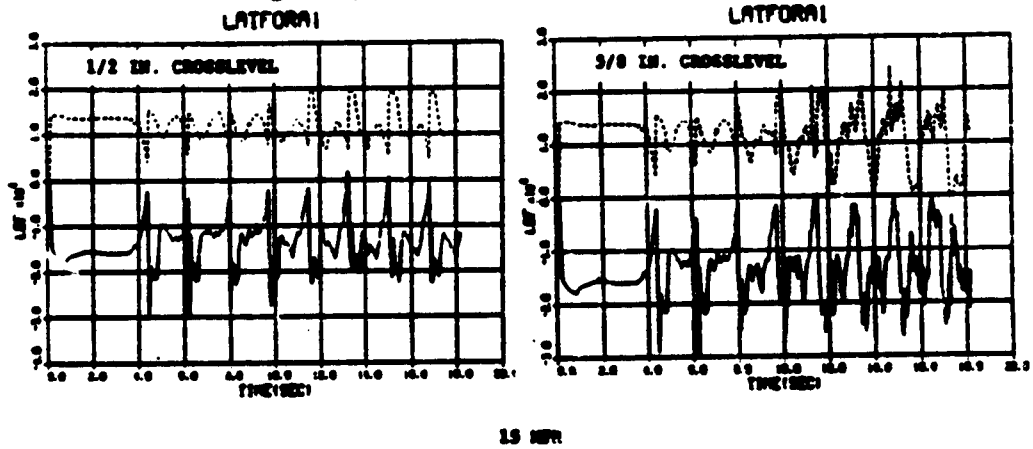

Figure 5.5-2 Lateral Force - Leading Axle-High Rail - 10° Curve with Crosslevel Variation on Gauge 56-1/2 in. to 57-3/4 in. (1-1/4 in. Cusps)

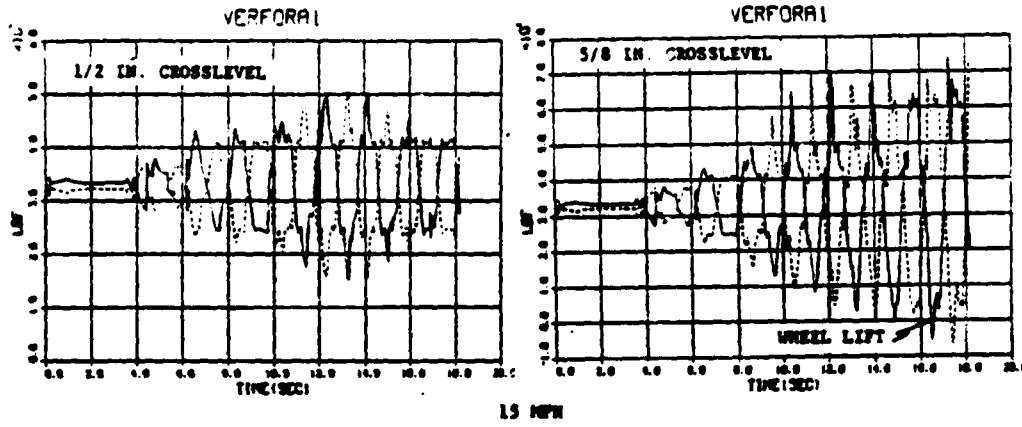

Figure 5.5-3 Vertical Force - Leading Axle-High Rail - 10° Curve with Crosslevel Variation and Gauge 56-1/2 in. to 57-3/4 in. (1-1/4 in. Cusps)

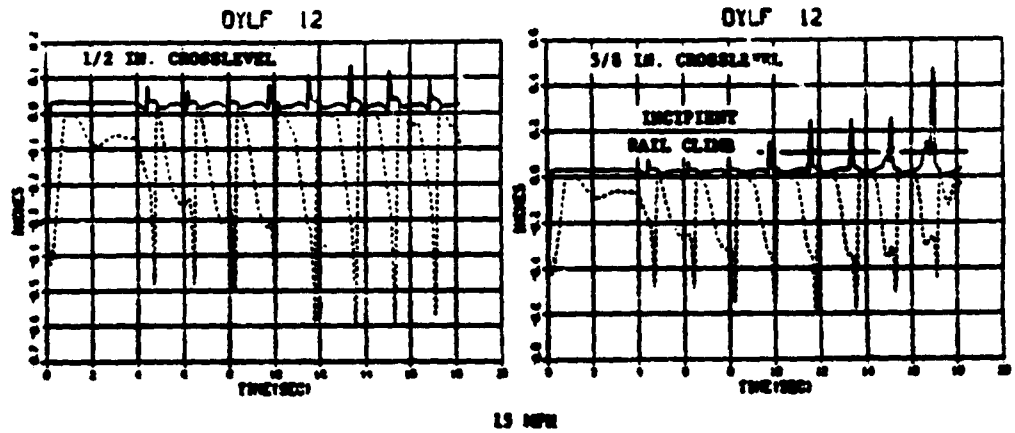

Figure 5.5-4 Rail Climb Tendency in 10 Degree Curve (1-1/4 in. Cusps) with Crosslevel Variation and Gauge 56-1/2 in. to 57-3/4 in.

wheel is represented by the solid line having positive values. No similar flange climb derailment is predicted for the 1/2 in. cross level variation, although an overlap of 0.1 is approached for very short intervals.

It is possible to conclude from these results for curvatures of 10° that a flange climb derailment is predicted for the combined excitation by track with values of crosslevel and gauge variation deemed just safe from separate excitation in earlier studies at the same speed. Thus the combined excitation suggests geometric limits smaller than those appropriate from the separate cross-level and gauge studies for the same curvature. Further studies are necessary to identify the new limits just providing safety from derailment.

5.6 SINUSOIDAL ALIGNMENT VARIATION WITH CONSTANT GAUGE

The track geometric variations discussed in the Sections 5.4 and 5.5 concern single rail perturbations. These correlate with gauge and cross level for the track geometry as measured. Although single rail alignment contributes to measured track alignment the results do not provide a particularly bad scenario for ascertaining values of track alignment which may provide derailment. The experience with measured track geometry (Ref 3) and knowledge of the most likely response in lowest damped kinematic mode of vehicle oscillation (Fig. 2.3-1) suggested that a sinusoidal track alignment with constant gauge be studied. This also includes conditions rather similar to transient irregularities such as those identified in Ref. 3 as the jog or sinusoidal (single wavelength) also occurring in spirals.

Initial studies were carried out on tangent track with a track wavelength of 90 ft, a gauge of 58.0 in. and 5.0 in. peak to peak (p/p) alignment amplitude. The chosen speed for these initial studies was 25 mph and the friction coefficient $\mu = 0.5$.

Figure 5.6-1 shows the path of the wheelset and the lateral force history for the widest gauge of 58.0 in. Increasing the gauge not only decreases the lateral distance before wheel drop is predicted, but also presents the outer wheel with a larger angle and tighter curvature at the point of flange contact, resulting in a larger lateral force. In the initial runs the largest lateral force occurring at the first peak in Fig. 5.6-1, for a gauge of 58.0 in., and 5 in. p/p alignment amplitude is 19,000 lb. This force reduces to 16,000 lb for 3 in. p/p input. The 3 in. p/p input with a gauge reduced to 56.5 in. gave a lateral force of 12,000 lb. The conclusion drawn from these initial results using the rail restraint curve described in Section 2.4.3, is that for the 90 ft wavelength the results indicate incipient wheel drop well before rail climb and a greater likelihood with increasing gauge and alignment amplitude.

The effect of wavelength is shown in Fig. 5.6-2 for a gauge of 58.0 in. and alignment amplitude of 3 in. peak/peak. While this amplitude suggests a marginally safe condition for the 90 ft wavelength, wheel drop is predicted for the smaller wavelengths. Indeed rail climb is predicted for the 50 ft and 39 ft wavelength as indicated by the sudden reduction in the distance to wheel drop (DISTDROP) at the Nadal value of L = 22,000 lb or L/V = 0.85. The vertical load at this point is reduced to 26,000 lb due to a body roll angle of more than 1.5°. In this condition, as seen from behind in a curve to the right, the left wheels are flanging as they are vertically unloaded dynamically due to clockwise body rotation. This combination of truck translation to the left and clockwise body rotation give an instantaneous center of rotation to the body above axle height. The motion is generally called upper center roll or sway and is one of the two modes of vehicle oscillation which may be excited during the kinematic oscillation known as hunting. It is discussed in Section 2.2.5. Since the hunting oscillation is least damped at a particular wavelength, generally below 75 ft, smaller alignment amplitudes are necessary at this wavelength to prevent incipient wheel drop and rail climb. This wavelength varies with the effective cone angle of the wheels and with track curvature.

Figure 5.6-3 shows the results for critical values of alignment amplitude and gauge for a wavelength of 50 ft. An increase in amplitude of 0.25 in. results in the need for a similar reduction in gauge at the incipient wheel drop prediction limit. In order to establish this limit and because of the variation in low rail lateral force, the lateral rail minimum stiffness curve is moved to suit the low rail force recorded as shown by the dotted line on Fig. 5.6-3. Also shown on Fig. 5.6-3 and subsequent figures are the mid-chord offset values for the particular run. These are calculated for a 62 ft chord (MCO) and 31 ft chord (MC31).

Critical values of alignment variation for the safe maximum gauge of 57.75 in., discussed previously in Section 5.4, are given in Fig. 5.6-4, along with the equivalent mid-chored offsets. The 50 ft wavelength excites the largest

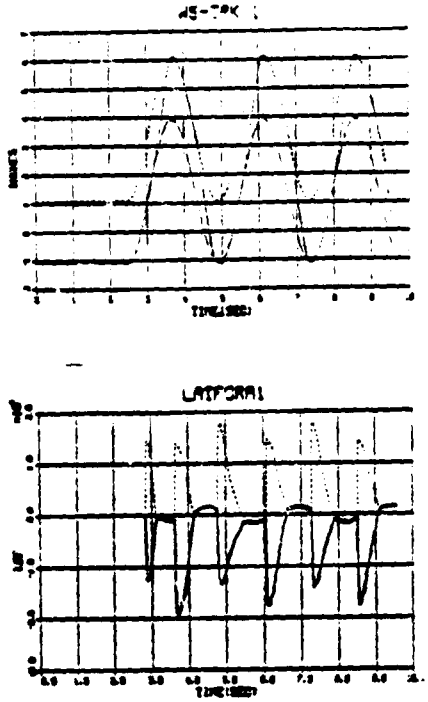

Figure 5.6-1 Wheelset Path and Lateral Forces Leading Wheelset - Tangent Track with Sinusoidal Alignment Variation Gauge = 58.0 in., Amplitude = 5 in. p/p

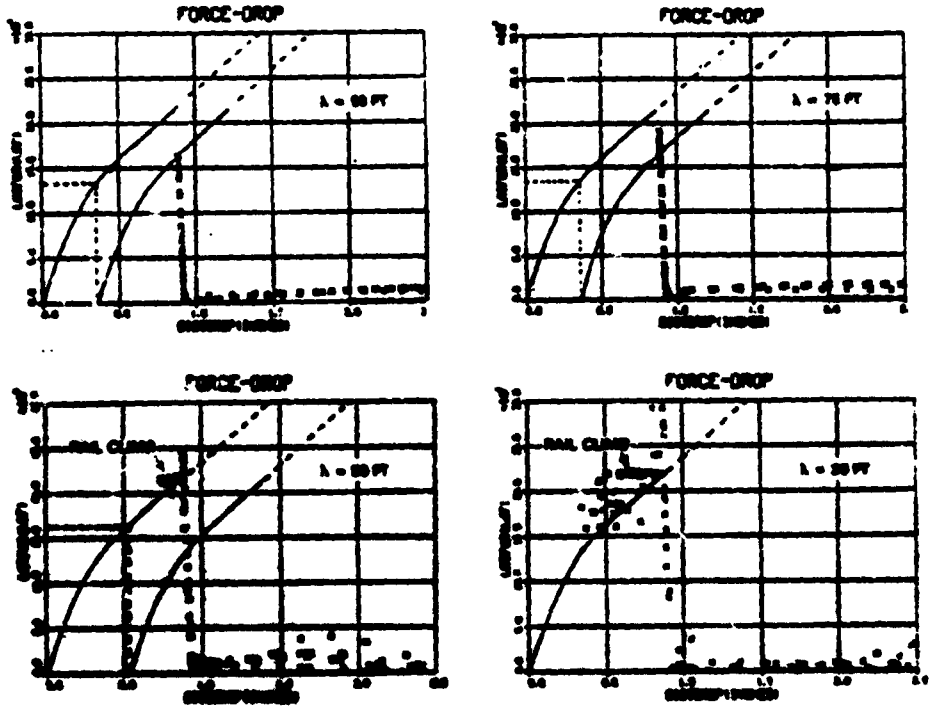

Figure 5.6-2 Incipient Wheel Drop Prediction 3 in. p/p - Sinusoidal Track Alignment Variation Tangent Track with 58.0. Gauge 25 mph

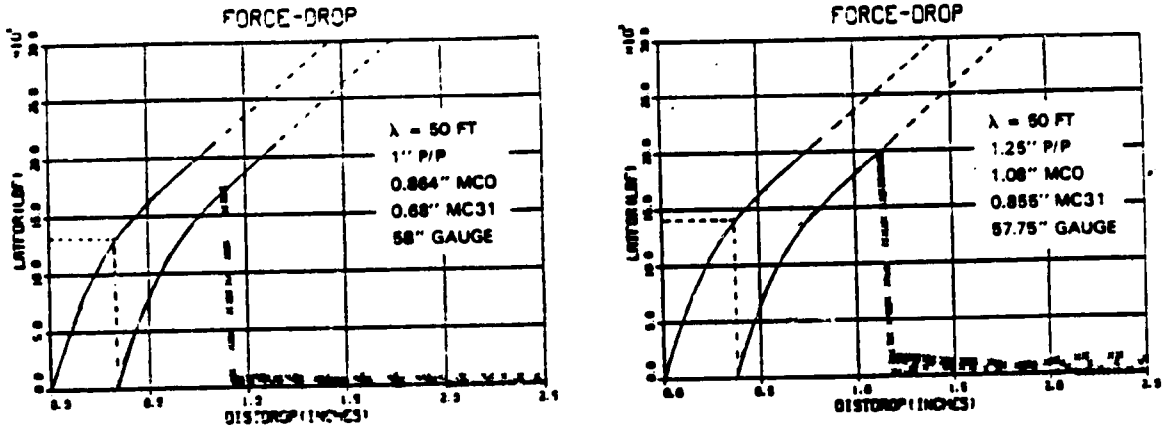

Figure 5.6-3 Incipient Wheel Drop Prediction Sinusoidal Track Alignment Variation Critical Amplitude at λ = 50 ft Tangent at 25 mph

response in the vehicle modeled on tangent track and consequently demands the smallest track alignment amplitude for avoidance of wheel drop. The probable proximity of this wavelength to the kinematic wavelength, in which tractive energy in transmitted through the wheel/rail interface into vehicle lateral dynamics, provoked a preliminary study into the effect of speed on the response of the truck at this wavelength of 50 ft. The result is shown in the lateral forces over the speed range of 5 to 100 mph in Fig. 5.6-5. There exists evidence of a peak in force just below 25 mph, which is accompanied in the output by a peak in roll angle, suggesting the excitation of a roll resonance. No attempt has yet been made to establish the precise speed which gives a maximum. At speeds above 60 mph, the short simulation runs did not settle in roll angle, although the peak forces in each time history were not increasing at the end of the run. Incipient wheel drop is predicted by all results for speeds above 40 mph. The results at high speeds are preliminary in this low speed study, but serve to place excitation with sinusoidal alignment variation into context of higher speed studies yet to be carried out. There is probably a wavelength at which the vehicle response and lateral forces are greater than those at 50 ft.

Further insight is possible from the study of sinusoidal alignment variations in curves. Figure 5.6-6 shows the sensitivity to alignment amplitude in a 5 degree curve at a wavelength of 39 ft and also shows the reduction due to the curvature at this wavelength. However not all wavelengths are similarly effected, as seen by the comparison between Fig. 5.6-7 for the 5 degree curve and the previous Fig. 5.6-4 for tangent track. The 39 ft wavelength is the only one requiring a substantially reduced amplitude to prevent a simulated incipient wheel drop response level at a curvature of 5 degrees.

In an alternative representation of the effect of curvature, Fig. 5.6-8 shows the leading axle lateral forces, for the alignment amplitudes, regarded as critical on tangent track. The increase in force between tangent and 5 degree curving on the 39 ft alignment wavelength is again apparent. All lateral forces increase beyond the force required for incipient wheel drop at 10 degrees of curvature and above. A first estimate of the simulation for critical values in the 10 degree curve is given in Fig. 5.6-9, which indicates the reduction in amplitude necessary to compensate for the increase in lateral force with curvature. The fact that the gauge has been kept constant for these alignment variation runs is apparent from the substantially constant value of distance to wheel drop in the results produced with the leading outer wheel flanging. The small slope is that due to the leading edge of the wheel/rail characteristic wheel lateral force vs lateral position, at flange contact, described previously in Section 3.3.1. However, assuming the gauge to be constant, say at 57.75 in. gives a constant distance to wheel drop of 1.17 in. Under potential derailment conditions, the forces on both wheels of the leading axle are large enough to be on the linear upper slope of the rail restraint characteristic used in allowing for rail deflection

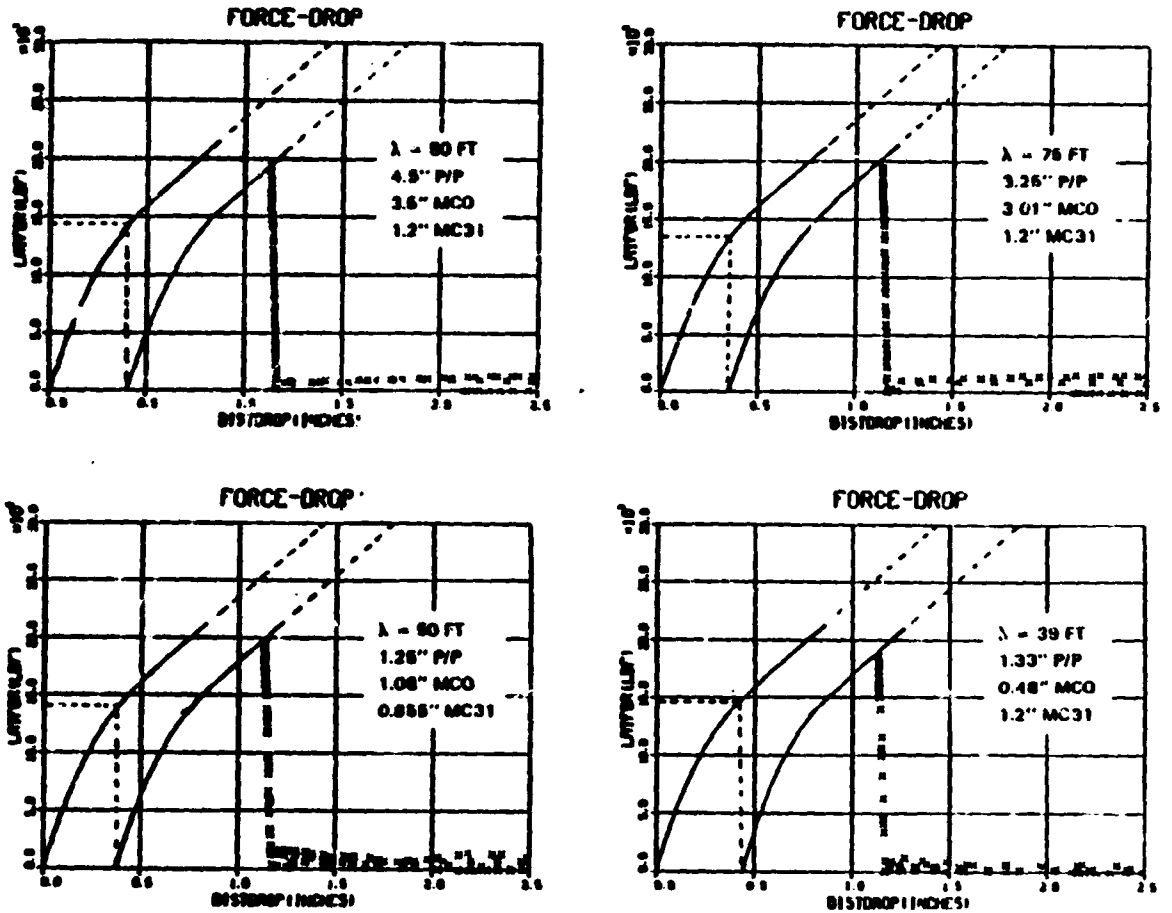

Figure 5.6-4 Incipient Wheel Drop Prediction
Sinusoidal Track Alignment Variation
Tangent · 57.75 in. Gauge · 25 mph · Critical Values

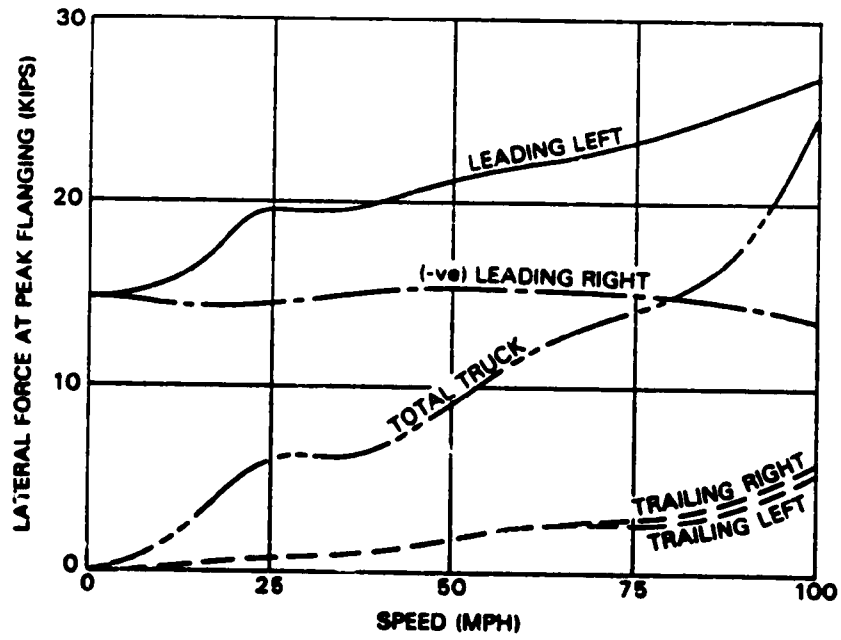

Figure 5.6-5 Effect of Speed
Sinusoidal Tangent Track Alignment Variation
(λ=50 ft - 57.75 in. Gauge - 1-1/8 in. p/p
Alignment)

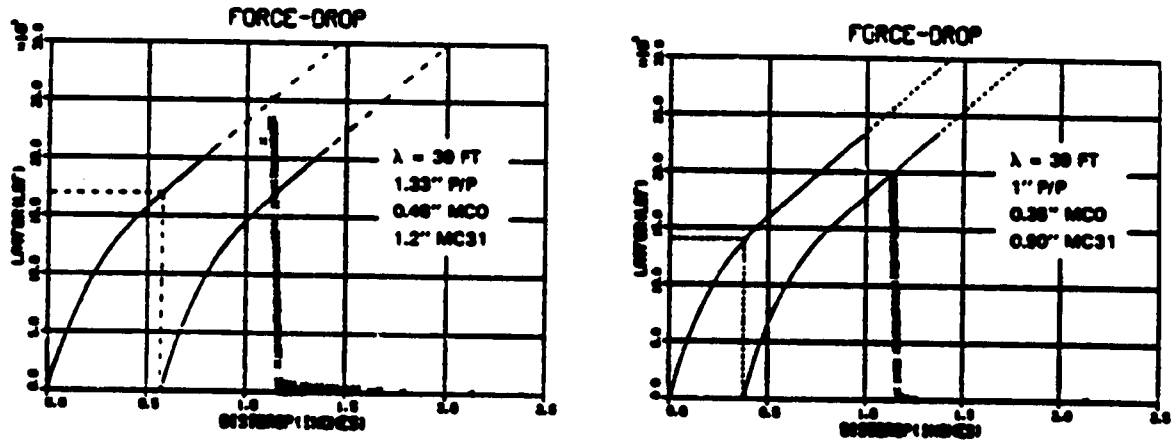

Figure 5.6-6 Incipient Wheel Drop Prediction
Sinusoidal Track Alignment Variation
Critical Amplitude at λ = 39 ft
5 Degree Curve at 25 mph,
57.75 in. Gauge

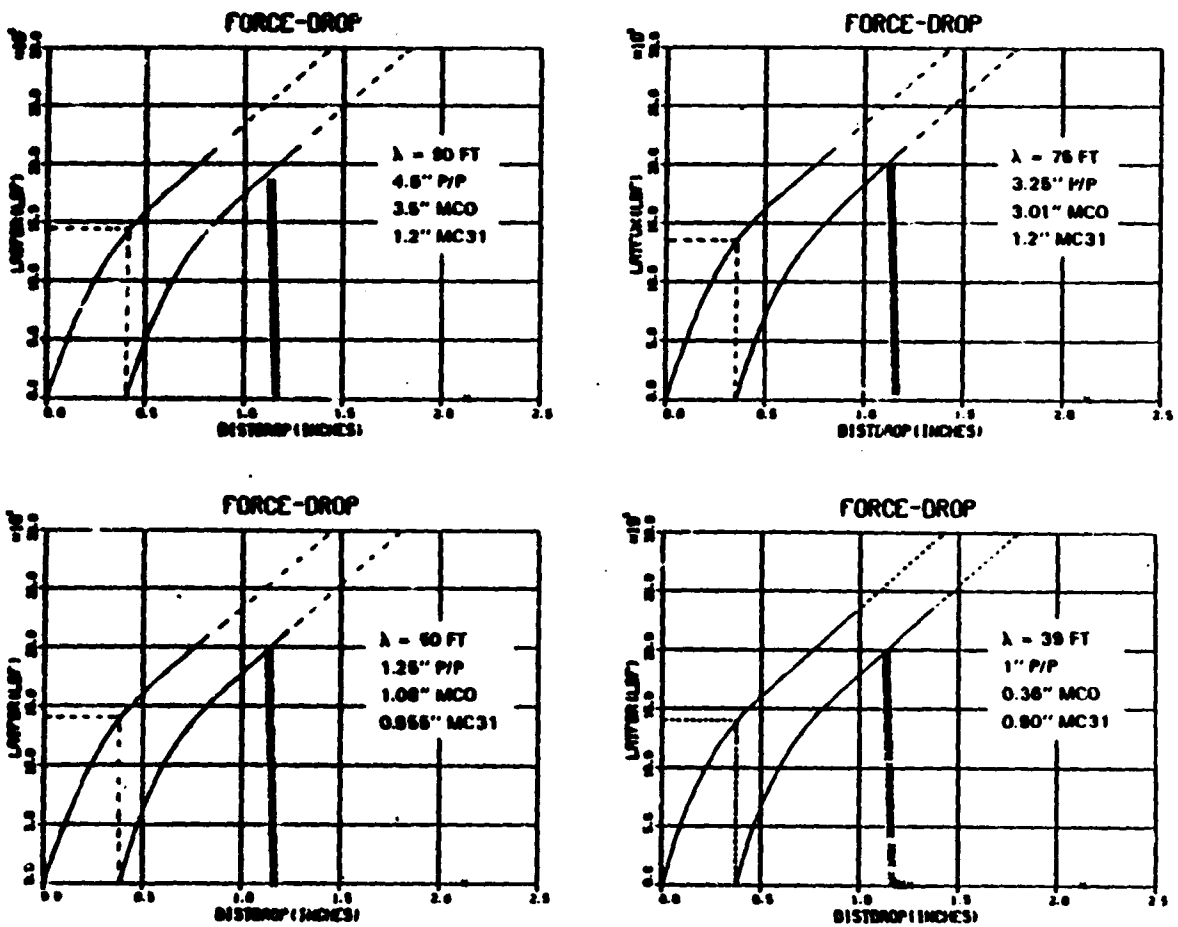

Figure 5.6-7 Incipient Wheel Drop Prediction
Sinusoidal Track Alignment Variation
5 Degree Curve · 57.75 in. Gauge · 25 mph · Critical Values

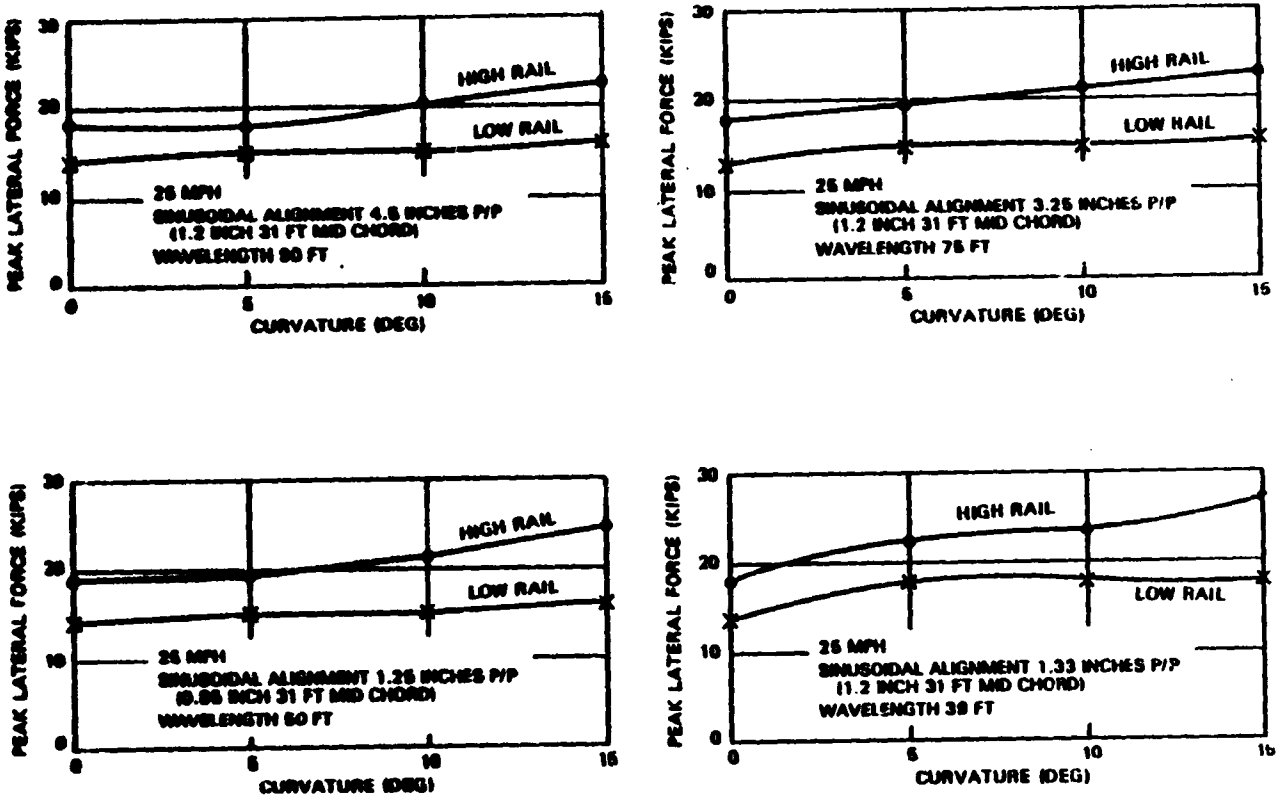

Figure 5.6-8 Effect of Curvature on Lead Axle Forces Under Sinusoidal Track Alignment Variation

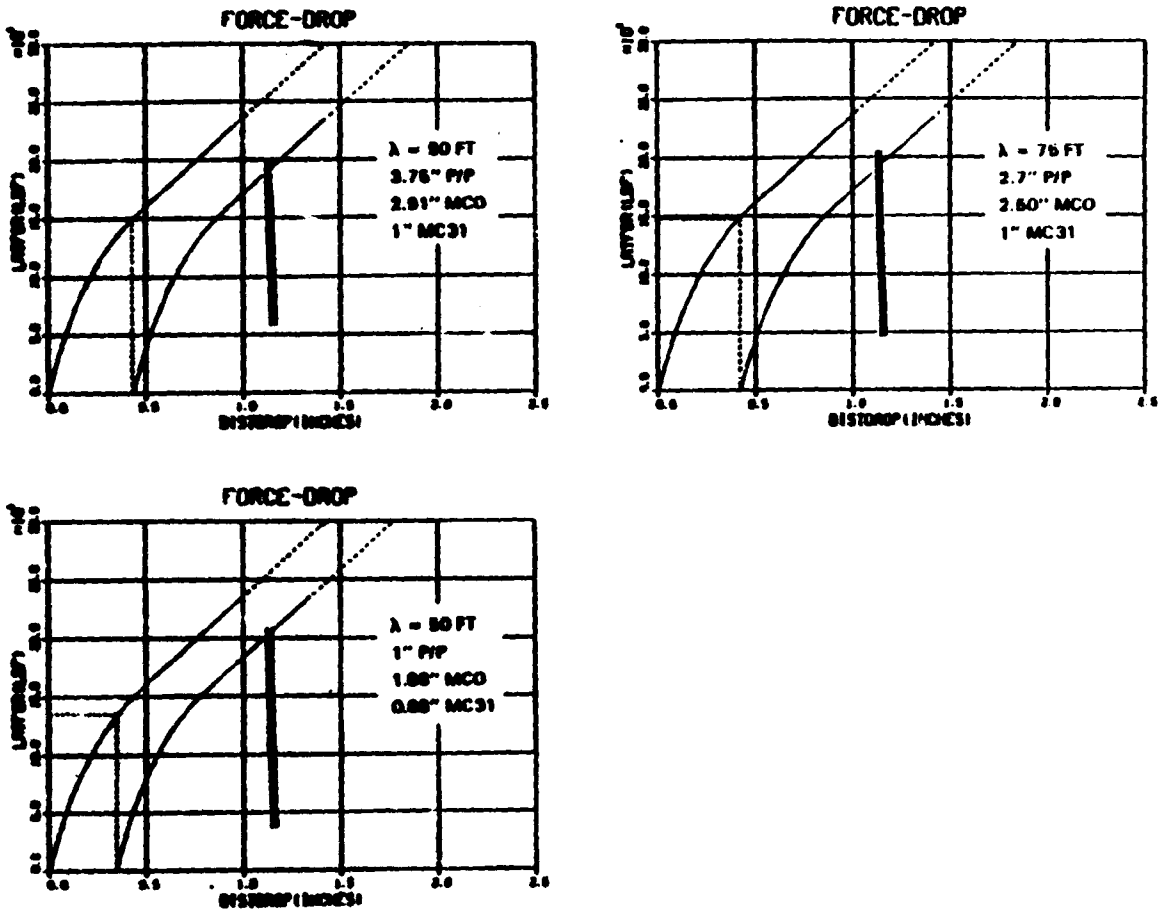

Figure 5.6-9 Incipient Wheel Drop Prediction
Sinusoidal Track Alignment Variation
10 Degree Curve · 57.75 in. Gauge · 25 mph · Critical Values

in the wheel drop studies. The equation governing this linear portion is,

$$\delta = 0.067L - 0.07$$

where

δ - lateral rail deflection, in

L - lateral rail force, kips.

Using δ_i for the inner rail and δ_o for the outer gives a total rail spreading deflection of $\delta = \delta_i + \delta_o$ or,

$$\delta = 0.067\ \Sigma L - 1.14 \text{ in.}$$

where

ΣL - sum of the rail spreading forces on the track

Since in the limiting case $\delta = 1.17$ in.

$$\Sigma L = \frac{1.17 + 1.14}{0.067} = 34.5 \text{ Kips}$$

A value of 30.7 Kips is similarly appropriate for a gauge of 58.0 in. Reference to Fig. 5.6-8 suggests that 34.5 Kips will be exceeded at curvatures just under 10 degrees for $\lambda = 90$ ft, close to 5 degrees for $\lambda = 75$ ft, between 5 and 10 degrees for $\lambda = 50$ ft, and at a very small curvature for $\lambda = 39$ ft, for the tangent track critical amplitudes stated. These results are consistent with the amplitude changes necessary in Fig. 5.6-7 and 5.6-9 to produce the critical values for incipient wheel drop. The tangent track values are good for all but the 39 ft wavelength in the 5 degree curve and all needed changing in the 10 degree curve.

Figure 5.6-10 shows a curve of total gauge spreading force at a speed of 25 mph, on both rails against sine wave double amplitude for $\mu = 0.5$, a wavelength of 50 ft, and gauge of 57.75 in. on tangent track. The critical value of amplitude is estimated to be 1.29 in., close to that given for the same wavelength in Fig. 5.6-4. The difference is solely due to the reading of lateral forces from the graphs, which was done by computer in previous results and by hand in Fig. 5.6-10. However this method of establishing critical values may be useful in interpreting quick-look data from field tests since it only involves the computation and comparison of a measured force with a predetermined critical value, for the measured or estimated track compliance and gauge.

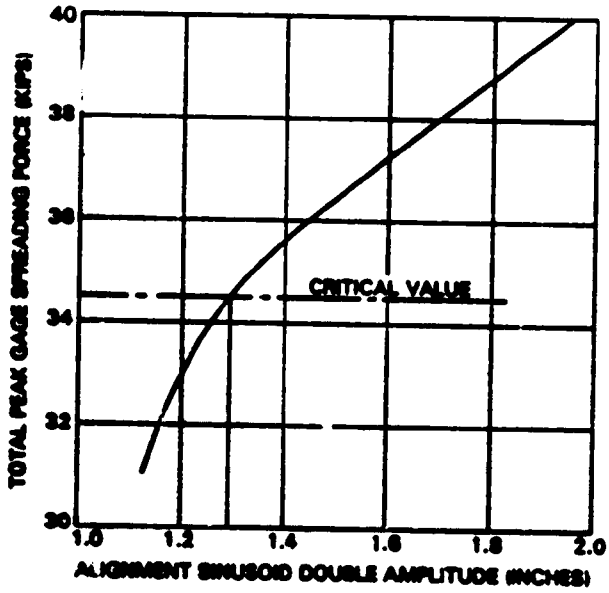

Figure 5.6-10 Rail Restraint Limited Gauge Spreading Forces on Tangent Track Gauge - 57.75 in. Wavelength - 50 ft $\mu = 0.5$ for a speed of 25 mph

6. CONCLUSIONS AND RECOMMENDATIONS

In this chapter, the outcome of the descriptions and discussion of the preceding chapters is summarized, separately, into conclusions and recommendations on the study, and on the relationship between track geometry and safety from derailment in the low speed range.

6.1 CONCLUSIONS

6.1.1 The Revised SIMCAR Model

The revised model and the computer simulation program developed under this effort have been shown to predict known freight vehicle behavior in the following modes.

- Roll - as compared to experimental results and the MIT model by Platin (Ref. 7), including jump phenomena due to body/bolster and truck suspension nonlinearities
- Steady Curving - as compared for constant conicity wheels and new rails with the model of Elkins (Ref. 22) and in general with published experimental results
- Dynamic Curving - as compared to the results of special tests for alignment and gauge variation on PTT track (Ref. 26) and UP track (Ref. 27) and for alignment, gauge and crosslevel variation, Chessie track (Ref. 28).

The revised model includes significant factors not found elsewhere in existing models in the required combination. The most important are,

- Gauge variation in addition to alignment and crosslevel in curving behavior
- Approximate wheel/rail characteristics which include linear and fully saturated regions for both tread and flange contact
- Snubbing and centerplate friction and vertical, yaw and lateral suspension nonlinearities between the bolster and side frames.

6.1.2 Steady State Vehicle Behavior

- It is apparent from the particular study of rail/wheel characteristics and their inclusion in the SIMCAR model, that the presence of 2-point contact between the wheel and rail, such as occurs during flanging with new AAR 1/20 wheels on new AREA 132 lb/yd rail, reduces the steering moment. This fact contributes to larger lateral forces during curving than are experienced with a single point of contact from profiled or worn wheels on many rail profiles.
- The studies of curving performance under conditions of incipient derailment indicate a limiting value to the force on the leading low rail/wheel as slipping commences in a predominantly lateral direction, a corresponding large lateral force on the flanging wheel (also spreading the rails), and a large yaw moment resisting curving from the rear axle in the truck due to its longitudinal wheel/rail forces.
- Increasing friction between wheel and rail adds significantly to the magnitude of the forces and potential for derailment.

6.1.3 Dynamic Curving Without Cross-Level But With Gauge Variation

- In the speed range of 10-25 mph, associated with present FRA track class 2, the predicted potential for incipient derailment is dominated by considerations of the lateral restraint capability of the rail. In the worst conditions investigated the limiting track geometry is that necessary to prevent the prediction of incipient wheel drop due to gauge spreading forces.
- With conditions representative of the poor track guidance in curves; including high friction level, new rail and wheel profiles, low track lateral rigidity and severe outer rail alignment cusps, the following represent gauge values within which no derailment and particularly no incipient wheel drop is predicted.

CURVE	MINIMUM GAUGE	MAXIMUM GAUGE
0-5	56.0	57.75
5-10	56.5	57.75
10-15	56.5	57.5
degrees	inches	inches

6.1.4 Dynamic Curving with Cross-Level and Gauge Variation

- For the 10 degree curve investigated, rail climb is predicted for the gauge variations defined to avoid wheel drop without track crosslevel, and when the amplitude of the crosslevel is 0.625 in. at each consecutive staggered joint, the value previously found safe on tangent track.
- The above result and predictions of incipient rail climb made at cross-level amplitudes of 0.625 in., and at critical speeds, confirm the fact that the gauge and alignment variations in the 10° curve significantly influences the safe response to cross-level.
- Further studies are recommended with varying cross-level and gauge to establish revised maximum limits to track geometry consistent with the safe performance of the vehicle in curves.

6.1.5 Sinusoidal Track Alignment Variation Alone

- The dominant mode of derailment predicted on rail with weakened lateral restraint, for the speed range of 10 to 25 mph, is wheel drop due to large gauge spreading forces.
- The sinusoidal track alignment amplitudes, for 57.75 in. gauge and 25 mph, below which the simulation of poor guidance conditions predicts no incipient wheel drop derailment, are,

WAVELENGTH	DOUBLE AMPLITUDE
for tangent track,	
39 ft	1.33 in.
50 ft	1.25 in.
75 ft	3.25 in.
90 ft	4.5 in.
for a 5 degree curve,	
39 ft	1.0 in.
50 ft	1.25 in.
75 ft	3.25 in.
90 ft	4.5 in.
and for a 10 degree curve,	
50 ft	1.0 in.
75 ft	2.7 in.
90 ft	3.75 in.

6.2 RECOMMENDATIONS

6.2.1 Present Rail/Wheel Characteristic

The approximation presently used to create wheel/rail forces and moments, while arranged to be accurate for wheels and rails providing constant tread conicity and two point contact at the flange, bears only asymptotic relationships to the physical process. New models, representing the basic rolling/creeping process, including the variation in wheelset rotational speed, and employing tabular representations for wheel/rail geometry and creep forces are in use and are computationally efficient. They are known from the literature to be very accurate in predicting wheel climb and gauge spreading forces and include the promise of further development into the prediction of dynamic wear and rolling resistance. This includes the prospect of further development beyond their present state of assumed Hertzian contact and dry interface conditions. A special consideration is that they are completely flexible for any measured or designed wheel or rail profile. It is recommended that the present model, used in the computer program SIMCAR, be modified to include this advance.

6.2.2 Present Computational Efficiency of the Simulation

As it presently exists, the program SIMCAR uses a process of state reduction to provide accurate integration of relevent dynamics with longer time steps. This process is presently compromised by the lack of a suitably robust algebraic algorithm for the highly non-linear equations governing the equilibrium of the trucks. The

present method uses values from the preceding step which reduces the advantage by making the accuracy step dependent. Because of the importance of the general problem in steady curving, in addition to the advantage of an efficient dynamic curving program for higher track speeds, it is recommended that an improved algorithm be sought and implemented for this purpose.

6.2.3 The Approach to Wheel/Rail Model Validation and to Determining Critical Track Geometries

From previous simulation studies and from published studies of track geometry it has been possible to choose outer rail and cross level cusps and sinusoidal alignment variation to provide severe geometric track inputs for the study of limiting track standards for gauge, cross level and alignment. Further studies of response to other shapes determined from the track geometric surveys are underway. However, the process of derailment has never been tested in full scale under controlled conditions in the United States, so that the physical condition under which derailments occur in the real world, in either rail climb or wheel drop, are not precisely known. It is likely that velocity, angle of attack, the state of wear of wheel and rail profiles, load, friction coefficient as well as track restraint and geometric history all play a role. A three part study could be undertaken to provide a better estimate of the probability of derailment on railroads in the United States.

In Part I it is proposed that an accurate model of a single wheelset on compliant track should be created to examine the criticality and sensitivity of the circumstantial variables which together give rise to the modes of derailment discussed in this report.

In Part II it is proposed that the model and simulation of the derailment process in Part I should be combined with a full scale experiment to provide validation up to and including a full derailment. For this it is proposed that a single wheelset test should be devised using a specially designed suspension from an existing heavy vehicle.

In Part III it is proposed that the resulting validated model results should be used to identify and rank the severity of track geometries recorded in the United States so far as their potential for derailment is concerned.

6.2.4 Extension of the Present Studies

The studies reported here have provided evidence of limiting or critical track geometries, for the response of a notably poorly performing vehicle over the speed range of 10-25 mph for track shapes, deemed to provide the most likely circumstance for derailment. The results have been demonstrated to be generally consistent with test results and with the known behavior of the high c.g. hopper car in service. The sections above have addressed improvements desirable in the simulation and model and its validity. Using these advances and any others found necessary through experience to simulate adequately the derailment process at higher speeds, it is recommended that studies continue into the safe performance limits of vehicles on poor track up to the highest speed envisaged for the operation of vehicles in freight and passenger service. This study should continue to use scenarios representative of known poorly behaving vehicles on track geometry and restraint conditions identified as providing the greatest hazard to the stable guidance process for the purpose of identifying relationships between track geometry and derailment potential.

APPENDIX A

RAIL VEHICLE DYNAMICS LIBRARY PROGRAM DESCRIPTIONS

A.1 OVERVIEW

The Rail Vehicle Dynamics Library (RVDL) programs are stored on tape. A program description and log system provides a data set on each program describing its origin and attributes. The programs can be sorted by means of a keyword system; presently allowable keywords are described in Section A.2. A complete listing of the descriptive material for each RVDL program is given in Section A.3.

A.2 KEYWORD DESCRIPTIONS

The program summary data sheets which comprise Section A.3 include a set of keywords for each program. These words are selected to describe the vehicle being modeled, the operating regime and the analysis methodology employed by the program. A special category of keywords is used to characterize wheel-rail analysis programs. The following four sections describe the keywords.

A.2.1 Vehicle Keywords

The vehicle under consideration is described by the keywords defined in the following paragraphs:

Train - This keyword indicates that the program analyzes an entire train, including locomotives.

Freight Car - This keyword indicates that the program analyzes a freight car. Typically, there is some attribute of the program that is specific to freight car behavior, although in some cases relatively simple program changes could result in passenger car models. The keyword "flexible freight car" indicates that the effects of car body flexibility are included.

Passenger Car - This keyword indicates that the program analyzes a passenger car or passenger rail car. Flexible car body analysis is indicated as for freight cars.

Loco - This keyword indicates that the vehicle being analyzed is a locomotive. The keyword "6-axle loco" indicates that the model is specifically built for a locomotive with two 3-axle trucks.

Loco Truck - This keyword indicates that only a locomotive truck is under analysis. This is appropriate when the carbody is in steady state, either due to the quasi-static nature of the problem or due to the emphasis on mid- and high-frequency truck and wheelset response. Keywords "passenger truck" and "freight truck", though not necessary as yet in the RVDL classification, would be similarly used.

A.2.2 Operating Regime Keywords

The operating regime and some attributes of the problem area under analysis are described by the following keywords:

Longitudinal Train Action - This keyword indicates that the longitudinal degree-of-freedom of each car is modeled for the purposes of detailing the buff and draft (train action) forces in the string of cars. This typically involves a simulation of locomotive and brake system performance as the train traverses a track exhibiting grade changes and curvature variations.

Curved Track - This keyword describes a model that is intended for curved track, and possibly also in entry/exit spirals. Since motion around a curve is inherently asymmetric, a model appropriate for curved track tends to be much more complex than one restricted to straight track.

Pitch-Heave - This keyword denotes a computer model which only evaluates vehicle response in the vertical plane. This includes both vertical translation (heave) and pitching motion.

Vertical - This keyword denotes a program which only models vertical translational motion.

Lateral-Roll-Yaw - This keyword describes a vehicle model including motion only out of the plane of symmetry. In general, three degrees-of-freedom (lateral, roll, and yaw) are necessary for each component of the vehicle.

Lateral Forces - This keyword is used for a program which explicitly calculates lateral forces between vehicles.

Hunting - This keyword denotes a model that is useful in analyzing the onset of hunting motion.

Non-Rigid Track - This keyword is used for a model which includes the effects of rail and track structure flexibility.

Fatigue Analysis - This keyword indicates that the program analyzes the fatigue life of the vehicle in question.

A.2.3 Mathematical Model Type and Analysis Method

The keywords which describe the type of mathematical model and the analysis method used in the rail vehicle dynamics programs are described in the following paragraphs. The first two keywords describe the type of model.

Linear - The mathematical model is based on the assumption of linearity: that the output of the system driven by the summation of two input signals is equal to the summation of the two separate output signals. This is often an approximation of reasonable validity for small perturbations about a static or quasi-static operating point. The usefulness of the assumption of linearity lies in the powerful systems analysis tools which have been developed for linear systems.

Nonlinear - This keyword describes a model for which linear input/output relationships are not valid. Certain important rail vehicle subsystems are inherently nonlinear (for example, coulomb dampers, flanging, centerplate and sidebearing contact geometry) and a nonlinear model is necessary to adequately portray these relationships.

The following analysis method keywords must be used with one of the above two mathematical model descriptors:

Time-History - This keyword denotes a program, one of the primary outputs of which is a time-history of vehicle component displacements, velocities, accelerations, or interface forces. For nonlinear systems, these time-histories are usually produced by numerical integration of the system differential equations; for linear systems a modal superposition or a state transition matrix approach is most efficient.

Eigenanalysis - This keyword indicates an analysis procedure that applies only to linear systems. Calculation of eigenvalues and eigenvectors is performed, and the results indicate the stability, frequency and damping of each vehicle mode, as well as the level of involvement of each vehicle component in each mode.

Transfer Function Calculation - This keyword indicates that the program evaluates important vehicle transfer functions from a linear model. A transfer function itself can be used for frequency domain input-output analysis; however, it is usually best visualized by evaluation at a range of frequencies and plotting the resulting gain and phase between input and output as a function of frequency.

PSD Analysis - This keyword -- a shortened form of power spectral density analysis -- is a method of describing the random response of a linear system to a stationary (statistically time-invariant) input. This analysis method is straightforward because the PSD of the observed vehicle response is linearly related to the PSD of the input, and the linear relationship depends only on the vehicle transfer function.

Quasi-Static - This keyword describes a nonlinear computer program that calculates a quasi-steady state equilibrium condition. Typically, this involves the solution of force and moment balance equations.

Limit Cycle - This keyword indicates that the program in question is suited to the analysis of limit cycles in nonlinear systems. Although limit cycles can be simulated using a time-history generation capability, the keyword is only used here if a portion of the program is especially adapted to limit cycle analysis. Typically, this involves the use of sinusoidal-input describing functions.

Random Response - This keyword is applied to a computer program set up to describe the random response of a nonlinear vehicle model to random track inputs. This may be done by direct simulation, which produces one of many possible random responses, or by a covariance analysis procedure, which produces a mean response and the variance about that mean response.

A.2.4 Special Wheel/Rail Keywords

Due to the unique and important part wheel/rail interactions play in rail vehicle dynamics, a set of keywords describing programs addressing wheel/rail interaction is included:

W/R Geometry - This keyword denotes a program that calculates the geometry of the wheel and rail profiles.

Contact Ellipse - This keyword is applied to a program that calculates the contact ellipse size and shape between the wheel and rail. The contact ellipse depends on material properties and the curvature of the surfaces involved.

Kalker's Theory - This keyword is used to denote programs which calculate wheel/rail interactions based on Kalker's theory of Rolling Contact.

Creep Coefs - This keyword indicates a program which calculates creep coefficients, which relate the wheel/rail forces to the degree of creepage, or deviation from pure rolling.

W/R Forces - This keyword applies to a program which explicitly calculates wheel/rail forces. Hence, this keyword can only appear in reference to a vehicle simulation program.

L/V Ratio - This keyword applies to a program which explicitly calculates the ratio between the lateral and vertical forces. This ratio is an important indicator of potential wheel climb.

A.3 DETAILED PROGRAM DESCRIPTIONS

The following pages reproduce the program descriptive data as stored on the computerized library management system. To a large extent, the headings are self-explanatory. Version 0 is used to refer to the program as initially delivered. Later versions are used for modifications or updates to the program code. The keyword line is especially important in rapid searches of the RVDL for programs dealing with a specific problem.

```
ID   V
--   -
001  S   TITLE  FLEXIBLE BODY RAILROAD FREIGHT CAR MODEL
         ORIGIN  AAR
         DATE_RECD  31 MAY 77
         KEYWORD  NONLINEAR FLEXIBLE FREIGHT CAR TIME HISTORY; W/R FORCES
         DESCRIPTION  SIMULATION OF FREIGHT CAR MOTION IN RESPONSE TO HALF OR FULL STAGGERED TRACK
         MODEL  EACH CARBODY HALF HAS 5 DOF, EACH BOLSTER AND WHEELSET HAS 2 DOF, 22-DOF
         METHOD  EQUATIONS OF MOTION ARE INTERGRATED. LAGRANGE'S METHOD IS USED.
         INPUTS  INERTIAL DAMPING AND STIFFNESS DATA. DIMENSIONAL AND RAIL DATA AND TRAIN SPEED.
         OUTPUTS  POSITION VELOCITY AND ACCELERATION OF EACH DOF. W/R AND INTERNAL FORCES
         DELIVERY  TAPE (0294 IN TASC LIBRARY)
         LANGUAGE  FORTRAN
         RESOURCES  INPUT: UNIT'  WORK FILES: UNITS 364  PRINT FILE: UNIT6  RESTART FILE: UNIT8
         COMPILE  TIME(SECS)=  1 35.89      COMPILE SIZE(K)=  150K
         RUN TIME(SECS)=  1109.85      RUN SIZE(K)=  316K
         STRUCTURE  COMPOSED OF ONE MAIN PROGRAM AND 6 SUBROUTINES
         TECH REPT  R-199  "FLEXIBLE BODY RAILROAD FREIGHT CAR
         PROGRAM SPEC  R-200  FLEXIBLE BODY RAILROAD FREIGHT CAR
         USER_GUIDE  R-200  FLEXIBLE BODY RAILROAD FREIGHT CAR
         MEMO

ID   V
--   -
002  S   TITLE  2-3-4 AXLE RIGID TRUCK CURVE NEGOTIATION MODEL
         ORIGIN  AAR
         DATE_RECD  31 MAY 77
         KEYWORD  NONLINEAR QUASI-STATIC LOCO TRUCK LATERAL FORCE; CURVED TRACK; W/R FORCES
         DESCRIPTION  CALC OF WHEEL/RAIL FORCES GIVEN TRACK CURVATURE AND TRUCK LOADS
         MODEL  A STATIC EQUILIBRIUM CURVING MODEL IS USED. NONLINEAR, LATERAL AND YAW DOF
         METHOD  LATERAL AND LONGITUDINAL FORCES AND YAW MOMENTS ARE CALC TO FIND AN EQUILIBRIUM
         INPUTS  TRUCK DATA, TRACTION/BRAKING LOADS; BUFF/DRAFT LOADS; TRACK CURVATURE
         OUTPUTS  LATERAL FLANGE AND CREEP FORCES AT EACH WHEEL, FRICTION CENTER LOCATION
         DELIVERY  TAPE (0397 IN TASC TAPE LIBRARY)
         LANGUAGE  FORTRAN
         RESOURCES  INPUT=UNIT5  OUTPUT=UNIT6  TEMPORARY WO  FILE=UNIT7
         COMPILE  TIME(SECS)=  3163.92      COMPILE SIZE(K)=  150K
         RUN TIME(SECS)=  3160.46      RUN SIZE(K)=  894K
         STRUCTURE  COMPOSED OF ONE MAIN PROGRAM AND 21 SUBROUTINES. MODULAR DESIGN.
         TECH REPT  R-204  2-3-4 AXLE RIGID TRUCK CURVE NEGOTIATION MODEL
         PROGRAM SPEC  R-204  2-3-4 AXLE RIGID TRUCK CURVE NEGOTIATION MODEL
         USER_GUIDE  R-204 2-3-4 AXLE RIGID TRUCK CURVE NEGOTIATION MODEL
         MEMO

ID   V
--   -
003  S   TITLE  QUASI-STATIC LATERAL TRAIN STABILITY MODEL (TRACK)
         ORIGIN  AAR
         DATE_RECD  31 MAY 77
         KEYWORD  NONLINEAR TRAIN LATERAL FORCE; QUASI-STATIC L/V RATIO; CURVED TRACK
         DESCRIPTION  SET UP TRACK DATA FILE FOR QSLAT(TRAIN)
         MODEL  NONLINEAR
         METHOD
         INPUTS  TRACK GEOM DESCRIPTION (TANGENT;SPIRALS;CURVTS;SUPER ELEVATION) AND DIRECTION
         OUTPUTS  TRACK GEOMETRY DATA PRINTOUT; TRACK FILE FOR USE BY QSLAT(TRAIN)
         DELIVERY  TAPE (0305 IN TASC LIBRARY)
         LANGUAGE  FORTRAN
         RESOURCES  CARD INPUT=UNIT5  OUTPUT=UNIT6  DISK STORAGE=UNIT3
         COMPILE  TIME(SECS)=  3164.22      COMPILE SIZE(K)=  150K
         RUN TIME(SECS)=  0128.20      RUN SIZE(K)=  310K
         STRUCTURE  COMPOSED OF ONE MAIN PROGRAM AND 2 SUBROUTINES
         TECH REPT  R-209 QUASI-STATIC LATERAL TRAIN STABILITY MODEL
         PROGRAM SPEC  R-209 QUASI-STATIC LATERAL TRAIN STABILITY MODEL
         USER_GUIDE  R-209 QUASI-STATIC LATERAL TRAIN STABILITY MODEL
         MEMO

ID   V
--   -
004  S   TITLE  QUASI-STATIC LATERAL TRAIN STABILITY MODEL (TRAIN)
         ORIGIN  AAR
         DATE_RECD  31 MAY 77
         KEYWORD  NONLINEAR TRAIN LATERAL FORCE; QUASI-STATIC L/V RATIO; CURVED TRACK
         DESCRIPTION  SIMULATES LATERAL FORCES THROUGHOUT A TRAIN (UP TO 100 CARS)
         MODEL  LONG. DOF: CAR, 4 DOF PER CAR; LAT. DOF: CAR, 4 DOF PER CAR; QUASI-DYNAMIC
         METHOD  EQUATIONS OF LATERAL FORCE EQUILIBRIUM ARE SOLVED FOR EACH CAR
         INPUTS  TRACK DATA; GEOMETRY OF EACH CAR; CAR DATA; TRAIN SPEED
         OUTPUTS  LATERAL FORCES AT EACH STEP; DERAILMENT MEAS; COUPLER ANGLES; L/V RATIOS
         DELIVERY  TAPE (0306 IN TASC LIBRARY)
         LANGUAGE  FORTRAN
         RESOURCES  INPUT=UNIT5  OUTPUT=UNIT6  TRACK DATA INPUT=UNIT3
         COMPILE  TIME(SECS)=  1166.33      COMPILE SIZE(K)=  162K
         RUN TIME(SECS)=  0116.01      RUN SIZE(K)=  324K
         STRUCTURE  COMPOSED OF ONE MAIN PROGRAM AND 3 SUBROUTINES
         TECH REPT  R-209 QUASI-STATIC LATERAL TRAIN STABILITY MODEL
         PROGRAM SPEC  R-209 QUASI-STATIC LATERAL TRAIN STABILITY MODEL
         USER_GUIDE  R-209 QUASI-STATIC LATERAL TRAIN STABILITY MODEL
         MEMO
```

```
ID   V
--   -
005  5   TITLE  TRAIN OPERATIONS SIMULATOR (EQUIP)
         ORIGIN  AAR
         DATE_RECD  01 MAY 77
         KEYWORD  NONLINEAR LONGITUDINAL TRAIN ACTION TIME HISTORY; L/V RATIO; CURVED TRACK
         DESCRIPTION  GENERATE A STANDARD VEHICLE DATA BASE REQUIRED BY TOS
         MODEL  LARGE VEHICLE DATA BASE
         METHOD
         INPUTS  VEHICLE DATA CARDS; LOCOMOTIVE DATA CARDS.
         OUTPUTS  BINARY DATA SET FOR USE BY TOS.
         DELIVERY  TAPE (1ST PART OF #309 ON TASC LIBRARY)
         LANGUAGE  FORTRAN
         RESOURCES  INPUT:CARDS(UNIT=)                    OUTPUT:DATA BASE(UNIT= 7) PRINTER(UNIT=6)
         COMPILE TIME(SECS)=  1309          COMPILE SIZE(K)=  120K
         RUN TIME(SECS)=  0147          RUN SIZE(K)=  314K
         STRUCTURE  COMPOSED OF ONE MAIN PROGRAM AND 6 SUBROUTINES
         TECH REPT  R-309 TRAIN OPERATIONS SIMULATOR
         PROGRAM SPEC
         USER_GUIDE  R-198 TRAIN OPERATIONS SIMULATOR
         MEMO  SIMILAR TO RVDL-009


ID   V
--   -
006  6   TITLE  TRAIN OPERATIONS SIMULATOR
         ORIGIN  AAR
         DATE_RECD  01 MAY 77
         KEYWORD  NONLINEAR LONGITUDINAL TRAIN ACTION TIME HISTORY; L/V RATIO; CURVED TRACK
         DESCRIPTION  SIM OF THE LONG. MOTION OF A TRAIN GIVEN CONSIST; TRACK DATA AND CP DETAILS
         MODEL  NONLINEAR MODEL OF LOCO AND CARS
         METHOD  INTEGRATION OF THE EQUATIONS OF MOTION
         INPUTS  VEHICLE DATA BASE FROM EQUIP; VEHICLE CONSIST; TRACK DATA; CP OF LOCOMOTIVE
         OUTPUTS  BUFF/DRAFT FORCES; TIME AND LOCATION ON TRACK; LOCO CONTROL POS; MAX L/V
         DELIVERY  TAPE (2ND PART OF #309 IN TASC LIBRARY)
         LANGUAGE  FORTRAN
         RESOURCES  INPUT:UNIT; UNIT4   OUTPUT:UNIT2 UNIT6 UNIT7 UNIT8
         COMPILE TIME(SECS)=  13128.78          COMPILE SIZE(K)=  144K
         RUN TIME(SECS)=  0108.37          RUN SIZE(K)=  318K
         STRUCTURE  COMPOSED OF ONE MAIN PROGRAM AND 30 SUBROUTINES
         TECH REPT  R-309 TRAIN OPERATIONS SIMULATOR
         PROGRAM SPEC
         USER_GUIDE  R-198 TRAIN OPERATIONS SIMULATOR
         MEMO  MANY SUBROUTINES SIMILAR TO THOSE FOUND IN RVDL-008 AND RVDL-010


ID   V
--   -
007  0   TITLE  LOCOMOTIVE TRUCK HUNTING MODEL (LTHNT)
         ORIGIN  AAR
         DATE_RECD  01 MAY 77
         KEYWORD  LINEAR 6-AXLE LOCO HUNTING EIGENANALYSIS
         DESCRIPTION  ANALYZES HUNTING STABILITY BY EIGENANALYSIS AT A RANGE OF SPEEDS
         MODEL  TWO AND THREE-AXLE TRUCK MODELS ALONG WITH A BODY MODEL. LINEAR, 17 OR 21-DOF
         METHOD  MASS; STIFFNESS & DAMPING MATS ARE CONVERTED TO LINEAR STATE EQNS. Q-R METHD USED
         INPUTS  VELOCITY RANGE; MASS;STIFFNESS; AND DAMPING DATA; DIMENSIONAL AND CREEP DATA.
         OUTPUTS  MASS; STIFFNESS; AND DAMPING MATRICES; EIGENVALUES AND EIGENVECTORS.
         DELIVERY  TAPE (#400 IN TASC LIBRARY)
         LANGUAGE  FORTRAN
         RESOURCES  INPUT:UNITS  OUTPUT:UNITS
         COMPILE TIME(SECS)=  3167.37          COMPILE SIZE(K)=  112K
         RUN TIME(SECS)=  0139.62          RUN SIZE(K)=  316K
         STRUCTURE  CONTAINS 33 SUBROUTINES AND 5 COMMON BLOCKS. FOR MORE INFO SEE PROGRAM LOG.
         TECH REPT  R-210 (AAR) LOCOMOTIVE TRUCK HUNTING MODEL
         PROGRAM SPEC  R-378 LOCOMOTIVE TRUCK HUNTING MODEL
         USER_GUIDE  R-227 (AAR) LOCOMOTIVE TRUCK HUNTING MODEL
         MEMO  PRINTS OUT EVERY OTHER EIGENVALUE


ID   V
--   -
007  1   TITLE  LOCOMOTIVE TRUCK HUNTING MODEL (LTHNT)
         ORIGIN  AAR
         DATE_RECD  01 MAY 77
         KEYWORD  LINEAR 6-AXLE LOCO HUNTING EIGENANALYSIS
         DESCRIPTION  ANALYZES HUNTING STABILITY BY EIGENANALYSIS AT A RANGE OF SPEEDS
         MODEL  TWO AND THREE-AXLE TRUCK MODELS ALONG WITH A BODY MODEL. LINEAR, 17 OR 21-DOF
         METHOD  MASS; STIFFNESS & DAMPING MATS ARE CONVERTED TO LINEAR STATE EQNS. Q-R METHD USED
         INPUTS  VELOCITY RANGE; MASS; STIFFNESS; AND DAMPING DATA; DIMENSIONAL AND CREEP DATA
         OUTPUTS  MASS; STIFFNESS; AND DAMPING MATRICES; EIGENVALUES AND EIGENVECTORS
         DELIVERY  TAPE (#400 IN TASC LIBRARY)
         LANGUAGE  FORTRAN
         RESOURCES  INPUT:UNITS  OUTPUT:UNITS
         COMPILE TIME(SECS)=  3167.37          COMPILE SIZE(K)=  112K
         RUN TIME(SECS)=  0139.62          RUN SIZE(K)=  316K
         STRUCTURE  CONTAINS 33 SUBROUTINES AND 5 COMMON BLOCKS.
         TECH REPT  R-210 (AAR) LOCOMOTIVE TRUCK HUNTING MODEL
         PROGRAM SPEC  R-378 LOCOMOTIVE TRUCK HUNTING MODEL
         USER_GUIDE  R-227 (AAR) LOCOMOTIVE TRUCK HUNTING MODEL
         MEMO  MODIFIED TO PRINT OUT EVERY EIGENVALUE
```

```
ID   V
---  -
308  3   TITLE  DETAILED LONGITUDINAL TRAIN ACTION MODEL (VEHICLE)
         ORIGIN  AAR
         DATE_RECD  31 MAY 77
         KEYWORD  NONLINEAR LONGITUDINAL TRAIN ACTION TIME HISTORY; CURVED TRACK
         DESCRIPTION  GENERATION OF A STANDARD VEHICLE LIBRARY FOR USE BY DLTAN SIMULATION
         MODEL  LARGE VEHICLE DATA BASE
         METHOD
         INPUTS  DESCRIPTION OF EACH TYPE OF FREIGHT CAR AND LOCOMOTIVE GENERALLY ENCOUNTERED.
         OUTPUTS  VEHICLE LIBRARY FOR DLTAN
         DELIVERY  TAPE (FIRST OF THREE PROGRAMS ON #398 IN TASC LIBRARY)
         LANGUAGE  FORTRAN
         RESOURCES  INPUT:CARDS(UNIT5)          OUTPUT:PRINTER(UNIT6)  DISK(UNIT8)
         COMPILE TIME(SECS)=  2:31.73     COMPILE SIZE(K)=  120K
         RUN TIME(SECS)=  2:56.03     RUN SIZE(K)=  310K
         STRUCTURE  CONSISTS OF ONE MAIN PROGRAM AND 6 SUBROUTINES
         TECH_REPT  R-221 DETAILED LONGITUDINAL TRAIN ACTION MODEL (VEHICLE)
         PROGRAM_SPEC
         USER_GUIDE  R-220 DETAILED LONGITUDINAL TRAIN ACTION MODEL
         MISC  SIMILAR TO AVOL-309
```



```
ID   V
---  -
309  3   TITLE  DETAILED LONGITUDINAL TRAIN ACTION MODEL (RUN)
         ORIGIN  AAR
         DATE_RECD  31 MAY 77
         KEYWORD  NONLINEAR LONGITUDINAL TRAIN ACTION TIME HISTORY; CURVED TRACK
         DESCRIPTION  PREPARE TRACK; VEHICLE AND INITIAL CONDITION DATA FOR THE DLTAN SIMULATION
         MODEL
         METHOD
         INPUTS  VEHICLE LIBRARY FROM VEHICLE; TRACK DATA (PROFILE; CURVATURE)
         OUTPUTS  DATA FOR DLTAN SIMULATION; CURVE FILE; PROFILE FILE; CONSIST FILE.
         DELIVERY  TAPE (#398 IN TASC LIBRARY)
         LANGUAGE  FORTRAN
         RESOURCES  INPUT:CARDS(UNIT5) TAPE(2)          OUTPUT:PRINTER(UNIT6)  TAPE(1-3-8-9)
         COMPILE TIME(SECS)=  3:50.17     COMPILE SIZE(K)=  314K
         RUN TIME(SECS)=  8:17.29     RUN SIZE(K)=  370K
         STRUCTURE  CONSISTS OF ONE MAIN PROGRAM AND 9 SUBROUTINES
         TECH_REPT  R-221 DETAILED LONGITUDINAL TRAIN ACTION MODEL
         PROGRAM_SPEC
         USER_GUIDE  R-220 DETAILED LONGITUDINAL TRAIN ACTION MODEL
         MISC  MANY SUBROUTINES SIMILAR TO THOSE FOUND IN AVOL-006
```

```
ID   V
---  -
310  6   TITLE  DETAILED LONGITUDINAL TRAIN ACTION MODEL (SIM)
         ORIGIN  AAR
         DATE_RECD  01 MAY 77
         KEYWORD  NONLINEAR LONGITUDINAL TRAIN ACTION TIME HISTORY; CURVED TRACK
         DESCRIPTION  SIMULATES TRAIN LONGITUDINAL BEHAVIOR WITH EMPHASIS ON BRAKE AND DRAFT GEAR OP
         MODEL  DETAILED LONGITUDINAL MODEL OF EACH VEHICLE INCLUDING BRAKE AND DRAFT GEAR OP
         METHOD  SPLITS TRAIN UP INTO 'DETAILED' AND 'NONDETAILED' SECTIONS; INTEGRATES EQNS
         INPUTS  CURVE FILE; PROFILE FILE; AND CONSIST FILE FROM RUN; LOCOMOTIVE OPERATION DATA.
         OUTPUTS  LOCATION ALONG TRACK; LOCOMOTIVE AND BRAKE STATE; DRAFT GEAR STATE.
         DELIVERY  TAPE (#398)
         LANGUAGE  FORTRAN
         RESOURCES  INPUT:CARDS(UNIT5) TAPE(UNITS(1-2-3-8-9))  OUTPUT:PRINTER(UNIT6) PLOTTER(UNIT7)
         COMPILE TIME(SECS)=  7:48.94     COMPILE SIZE(K)=  130K
         RUN TIME(SEC)=
         STRUCTURE  CONSISTS OF ONE MAIN ROUTINE AND 30 SUBROUTINES. PLOTTING REFERENCES DELETED
         TECH_REPT  R-221 DETAILED LONGITUDINAL TRAIN ACTION MODEL
         PROGRAM_SPEC
         USER_GUIDE  R-220 DETAILED LONGITUDINAL TRAIN ACTION MODEL
         MISC  NOT RUN DUE TO LARGE CPU TIME REQUIREMENT; SOME SUBROUTINES SIMILAR TO AVOL-006
```

```
ID   V
---  -
311  6   TITLE  FLEX
         ORIGIN  TSC
         DATE_RECD  10 MAY 77
         KEYWORD  LINEAR PITCH-HEAVE FLEXIBLE PASSENGER CAR TRANSFER FUNCTION ANALYSIS
         DESCRIPTION  FIND THE [illegible] OF A FLEX LINEAR RAIL VEHICLE TO SINUS TRACK BUMP [illegible]
         METHOD  THE TRANSFER FUNC IS CALC FROM THE [illegible]
         INPUTS  [illegible]
         OUTPUTS  [illegible]
         DELIVERY  TAPE [illegible]
         LANGUAGE  FORTRAN
         RESOURCES  [illegible]
         COMPILE TIME(SECS)=  [illegible]
         RUN TIME(SEC)=  [illegible]
         STRUCTURE  [illegible]
         TECH_REPT  [illegible]
         PROGRAM_SPEC  [illegible]
         USER_GUIDE  [illegible]
         MISC
```

```
ID   1
--   -
012  0    TITLE  HALF#5
          ORIGIN  TSC
          DATE_RECD   16 MAY 77
          KEYWORD  LINEAR VERTICAL PASSENGER CAR TRANSFER FUNCTION CALCULATION
          DESCRIPTION   FIND VERT WHEEL/RAIL FORCES AND TRACK DEFLECTION DUE TO SINUS TRACK SURF IRREG
          MODEL   HALF-CAR BODY; ONE TRUCK AND TRACK STRUCTURE (4#FREDANCE.   4-DOF
          METHOD   COMPLX COEF MAT IS FORMED AND REPEATEDLY EVAL OVER THE RANGE OF FREQ OF INTEREST
          INPUTS   MASS STIFF AND DAMPING OF PRIMARY AND 2NDARY SUSPENSIONS AND TRK STRUCTURE. VEL.
          OUTPUTS   MAG AND PHASE OF EACH DOF AS WELL AS THE TRACK DEFLECTION AND FORCE TRANSFR FUNC
          DELIVERY   TAPE (#274 IN TASC LIBRARY
          LANGUAGE   FILE#4
          RESOURCES   1 TRACK)
          COMPILE TIME(SECS)=   3101.35      COMPILE SIZE(K)=   320K
          RUN TIME(SECS)=   0119.99      RUN SIZE(K)=   220K
          STRUCTURE   CONSISTS OF A MAIN PROGRAM AND 9 SUBRUUTINES. PLOTTING REFERENCES DELETED
          TECH REPT   FRA-ORED-76-135.I
          PROGRAM SPEC   FRA-ORED-76-135.II
          USER_GUIDE   FRA-ORED-76-135.II
          #EMO
```

```
ID   1
--   -
013  0    TITLE  FULL#5
          ORIGIN   TSC
          DATE_RECD   16 MAY 77
          KEYWORD  LINEAR PITCH-HEAVE PASSENGER CAR TRANSFER FUNCTION CALCULATION
          DESCRIPTION   CALC OF PITCH-HEAVE CAR RESPONSE TO VERTICAL SINUSOIDAL TRACK IRREGULARITIES
          MODEL   BODY HEAVE AND  PITCH TRNSFR FUNCTS (BOTH 4TH ORDER) FORM THE MODEL
          METHOD   TRANSFER FUNCTION EVALUATION (TRUCK PITCH MODES NEGLECTED)
          INPUTS   VELOCITY; VEHICLE MASS; INERTIA AND SUSPENSION DATA
          OUTPUTS   TABULATION OF TRANSFER FUNCTION AMPLITUDES AS A FUNCTION OF FREQUENCY
          DELIVERY   TAPE (#274 IN TASC LIBRARY; FILE#7; 9TRACK)
          LANGUAGE   FORTRAN
          RESOURCES   INPUT:CARDS(UNIT20)      OUTPUT:PRINTER(UNIT6)
          COMPILE TIME(SECS)=   0731.36      COMPILE SIZE(K)=   360K
          RUN TIME(SECS)=   0119.97      RUN SIZE(K)=   310K
          STRUCTURE   CONTAINS ONE MAIN PROGRAM AND THREE SUBROUTINES. ALL PLOTTING REFERENCES DELETED
          TECH REPT   FRA-ORED-76-135.I
          PROGRAM SPEC   FRA-ORED-76-135.II
          USER_GUIDE   FRA-ORED-76-135.II
          #EMO
```

```
ID   1
--   -
014  0    TITLE  LATERAL
          ORIGIN   TSC
          DATE_RECD   16 MAY 77
          KEYWORD  LINEAR LATERAL-ROLL-YAW PASSENGER CAR TRANSFER FUNCTION CALCULATION
          DESCRIPTION   CALC THE LATERAL FREQ RESP OF A LINEAR RAIL VEHICLE TO SINUSOIDAL TRK IRREG
          MODEL   CARBODY WITH TWO TRUCKS; LINEAR, 10-DOF
          METHOD   THE COMPLEX COEFFICIENT MATRICES ARE FORMED AND REPEATEDLY SOLVED
          INPUTS   LATERAL OR CROSSLEVEL SINUSOIDAL IRREG, SPECIAL VEHICLE DATA
          OUTPUTS   NORMALIZED DISPLACEMENTS AND ACCELERATIONS OF ALL DOF'S ARE PRINTED
          DELIVERY   TAPE (#274 IN TASC LIBRARY; FILE#7; 9 TRACK)
          LANGUAGE   FORTRAN
          RESOURCES   INPUT:CARDS(UNIT2)      OUTPUT:PRINTER(UNIT6)
          COMPILE TIME(SECS)=   0134.34      COMPILE SIZE(K)=   360K
          RUN TIME(SECS)=   1183.71      RUN SIZE(K)=   280K
          STRUCTURE   CONSISTS OF ONE MAIN PROGRAM AND FOUR SUBROUTINES. ALL PLOTTING REFS DELETED
          TECH REPT   FRA-76-136.I
          PROGRAM SPEC   FRA-76-136.II
          USER_GUIDE   FRA-76-136.II
          MEMO  VERSION II INCLUDES EXPANDED CAPABILITY
```

```
ID   1
--   -
015  0    TITLE  TEST DATA
          ORIGIN   TSC
          DATE_RECD   16 MAY 77
          KEYWORD
          DESCRIPTION   TEST DATA FOR RUNS 0111 0104 0171 014
          MODEL
          METHOD
          INPUTS
          OUTPUTS
          DELIVERY
          LANGUAGE
          RESOURCES
          COMPILE TIME(SECS)=      COMPILE SIZE(K)=
          RUN TIME(SECS)=      RUN SIZE(K)=
          STRUCTURE
          TECH REPT
          PROGRAM SPEC
          USER_GUIDE
          MEMO
```

```
ID   V
--   -
017  5   TITLE  KNEEPS
         ORIGIN  TSC
         DATE_RECD  16 MAY 77
         KEYWORD  NONLINEAR W/R GEOMETRY CREEP COEFS; KALKER'S THEORY; W/R FORCES
         DESCRIPTION  KALKER'S THEORY PROGRAM
         MODEL  SIMPLIFIED ROLLING CONTACT
         METHOD
         INPUTS  CONTACT PATCH GEOMETRY
         OUTPUTS  CREEP FORCES
         DELIVERY  CARDS (029 PUNCH)
         LANGUAGE  FORTRAN
         RESOURCES  INPUT:CARDS(UNIT5)              OUTPUT:PRINTER(UNIT6)
         COMPILE TIME(SECS)=  0:10.33      COMPILE SIZE(K)=  362K
         RUN TIME(SECS)=  1:34.66      RUN SIZE(K)=  326K
         STRUCTURE  CONSISTS OF ONE MAIN PROGRAM AND 2 SUBROUTINES
         TECH REPT
         PROGRAM SPEC
         USER_GUIDE
         NEWS  SUPERCEDED BY RVOL-021-8
```

```
ID   V
--   -
016  0   TITLE  PLOTTING PACKAGE
         ORIGIN  TSC
         DATE_RECD  16 MAY 77
         KEYWORD
         DESCRIPTION  PLOT PACKAGE FOR RVOL 011; 012; 013; 014
         MODEL
         METHOD
         INPUTS
         OUTPUTS
         DELIVERY
         LANGUAGE
         RESOURCES
         COMPILE TIME(SECS)=              COMPILE SIZE(K)=
         RUN TIME(SECS)=              RUN SIZE(K)=
         STRUCTURE
         TECH REPT
         PROGRAM SPEC
         USER_GUIDE
         NEWS
```

```
ID   V
--   -
016  0   TITLE  WHRAIL
         ORIGIN  ARIZONA STATE UNIVERSITY
         DATE_RECD  01 JUN 77
         KEYWORD  NONLINEAR W/R GEOMETRY
         DESCRIPTION  GIVEN WHEEL AND RAIL PROFILE DATA; FIND W/R CONTACT PTS AND GEOMETRY
         MODEL  CONTACT GEOMETRY IS FOUND FOR A RANGE OF WHEELSET LATERAL POSITIONS
         METHOD  4TH ORDER CRVS ARE FITTED TO THE DATA. CONTACT PTS ARE FOUND AND PRINTED.
         INPUTS  WHEEL AND RAIL PROFILES(RAIL CANT,GAUGE,WHEEL AND RAIL PROFILES)RAIL CANT,GAUGE,CONTROL INFO
         OUTPUTS  W/R CURVE FIT COEFFS; TABLES OF CONTACT PT GEOM AND ROLLING RADIUS VS LAT POS
         DELIVERY  CARDS (FOR UNIVAC 1108)
         LANGUAGE  FORTRAN
         RESOURCES  INPUT:CARDS(UNIT5)              OUTPUT:PRINTER(UNIT6)
         COMPILE TIME(SECS)=  1:40.44      COMPILE SIZE(K)=  368K
         RUN TIME(SECS)=  0:30.59      RUN SIZE(K)=  279K
         STRUCTURE  CONSISTS OF ONE MAIN PROGRAM AND 13 SUBROUTINES. PLOTTING REPS DELETED
         TECH REPT
         PROGRAM SPEC
         USER_GUIDE  FRA-ORD&D-76/264 APPENDIX A. WHEEL/RAIL CONTACT CHARACTERIZATION PROGRAM
         NEWS
```

```
ID   V
--   -
019  0   TITLE  WHEELDAT
         ORIGIN  TSC
         DATE_RECD  26 AUG 77
         KEYWORD  NONLINEAR W/R GEOMETRY
         DESCRIPTION  GENERATE TEST DATA (ROUND RAIL AND SIMPLE FLANGED CONED WHEEL) FOR WHRAIL
         MODEL
         METHOD  CIRCULAR ARCS AND STRAIGHT LINES FORM THE PROFILES
         INPUTS
         OUTPUTS  PROFILE DATA FOR ROUND RAIL AND CONED; FLANGED WHEEL
         DELIVERY
         LANGUAGE  FORTRAN
         RESOURCES  INPUT:CARDS(UNIT5)              OUTPUT:PRINTER(UNIT6)  TEMP DISK(UNIT7&8)
         COMPILE TIME(SECS)=  1:00.00      COMPILE SIZE(K)=  340K
         RUN TIME(SECS)=  0:00.00      RUN SIZE(K)=  [illegible]
         STRUCTURE  ONE SUBROUTINE CALLED; OUTPUT DATA FILE IN CORRECT FORMAT TO BE USED BY WHRAIL
         TECH REPT
         PROGRAM SPEC
         USER_GUIDE
         NEWS
```

```
ID   V
--   -
020  0   TITLE  AVOCADET
        ORIGIN  TASC
        DATE_RECD  27 SEP 77
        KEYWORD  NONLINEAR FREIGHT CAR LIMIT CYCLE AND RANDOM RESPONSE TIME HISTORY
        DESCRIPTION  NONLINEAR OR QUASI-LINEAR VEHICLE STATISTICAL DYNAMICS
         MODEL  14-DOF FREIGHT CAR; TRUCK LATERAL; YAW AND TRANS 3 RIGID; 3 FLEX BODY MODES
        METHOD  INTEGRATION OF NONLINEAR EQS; SINUSOIDAL OR RANDOM INPUT QUASI LINEARIZATION
        INPUTS  VEHICLE DATA; SPEED; STATISTICS OF VEHICLE AND TRACK PARAMS
        OUTPUTS  QUASI LINEARIZED EIGENANALYSIS; LIMIT CYCLE DATA; COVARIANCE PROPAGATION
        DELIVERY  IN HOUSE
        LANGUAGE  FORTRAN
        RESOURCES  INPUT:CARDS(UNITS)                    OUTPUT:PRINTER(UNITS)  TECHTRONIX PLOTTER
        COMPILE TIME(SECS)=  3:30.00     COMPILE SIZE(K)=  344K
        RUN TIME(SECS)=  2.5 PER FT  RUN SIZE(K)=  434K
        STRUCTURE  MODULAR; GENERAL PURPOSE EXECUTIVE; 2 VEHICLE SPECIFIC SUBROUTINES
        TECH_REPT  WORKING NOTES
        PROGRAM_SPEC  WORKING NOTES
        USER_GUIDE  NONE
        MEMO  ION 6/13/78 AVOCADET VER#2  -  ION 11/27/78 AVOCADET MODIFICATIONS
```



```
ID   V
--   -
021  0   TITLE  KALKER'S SIMPLIFIED THEORY OF ROLLING CONTACT (FORCES)
        ORIGIN  CLEMSON
        DATE_RECD  12 SEP 77
        KEYWORD  NONLINEAR W/R GEOMETRY; CREEP COEFS; KALKER'S THEORY
        DESCRIPTION  GIVEN CONTACT PATCH GEOM; FIND CREEP COEFFS.  GIVEN CREEPAGE FIND CREEP FORCES
        MODEL  KALKER'S TABLES GIVE CREEP COEFFICIENTS. NONLINEAR.
        METHOD  KALKER'S TABLES AND ASSYMPTOTIC EXPANSIONS YIELD CREEP COEFFS
        INPUTS  NORMALIZED CONTACT ELLIPSE PARAMS; POISSON'S RATIO; CREEPAGE (LONG; SPIN & LAT)
        OUTPUTS  LONGITUDINAL AND LATERAL CREEP FORCES
        DELIVERY  CARDS
        LANGUAGE  FORTRAN
        RESOURCES  INPUT:CARDS(UNITS)                    OUTPUT:PRINTER(UNITS)
        COMPILE TIME(SECS)=  0:30.44     COMPILE SIZE(K)=  356K
        RUN TIME(SECS)=  0:47.01     RUN SIZE(K)=  316K
        STRUCTURE  ONE MAIN PROGRAM AND 4 SUBROUTINES. WELL COMMENTED WITH REF TO TECH LITERATURE.
        TECH_REPT
        PROGRAM_SPEC
        USER_GUIDE  FRA-ORSD-78/96 USER'S MANUAL FOR KALKER'S SIMPLIFIED NONLINEAR CREEP THEORY
        MEMO
```

```
ID   V
--   -
022  0   TITLE  TRKVP80 VOD II
        ORIGIN  BATTELLE COLUMBUS LABORATORIES
        DATE_RECD  22 SEP 77
        KEYWORD  LINEAR FREIGHT CAR PSD ANALYSIS; W/R FORCES; NON-RIGID TRACK
        DESCRIPTION  CALC OF PSD'S OF CAR VERT/HEAVE RESPNS AND CAR LATERAL/ROLL/YAW RESPNS
        MODEL  PITCH HEAVE (7 DOF) IS DECOUPLED FROM LATERAL/ROLL/YAW MOTION (11 DOF); LINEAR
        METHOD  THE OUTPUT PSD IS CALC FROM PSD OF THE TRANSFER FUNC TIMES THE INPUT PSD
        INPUTS  SPEED; PARS; SPRINGS AND STIFFNESS INPUT DID DATA; WHEEL/RAIL DATA
        OUTPUTS  VEHICLE RESPONSE PSD'S OF TRACK FORCES; ACCELS DISPLACEMENTS & SUMMARIES PRTED
        DELIVERY  CARDS
        LANGUAGE  FORTRAN
        RESOURCES  INPUT:CARDS(UNITS)                    OUTPUT:PRINTER(UNITS)
        COMPILE TIME(SECS)=  3:30.30     COMPILE SIZE(K)=  384K
        RUN TIME(SECS)=  0:31.18     RUN SIZE(K)=  356K
        STRUCTURE  ONE MAIN PROGRAM AND 2 SUBROUTINES AND 1 FUNCTION SUBPROGRAM
        TECH_REPT  SUMMARY ON PROGRAM TRKVP80 VOD II (DOT REPORT)
        PROGRAM_SPEC  SUMMARY ON PROGRAM TRKVP80 VOD II (DOT REPORT)
        USER_GUIDE  SUMMARY ON PROGRAM TRKVP80 VOD II (DOT REPORT)
        MEMO  RECEIVED A LETTER FROM D.A. ANLOCH CONCERNING TWO MINOR CHANGES DATED 9/14/77
```

```
ID   V
--   -
023  0   TITLE  A [illegible] FREIGHT CAR [illegible]/EIGENVECTOR PROGRAM
        ORIGIN  CLEMSON
        DATE_RECD  01 SEP 77
        KEYWORD  LINEAR FREIGHT CAR EIGENANALYSIS
        DESCRIPTION  [illegible] CALCULATION FOR A NORTH AMERICAN FREIGHT CAR
        MODEL  [illegible] CAR; [illegible] LAT; ROLL; YAW MOD. LINEAR; 0-60?
        METHOD  [illegible] EIGENVALUES & EIGENVECTORS; [illegible] SUBROUTINE
        INPUTS  CAR [illegible] SPEED; STATISTICS OF [illegible] & SPRING RATES
        OUTPUTS  [illegible] & EIGENVECTORS; [illegible]
        DELIVERY  CARDS
        LANGUAGE  FORTRAN
        RESOURCES  INPUT:CARDS READER (UNITS)            OUTPUT:PRINTER(UNITS)
        COMPILE TIME(SECS)=  0:00.00     COMPILE SIZE(K)=  [illegible]
        RUN TIME(SECS)=  0:00.14     RUN SIZE(K)=  [illegible]
        STRUCTURE  [illegible] AND 17 SUBROUTINES. SOME NON-ANSI STANDARD FORTRAN USED
        TECH_REPT
        PROGRAM_SPEC
        USER_GUIDE
        MEMO
```

```
ID   V
--   -
024  1   TITLE  NINE DEGREES OF FREEDOM INTEGRATION PROGRAM
         ORIGIN  CLEMSON
         DATE_RECD  31 SEP 77
         KEYWORD  NONLINEAR FREIGHT CAR TIME HISTORY
         DESCRIPTION  INTEGRATION OF A 9 DOF NORTH AMERICAN FREIGHT CAR SET OF EQUATIONS OF MOTION
         MODEL  LINEAR AS NINEDIG BUT FRICTION CAN BE INSERTED AT THE CNTR PLATES OR SIDES( 9-DOF
         METHOD  EQUATIONS OF MOTION ARE INTEGRATED BY 4TH ORDER PREDICTOR-CORRECTOR METHOD
         INPUTS  CAR MASS DAMPING(VISCIOUS OR DRY) ; STIFFNESS DATA; DIM DATA; SPEED; CREEP DATA
         OUTPUTS  STATE TIME HISTORIES
         DELIVERY  TAPE (#1094 FILE #2)
         LANGUAGE  FORTRAN
         RESOURCES  INPUT:CARDS(UNIT1)                    OUTPUT:PRINTER(UNIT3)
         COMPILE TIME(SECS)=  3139.41     COMPILE SIZE(K)=  140K
         RUN TIME(SECS)=  1140.78     RUN SIZE(K)=  210K
         STRUCTURE  CONSISTS OF ONE MAIN PROGRAM AND 17 SUBROUTINES
         TECH_REPT
         PROGRAM_SPEC
         USER_GUIDE
         MEMO
```

```
ID   V
--   -
025  3   TITLE  CREEP
         ORIGIN  CLEMSON
         DATE_RECD  31 SEP 77
         KEYWORD  W/R GEOMETRY LINEAR CREEP COEFFS( KALKER'S THEORY( W/R FORCES
         DESCRIPTION  FIND CONTACT ELLIPSE GEOMETRY AND LINEAR CREEP COEFFS FOR CENTERED ANGULAR
         MODEL  ELASTIC DEFORM THRY GIVES CONTACT ELLIPSE(KALKER'S TABLES FOR LINEAR CREEP COEFS
         METHOD  CONTACT ELLIPSE FROM MATERIAL PROPS AND GEOM( CREEP COEFS FROM KALKER'S TABLES
         INPUTS  WHEEL AND RAIL HEAD PROFILE AND ROLLING RADII MATERIAL PROPERTIES( NORMAL FORCE
         OUTPUTS  CREEP COEFFICIENTS( LATERAL( LATERAL/SPIN( SPIN( AND LONGITUDINAL CREEP FORCES
         DELIVERY  TAPE (#1094  FILE-3)
         LANGUAGE  FORTRAN                                OUTPUT:PRINTER(UNIT3)
         RESOURCES  INPUT:CARDS(UNIT1)
         COMPILE TIME(SECS)=  3110.05     COMPILE SIZE(K)=  352K
         RUN TIME(SECS)=  0101.27     RUN SIZE(K)=  310K
         STRUCTURE  CONSISTS OF ONE MAIN PROGRAM AND TEN SUBROUTINES
         TECH_REPT
         PROGRAM_SPEC
         USER_GUIDE  USER'S MANUAL FOR PROGRAM FOR CALC OF KALKER'S LINEAR CREEP COEFFS (DRAFT)
         MEMO
```

```
ID   V
--   -
026  8   TITLE  DYNALIST II
         ORIGIN  TSC
         DATE_RECD  28 MAY 78
         KEYWORD  LINEAR SIGENANALYSIS( TRANSFER FUNCTION CALCULATION( PSD ANALYSIS
         DESCRIPTION  LINEAR SYSTEM ANALYSIS( SINUSOIDAL OR STATIONARY RANDOM INPUT RESPONSE
         MODEL  MODELS ARE CONSTRUCTED OF MODES WITH SUBSYSTEM MODELS EASILY HANDLED
         METHOD  MODEL SYNTHESIS USING COMPLEX EIGENVECTORS
         INPUTS  GENERAL SUBSYSTEM DATA
         OUTPUTS  EIGEN PROBLEM SOLUTION( FREQUENCY RESPONSE( MAGNITUDE( RANDOM RESPONSE AMPLITUDE
         DELIVERY
         LANGUAGE  FORTRAN
         RESOURCES
         COMPILE TIME(SECS)=                  COMPILE SIZE(K)=
         RUN TIME(SECS)=                  RUN SIZE(K)=
         STRUCTURE
         TECH_REPT
         PROGRAM_SPEC
         USER_GUIDE  DYNALIST II: USER'S MANUAL; FRA-CR&D-78.88.11
         MEMO
```

```
ID   V
--   -
027  8   TITLE  TRANSIT
         ORIGIN  DOT/TSC
         DATE_RECD
         KEYWORD  RUNNING EIGENANALYSIS
         DESCRIPTION  LATERAL STABILITY( 2 AXLE TRUCK AS FUNCTION OF SPEED
         MODEL  LINEAR
         METHOD  EIGENPROBLEM
         INPUTS
         OUTPUTS
         DELIVERY
         LANGUAGE
         RESOURCES
         COMPILE TIME(SECS)=                  COMPILE SIZE(K)=
         RUN TIME(SECS)=                  RUN SIZE(K)=
         STRUCTURE
         TECH_REPT
         PROGRAM_SPEC
         USER_GUIDE
         MEMO  PROGRAM PROPRIETARY WITH BCL
```

```
ID   4
--   -
028  3   TITLE  CAHNNY
         ORIGIN  DOT/TSC
         DATE_RECD
         KEYWORD  LINEAR LATERAL-ROLL-YAW EIGENANALYSIS
         DESCRIPTION  LATERAL STABILITY; CAR PLUS 2 TRUCKS; AS FUNCTION OF SPEED
         MODEL  LINEAR
         METHOD  EIGENVALUE
         INPUTS
         OUTPUTS
         DELIVERY
         LANGUAGE
         RESOURCES
         COMPILE TIME(SECS)=              COMPILE SIZE(K)=
         RUN TIME(SECS)=                  RUN SIZE(K)=
         STRUCTURE
         TECH_REPT
         PROGRAM_SPEC
         USER_GUIDE
         KEND  PROGRAM PROPRIETARY WITH DCL
```

```
ID   V
--   -
025  3   TITLE  TRKVSM
         ORIGIN  DOT/TSC
         DATE_RECD
         KEYWORD  LINEAR TIME HISTORY
         DESCRIPTION  RESPONSE TO RECTIFIED SINE; VERTICAL AND LATERAL
         MODEL  7 DOF PITCH/HEAVE; 7 DOF LATERAL
         METHOD
         INPUTS
         OUTPUTS
         DELIVERY
         LANGUAGE
         RESOURCES
         COMPILE TIME(SECS)=              COMPILE SIZE(K)=
         RUN TIME(SECS)=                  RUN SIZE(K)=
         STRUCTURE
         TECH_REPT
         PROGRAM_SPEC
         USER_GUIDE
         KEND  PROGRAM PROPRIETARY WITH DCL
```



```
ID   V
--   -
030  3   TITLE  6-AXLE LOCOMOTIVE RESPONSE MODEL
         ORIGIN  AAR
         DATE_RECD  01 JUN 78
         KEYWORD  LINEAR 6-AXLE LOCO TIME HISTORY; NON-RIGID RAIL
         DESCRIPTION  LOCOMOTIVE TRUCK AND BODY RESPONSE TO LATERAL AND VERTICAL TRACK INPUTS
         MODEL  DECOUPLED PITCH-HEAVE (10 DOF) AND LATERAL-YAW-ROLL (21 DOF)
         METHOD  NUMERICAL INTEGRATION OF LINEAR MODEL
         INPUTS  VEHICLE & TRACK SINUSOIDAL PARAMETERS
         OUTPUTS  POSITION; VELOCITY & ACCELERATION OF EACH DOF; CAN FIND W/R FORCES FROM OUTPUT
         DELIVERY  TAPE(LRECL=80)
         LANGUAGE  FORTRAN
         RESOURCES  CARD READER (UNIT=5) PRINTER (UNIT=6)
         COMPILE TIME(SECS)=  1140.00          COMPILE SIZE(K)=  396K
         RUN TIME(SECS)=  2130.00          RUN SIZE(K)=  512K
         STRUCTURE  MAIN PROGRAM AND TWENTY NINE SUBROUTINES
         TECH_REPT  A-296 LOCOMOTIVE RESPONSE MODEL
         PROGRAM_SPEC
         USER_GUIDE  A-296 LOCOMOTIVE RESPONSE MODEL
         KEND
```

```
ID   V
--   -
030  3   TITLE  6-AXLE LOCOMOTIVE RESPONSE MODEL
         ORIGIN  AAR
         DATE_RECD  01 JUN 78
         KEYWORD  LINEAR 6-AXLE LOCO TIME HISTORY; NON-RIGID RAIL
         DESCRIPTION  LOCOMOTIVE TRUCK AND BODY RESPONSE TO LATERAL AND VERTICAL TRACK INPUTS
         MODEL  DECOUPLED PITCH-HEAVE (10 DOF) AND LATERAL-YAW-ROLL (21 DOF)
         METHOD  NUMERICAL INTEGRATION OF LINEAR MODEL
         INPUTS  VEHICLE & TRACK SINUSOIDAL PARAMETERS
         OUTPUTS  POSITION; VELOCITY & ACCELERATION OF EACH DOF; CAN FIND W/R FORCES FROM OUTPUT
         DELIVERY  TAPE(LRECL=80)
         LANGUAGE  FORTRAN
         RESOURCES  CARD READER (UNIT=5)          OUTPUT PRINTER(UNIT=6)
         COMPILE TIME(SECS)=  1140.00          COMPILE SIZE(K)=  396K
         RUN TIME(SECS)=  2130.00          RUN SIZE(K)=  512K
         STRUCTURE  MAIN PROGRAM AND TWENTY NINE SUBROUTINES. THIS WILL BE UPDATED
         TECH_REPT  A-296 LOCOMOTIVE RESPONSE MODEL
         PROGRAM_SPEC
         USER_GUIDE  A-296 LOCOMOTIVE RESPONSE MODEL
         KEND  ADD TO ACCOUNT STRUCTURE CLN THE PORTRAN77 ERROR COMP TIME FOR NEW ROUTINES
```

```
ID    V
--    -
031   0   TITLE  FREIGHT CAR HUNTING MODEL
          ORIGIN  AAR
          DATE_RECD  31 JUN 78
          KEYWORD  LINEAR FREIGHT CAR HUNTING EIGENANALYSIS
          DESCRIPTION  LATERAL STABILITY OF A FREIGHT CAR
          MODEL  28 DOF LATERAL MODEL; 3 DOF BODY; 4 DOF TRUCKS; 2 DOF AXLES
          METHOD  FIND MASS; STIFFNESS & DAMPING MATRICES; SOLVE EIGEN PROBLEM
          INPUTS  VEHICLE DATA; SPEED
          OUTPUTS  EIGENVALUES AND EIGENVECTORS
          DELIVERY  TAPE(FCH003)
          LANGUAGE  FORTRAN
          RESOURCES  CARD READER (UNIT5) PRINTER (UNIT6)
          COMPILE TIME(SECS)=  1:18.49      COMPILE SIZE(K)=  356K
          RUN TIME(SECS)=  1145.73      RUN SIZE(K)=  216K
          STRUCTURE  ONE MAIN ROUTINE AND THIRTEEN SUBROUTINES. WELL COMMENTED.
          TECH REPT
          PROGRAM SPEC
          USER_GUIDE  A-351 FREIGHT CAR HUNTING MODEL - USER'S MANUAL
          MEMO  INSTALLATION GUIDE DELIVERED WITH PROGRAM

ID    V
--    -
032   0   TITLE  DETAILED LATERAL STABILITY MODEL
          ORIGIN  AAR
          DATE_RECD
          KEYWORD
          DESCRIPTION  LATERAL FORCES OF AN ARBITRARY CONSIST OVER A HYPOTHETICAL TRACK
          MODEL
          METHOD
          INPUTS
          OUTPUTS
          DELIVERY
          LANGUAGE
          RESOURCES
          COMPILE TIME(SECS)=              COMPILE SIZE(K)=
          RUN TIME(SECS)=              RUN SIZE(K)=
          STRUCTURE
          TECH REPT
          PROGRAM SPEC
          USER_GUIDE
          MEMO  NOT YET AVAILABLE

ID    V
--    -
033   0   TITLE  DETAILED VERTICAL TRAIN STABILITY MODEL
          ORIGIN  AAR
          DATE_RECD
          KEYWORD
          DESCRIPTION  VERTICAL FORCES OF AN ARBITRARY CONSIST ALONG A HYPOTHETICAL TRACK
          MODEL
          METHOD
          INPUTS
          OUTPUTS
          DELIVERY
          LANGUAGE
          RESOURCES
          COMPILE TIME(SECS)=              COMPILE SIZE(K)=
          RUN TIME(SECS)=              RUN SIZE(K)=
          STRUCTURE
          TECH REPT
          PROGRAM SPEC
          USER_GUIDE
          MEMO  NOT YET AVAILABLE

ID    V
--    -
034   0   TITLE  LATERAL/VERTICAL FORCE MODEL
          ORIGIN  AAR
          DATE_RECD
          KEYWORD
          DESCRIPTION  WHEEL/RAIL INTERACTION FORCES OF A FREIGHT CAR TRUCK
          MODEL
          METHOD
          INPUTS
          OUTPUTS
          DELIVERY
          LANGUAGE
          RESOURCES
          COMPILE TIME(SECS)=              COMPILE SIZE(K)=
          RUN TIME(SECS)=              RUN SIZE(K)=
          STRUCTURE
          TECH REPT
          PROGRAM SPEC
          USER_GUIDE
          MEMO  NOT YET AVAILABLE; A-237 (USER'S MANUAL) IS LISTED
```

```
ID    V
---   -
035   1   TITLE  WHRAILA
          ORIGIN  CLEMSON
          DATE_RECD  04 MAY 79
          KEYWORD  NONLINEAR W/R GEOMETRY
          DESCRIPTION  COMPUTES THE WHEEL/RAIL CONTACT POSITIONS; GEOMETRY FROM W/R PROFILES
          MODEL  ACCEPTS ASYMMETRIC W/R DATA; PROFILE DATA CAN BE VERY GENERAL
          METHOD  6TH ORDER CURVES ARE FITTED TO DIGITAL PROFILE DATA. ITERATE FOR W/R CONTACT
          INPUTS  WHEEL AND RAIL GAGE; WHEEL AND RAIL PROFILES; RAIL CANT; PROGRAM CONTROL INFO
          OUTPUTS  WHEEL AND RAIL CRV FIT COEFFS; TABLES OF CONTACT PT GEOM AS A FUN OF LATERAL POS.
          DELIVERY  CARDS
          LANGUAGE  FORTRAN
          RESOURCES
          COMPILE TIME(SECS)=                COMPILE SIZE(K)=
          RUN TIME(SEC/MI)=                  RUN SIZE(K)=
          STRUCTURE  MAIN PROGRAM AND 14 SUBROUTINES
          TECH REPT
          PROGRAM SPEC
          USER GUIDE  FRA-ORED-78/05 USER'S MANUAL
          MEMO  ALSO CALCULATES SINUSOIDAL INPUT DESCRIBING FUNCTIONS


ID    V
---   -
035   1   TITLE  WHRAILA
          ORIGIN  CLEMSON
          DATE_RECD  03 MAY 79
          KEYWORD  NONLINEAR W/R GEOMETRY
          DESCRIPTION  COMPUTES THE WHEEL/RAIL CONTACT POSITIONS; GEOMETRY FROM W/R PROFILES
          MODEL  ACCEPTS ASYMMETRIC W/R DATA; PROFILE DATA CAN BE VERY GENERAL
          METHOD  6TH ORDER CURVES ARE FITTED TO DIGITAL PROFILE DATA. ITERATE FOR W/R CONTACT
          INPUTS  WHEEL AND RAIL GAGE; WHEEL AND RAIL PROFILES; RAIL CANT; PROGRAM CONTROL INFO
          OUTPUTS  WHEEL AND RAIL CRV FIT COEFFS; TABLES OF CONTACT PT GEOM AS A FUN OF LATERAL POS
          DELIVERY  TAPE 60504 (9 TRK; 80 CHAR RECD; 10 REC BLKING; FILE #1)
          LANGUAGE  FORTRAN
          RESOURCES
          COMPILE TIME(SECS)=                COMPILE SIZE(K)=
          RUN TIME(SECS)=                    RUN SIZE(K)=
          STRUCTURE  MAIN PROGRAM AND 14 SUBROUTINES
          TECH REPT
          PROGRAM SPEC
          USER GUIDE  FRA-ORED-78/05 USER'S MANUAL
          MEMO  ALSO CALCULATES SINUSOIDAL INPUT ...RIBING FUNCTIONS; NEW VERSION FROM TSC


ID    V
---   -
036   0   TITLE  DYCAR MODEL
          ORIGIN  AAR
          DATE_RECD  01 JUN 79
          KEYWORD  NONLINEAR FLEXIBLE FREIGHT CAR TIME HISTORY; W/R FORCES
          DESCRIPTION  PREP AND POST PROCESSORS FOR FLEXIBLE BODY FREIGHT CAR
          MODEL  23 DOF FLEXIBLE BODY FREIGHT CAR
          METHOD  FREE FORM (INPUTS ARE FORMATTED FOR PROGRAM RVDL-401)
          INPUTS  VEHICLE DATA; TRACK DATA; CAR SPEED
          OUTPUTS  POSITION; VELOCITY; AND ACCELERATION OF EACH DOF; RAIL REACTIONS
          DELIVERY  TAPE0926
          LANGUAGE  FORTRAN
          RESOURCES  VERY LARGE TEMPORARY DISK DATA SETS ARE REQUIRED
          COMPILE TIME(SECS)=  3134.36       COMPILE SIZE(K)=  256K
          RUN TIME(SECS)=  8118.18           RUN SIZE(K)=  512K
          STRUCTURE  69 FORTRAN SOURCE ROUTINES PLUS ONE ASSEMBLER ROUTINE (KRONOS)
          TECH REPT
          PROGRAM SPEC
          USER GUIDE
          MEMO  INSTALLATION GUIDE DELIVERED WITH PROGRAM


ID    V
---   -
037   0   TITLE  FATIGUE LIFE ANALYSIS
          ORIGIN  AAR
          DATE_RECD  01 JUN 79
          KEYWORD  FREIGHT CAR FATIGUE ANALYSIS
          DESCRIPTION  CALCULATES FATIGUE LIFE OF A FREIGHT CAR
          MODEL
          METHOD
          INPUTS  STRESS SPECTRUMS; EMPTY/LOAD RATIO; IMPACT LOADING
          OUTPUTS  FATIGUE LIFE IN MILES
          DELIVERY  TAPE; PLACED
          LANGUAGE  FORTRAN
          RESOURCES  INPUT/CARD READER(UNITS)                OUTPUT/PRINTER(UNITS)
          COMPILE TIME(SECS)=  0117.00       COMPILE SIZE(K)=  256K
          RUN TIME(SECS)=  018.33            RUN SIZE(K)=  256K
          STRUCTURE  ONE MAIN ROUTINE AND 5 SUBROUTINES. UNDOCUMENTED CODE
          TECH REPT
          PROGRAM SPEC
          USER GUIDE
          MEMO  INSTALLATION GUIDE DELIVERED WITH PROGRAM
```

```
ID   A
--   -
138  3   TITLE  CURVELOCO
         ORIGIN  TSC/ARIZONA STATE
         DATE_RECD  08 MAY 79
         KEYWORD  NONLINEAR 6-AXLE LOCO TIME HISTORY; CURVED TRACK L/V RATIO; W/R FORCES
         DESCRIPTION  DYNAMIC RESPONSE OF A 6-AXLE LOCO ON TANGENT; SPIRAL OR CURVED TRACK.SEE ENG SUM
         MODEL  6-AXLE LATERAL RESPONSE (21 DOF) WITH 3 EXTRA STATE EQUATIONS FOR AXLE ROTATION
         METHOD  INTEGRATION OF EQUATIONS OF MOTION. NONLINEAR W/R LOCATION.
         INPUTS  VEHICLE DATA; TRACK CHARACTERISTICS; W/R DATA; CREEP DATA
         OUTPUTS  STATE TIME HISTORY; L/V RATIOS
         DELIVERY  CARDS
         LANGUAGE  FORTRAN
         RESOURCES
         COMPILE TIME(SECS)=              COMPILE SIZE(K)=
         RUN TIME(SECS)=                  RUN SIZE(K)=
         STRUCTURE  MAIN PROGRAM AND 12 SUBROUTINES
         TECH_REPT
         PROGRAM_SPEC
         USER_GUIDE  LOCOMOTIVE DYNAMIC CURVING ANALYSIS PROGRAM USER'S MANUAL
         MEMO

ID   V
836  1   TITLE  CURVELOCO
         ORIGIN  TSC/ARIZONA STATE
         DATE_RECD  03 MAY 79
         KEYWORD  NONLINEAR 6-AXLE LOCO TIME HISTORY; CURVED TRACK L/V RATIO; W/R FORCES
         DESCRIPTION  DYNAMIC RESPONSE OF A 6-AXLE LOCO ON TANGENT; SPIRAL OR CURVED TRA. SEE ENG SUM
         MODEL  6-AXLE LATERAL RESPONSE (21 DOF) WITH 6 EXTRA STATE EQUATIONS FOR AXLE ROTATION
         METHOD  INTEGRATION OF EQUATIONS OF MOTION. NONLINEAR W/R LOCATION
         INPUTS  VEHICLE DATA; TRACK CHARACTERISTICS; W/R DATA; CREEP DATA
         OUTPUTS  STATE TIME HISTORY; L/V RATIOS
         DELIVERY  TAPE #4864 (9 TRK; 80 CHAR REC; 10 REC BLKING; FILE #3)
         LANGUAGE  FORTRAN
         RESOURCES
         COMPILE TIME(SECS)=              COMPILE SIZE(K)=
         RUN TIME(SECS)=                  RUN SIZE(K)=
         STRUCTURE  MAIN PROGRAM AND 12 SUBROUTINES
         TECH_REPT
         PROGRAM_SPEC
         USER_GUIDE  LOCOMOTIVE DYNAMIC CURVING ANALYSIS PROGRAM USER'S MANUAL
         MEMO  LOCOMOTIVE DYNAMIC CURVING ANALYSIS PROGRAM USER'S MANUAL; NEW VERSION PRG4 TSC

ID   V
838  2   TITLE  WHEELSET/RAIL GEOMETRY
         ORIGIN  ARIZONA STATE
         DATE_RECD  08 MAY 79
         KEYWORD  CREEP COEFS; CONTACT ELLIPSE; KALKER'S THEORY; W/R GEOMETRY
         DESCRIPTION  GIVEN W/R GEOMETRY AS FUNCTION OF LATERAL POSITION FIND CREEP
         MODEL  FINDS W/R FOR CONTACT ELLIPSE; KALKER FOR CREEP COEFS
         METHOD  CALCULATE LOCAL CURVATURE; FIND CONTACT ELLIPSE; FIND CREEP COEFS
         INPUTS  WHEEL AND RAIL CONTACT ANGLES AND CURVATURE VS A PCN OF LATERAL PUS
         OUTPUTS  CREEP COEFS AS PCN OF WHEELSET LATERAL
         DELIVERY  CARDS
         LANGUAGE  FORTRAN
         RESOURCES
         COMPILE TIME(SECS)=              COMPILE SIZE(K)=
         RUN TIME(SECS)=                  RUN SIZE(K)=
         STRUCTURE
         TECH_REPT
         PROGRAM_SPEC
         USER_GUIDE
         MEMO

ID   V
839  1   TITLE  WR DATA REDUC
         ORIGIN  Arizona STATE
         DATE_RECD  01 MAY 79
         KEYWORD  CREEP COEFS; CONTACT ELLIPSE; KALKER'S THEORY; W/R GEOMETRY
         DESCRIPTION  GIVEN W/R GEOMETRY AS FUNCTION OF LATERAL POSITION FIND CREEP
         MODEL  FINDS W/R FOR CONTACT ELLIPSE; KALKER FOR CREEP COEFS
         METHOD  CALCULATE LOCAL CURVATURE; FIND CONTACT ELLIPSE; FIND CREEP COEFS
         INPUTS  WHEEL AND RAIL CONTACT ANGLES AND CURVATURE VS A PCN OF LATERAL PUS
         OUTPUTS  CREEP COEFS AS PCN OF WHEELSET LATERAL
         DELIVERY  TAPE 30004 (9TRK; 80 CHAR REC; 10 REC BLKING; FILE #3)
         LANGUAGE  FORTRAN
         RESOURCES
         COMPILE TIME(SECS)=              COMPILE SIZE(K)=
         RUN TIME(SECS)=                  RUN SIZE(K)=
         STRUCTURE
         TECH_REPT
         PROGRAM_SPEC
         USER_GUIDE
         MEMO  NEW VERSION PRG4 TSC
```

```
ID    V
--    -
040   3    TITLE  FRATE
           ORIGIN  WITRE (VIRGINIA)
           DATE_RECD
           KEYWORD  NONLINEAR FLEXIBLE FREIGHT CAR TIME HISTORY
           DESCRIPTION  FULL-ORDER TOPIC EQUATIONS OF MOTION ARE NUMERICALLY INTEGRATED
           MODEL  11-DOF RGT CAR; 4-DOF FLEX; TWO 4-DOF TRAILERS; VISCOUS DAMPING; NONLIN SPRINGS
           METHOD  SNGL-FREQ LAT; ROLL; HEAVE POSITION; VELOCITY OR ACCEL INPUT DRIVES CAR MOTION
           INPUTS  VEHICLE DATA; TRAILER DATA; SINGLE-FREQUENCY SINUSOIDAL INPUT AMP AND PHASE
           OUTPUTS  RESPONSE TIME HISTORY; RESPONSE ENVELOPES
           DELIVERY
           LANGUAGE  FORTRAN
           RESOURCES
           COMPILE TIME(SECS)=                    COMPILE SIZE(K)=
           RUN TIME(SECS)=                    RUN SIZE(K)=
           STRUCTURE  MAIN PROGRAM AND FIVE SUBROUTINES
           TECH REPT  FRATE VOLUME 2: TECHNICAL MANUAL
           PROGRAM SPEC
           USER GUIDE  FRATE VOLUME 1: USER'S MANUAL (FRA/ORD0-78/50)
           REMD  DEVELOPED FREIGHT CYCLE PROGRAM FOR VTU CALIBRATION


ID    V
--    -
041   3    TITLE  FPS
           ORIGIN  PRINCETON (JOE SIVAK)
           DATE_RECD  19 FEB 79
           KEYWORD  W/R FORCES; CREEP COEFS; KALKER'S THEORY
           DESCRIPTION  GIVEN W/R GEOMETRY AS FCN OF LAT POS AND YAW; FIND LAT FORCE AND YAW MOMENT
           MODEL  TIMOSHENKO FOR CONTACT ELLIPSE; KALKER FOR CREEP COEFS
           METHOD  FIND CONTACT ELLIPSE; LOOK UP CREEP; APPLY VECTOR SLIPPAGE LIMIT
           INPUTS  W/R GEOMETRY AS FCN OF LAT POS; YAW RANGE; COEF OF FRICTION; NORMAL FORCE
           OUTPUTS  LAT FORCE AND YAW MOMENT VS LAT POS AND YAW
           DELIVERY  LISTING
           LANGUAGE  APL
           RESOURCES
           COMPILE TIME(SECS)=                    COMPILE SIZE(K)=
           RUN TIME(SECS)=                    RUN SIZE(K)=
           STRUCTURE  MAIN PROGRAM AND 0 SUBROUTINES. NO COMMENTS
           TECH REPT
           PROGRAM SPEC
           USER GUIDE
           REMD
```

APPENDIX B

SIXTEEN DEGREE OF FREEDOM MODEL

B.1 INTRODUCTION

This appendix describes the freight car model used with the exception of the rail/wheel interactions discussed in Chapter 3. The model consists of sixteen degrees of freedom with piecewise-linear suspension elements.

B.2 EQUATIONS OF MOTION

The complete vehicle described by the model is that of a freight car having two 3-piece trucks. The trucks have motion variables subscripted A and B on the leading and trailing ends. The body motion variables are subscripted C. The rigid body coordinates for the carbody are shown in Fig. B.2-1. The motion is expressed in rectangular coordinates having their origin at a point moving with the carbody center of gravity at constant speed v along the track. In the vertical cross section this point has the static loaded position of the body center of gravity relative to unsuperelevated track.

The five variables describing rigid body motion of the carbody, given in Fig. B.2-1, are:

- Lateral displacement (y_c)
- Vertical displacement or heave (z_c)
- Roll angle (ϕ_c)
- Pitch angle (θ_c)
- Yaw angle (ψ_c).

In addition, carbody flexibility is modeled by twisting, and by lateral and vertical bending modes with motion variables ξ_x, ξ_y and ξ_z respectively. The subscripts indicate the axis of rotation. The first mode only is used to characterize each carbody flexibility. The modes are illustrated in Fig. B.2-2. The deflection of these modes at the carbody bolster per unit motion is given by the Γ parameters. Hence, Γ_z is the lateral deflection due to lateral bending, Γ'_z is the yaw deflection due to lateral bending, Γ_y is the vertical deflection due to vertical bending and Γ_x is the roll deflection due to torsion.

The external forces and moments acting upon the carbody are shown reacting to positive movement in Fig. B.2-3. In this diagram, F_{yA}, F_{yB} are the lateral forces provided by the bolster at trucks A and B. F_{yC} is the force due to the centrifugal overbalance at the body center of gravity, W_c is the static body weight assumed equally distributed, T_{GA} and T_{GB} are the moments due to the lateral load shift relative to the central axis during roll at positions A and B. $F_{zA,B}$ are the dynamic vertical forces at the bolster centers A and B and $T_{xA,B}$ are the roll moments between the carbody and bolster at each truck. T_{zA} and T_{zB} are the moments in yaw at the center plates at A and B. The characteristics of these moments and forces are given later in terms of their local coordinates and motion variables.

Each bolster is modeled as having a separate degree of freedom, in roll about the x axis, but is assumed to move vertically and laterally with the body. The roll angles are ϕ_{BA} at truck A and ϕ_{BB} at truck B. The forces and moments acting upon the A bolster are shown in Fig. B.2-4. The bolster moves in yaw with the truck wheelsets, being assumed guided at its ends in the sideframes.

Each truck is modeled as two wheelsets connected to the sideframes by frictionless "pin joints" at the bearings, as shown in Fig. B.2-5. This model was used by Blader and Kurtz and by Law, Hadden and Cooperrider (Ref. 8). Truck characteristics have been measured by Martin Marietta Corp. (Ref. 13). The three motion variables for each truck, shown in the plan view for truck are:

- Truck center lateral displacement (y_A, y_B)
- Wheelset (bolster) yaw (ψ_A, ψ_B)
- Sideframe yaw (γ_A, γ_B).

They are in rectangular coordinates parallel to those specified for the body and moving with it at the nominal position for each truck.

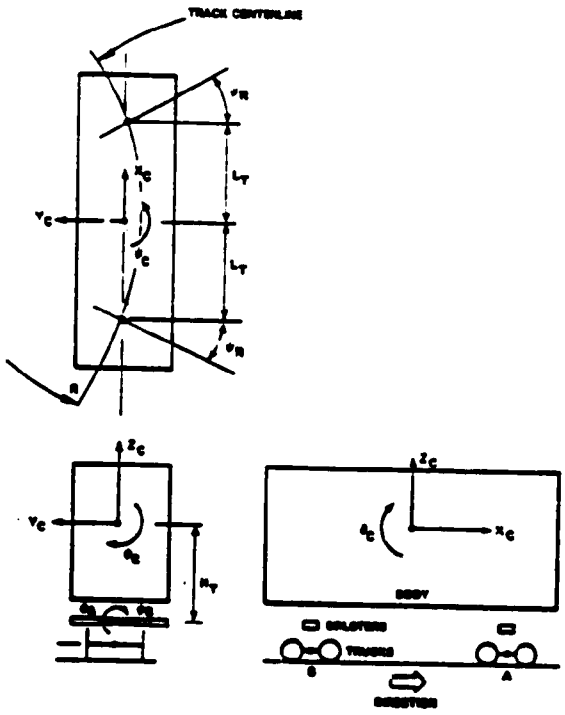

Figure B.2-1 Rigid Body Coordinates

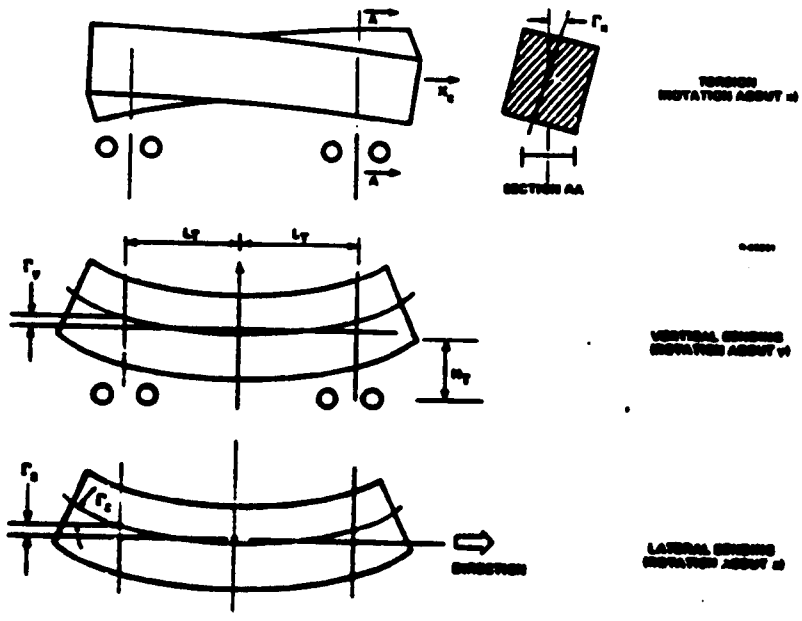

Figure B.2-2 Flexible Carbody Model Parameters

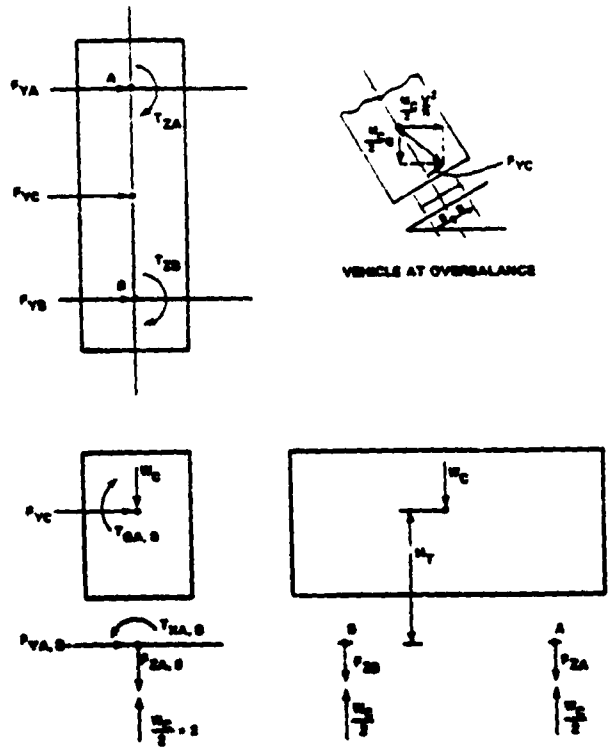

Figure B.2-3 External Forces and Moments on the Body

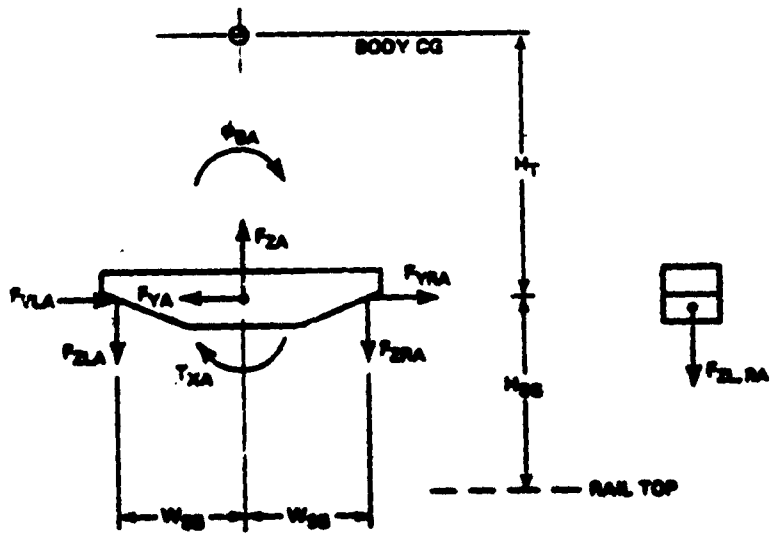

Figure B.2-4 External Forces and Moments on Bolster A

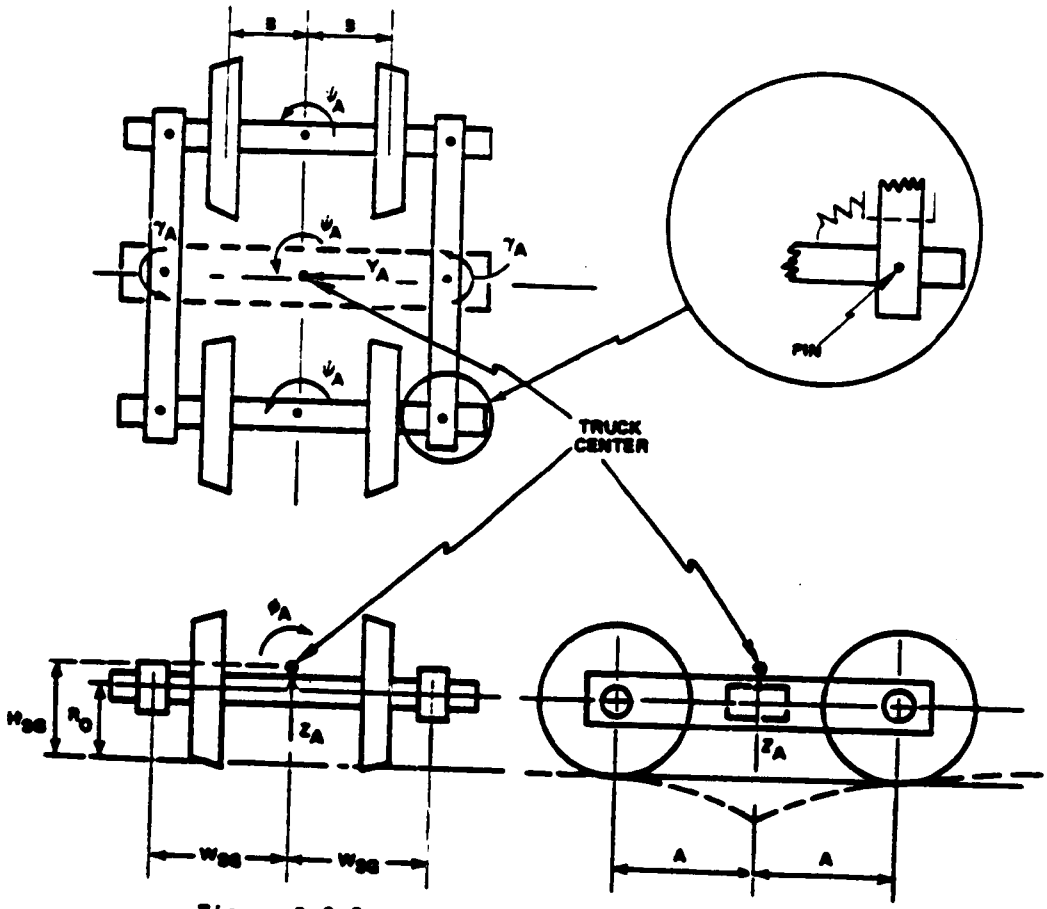

Figure 8.2-5 Truck Parameters (Truck A Shown)

The vertical displacement z_A and z_B and the mean roll angle ϕ_A and ϕ_B for each truck are computed directly from the rail input, since there is no primary suspension and full "equalization" is assumed between axles of the load and the sideframes. Thus in Fig. 8.2-6, F_{zAL1} and F_{zAL2} are equal as are F_{zAR1} and F_{zAR2}. The lateral force on the wheelsets from the rails are shown as F_{yA1} and F_{yA2} and contain both tread and flange forces as do the yaw moments T_{zA1} and T_{zA2}. $F_{y_{SA}}$ and T_{zA} arise from the body suspension. F_{GA} includes the force due to centrifugal unbalance on the truck. T_{BA} represents a stiffening element at all pins between axle and bolster and sideframe. Since the linear spring elements are represented at the truck center by moment T_{BA} and force F_{yA}, forces F_{zRA} and F_{zLA} are the remaining suspension force due to the snubber. Similar forces and moments are found on the B truck.

The equations of motion for the degrees for freedom in terms of the external forces and moments about static balanced equilibrium values are as follows:

8.2.1 Rigid Body Motion

1. Lateral

$$M_C \ddot{y}_C = -F_{yC} - F_{yA} - F_{yB}$$

2. Bounce

$$M_C \ddot{z}_C = -F_{zA} - F_{zB}$$

3. Roll

$$I_{xC} \ddot{\phi}_C = -H_t F_{yA} - H_t F_{yB} - T_{zA} - T_{zB} + T_{GA} + T_{GB}$$

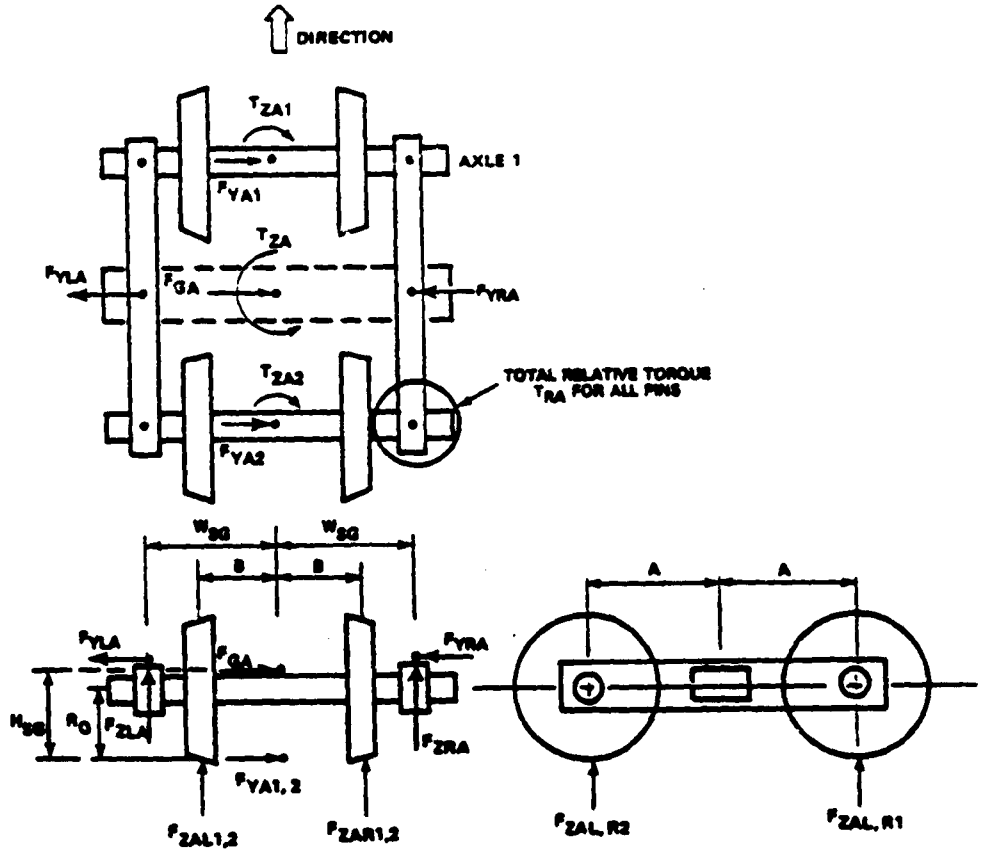

Figure B.2-6 External Forces and Moments (Truck A Shown)

4. Pitch

$$I_{yC}\ddot{\theta}_C = L_T F_{zA} - L_T F_{zB}$$

5. Yaw

$$I_{zC}\ddot{\psi}_C = -L_T F_{yA} + L_T F_{yB} - T_{zA} - T_{zB}$$

B.2.2 Flexible Body Motion (Free-Free Mode)

6. Twist

$$M_{xC}\ddot{\xi}_x = -M_x\omega_x^2\xi_x - H_T\Gamma_x F_{yA} + H_T\Gamma_x F_{yB} - \Gamma_x T_{xA} + \Gamma_x T_{xB}$$

7. Vertical Bending (about y)

$$M_{yC}\ddot{\xi}_y = -M_{yC}\omega_y^2\xi_y - \Gamma_y F_{zA} - \Gamma_y F_{zB}$$

8. Lateral Bending (about z)

$$M_{zC}\ddot{\xi}_z = -M_{zC}\omega_z^2\xi_z - \Gamma_z F_{yA} - \Gamma_z F_{yB} - \Gamma_z' T_{zA} + \Gamma_z' T_{zB}$$

B.2.3 Truck A - Leading

9. Lateral

$$(2M_S + 2M_w)\ddot{y}_A = F_{yLA} + F_{yRA} - F_{YA1} - F_{yA2} - F_{GA} + (2M_S + 2M_w) H_{SC}\ddot{\phi}_A$$

10. Yaw (wheelsets)

$$(I_{Bz}+2W_{SG}^2M_S+2I_w)\ddot{\psi}_A = T_{zA} - T_{zA1} - T_{zA2} - T_{RA}$$

11. Yaw (side frames)

$$(2I_S+2A^2M_w)\ddot{\gamma}_A = T_{RA} - AF_{yA1} + AF_{yA2}$$

B.2.4 Truck B - Trailing (Not Shown)

12. Lateral

$$(2M_S+2M_w)\ddot{y}_B = F_{yLB} + F_{yRB} - F_{yB1} - F_{yB2} - F_{GB} + (2M_S + 2M_w) H_{SG} \ddot{\phi}_B$$

13. Yaw (wheelsets)

$$(I_{Bz}+2W_{SG}^2M_S+2I_w)\ddot{\psi}_B = T_z - T_{zB1} - T_{zB1} - T_{zB2} - T_{RB}$$

14. Yaw (sideframes)

$$(2I_S+2A^2M_w)\ddot{\gamma}_B = T_{RB} - AF_{yB1} + AF_{yB2}$$

B.2.5 Bolster Motion

15. Roll - Bolster A

$$I_{Bx}\ddot{\phi}_{BA} = T_{xA} + W_{SG} F_{zRA} - W_{SG} F_{zLA}$$

16. Roll - Bolster B

$$I_{Bx}\ddot{\phi}_{BB} = T_{xB} + W_{SG} F_{zRB} - W_{SG} F_{zLB}$$

B.2.6 Other Relationships

- Lateral Forces at Bolster

$$F_{yA} = F_{yLA} + F_{yRA}$$
$$F_{yB} = F_{yLB} + F_{yRB}$$

- Vertical Forces at Bolster

$$F_{zA} = F_{zLA} + F_{zRA}$$
$$F_{zB} = F_{zLB} + F_{zRB}$$

- Pitch Equalization

$$F_{zAR} = F_{zAR1} = F_{zAR2}$$
$$F_{zAL} = F_{zAL1} = F_{zAL2}$$
$$F_{zBR} = F_{zBR1} = F_{zBR2}$$
$$F_{zBL} = F_{zBL1} = F_{zBL2}$$

- Vertical - Trucks A and B

$$-F_{zLA} - F_{zRA} = 2F_{zAL} + 2F_{zAR}$$
$$-F_{zLB} - F_{zRB} = 2F_{zBL} + 2F_{zBR}$$

- Roll - Trucks A and B

$$H_{SG} F_{yA} - H_{SG} F_{GA} + W_{SG} F_{zRA} - W_{SG} F_{zLA} = 2B F_{zAL} - 2B F_{zAR}$$

$$H_{SG} F_{yB} - H_{SG} F_{GB} + W_{SG} F_{zRB} - W_{SG} F_{zLB} = 2B F_{zBL} - 2B F_{zBR}$$

B.3 SYSTEM CHARACTERISTICS

In the following description, each system force or moment is given in terms of the local coordinate, e.g., a local spring deflection. These, including the wheel/rail characteristics, are linearly related to the state variables chosen for equations of motion. Nonlinear relationships are given in graphical form.

B.3.1 Local Coordinates for the Wheelsets

The characteristic interactions described in Chapter 3 are given in local wheelset coordinates relative to the track. These are therefore redefined in the frame of reference of the motion or state variables, relative to the vehicle position when in balance and placed centrally upon the track. The following relationships are required to convert the local coordinates, subscripted A1, A2, B1, B2 for each wheelset to the state variables.

- Leading Truck - A - Wheelset 1

$$y_{A1} = y_A + A(\gamma_A - \psi_R) - y_{R1};$$
$$\dot{y}_{A1} = \dot{y}_A + A\dot{\gamma}_A$$

$$\psi_{A1} = \psi_A - \psi_r\left(1+\frac{A}{L_T}\right);$$

$$\dot{\psi}_{A1} = \dot{\psi}_A + \frac{v}{R}$$

- wheelset 2

$$y_{A2} = y_A - A(\gamma_A - \psi_R) - y_{R2}$$
$$\dot{y}_{A2} = \dot{y}_A - A\dot{\gamma}_A$$

$$\psi_{A2} = \psi_A - \psi_R\left(1-\frac{A}{L_T}\right);$$

$$\dot{\psi}_{A2} = \dot{\psi}_A + \frac{v}{R}$$

- Trailing Truck - B - Wheelset 1

$$y_{B1} = y_B + A(\gamma_B + \psi_R) - y_{R3};$$
$$\dot{y}_{B1} = \dot{y}_B + A\dot{\gamma}_B$$

$$\psi_{B1} = \psi_B + \psi_R\left(1-\frac{A}{L_T}\right)$$

$$\dot{\psi}_{B1} = \dot{\psi}_B + \frac{v}{R}$$

- wheelset 2

$$y_{B2} = y_B - A(\gamma_B + \psi_R) - y_{R4};$$
$$\dot{y}_{B2} = \dot{y}_B - A\dot{\gamma}_B$$

$$\psi_{B2} = \psi_B + \psi_R\left(1+\frac{A}{L_T}\right)$$

$$\dot{\psi}_{B2} = \dot{\psi}_B + \frac{v}{R}$$

where

$y_{R1} - y_{R4}$ - lateral track center offset (alignment variation) at wheelsets 1 - 4

A - semi wheelbase in truck

L_T - semi-truck base in car

$\frac{v}{R}$ - apparent track yaw velocity relative to the wheelset due to the curve, radius R, for speed v

x - truck rotation due to curve (see Fig. B.2-1).

Using the above relationships, values are determined for the linear combinations required to compute the wheel/rail forces and moments. Thus for the leading wheelset the additional relationships required from Section 3.3.1 are:

- Lateral creepage in the horizontal plane

$$\left(\frac{\dot{y}_{A1}}{v} - \psi_{A1}\right) = \frac{1}{v}(\dot{y}_A + A\dot{\gamma}_A) - \psi_A + \psi_R\left(1 + \frac{A}{L_T}\right)$$

- Longitudinal creepage in the horizontal plane for the right wheel

$$\left(\frac{a}{r_o} y_{A1} + \frac{B}{v}\dot{\psi}_{A1}\right) = \frac{a}{r_o}\left(y_A + A(\gamma_A - \psi_R) - y_{R1}\right) + \frac{B}{v}\left(\dot{\psi}_A + \frac{v}{R}\right)$$

B.3.2 Lateral Suspension and Truck Forces

- Forces F_{yA}, F_{yB}, F_{GA} and F_{GB}

The lateral forces modeled arise from lateral springing F'_{YA}, F'_{YB}, lateral damping F''_{YA}, F''_{YB} and the forces due to superelevation deficiency in curves, F_{GA} and F_{GB}.

The local coordinates $y_{local(A)}$ and $y_{local(B)}$ are given by:

$$y_{local(A)} = y_C + H_T\phi_C + L_T\psi_C + H_T r_x \xi_x + r_z\xi_z - y_A + H_{SG}\phi_A$$

$$y_{local(B)} = y_C + H_T\phi_C - L_T\psi_C - H_T r_x \xi_x + r_z\xi_z - y_B + H_{SG}\phi_B$$

The spring characteristic is given in Fig. B.3-1. In addition to the spring forces, linear damping forces, F''_{yA} and F''_{yB}, are used to approximate energy dissipation, where,

$$F''_{yA} = B_{yA}\,(\dot{y}_c + H_T\dot{\phi}_c + L_T\dot{\psi}_c + H_T\Gamma_x\dot{\xi}_x + \Gamma_z\dot{\xi}_z - \dot{y}_A + H_{SG}\,\dot{\phi}_A)$$

and,

$$F''_{yB} = B_{yB}\,(\dot{y}_c + H_T\dot{\phi}_c - L_T\dot{\psi}_c - H_T\Gamma_x\dot{\xi}_x + \Gamma_z\dot{\xi}_z - \dot{y}_B + H_{SG}\,\dot{\phi}_B)$$

The total lateral forces F_{yA} and F_{yB} are,

$$F_{yA} = F'_{yA} + F''_{yA}$$

and,

$$F_{yB} = F'_{yB} + F''_{yB}$$

Forces F_{GA} and F_{GB} are due to the unbalanced centrifugal force on the truck masses. They are given by,

$$F_{GA} = 2G(M_{WA} + M_{SA})\varepsilon$$

$$F_{GB} = 2G(M_{WB} + M_{SB})\varepsilon$$

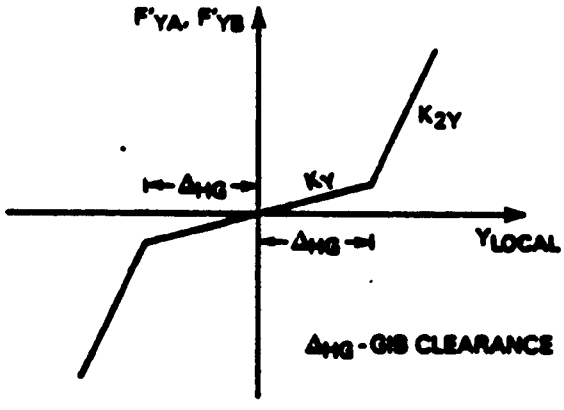

Figure B.3-1 Lateral Spring Forces at Each Truck

where,

G - gravitational constant in./sec^2

M_W - wheelset mass lb sec^2/in.

M_S - sideframe mass lb sec^2/in.

ε - angle of apparent weight vector to track normal.

B.3.3 Vertical Suspension

Snubbing Forces -

$$F_{zLA},\ F_{zLB},\ F_{zRA},\ F_{zRB}$$

Each local suspension force is comprised of the sum of a vertical spring force with provision for becoming "free" for "close-coiled" and a snubber force at each sideframe. The spring force has the characteristic given in Fig. B.3-2.

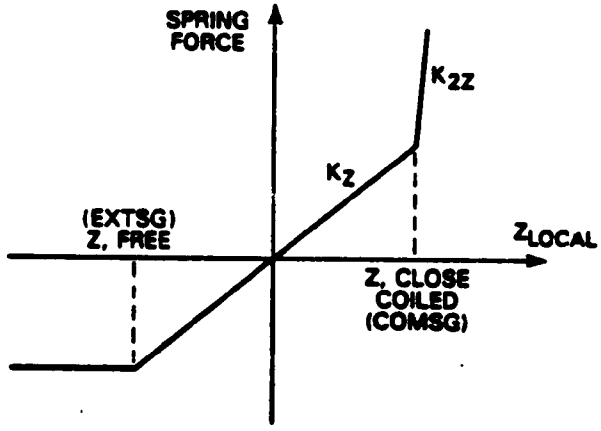

Figure B.3-2 Vertical Spring Characteristic

The local deflections for each spring are,

$$z_{local(RA)} = z_C - L_T\theta_C + \Gamma_y\xi_y - W_{SG}(\phi_{BA}-\phi_A) - z_A$$

$$z_{local(LA)} = z_C - L_T\theta_C + \Gamma_y\xi_y + W_{SG}(\phi_{BA}-\phi_A) - z_A$$

$$z_{local(RB)} = z_C + L_T\theta_C + r_y\xi_y - W_{SG}(\phi_{BB}-\phi_B) - z_B$$

$$z_{local(LB)} = z_C + L_T\theta_C + r_y\xi_y + W_{SG}(\phi_{BB}-\phi_B) - z_B$$

For the snubbers, each force is a function of local velocity across the suspension at each sideframe center. The characteristic is given in Fig. B.3-3.

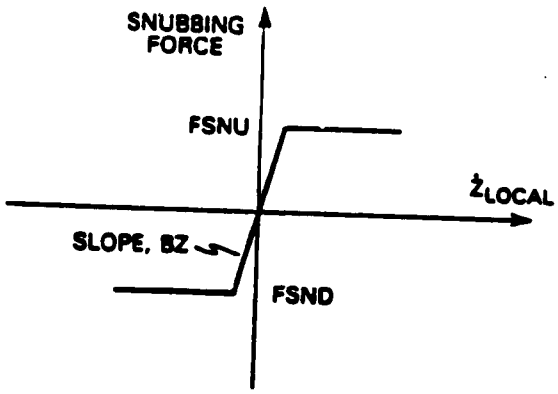

Figure B.3-3 Snubbing Characteristics

The local values of the velocity of each snubber are,

$$\dot{z}_{local(RA)} = \dot{z}_C - L_T\dot{\theta}_C + r_y\dot{\xi}_y - W_{SG}(\dot{\phi}_{BA}-\dot{\phi}_A) - z_A$$

$$\dot{z}_{local(LA)} = \dot{z}_C - L_T\dot{\theta}_C + r_y\dot{\xi}_y + W_{SG}(\dot{\phi}_{BA}-\dot{\phi}_A) - z_A$$

$$\dot{z}_{local(RB)} = \dot{z}_C + L_T\dot{\theta}_C + r_y\dot{\xi}_y - W_{SG}(\dot{\phi}_{BB}-\dot{\phi}_B) - \dot{z}_B$$

$$\dot{z}_{local(LB)} = \dot{z}_C + L_T\dot{\theta}_C + r_y\dot{\xi}_y + W_{SG}(\dot{\phi}_{BB}-\dot{\phi}_B) - \dot{z}_B$$

B.3.4 Body Roll Characteristic

- Moments T_{xA}, T_{xB}, T_{GA}, T_{GB}

The total characteristic for the carbody in roll follows the configurations shown in Fig. B.3-4 suggested by Platin, Beaman, Hedrick and Wormley (Ref 7). During configuration C-1, the roll stiffness characteristic is linear.

The sequence of events described by Fig. B.3-4 is as follows:

C-1 - The centerplate remains in full contact

$T_{xA,B}$ - large linear stiffness K_{xxR} between bolster and body

C-2 - Body rotates over the edge of the centerplate of radius R_{CP}

$T_{xA,B}$ = constant, $\frac{1}{2} W_C R_{CP}$ per truck.

C-3 - Body contacts both centerplate and side bearer following a rotation of angle ϕ_2

$T_{xA,B}$ - large linear stiffness K_{xxR} between bolster and body

$$\phi_2 = CL_{SB}/(L_{SB}-R_{CP})$$

where CL_{SB} - clearance of the sidebearer

$(L_{SB}-R_{CP})$ - distance between sidebearer and edge of centerplate

C-4 - Body rotates over sidebearer

$T_{xA,B}$ = constant, $\frac{1}{2} W_C L_{SB}$ per truck.

The complete characteristic is given in Fig. B.3-5. The local values of the relative roll angle between the car body and the bolster are,

$$\phi_{BA} = (\phi_C + r_x\xi_x) - \phi_{BA}$$

$$\phi_{BB} = (\phi_C - r_x\xi_x) - \phi_{BB}$$

In addition to the roll moment sustained between the body and bolster, T_{xA} and T_{xB}, there exists an overturning

CONFIGURATION	#	DESCRIPTION
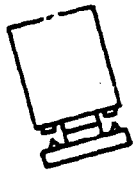	C-1	BOLSTER ROLLING
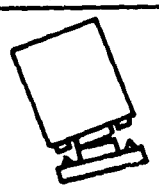	C-2	CENTERLINE ROCKING
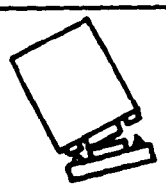	C-3	CENTERPLATE/SIDEBEARING ROCKING
	C-4	SIDEBEARING ROCKING

Figure B.3-4 Body-Bolster Roll Configurations

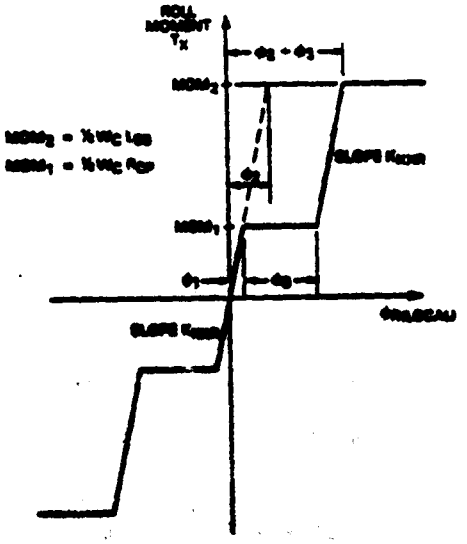

Figure B.3-5 Roll Moment Characteristic

moment, due to the lateral movement of the center of gravity of the body with its load. These are given by:

$$T_{GA} = \frac{1}{2} W_C H_T(\phi_C + \Gamma_x \xi_x)$$

$$T_{GB} = \frac{1}{2} W_C H_T(\phi_C - \Gamma_x \xi_x)$$

B.3.5 Centerplate Friction

- Moments T_{zA}, T_{zB}

The characteristic used to represent centerplate friction is that shown in Fig. B.3-6.

This characteristic represents a small unhindered relative velocity below Δ_{cp} about the steady state position allowing for clearances to be taken up. The local relative yaw velocities, $\dot{\psi}_{local}$, are,

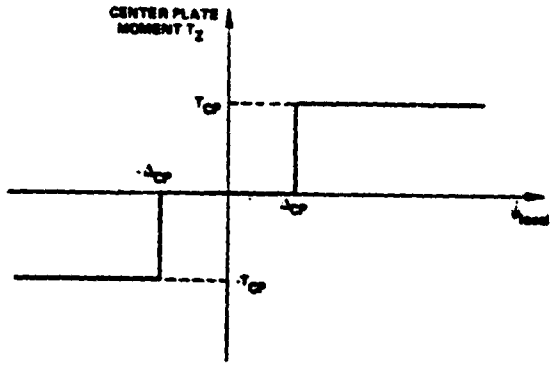

Figure B.3-6 Centerplate Friction Moment

$$\dot{\psi}_{local(A)} = \dot{\psi}_c + r_z\dot{\xi}_z - \dot{\psi}_A$$

$$\dot{\psi}_{local(B)} = \dot{\psi}_c - r_z\dot{\xi}_z - \dot{\psi}_B$$

B.3.6 Tramming Torque

- Moments T_{RA}, T_{RB}

The total effect of yaw movement between the axles (and bolster) and the sideframes within each truck is modeled as a relative rotational stiffness having two rates as shown in Fig. B.3-7. The first rate is associated with the spring groups and the second follows take up of clearances in the gibs and bearings.

For trucks A and B the local, relative yaw angles are,

$$\psi_{rel(A)} = \psi_A - \gamma_A$$

$$\psi_{rel(B)} = \psi_B - \gamma_B$$

B.3.7 Jointed Rail Inputs

All dynamic inputs to the vehicle model are associated with track curvature or rail geometry. Any track geometry may be specified having elements of constant track curvature and rail perturbations. Jointed rail is of particular interest to the study reported since it provides a harmonic input to the vehicle.

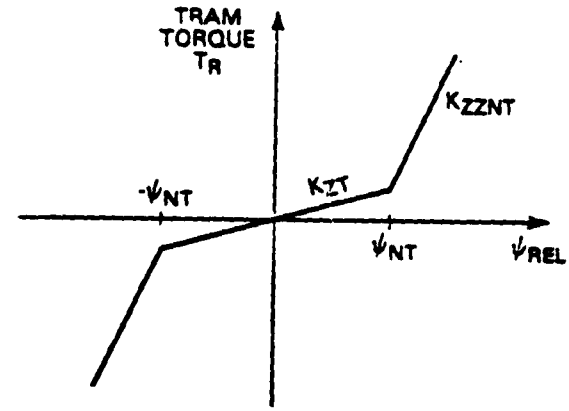

Figure B.3-7 Tramming Torque

The model rail shape used is described fully here.

The rail geometry chosen to represent the jointed rail in both vertical and horizontal perturbations is made up of exponentials as shown in Fig. B.3-8.

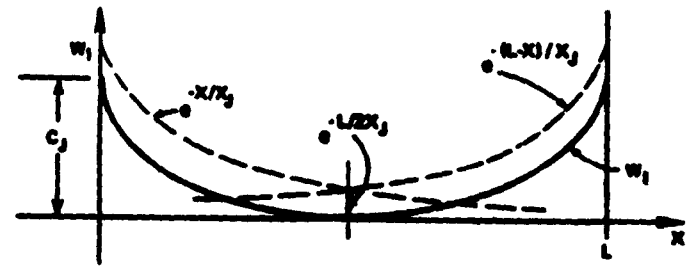

Figure B.3-8 Single Jointed Rail Geometry

The equations of w_1 and its time derivative $\frac{dw_1}{dt} = w_2$ are,

$$w_1 = C_j \frac{e^{-x/x_j} + e^{-(L-x)/x_j} - 2e^{-L/2x_j}}{1 + e^{-L/x_j} - 2e^{-L/2x_j}} \text{ in.}$$

and

$$w_2 = \frac{C_J}{x_J} v. \frac{-e^{-x/x_J} + e^{-(L-x)/x_J}}{1 + e^{-L/x_J} - 2e^{-L/2x_J}} \text{ in. sec}$$

where,

C_J - joint amplitude, in.

x_J - characteristic length, in.

L - rail length, in.

For each wheelset the distance along the track varies,

for wheelset 1, $x_1 = x$

for wheelset 2, $x_2 = x - 2A$

for wheelset 3, $x_3 = x - 2L_T$

for wheelset 4, $x_4 = x-2(A+L_T)$

A further distance difference along the rail of $\frac{L}{2}$ is modeled between left and right rails when the joints are staggered. Thus for any distance along the track the vertical and lateral position of each rail are defined. Using the subscripts A, B to designate the truck; 1,2 to designate the wheelset and L, R to indicate the left or right wheel, the input parameters for truck A in the vertical direction, are,

$$z_A = (z_{A1L} + z_{A1R} + z_{A2L} + z_{A2R})/4$$

$$\dot{z}_A = (\dot{z}_{A1L} + \dot{z}_{A1R} + \dot{z}_{A2L} + \dot{z}_{A2R})/4$$

$$\phi_A = (z_{A1L} + z_{A2L} - z_{A1R} - z_{A2R})/4B$$

$$\dot{\phi}_A = (\dot{z}_{A1L} + \dot{z}_{A2L} - \dot{z}_{A1R} - \dot{z}_{A2R})/4B$$

the lateral perturbation of the truck center,

$$y_{R1} = (y_{A1L} + y_{A1R})/2$$

$$y_{R2} = (y_{A2L} + y_{A2R})/2$$

and the variation in gauge,

$$y_{G1} = y_{A1L} - y_{A1R}$$

$$y_{G2} = y_{A2L} - y_{A2R}$$

Similar expressions exist for truck B parameters z_B, $\dot{z}_B$, ϕ_B, $\dot{\phi}_B$, y_{R3}, y_{R4}, y_{G3}, y_{G4}. Clearances used in the computation of the wheelset-rail nonlinearities are,

$$CR1 = CR + y_{G1}/2$$

$$CR2 = CR + y_{G2}/2$$

$$CR3 = CR + y_{G3}/2$$

$$CR4 = CR + y_{G4}/2$$

where,

CR - nominal clearance each side

CRi - total one sided instantaneous clearance at axle i

B.3.8 Track Curvature

It is customary in railroad practice to define track curvature in degrees, D, subtended by a 100 ft chord. An approximation is used that the radius of the curve R ft is related to the degree of curvature, D by

$$R = 5729.6/D \text{ ft}$$

This leads to further approximations for the input variables. For ε, the unbalanced superelevation angle

$$\varepsilon = 3.767\times10^{-8} V^2.D - E/2B \text{ radians},$$

where,

V = velocity along the track, in./sec

E = elevation of outer rail over inner, in.

B = semi-distance between rails, in.

for the yaw velocity of the track frame of reference represented by the difference ΔV in the rail velocity relative to the wheelset,

$$\Delta V = 1.4544\times10^{-5} \cdot B.V.D \text{ in./sec}$$

and for the offset angle of each truck ψ_R.

$$\psi_R = 1.4544\times10^{-5} \cdot L_T \cdot D \quad \text{radians}$$

B.4 STATE EQUATIONS AND REDUCTION

The simultaneous equations of motion in the 14 degrees of freedom described are of the form,

$$M\,\ddot{\underline{d}} + B\,\dot{\underline{d}} + K\,\underline{d} + \underline{g}\,(\underline{d},\dot{\underline{d}},\underline{u},\dot{\underline{u}}) = \underline{h}\,(\underline{u},\dot{\underline{u}})$$

where

- $\underline{d}$ - vector of motion variables
- M - mass matrix
- B - damping matrix
- K - stiffness matrix
- $\underline{g}$ - vector of nonlinearities
- $\underline{h}$ - input vector.

For the purposes of step by step integration this set of second order differential equations is reduced to first order as a state equation.

B.4.1 Full State Equations

The form of the state equation is,

$$\dot{\underline{x}}_o = F\,\underline{x}_o + D\,\underline{f}\,(\underline{x}_o,\underline{u}) + G\,\underline{u}$$

where,

- $\underline{x}$ - state vector
- $\underline{f}(\underline{x},\underline{b})$ - nonlinear vector function
- $\underline{u}$ - input vector
- F, D, G - dynamics matrices.

The transformation is made using

$$\dot{\underline{d}} = \underline{v}$$

and

$$\dot{\underline{v}} = M^{-1}\,(-B\underline{v} - K\underline{d} - \underline{g} + \underline{h})$$

The ordering of the equations is used here is,

$\underline{x}_o = ($[illegible]$)^T$ (elements numbered 1 to 32)

where the first 10 states describe the rigid body motion of the freight car, the next 6 states describe the torsional, vertical and lateral bending modes and the two trucks (subscripted A and B) provide the next 12 states and the bolsters the final 4 states.

Hence, in the linear system matrix F, the elements $f_{odd,even}$ comprise a unit matrix, the elements $f_{even,odd}$ give $-M^{-1}K$ and the elements from $f_{even,even}$ give the matrix $-M^{-1}B$. Since M is diagonal, M^{-1} is also diagonal consisting of reciprocals of the appropriate masses and inertias. The elements in F, D and G contain multiplication by these. Where linear springs and dampers occur in the physical model described, they give rise to linear coefficients in K and B, positive on the diagonal and negative in the element of the coupled variable. The signs are therefore reversed in F. Moment arms appear from the model to create moments from forces. The resulting terms are apparent from the listing of the elements in the matrix F provided in Appendix C.

B.4.2 Elimination of Truck Masses - State Reduction

The range of frequencies associated with the tracking performance of freight vehicles is generally less than 15 Hz. However, the response of the vehicle as modeled in SIMCAR includes rapidly decaying phenomena, or "hard states", associated with the truck masses. Inclusion of these states would require an extremely small computation time step increasing cost of simulation. To order computation cost and contain sufficient accuracy the inertia forces in the truck and bolster have been set to zero for the study in this report. This has been carried out in the program without changing the basic model by a process of state reduction. The state vector is first permuted such that $\underline{x}_p = \Pi\,\underline{x}_o$ where,

$$\underset{(28\times1)}{\underline{x}_p} = \begin{bmatrix} \underline{x}_c \\ \underline{x}_T \\ \underline{x}_2 \end{bmatrix} \begin{matrix} \text{- body states} \\ \text{- truck and bolster displacements} \\ \text{- truck velocities} \end{matrix}$$

and,

$$\underline{x}_C = y_C, \dot{y}_C, z_C, \dot{z}_C, \phi_C, \dot{\phi}_C, \theta_C, \dot{\theta}_C, \psi_C, \dot{\psi}_C, \xi_x, \dot{\xi}_x, \xi_y, \dot{\xi}_y, \xi_z, \dot{\xi}_z$$

$$\underline{x}_T = y_A, \psi_A, \gamma_A, y_B, \psi_B, \gamma_B, \phi_{BA}, \phi_{BB}$$

$$\underline{x}_1 = (\underline{x}_C, \underline{x}_T)^T$$

$$\underline{x}_2 = \dot{y}_A, \dot{\psi}_A, \dot{\gamma}_A, \dot{y}_B, \dot{\psi}_B, \dot{\gamma}_B, \dot{\phi}_{BA}, \dot{\phi}_{BB} = \dot{\underline{x}}_2$$

The permutation matrix, π can be selected for particular application in SIMCAR and the permutation above is that chosen for the studies reported here. The permuted system, $\underline{x}_p$ is governed by,

$$\dot{\underline{x}}_p = F_p \underline{x}_p + D_p \underline{f}(\underline{x}_o, \underline{u}) + G_p \underline{u}$$

where

$\underline{x}_o$ - original state vector

$F_p = \pi F_o \pi^T$

$D_p = \pi D_o$

$G_p = \pi G_o$

$\underline{x}_p$ is partitioned into, $\underline{x}_p = \begin{bmatrix} \underline{x}_1 \\ \hline \underline{x}_2 \end{bmatrix}$

This implies the further partitions,

$$F_p = \left[\begin{array}{c|c} F_{11} & F_{12} \\ \hline F_{21} & F_{22} \end{array}\right]; \quad D_p = \begin{bmatrix} D_1 \\ \hline D_2 \end{bmatrix}; \quad G_p = \begin{bmatrix} G_1 \\ \hline G_2 \end{bmatrix}$$

The system equations are rewritten,

$$\dot{\underline{x}}_1 = F_{11} \underline{x}_1 + F_{12} \underline{x}_2 + D_1 \underline{f}(\underline{x}_o, \underline{u}) + G_1 \underline{u}$$

$$0 \simeq \dot{\underline{x}}_2 = F_{21} \underline{x}_1 + F_{22} \underline{x}_2 + D_2 \underline{f}(\underline{x}_o, \underline{u}) + G_2 \underline{u}$$

hence

$$\underline{x}_2 = - F_{22}^{-1} F_{21} \underline{x} - F_{22}^{-1} D_2 \underline{f}(\underline{x}_o, \underline{u}) - F_{22}^{-1} G_2 \underline{u}$$

However, $\underline{x}_o = \pi^T \underline{x}_p = \pi^T (\underline{x}_1, \underline{x}_2)^T$. Hence the vector of nonlinearities, $\underline{f}$, is also a function of $\underline{x}_2$ the unknown. For the severe non-linearities of a freight car, a fast general algebraic solution, at each integration step, is difficult. This has been avoided by using the values from the preceeding step. Thus initially,

$$\left[\dot{\underline{x}}_1\right]_n = F_u \left[\underline{x}_1\right]_n + F_{12} \left[\underline{x}_2\right]_n + D_1 \underline{f}\left(\left[\underline{x}_1\right]_n, \left[\underline{x}_2\right]_n, \left[\underline{u}\right]_n\right) + G_1 \underline{u}_n$$

Then,

$$\left[\underline{x}_2\right]_{n+1} = - \bar{F}_{21} \left[\underline{x}_1\right]_n - \bar{D}_2 \underline{f}\left(\left[\underline{x}_1\right]_n, \left[\underline{x}_2\right]_n, \left[\underline{u}\right]_{n+1}\right) - \bar{G}_2 \underline{u}_{n+1}$$

where

$$\bar{F}_{21} = F_{22}^{-1} F_{21}$$

$$\bar{D}_2 = F_{22}^{-1} D_2$$

$$\bar{G}_2 = F_{22}^{-1} G_2$$

Then,

$$\left[\dot{\underline{x}}_1\right]_{n+1} = F_{11} \left[\underline{x}_1\right]_n + F_{12} \left[\underline{x}_2\right]_n + D_1 \underline{f}\left(\left[\underline{x}_1\right]_n, \left[\underline{x}_2\right]_{n+1}, \left[\underline{u}\right]_{n+1}\right) + G_1 \left[\underline{u}\right]_{n+1}$$

Integration is by means of the "trapezoidal" method as follows:

$$\left[x_1\right]_{n+1} = \left[x_1\right]_n + 0.5\left(\left[\dot{x}_1\right]_n + \left[\dot{x}_1\right]_{n+1}\right)\Delta T$$

where ΔT is the time step and $[\ ]_n$, $[\ ]_{n+1}$ represent values at the n^{th} and $(n+1)^{th}$ integration time step.

APPENDIX C

NOMENCLATURE AND PARAMETRIC VALUES

C.1 INTRODUCTION

The nomenclature used in this report is similar to that used in the program, SIMCAR, also used in the study reported. In general symbols have been identified where they arose through statement of definition on a figure. In this appendix they are listed, along with the dynamics matrices in the program SIMCAR. The parametric values, used for the study reported in Chapters 4 and 5, are also given.

C.2 NOMENCLATURE

The symbols used in this report and in the program SIMCAR have the meaning identified in the following sections.

C.2.1 Masses (M) and Inertias (I)

SYMBOL	DEFINITION
M_C	Car body mass
M_{XC}	Car body effective ξ_x mass
M_{YC}	Car body effective ξ_y mass
M_{ZC}	Car body effective ξ_z mass
M_B	Bolster mass
M_S	Sideframe mass
M_W	Wheelset mass
I_{XC}	Car body inertia about x axis
I_{YC}	Car body inertia about y axis
I_{ZC}	Car body inertia about z axis
I_{BX}	Bolster inertia, roll
I_{BZ}	Bolster inertia, yaw
I_S	Sideframe inertia, yaw
I_W	Wheelset inertia, yaw

C.2.2 Inverse Masses and Inertias

```
MCINC = 1.0 / MC
IXCINV = 1.0 / IXC
IYCINV = 1.0 / IYC
IZCINV = 1.0 / IZC
MXCINV = 1.0 / MXC
MYCINV = 1.0 / MYC
MZCINV = 1.0 / MZC
MTINV  = 0.5 / (MW + MS)
IWINV  = 1.0 / ( ( IW + B * B * MS )
                                * 2.0 + IB )
ISINV  = 0.5 /     ( IS + A * A * MW )
IBINV  = 1.0 / IBX
```

C.2.3 Stiffnesses (K) and Dampings (B)

SYMBOL	DEFINITION
K_Y	Car body to sideframe lateral stiffness front/rear trucks - small deflections
K_{2Y}	Same - following gib clearance
K_Z	Car body to truck vertical stiffness front/rear trucks - linear range
K_{2Z}	Same - following spring closure
K_{XXR}	Car body to bolster roll stiffness - small relative deflections
K_{ZZ}	Car body to bolster yaw stiffness - linear
K_{ZT}	Tram stiffness in yaw front/rear trucks - small deflections
K_{ZZNT}	Tram stiffness - large deflections
	All B's are Analogous Damping to Above Stiffness Where They Occur

C.2.4 Car and Component Dimensions

SYMBOL	DEFINITION
L_T	Car body CM to truck CM distance, in x direction
H_T	Distance of car body CM from the truck center, in z direction
a	Half truck wheelbase, in x direction
b	Half track gauge, in y direction
W_{SG}	Half lateral distance between spring groups

SYMBOL	DEFINITION
H_{SG}	Height of top of springs (= Truck CM) above rail
Δ_{HG}	Clearance at gibs in y direction
R_o	Wheel radius - centered contact with rail
L_{SB}	Half lateral distance between sidebearers
CL_{SB}	Clearance of the sidebearers
R_{CP}	Centerplate radius
COM_{SG}	Close-coiled compression of spring group
EXT_{SG}	Extension to free length of spring group

C.2.5 Flexibility Parameters for the Car body

SYMBOL	DEFINITION
$\Omega_x, \Omega_y, \Omega_z$	Natural frequencies of modes ξ_x, ξ_y, ξ_z
$\Gamma_x, \Gamma_y, \Gamma_z$	Modal shapes at $+L_T$
$\Gamma'_x, \Gamma'_y, \Gamma'_z$	Modal derivatives at $+L_T$

C.2.6 Non-Linear Characteristics (Not included elsewhere)

SYMBOL	DEFINITION
FSNU	Upwards snubbing force limit
FSND	Downwards snubbing force limit
ϕ_1	Roll angle between body and bolster at which body tips on center plate
ϕ_2	Roll angle between body and bolster at which body would tip over sidebearer with no sidebearer clearance
ϕ_3	Roll angle between body and bolster during tipping on center plate up to sidebearer contact
MOM_1	Roll moment at which the car body tips over the edge of the center plate
MOM_2	Roll moment at which the car body tips over the sidebearer
T_{CP}	Frictional center plate moment in yaw
Δ_{CP}	Free rotational velocity for center plate
ψ_{NT}	Relative yaw angle between sideframes and bolster (or wheelsets) at which the relative moment stiffens.

C.2.7 Track Parameters

SYMBOL	DEFINITION
C_J	Amplitude at the joint
x_J	Characteristic length
L	Rail length
CR	Nominal flangeway clearance
D(DEG)	Degree of curvature

C.2.8 Wheel/Rail Parameters

SYMBOL	DEFINITION
α	Tread conicity
δ	Flange angle (maximum)
μ	Coefficient of friction

C.3 DYNAMICS MATRICES

The elements of the dynamics matrices F, D and G are identified in this section for the state equation.

$$\dot{\underline{x}} = F\,\underline{x} + D\underline{f}(\underline{x},\underline{u}) + G\,\underline{u}$$

These are followed by a statement of the vectors $\underline{f}$ (nonlinearities), and $\underline{u}$ (inputs).

C.3.1 Linear System Matrix F

```
      F( 2, 1) =-MCINV * ( KY + KY )
      F( 2, 2) =-MCINV * ( BY + BY )
      F( 2, 5) =-MCINV * ( KY + KY ) * HT
      F( 2, 6) =-MCINV * ( BY + BY ) * HT
      F( 2.15) =-MCINV * ( KY + KY ) * GAMSZ
      F( 2.16) =-MCINV * ( BY + BY ) * GAMSZ
      F( 2.17) = KY * MCINV
      F( 2.18) = BY * MCINV
      F( 2.23) = KY * MCINV
      F( 2.24) = BY * MCINV

      F( 4, 3) =-MCINV * ( KZ + KZ)
      F( 4, 4) =-MCINV * ( BZ + BZ)
      F( 4.13) =-MCINV * ( KZ + KZ ) * GAMSY
      F( 4.14) =-MCINV * ( BZ + BZ ) * GAMSY

      F( 6, 1) =-IXCINV * ( KY + KY ) * HT
      F( 6, 2) =-IXCINV * ( BY + BY ) * HT
      F( 6, 5) =-IXCINV * ( 2.0 * ( KXXR - KXXG ) + ( KY + KY )
     $           * HT * HT )
      F( 6, 6) =-IXCINV * ( BY + BY ) * HT * HT  - 2.0 * IXCINV * BXXR
      F( 6.15) =-IXCINV * ( KY + KY ) * GAMSZ * HT
      F( 6.16) =-IXCINV * ( BY + BY ) * GAMSZ * HT
      F( 6.17) = IXCINV * KY * HT
      F( 6.18) = IXCINV * BY * HT
      F( 6.23) = IXCINV * KY * HT
      F( 6.24) = IXCINV * BY * HT
      F( 6.29) = IXCINV * KXXR
      F( 6.30) = IXCINV * BXXR
      F( 6.31) = IXCINV * KXXR
      F( 6.32) = IXCINV * BXXR

      F( 8, 7) =-IYCINV * ( KZ + KZ ) * LT * LT
      F( 8, 8) =-IYCINV * ( BZ + BZ ) * LT * LT
      F(10, 9) =-IZCINV * ( KZZ + KZZ + ( KY + KY ) * LT * LT )
      F(10.10) =-IZCINV * ( BZZ + BZZ + ( BY + BY ) * LT * LT )
      F(10.11) =-IZCINV * ( KY + KY ) * GAMSX * HT * LT
      F(10.12) =-IZCINV * ( BY + BY ) * GAMSX * HT * LT
      F(10.17) = IZCINV * KY * LT
      F(10.18) = IZCINV * BY * LT
      F(10.19) = IZCINV * KZZ
      F(10.20) = IZCINV * BZZ
      F(10.23) =-IZCINV * KY * LT
      F(10.24) =-IZCINV * BY * LT
      F(10.25) = IZCINV * KZZ
      F(10.26) = IZCINV * BZZ

      F(12, 9) =-MXCINV * ( KY + KY) * GAMSX * HT * LT
      F(12.10) =-MXCINV * ( BY + BY) * GAMSX * HT * LT
      F(12.11) =-MXCINV * ( ( 2.0 * ( KXXR - KXXG ) + ( KY + KY )
     $           * HT * HT ) * GAMSX * GAMSX + MXC * OMX * OMX )
      F(12.12) =-MXCINV * ( BY + BY ) * HT * HT * GAMSX * GAMSX
     *           - 2.0 * MXCINV * BXXR * GAMSX * GAMSX
      F(12.17) = KY * MXCINV * GAMSX * HT
      F(12.18) = BY * MXCINV * GAMSX * HT
      F(12.23) =-KY * MXCINV * GAMSX * HT
      F(12.24) =-BY * MXCINV * GAMSX * HT
      F(12.29) = MXCINV * KXXR * GAMSX
      F(12.30) = MXCINV * BXXR * GAMSX
      F(12.31) =-MXCINV * KXXR * GAMSX
      F(12.32) =-MXCINV * BXXR * GAMSX

      F(14, 3) =-MYCINV * ( KZ + KZ ) * GAMSY
      F(14, 4) =-MYCINV * ( BZ + BZ ) * GAMSY
      F(14.13) =-MYCINV * ( ( KZ + KZ ) * GAMSY * GAMSY
     $                      + MYC * OMY * OMY )
      F(14.14) =-MYCINV * ( BZ + BZ ) * GAMSY * GAMSY

      F(16, 1) =-MZCINV * ( KY + KY ) * GAMSZ
      F(16, 2) =-MZCINV * ( BY + BY ) * GAMSZ
      F(16, 5) =-MZCINV * ( KY + KY ) * GAMSZ * HT
      F(16, 6) =-MZCINV * ( BY + BY ) * GAMSZ * HT
      F(16.15) =-MZCINV * ( ( KZZ + KZZ ) * GAMPSZ * GAMPSZ
     $                    + ( KY + KY ) * GAMSZ * GAMSZ
     $                    + MZC * OMZ * OMZ )
      F(16.16) =-MZCINV * ( ( BZZ + BZZ ) * GAMPSZ * GAMPSZ
     $                    + ( BY + BY ) * GAMSZ * GAMSZ )
      F(16.17) = KY * MZCINV * GAMSZ
      F(16.18) = BY * MZCINV * GAMSZ
      F(16.19) = KZZ * MZCINV * GAMPSZ
      F(16.20) = BZZ * MZCINV * GAMPSZ
      F(16.23) = KY * MZCINV * GAMSZ
      F(16.24) = BY * MZCINV * GAMSZ
      F(16.25) =-KZZ * MZCINV * GAMPSZ
      F(16.26) =-BZZ * MZCINV * GAMPSZ
```

(C.3.1 Continued)

```
F(18, 1) = KY * MTINV
F(18, 2) = BY * MTINV
F(18, 5) = KY * MT * MTINV
F(18, 6) = BY * MT * MTINV
F(18, 9) = KY * LT * MTINV
F(18,10) = BY * LT * MTINV
F(18,11) = KY * GAMSX * MT * MTINV
F(18,12) = BY * GAMSX * MT * MTINV
F(18,15) = KY * GAMSZ * MTINV
F(18,16) = BY * GAMSZ * MTINV
F(18,17) =-KY * MTINV
F(18,18) =-MTINV * ( BY + 4.0 * F22 / VIPS )
F(18,19) = F22 * MTINV * 4.0

F(20, 9) = KZZ * IWINV
F(20,10) = BZZ * IWINV
F(20,15) = KZZ * GAMPSZ * IWINV
F(20,16) = BZZ * GAMPSZ * IWINV
F(20,17) =-B * F11 * ALPHA / RO * IWINV * 4.0
F(20,19) =-( KZT + KZZ) * IWINV
F(20,20) =-( BZT + BZZ + B * B * F11 / VIPS * 4.0 ) * IWINV
F(20,21) = KZT * IWINV
F(20,22) = BZT * IWINV

F(22,19) = KZT * ISINV
F(22,20) = BZT * ISINV
F(22,21) =-KZT * ISINV
F(22,22) =-( BZT + F22 * A * A * 4.0 / VIPS ) * ISINV
F(24, 1) = KY * MTINV
F(24, 2) = BY * MTINV
F(24, 5) = KY * MT * MTINV
F(24, 6) = BY * MT * MTINV
F(24, 9) =-KY * LT * MTINV
F(24,10) =-BY * LT * MTINV
F(24,11) =-KY * GAMSX * MT * MTINV
F(24,12) =-BY * GAMSX * MT * MTINV
F(24,15) = KY * GAMSZ * MTINV
F(24,16) = BY * GAMSZ * MTINV
F(24,23) =-KY   * MTINV
F(24,24) =-( BY + F22 * 4.0 / VIPS ) * MTINV
F(24,25) = F22 * MTINV * 4.0

F(26, 9) = KZZ * IWINV
F(26,10) = BZZ * IWINV
F(26,15) =-KZZ * GAMPSZ * IWINV
F(26,16) =-BZZ * GAMPSZ * IWINV
F(26,23) =-B * F11 * ALPHA / RO *  IWINV  *  4.0
F(26,25) =-( KZT + KZZ ) * IWINV
F(26,26) =-( BZT + BZZ + B * B * F11 / VIPS * 4.0 ) * IWINV
F(26,27) = KZT * IWINV
F(26,28) = BZT * IWINV

F(28,25) = KZT * ISINV
F(28,26) = BZT * ISINV
F(28,27) =-KZT * ISINV
F(28,28) =-( BZT + F22 * A * A * 4.0 / VIPS ) * ISINV

F(30, 5) = ISINV * KXXR
F(30, 6) = ISINV * BXXR
F(30,11) = ISINV * KXXR * GAMSX
F(30,12) = ISINV * BXXR * GAMSX
F(30,29) =-ISINV * ( KXX + KXXR )
F(30,30) =-ISINV * BXX - ISINV * BXXR

F(32, 5) = ISINV * KXXR
F(32, 6) = ISINV * BXXR
F(32,11) =-ISINV * KXXR * GAMSX
F(32,12) =-ISINV * BXXR * GAMSX
F(32,31) =-ISINV * ( KXX + KXXR )
F(32,32) =-ISINV * BXX - ISINV * BXXR
```

C.3.2 **Nonlinear Dynamics Matrix D**

```
D( 5,19) = MSINV
D( 5,25) = MSINV

D( 6,11) = MSINV
D( 6,12) = MSINV
D( 6,15) = MSINV
D( 6,16) = MSINV
D( 6,17) = MSINV
D( 6,18) = MSINV
D( 6,23) = MSINV
D( 6,24) = MSINV
D( 6,29) = MSINV
D( 6,30) = MSINV
D( 6,31) = MSINV
D( 6,32) = MSINV
```

```
D( 8,11) =-IYCINV * LT
D( 8,12) = D(8,11)
D( 8,13) =-D(8,11)
D( 8,14) = D(8,13)
D( 8,29) = D(8,11)
D( 8,30) = D(8,11)
D( 8,31) = D(8,13)
D( 8,32) = D(8,13)

D(10,15) = IZCINV
D(10,16) = IZCINV
D(10,19) = IZCINV * LT
D(10,20) =-D(10,19)

D(12, 9) = MXCINV * GAMSX
D(12,10) =-D(12,9)
D(12,19) = D(12,9) * MT
D(12,20) =-D(12,19)

D(14,11) = GAMSY * MYCINV
D(14,12) = D(14,11)
D(14,13) = D(14,11)
D(14,14) = D(14,11)
D(14,29) = D(14,11)
D(14,30) = D(14,11)
D(14,31) = D(14,11)
D(14,32) = D(14,11)

D(16,15) = MZCINV * GAMPSZ
D(16,16) =-D(16,15)
D(16,19) = MZCINV * GAMSZ
D(16,20) = D(16,19)

D(18, 1) = MTINV
D(18, 2) = MTINV
D(18, 3) = MTINV
D(18, 4) = MTINV
D(18,19) =-MTINV

D(20,15) =-IWINV
D(20,17) =-IWINV
D(20,21) = IWINV
D(20,22) = IWINV
D(20,23) = IWINV
D(20,24) = IWINV

D(22, 1) = A * ISINV
D(22, 2) = D(22,1)
D(22, 3) =-D(22,1)
D(22, 4) =-D(22,1)
D(22,17) = ISINV

D(24, 5) = MTINV
D(24, 6) = MTINV
D(24, 7) = MTINV
D(24, 8) = MTINV
D(24,20) =-MTINV

D(26,16) =-IWINV
D(26,18) =-IWINV
D(26,25) = IWINV
D(26,26) = IWINV
D(26,27) = IWINV
D(26,28) = IWINV

D(28, 5) = D(22,1)
D(28, 6) = D(22,1)
D(28, 7) =-D(22,1)
D(28, 8) =-D(22,1)
D(28,18) = ISINV

D(30, 9) =-IBINV
D(30,11) =-IBINV * WSG
D(30,12) =-D(30,11)
D(30,29) = D(30,11)
D(30,30) =-D(30,11)

D(32,10) =-IBINV
D(32,13) = D(30,11)
D(32,14) =-D(30,11)
D(32,31) = D(30,11)
D(32,32) =-D(30,11)
```

C.3.3 Input Dynamics Matrix G

```
G( 2, 1) =-1
G( 2, 8) =-MCINV * MSG * KY
G( 2, 9) =-MCINV * MSG * BY
G(3,14) = G( 2, 8)
G(3,15) = G( 2, 9)

G( 4, 8) = KZ * MCINV
G( 4, 9) = BZ * MCINV
G(4,12) = G( 4, 8)
G(4,13) = G( 4, 9)

G( 6, 8) =-IXCINV * HT * KY * MSG
G( 6, 9) =-IXCINV * HT * BY * MSG
G(6,16) = G( 6, 8)
G(6,18) = G( 6, 9)

G( 8, 6) =-IYCINV * KZ * LT
G( 8, 7) =-IYCINV * BZ * LT
G( 8,12) =-G( 8, 6)
G( 8,13) =-G( 8, 7)

G(10, 8) =-IZCINV * LT * KY * MSG
G(10, 9) =-IZCINV * LT * BY * MSG
G(10,16) =-G(10, 8)
G(10,18) =-G(10, 9)

G(12, 8) =-MCINV * HT * KY * MSG * GAMSX
G(12, 9) =-MCINV * HT * BY * MSG * GAMSX
G(12,16) =-G(12, 8)
G(12,18) =-G(12, 9)

G(14, 6) = KZ * GAMSY * MYCINV
G(14, 7) = BZ * GAMSY * MYCINV
G(14,12) = G(14, 6)
G(14,13) = G(14, 7)

G(16, 1) =-G( 8) * MZCINV * GLOADZ
G(16, 8) =-MZCINV * KY * MSG * GAMSZ
G(16, 9) =-MZCINV * BY * MSG * GAMSZ
G(16,16) = G(16, 8)
G(16,18) = G(16, 9)

G(18, 1) =-G(
G(18, 3) =-FSS * MTINV * 4.0
G(18, 8) = MTINV * KY * MSG
G(18, 9) = MTINV * BY * MSG

G(20, 2) =-G * FII / VIPS * IWINV * 4.0
G(20, 4) = G * FII * ALPHA / RS * IWINV * 2.0
G(20, 5) = G(20, 4)

G(22, 3) =-FSS * ISINV * 4.0 * A * A / LT

G(24, 1) =-G(
G(24, 3) =-G(18, 3)
G(24,16) = G(18, 8)
G(24,18) = G(18, 9)

G(25, 2) = G(20, 2)
G(25,16) = G(20, 4)
G(25,11) = G(20,16)
G(25, 3) = G(22, 3)

G(30, 8) = IBINV * KRR
G(33, 8) = IBINV * BRR

G(32,16) = IBINV * KRR
G(32,18) = IBINV * BRR
```

C.3.4 Input and Non-linearity Vectors

The full input vector $\underline{u}$ is

u_1 - ε unbalanced super-elevation/track gauge

u_2 - ΔV ($\approx$ Vb/R); R-curve radius, b-semigauge

u_3 - ϕ_R, yaw angle of track under truck in curve (see Fig. B.2-1)

u_4 - y_{R1}, rail offset in curve at axle 1

u_5 - y_{R2}, rail offset in curve at axle 2

u_6 - z_A, truck A mean vertical displacement (see Fig. B.2-5)

u_7 - $\dot{z}_A$, truck A mean vertical rate

u_8 - ϕ_A, truck A mean roll angle (see Fig. B.2-5)

u_9 - $\dot{\phi}_A$, truck A mean roll rate

u_{10} to u_{15} - as b_4 to b_9 for Truck B

u_{16} to u_{19} - gauge variation of track at axles 1 to 4.

The total vector on nonlinearities $\underline{f}$ is,

f_1 to f_8 - lateral wheel-rail forces

f_9 to f_{10} - roll stiffness at bolster A, bolster B

f_{11} to f_{12} - vertical snubbing force truck A, right, left

f_{13} to f_{14} - vertical snubbing force truck B, right, left

f_{15} to f_{16} - centerplate yaw moment truck A, truck B

f_{17} to f_{18} - tramming torque truck A, truck B

f_{19} to f_{20} - lateral stiffness truck A, truck B

f_{21} to f_{27} - yaw wheel-rail torques

f_{29} to f_{32} - vertical stiffness nonlinearity each spring group.

C.4 100 TON HOPPER CAR PARAMETER LIST

The parametric values used in the study described in Chapters 4 and 5 are listed below. The truck values were taken from measurements reported by Martin-Marietta Corporation (Ref. 35). The body and certain suspension parameters were those used by Platin, Beaman, Hedrick, and Wormley (Ref. 7) in their study of "rock and roll." No particular vehicle has these dimensions, it is designed to be realistic but to exhibit poor response to track input. In this list, since the trucks are identical, only values for Truck A have been given.

Masses and Inertias

M_C	= 630.77	lb sec^2/in.	-	Ref. 7
M_{XC}	= 912,000.0	lb-in.-sec^2	-	Note 1
M_{YC}	= 317.2	lb sec^2/in.	-	Note 1
M_{ZC}	= 317.2	lb sec^2/in.	-	Note 1
M_B	= 3.78	lb sec^2/in.	-	Ref. 35
M_S	= 2.983	lb sec^2/in.	-	Ref. 35
M_W	= 7.731	lb sec^2/in.	-	Ref. 35
I_{XC}	= 1,824,000	lb-in.-sec^2	-	Ref. 7
I_{YC}	= 16,800,000	lb-in.-sec^2	-	Ref. 7
I_{ZC}	= 16,657,000	lb-in.-sec^2	-	Ref. 7
I_{BX}	= 2,757.0	lb-in.-sec^2	-	Ref. 35
I_{BZ}	= 2,757.0	lb-in.-sec^2	-	Ref. 35
I_S	= 1,366.0	lb-in.-sec^2	-	Ref. 35
I_W	= 5,889.0	lb-in.-sec^2	-	Ref. 35

Stiffnesses per Truck

K_Y	= 20,400.0	lb/in.	-	Ref. 7
K_{2Y}	= 1,020,000.0	lb/in.	-	Ref. 7
K_Z	= 44,200.0	lb/in.	-	Ref. 7
K_{2Z}	= 2,406,000.0	lb/in.	-	Ref. 7
K_{XR}	= 10^9	lb/in.	-	nominal
K_{ZT}	= 34,300,000	lb-in./rad	-	Ref. 35
K_{ZZT}	= $K_{ZT} \times 10$	lb-in./rad	-	Ref. 35

Damping per Truck

B_Y	= 3,242.0	lb-sec/in.	-	Note 2
B_Z	= 20,000.0	lb-sec/in.	-	nominal

Other linear coefficients = 0.0

FSNU = FSND = 4000.0 lb - Ref. 7
each side - see Fig. B.3-3

T_{CP} = 56,190.0 lb in. - Ref. 35
See Fig. B.3-6

Vehicle Dimensions

L_T	= 243.0 in.	-	Ref. 7
H_T	= 60.0 in.	-	Ref. 7
a	= 35.0 in.	-	Ref. 35
b	= 29.75 in.	-	standard
w_{SG}	= 39.52 in.	-	Ref. 7
h_{SG}	= 21.7 in.	-	standard
Δ_{hg}	= 0.375 in.	-	Ref. 7
R_o	= 18.0 in.	-	Standard
L_{SB}	= 25.0 in.	-	Standard
CL_{SB}	= 0.25 in.	-	Estimate
R_{CP}	= 7. in.	-	Standard
COM_{SG}	= 0.91 in.	-	Estimate
EXT_{SG}	= 2.78 in.	-	Estimate

Flexibility Parameters

Ω_x	= 44.08	rad/sec	-	Note 1
Ω_y	= 108.45	rad/sec	-	Note 1
Ω_z	= 63.90	rad/sec	-	Note 1
Γ_x	= 0.9274		-	Note 1
Γ_y	= 0.6237		-	Note 1
Γ_z	= 0.6237		-	Note 1
Γ_z	= 0.01028/in.		-	Note 1

Other Nonlinear Parameters

λ_{CP}	= 1.745×10^{-3}	rad/sec	-	Estimate
ϕ_1	= 8.52×10^{-4}	rad	-	Estimate
ϕ_2	= 3.04×10^{-3}	rad	-	Estimate
ϕ_3	= 0.0139	rad	-	Estimate
ψ_{NT}	= 0.05236	rad	-	Ref. 35

Rail Wheel Parameters

α	= 0.05	(or 0.071 or 0.18)	-	see Chapter 3
f_{11}	= 1.96×10^6 lb			
f_{22}	= 1.83×10^6 lb			
MU(μ)	= 0.375	(or 0.5)	-	see Chapter 3
δ	= 67°	(or 70°)	-	see Chapter

Note 1 - The flexible modes assume a free-free beam shape. The values of GAMSX (Γ_x), GAMSY, (Γ_y), GAMSZ (Γ_z), GAMPSZ (Γ_z') are derived from these modes,

$$\Gamma_{y,z} = \cos(2.365 \frac{x}{\ell_c}) - 0.1329 \cosh(2.365 \frac{x}{\ell_c})$$

$$\Gamma_x = \sin(\frac{\pi}{2} \frac{x}{\ell_c})$$

for the value $\frac{x}{\ell_c} = 0.756$, also,

$$M_{xc} = \frac{I_{xc}}{2\ell_c} \int_{-\ell}^{+\ell} \Gamma_x^2 (x)dx = 0.5 I_{xc}$$

$$M_{Y,zc} = \frac{M_c}{2\ell_c} \int_{-\ell}^{+\ell} \Gamma_{y\,z}^2 (x)dx = 0.509 M_c$$

Note 2 - This is an approximate linear viscous damping equivalent to a friction force of 4000 lb per side in the range of frequencies and amplitudes investigated. The results are not sensitive to this value.

C.5 AUXILIARY STATES AND OUTPUTS LIST

In the following list, the first 32 entries are the vehicle states, followed by the 55 auxiliary states computed in the program SIMCAR. The dimensions as they appear on output are also given. In some cases (especially angles) these are not the "natural units" used to solve the problem.

Original State Number	Description	Units
1	Body lateral position	inches
2	Body lateral velocity	in./sec
3	Body vertical position	inches
4	Body vertical velocity	in./sec
5	Body roll angle	deg
6	Body roll rate	deg/sec
7	Body pitch angle	deg
8	Body pitch rate	deg/sec
9	Body yaw angle	deg
10	Body yaw rate	deg/sec
11	Body torsion displacement	rad
12	Body torsional rate	rad/sec
13	Body vertical bending displacement	rad
14	Body vertical bending velocity	rad/sec
15	Body lateral bending displacement	rad
16	Body lateral bending velocity	rad/sec
17	Truck A lateral position	inches
18	Truck A lateral velocity	in./sec
19	Truck A wheelset yaw angle	deg
20	Truck A wheelset yaw rate	deg/sec
21	Truck A sideframe yaw angle	deg
22	Truck A sideframe yaw rate	deg/sec
23	Truck B lateral position	inches
24	Truck B lateral velocity	in./sec
25	Truck B wheelset yaw angle	deg
26	Truck B wheelset yaw rate	deg/sec
27	Truck B sideframe yaw angle	deg
28	Truck B sideframe yaw rate	deg/sec
29	Truck A bolster roll angle	deg
30	Truck A bolster roll rate	deg/sec
31	Truck B bolster roll angle	deg
32	Truck B bolster roll rate	deg/sec

Auxiliary State	Description	Units
1	First axle lateral force, left wheel	lbf
2	Second axle lateral force, left wheel	lbf
3	Third axle lateral force, left wheel	lbf

Auxiliary State	Description	Units
4	Fourth axle lateral force, left wheel	lb_f
5	First axle lateral position	inches
6	Second axle lateral position	inches
7	Third axle lateral position	inches
8	Fourth axle lateral position	inches
9	Vertical force on right weels of Truck A (per wheel)	lb_f
10	Vertical force on left wheels of Truck A (per wheel)	lb_f
11	Vertical force on right wheels of Truck B (per wheel)	lb_f
12	Vertical force on left wheels of Truck B (per wheel)	lb_f
13	Lateral position of rail center under Truck A	inches
14	Lateral position of rail centerline under Truck B	inches
15	Lateral position of rail centerline under body	inches
16	Average of front and rear crosslevel	deg
17	Rail lateral position, front right wheel of Truck A	inches
18	Rail lateral position, rear right wheel of Truck A	inches
19	Pitch angle of track due to profile at truck centers	deg
20	Yaw angle of track due to alignment at truck centers	deg
21	Average of front and rear rail vertical position	inches
22	Yaw moment due to rail and wheel-wheelset 1	lb in.
23	Yaw moment due to rail and wheel-wheelset 2	lb in.
24	Rail lateral position, front left wheel of Truck A	inches
25	Rail lateral position, rear left wheel of Truck A	inches
26	Rail lateral position, front left wheel of Truck B	inches
27	Rail lateral position, rear left wheel of Truck B	inches
28	Rail lateral position, front right wheel of Truck B	inches
29	Rail lateral position, rear right wheel of Truck B	inches
30	Linear lateral creepage, first axle	rad
31	Angle-of-attack (neg), first axle	rad

Auxiliary State	Description	Units
32	Lateral creepage, second axle	rad
33	Angle-of-attack (neg), second axle	rad
34	Lateral creepage, third axle	rad
35	Lateral creepage, fourth axle	rad
36	First axle lateral force, right wheel	lb_f
37	Second axle lateral force, right wheel	lb_f
38	Third axle lateral force, right wheel	lb_f
39	Fourth axle lateral force, right wheel	lb_f
40	L/V of first axle, left wheel	---
41	Lateral force, left wheels of Truck A	lb_f
42	L/V of left side of Truck A	---
43	Total lateral force of Truck A	lb_f
44	L/V of first axle, right wheel	---
45	Lateral force, right wheels of Truck A	lb_f
46	L/V of right side of Truck A	---
47	First left wheel flange to rail overlap	inches
48	First right wheel flange to rail overlap	inches
49	Second left wheel flange to rail overlap	inches
50	Second right wheel flange to rail overlap	inches
51	Third left wheel flange to rail overlap	inches
52	Third right wheel flange to rail overlap	inches
53	Fourth left wheel flange to rail overlap	inches
54	Fourth right wheel flange to rail overlap	inches
55	Ratio of leading left wheel lateral force over distance to wheel drop on leading right wheel	inches

APPENDIX D
REPORT OF NEW TECHNOLOGY

No patentable item has been found in the work performed and described in this report. However, it contributes to the state-of-the-art in the area of rail vehicle simulation.

A computer program, SIMCAR, of a freight car analytical model has been developed, capable of indicating the response of real freight cars to track geometry variations, including curvature, alignment, gage and crosslevel.

Values have been computed of the largest track geometry variations which do not indicate incipient derailment for a standard 100 ton hopper car in the speed range 10 to 25 mph.

REFERENCES

1. DiMasi, F., "Correlation of Accident Data with Physical Characteristics of Derailed Freight Vehicles," TSC Report, No. DOT-TSC-RR219-PM-82-6.

2. DiMasi, F.P., P.G. Przybylinski and G.B. Anderson. Engineering Data Characterizing the Fleet of U.S. Railway Rolling Stock. Washington: U.S. Department of Transportation, Federal Railroad Administration 1981. Report No. FRA/ORD-81/75.1 & 81/75.2 (2 vols.). NTIS: PB82-181546 and PB82-181553.

3. Hamid, A., Owings, R., and Kenworthy, M., "Characterization of Relatively Large Track Geometry Variations," DOT Report No. FRA/ORD-81/13, March 1982.

4. Martin, G.C., Plouffe, W.E., Ahmed, S., Antczak, H., and Tideman, H., "User's Manual Detailed Longitundinal Train Action Model," AAR/TTD Report R-220, 1975.

5. Law, E.H., and Cooperrider, N.K., "Literature Survey of Railway Vehicle Dynamics Research," Journal of Dynamic Systems Measurements and Control, (Trans ASME), Vol. 31-E, No. 2, June 1974, pp. 338.

6. Lee, H.S., Weinstock, H., "Rail Car Harmonic roll Response to Periodic Track Crosslevel Variations," TSC Report No. WP-743-C-15-075, December 1979.

7. Platin, B.E., Beaman, J.J., Hedrick, J.K., and Wormley, D.N., "Computational Methods to Predict Railcar Response to Track Crosslevel Variations," MIT, Final Report, DOT Report No. FRA/OR&D-76/293, September 1976.

8. Law, E.H., Hadden, J.A., and Cooperrider, N.K., "General Models for Lateral Stability Analyses of Railway Freight Vehicles," Clemson University and Arizona State University, Interim Report, FRA Contract No. DOT-05-40018, June 1977.

9. Nadal, M.J., "Theorie de la Stabilite des Locomotives," pt. 2, Movement de Lacet, Annales des Mines, 10, 232 (1896).

10. Porter, S.R.M., "The Mechanics of a Locomotive on Curved Track," The Railway Gazette, London, 1935.

11. Mackenzie, J., "Proceedings of Institute of Civil Engineering," Vol. LXXIV, 1883, pp. 1-57.

12. Carter, F.W., "On the Lateral Stability of Running Locomotives," Proc. Roy. Soc., 121A, 585 (1928).

13. Boocock, D., "The Steady-State Motion of Railway Vehicles on Curved Track," Journal of Mechanical Engineering Science, Vol. II, No. 6, 1969.

14. Newland, D., "Steering Characteristics of Bogies," The Railway Gazette, London, 1968.

15. Kalker, J.J., "On the Rolling Contact of Two Elastic Bodies in the Presence of Dry Friction," (plus table book) Doctoral Thesis, Delft, 1967.

16. Gilchrist, A.O., and Brickle, B.V., "A Re-Examination of the Processes to Derailment of a Railway Wheelset," Journal of Mechanical Engineering Science, Vol. 18, No. 3, 1976, pp. 131-141.

17. Elkins, J.A., and Gostling, R.J., "A General Quasi-Static Curving Theory for Railway Vehicles," Proceedings from 5th VSD-2nd IUTAM Symposium, Vienna, September 1977.

18. Sweet, L.M., Sivek, J.A., and Putman, W.F., "Nonlinear Wheelset Forces in Flange Contact - Parts 1and 2," Journal of Dynamic Systems, Measurement and Control, Vol. 101, No. 3, September 1979.

REFERENCES (Continued)

19. Smith, K.R., MacMillan, R.D., and Martin, G.C., "Two, Three, and Four Axle Rigid Truck Curve Negotiation Model," International Government Industry Research Program of Track-Train Dynamics, administered by Association of American Railroads, 1975.

20. Doyle, G.R., "Conventional Versus Self-Steering Radial Trucks for High-Speed Passenger Trains," ASME Paper 79/RT/3, April 1974.

21. Apparao, T., "Digital Simulation of the Curve Entry Dynamics of a Rail Transit Vehicle," 4th Symposium on Engineering Applications of Solid Mechanics, Mississauga, Ontario, September 1978.

22. Elkins, J.A., and Eickhoff, B.M., "Advances in Nonlinear Wheel/Rail Force Prediction Methods and their Validation," presented at the ASME Winter Annual Meeting, New York, December 1979, to be published.

23. Elkins, J.A., and Weinstock, H., "The Effect of Two-Point Contact on the Curving Behavior of Railroad Vehicles," submitted ASME Winter Annual Meeting, Phoenix, November, 1982.

24. Kalousek, J., "Rail Corrugations,: Canadian Pacific Ltd., Dept. of Research, Report No. S488-75, February 1975.

25. Marcotte, P.P., "Theoretical Study Concerning the Use of Profiled Wheels on Freight Car Trucks," Canadian National Railways, Rail Research, Internal Report No. 115, August 1973.

26. Coltman, M., Brantman, R., and Tong, P., "A Description of the Tests Conducted and Data Obtained during the Perturbed Track Test," DOT Report No. FRA/ORD-80/15, January 1980.

27. Results of the U/P Tests communicated to TASC directly by Dr. H. Weinstock of TSC, Report to be published.

28. Coltman, M., "Quick Look Data Analysis from Vehicle/Track Interaction Test at Starr, Ohio," October 1981, to be published.

29. Harvey, S. Lee, "Simulation of Tangent Track Crosslevel Variation Tests Conducted at Starr, Ohio, May-June 1981," Internal TSC Memorandum.

30. RamaChandran, P.V., and El Madany, M.M., "Performance Characterization of Type I Freight Car Trucks," TDOP Phase II, Wyle Laboratories, DOT Report No. FRA/ORD-80-55, available through NTIS.

31. Tuten, J.M., and Ahlbeck, D.R., "Characterization and Analysis of the Wheel/Rail Load Environment at FAST," Battelle Columbus Labs. presented at ASME Winter Annual Meeting, November 1981.

32. Allen, R.A., and Jolley, J.P., "The Mechanical Aspects of Wheel/Rail Wear," Proc. FAST Eng. Conf. 1981, Denver, Colorado, November 1981, p. 217.

33. Gonsalves, R., Pak, W., and Izbinsky, G., "Railroad Dynamics Inc. (RDI) Truck Evaluation Test," Canadian Pacific Ltd., Report No. 5670-81, March 1981.

34. Ahlbeck, D.R., Johnson, H.R., Harrison, H.D., and Tuten, J.M., "Measurements of Wheel/Rail Loads on Class 5 Track," DOT Report No. FRA/ORD-80/19, February 1980.

35. Abbott, P.W., "Barker S-2 Static Test," Martin Marietta Corp., Report TR-006-5, NASA-CR-144272, February 1976.